Characterization of the zebrafish pigment pattern mutant parade

Muller, Jeanette

Award date:
2007

Awarding institution:
University of Bath

Characterization of the zebrafish pigment pattern mutant *parade*

Jeanette Müller

A thesis submitted for the Degree of Doctor of Philosophy

University of Bath
Department of Biology and Biochemistry
May 2007

ProQuest LLC
789 East Eisenhower Parkway
P.O. Box 1346
Ann Arbor, MI 48106-1346

Table of contents

Acknowledgements

First and foremost I would like to thank my supervisor Robert Kelsh for his continuous support, enthusiasm and inspiring discussions.

I would like to thank all the people who have helped me during the past years.
My two project students Kuisoon Lee and Agnes Wyzgol for their help with the characterization of *id2*. Ursula Potter performed the sectioning of embryos for TEM analysis and was a great help in interpreting the sections. Edward Feil for help with statistical analysis.
I am grateful to Derek Stemple and Elisabeth Busch- Nentwich from the Welcome Trust Sanger Institute for teaching me how to map genes and to Mario Coccamo for providing me with unpublished assembly information. Thank you to Hans-Martin Pogoda for additional advice on creating markers for mapping. Thank you also to Emma Greenhill for proof-reading parts of my thesis.

I would also like to thank Richard Squire and Marc Shedden for excellent fish care.

Thank you to all former and present members of the Kelsh and Ward labs, especially Tom Carney, for help and discussion. Thank you to Al Garfield for providing 'in lab entertainment' throughout my PhD.

Abbreviations

AVS	anterior ventral stripe
BACs	Bacterial Artificial Chromosomes
BCIP	5-Bromo-4-chloro-3-indolyl phosphate,toluidine salt
BMP	Bone Morphogenetic Protein
Bp	base pair
BSA	Bovine serum albumin
°C	Degrees Celcius
$CaCl_2$	Calcium chloride
cDNA	complementary DNA
cho	*choker*
cls	*colourless*
c-kit	*kit oncogene*
cM	centi Morgan
cR	centi Ray
C6S	chondoritin-6-sulfate
CTP	cytidine triphosphate
DAB	3,3'-Diaminobenzidine
dct	*dopachrome tautomerase*
DIG	Digoxygenin
DMSO	Dimethyl Sulfoxide
DNA	Deoxyribonucleic acid
dpf	days post fertilization
Dom	*Dominant megacolon*
DS	dorsal stripe
Dsk	*Dark skin*
E	Embronic day
ECM	Extracellular Matrix
ednrb1	*endothelin receptor 1b*
EDTA	Ethylenediaminetetra-acetic acid
EMT	Epithelial-to-mesenchymal transition
ENU	N-ethyl-N-nitrosourea
ER	Endoplasmatic Reticulum
ESM	Early stripe melanophores
EST	Expressed Sequence Tags
Fig.	Figure
FGF	Fibroblast Growth Factor
g	gram
GAT	Gates et al
gch	*GTPI cyclohydrolase*
GFP	Green Fluorescent Protein
GMP synthetase	Guanine Monophosphate synthetase
GTP	guanosine triphosphate
HCl	Hydrochloric acid
HOAc	acetic acid
H_2O_2	Hydrogen peroxide
HM	Hybridisation mix
HNK-1	Human Natural Killer-1
hpf	hours post fertilization

HS	Heat shock
Hyb	Hybridisation mix
id	*inhibitor of DNA binding*
KCl	potassium chloride
kD	kilo Dalton
KOD	Thermococcus kodakaraensis
KOH	Potassium hydroxide
l	litre
LB	Luria Bertani
LiCl	Lithium Chloride
LN54	Loeb, NIH, 5000rad, 4000rad
LOD	logarithm of likelihood ratio for linkage
LS	lateral stripe
LSM	Late stripe melnaophores
mitf	*microphthalmia related transcription factor*
nac	*nacre*
m	milli
μ	micro
$MgSO_4$	Magnesium sulfate
MOP	Mother of Pearl
NaAc	Sodium acetate
NaCl	Sodium chloride
NBT	Nitro blue tetrazolium chloride
N-terminal	amino-terminal
NTP	nucleoside triphosphate
OMIM	Online Mendelian Inheritence in Men
PACs	P1 artificial chromosomes
PBS	Phosphate Buffered Saline
PCR	Polymerase Chain Reaction
PCI	Phenol:Chloroform:Isoamyl Alcohol
pde	*parade*
Penn/Strep	Pennicillin/Streptomycin
PFA	Paraformaldehyde
PH3	Phospho Histone 3
PLLn	Posterior lateral line nerve
PNA	Peanut agglutinin lectin
PNS	Peripheral nervous system
PTU	1-phenyl-2-thiourea
PVS	posterior ventral stripe
RD	Reaction-Diffusion
RFLP	Restriction Fragment Length Polymorphism
RNA	Ribonucleic acid
RPE	Retinal Pigmented Epithelium
rpm	revolutions per minute
RT	reverse transcriptase
s	*piebald lethal*
Sdf1a	*stromal derivel cell factor 1a*
SDS	Sodium dodecyl sulfate
shd	*shady*
SL	Smyth line serum

Sl	Steel
SNPs	Single Nucleotide Polymorphism)
sox 10	*SRY-box containing gene 10*
Sry	sex-determining region of Y chromosome
SSC	saline sodium citrate
SSLP	Single Sequence Length Polymorphism
SSR	Simple Sequence Repeats
TAE	Tris-Acetate-EDTA
TE	Tris EDTA
TEM	Transmission Electron microscope
TGFβ	Transforming Growth Factor β
TILLING	Targeting Induced Local Lesions in Genomes
TUNEL	Terminal deoxynucleotidyl Transferase Biotin-dUTP Nick End Labelling
tyr	*tyrosinase*
u	units
UTP	uridine triphosphate
UV	ultra violet
VS	ventral stripe
W	*Dominant spotting*
wt	wild-type
xdh	*xanthine dehodrogenase*
YAC	Yeast Artificial Chromosome
YSS	yolk sac stripe
ZFIN	Zebrafish Information Network
Zv	Zebrafish version

Abstract

In vertebrates, pigment cells are a biologically and medically important derivative of the neural crest. Zebrafish have multiple distinct pigment cell types, including melanophores, iridophores and xanthophores, that form a characteristic stereotypic pattern comprising four body stripes-dorsal, lateral, ventral and yolk sac stripe. The mechanisms necessary for forming this pattern are only poorly understood. In order to further understand how pigment pattern formation in zebrafish occurs we characterize *parade*, a pigmentation mutant with ectopic chromatophores in the trunk, located just below the notochord (Kelsh et al., 1996). We propose 4 different models – mixed cell fate, transdifferentiation, cell number and migration- explaining the appearance of the ectopic chromatophores and test each in turn.

We show that *parade*^{tj262} mutants have an early increase in iridophore numbers. The *sox10*-dependent appearance of the ectopic chromatophores -sometimes closely associated- melanophores and iridophores seems (at least partly) independent of this increase. Analysis of double mutants, lacking either melanophores or iridophores, indicates that environmental cues are involved in the ectopic appearance as loss of one pigment cell type does not appear sufficient to completely loose the ectopic cells.

We also observe a reduction in sympathetic neuron numbers in the trunk at 7 dpf. It remains unclear whether the pigment and sympathetic neuron phenotypes have a shared mechanism.

To advance the study of the iridophore phenotype we characterised *alk* expression further and identified and characterised *cb632* and *id 2* as iridophore markers. We show that their expression is not restricted to iridophores at early developmental stages.

In preparation for positional cloning of *parade* we mapped it, using bulk segregant analysis, to linkage group 1. Using fine mapping we located a marker only ~ 0.2 cM away from the mutation. We are now nicely positioned for rapid positional cloning as the coverage of this region of the genome has improved.

Chapter I Introduction

During development an organism develops from a single cell to a multicellular and 3 dimensional organism with a number of different organs and tissues. A complex series of developmental events have to take place to ensure formation of the correct body plan. This 'process by which embryonic cells form ordered spatial arrangements of differentiated tissues' (Gilbert, 2000) is called pattern formation. Correct pattern formation is crucial for essential steps in development, such as axis formation and vertebrate limb development (Gilbert, 2000; Tickle, 2000). Defects in pattern formation can result in death, severe illnesses and disabilities such as the loss or malformation of limbs. A classic example of pattern formation that has been studied for many years is pigment pattern formation. The beauty and variety of pigment patterns in different animal species has fascinated scientists and laypersons alike. Defects in pigment cell patterning can easily be detected due to the intrinsic properties of the pigment cells. A large number of naturally occurring and laboratory generated pigmentation mutants are known, providing an excellent source to study pigment pattern formation (Kelsh et al., 1996; Kelsh et al., 2004; Nakamura et al., 2002). Pigment cells are a derivative of the neural crest and understanding of the mechanisms involved in pigment pattern formation might also provide insight into the mechanisms involved in the pattern formation of other neural crest derivatives.

I.1. Neural crest

First discovered by Wilhelm His in 1868 the neural crest is a transitory, pluripotent and highly migratory population of cells characteristic of vertebrates. The development of the neural crest has been studied in a variety of model organisms including chick, frog, mouse and zebrafish (Aybar and Mayor, 2002; Kelsh and Raible, 2002; Le Douarin, 2004). The ectoderm-derived neural crest arises at the dorsal edge of the neural tube during embryonic development and gives rise to a variety of different derivatives that contribute to a large number of different organs and tissues. The development of the neural crest consist of the following main steps: induction of neural crest, epithelial-to-mesenchymal transition (EMT), migration of neural crest cells and specification and differentiation into the various derivatives (Halloran and Berndt, 2003).

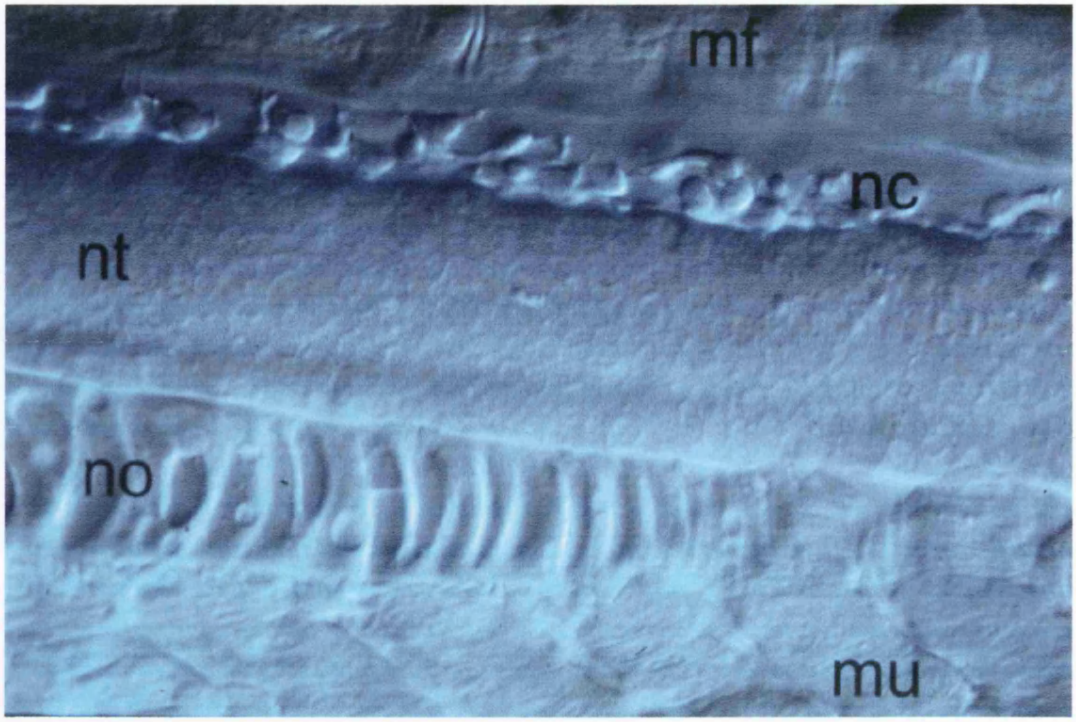

Fig. 1.1: Neural crest in zebrafish embryos
At about 22 hpf neural crest cells (nc) can be seen lying on top of the neural tube (nt) in the tail of zebrafish embryos. Lateral view of the dorsal trunk of the embryo with dorsal to the top. mf: medial fin, no: notochord and mu: muscle.
In this and all other pictures anterior is to the left and posterior to the right.
picture with permission of R.N. Kelsh

The induction of neural crest is a multistep process and while it is similar in different species, some differences can be detected (Aybar and Mayor, 2002). The ectodermally derived neural crest cells are induced at the border of prospective epidermis and neural plate by signals including members of the *Bone Morphogenic Protein* (*Bmp*), *Wnt* and *Fibroblast Growth Factor* (*Fgf* (Aybar and Mayor, 2002) families. During primary neurulation the neural plate folds to form the neural tube. As a result of this process combined with delamination of neural crest from the epithelium the neural crest cells come to lie on top of the neural tube underneath the epidermis (Fig. 1.1). From here they migrate along two main distinct pathways –called medial and lateral in zebrafish (ventromedial and dorsolateral in chick)- and give rise to a prodigious number of derivatives. The derivatives include pigment cells, neurons and glia of the sensory, autonomic and enteric nervous system, craniofacial cartilage and bone (LaBonne and Bronner-Fraser, 1999; Le Douarin and Kalcheim, 1999). Neural crest gives rise to multiple derivatives in the head and defects in differentiation and distribution of those can lead to severe patterning defects such as the cleft palate. However, for the purpose of this thesis we will concentrate on neural crest, specifically pigment cell, development in the trunk as no defects in the head of the mutant characterised here have been observed.

I.2. Neural crest derived pigment cell types

Pigment cells are an excellent model for studying pattern formation. Differences in pigmentation and pigment cell distribution are easily visible due to the intrinsic properties of pigment cells like the production of melanin.

The colouration in mammals and birds is generated by melanocytes only (Fujii, 2000). Homeotherms have two types of melanin, the brown-black eumelanin and the red-brown pheomelanin (Bagnara, 1998). In contrast, poikilothermic vertebrates and invertebrates can have up to six different pigment cell types -called chromatophores: black melanophores (homologous to melanocytes)(Fig. 1.2 A), iridescent iridophores (Fig. 1.2 B), white leucophores, yellow xanthophores (Fig. 1.2 C), red erythrophores, and blue cyanophores (Bagnara, 1998; Fujii, 2000). The pigment pattern in salamander is made up of melanophores, iridophores and xanthophores (Parichy, 1996a). The fish medaka (Oryzias latipes) possesses all these three pigment cell types and also

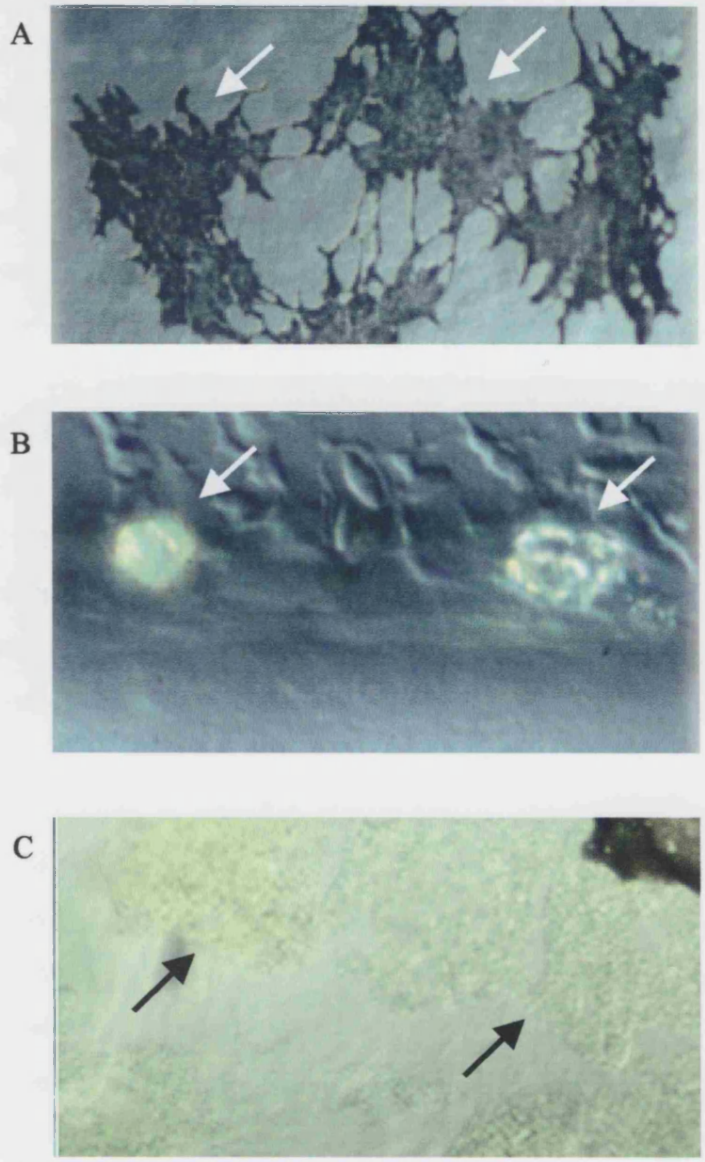

Fig. 1.2: Neural crest derived pigment cell derivatives
In zebrafish neural crest gives rise to three distinct types of pigment cells: the black melanin containing melanophores (A, arrows), the silver, reflecting iridophores (B, arrows) and the yellow green xanthophores (C, arrows).

leucophores (Kelsh et al., 2004). As adults *Danio rerio* display melanophores, iridophoreas and xanthophores and presence of leucophores has been described for the tail (Johnson et al., 1995). Other *Danio* species, such as *Danio albolineatus*, have been shown to also have erythrophores (Parichy, 2006). Embryonic zebrafish are known to have three different pigment cell types: melanophores (Fig. 1.2 A), iridophores (Fig. 1.2 B) and xanthophores (Fig.1.2 C).

The light absorbing black/brown melanophores contain eumelanin producing spherical shaped melanosomes (Bagnara, 1978). Melanophores often have a spider-like appearance due to the formation of multiple dendrites (Bagnara, 1998). The second pigment cell type, the light reflecting iridophore is mainly found in cold- blooded vertebrates (Fig.1.2 B), but iridophores have also been observed in the eyes of doves (Bagnara, 1999). The organelles of iridophores, the reflecting platelets, can often be seen forming various oriented stacks within a cell and are endoplasmatic reticulum (ER) derived (Bagnara, 1978) leading to each reflective platelet being surround by a cell membrane (Zarnescu, 2007). After fixing with Paraformaldehyde (PFA) and subsequent sectioning the reflecting platelets look like empty spaces, but *in vivo* they contain guanine. While iridophores in zebrafish appear brown when viewed with transmitted light, they reflect silver or gold under incident light. The third pigment cell type in embryonic zebrafish is the yellow xanthophore (Fig. 1.2 C). The pigmented organelles of xanthophores, carotenoid vesicles and pterinosomes, contain carotenoids and pteridines respectively (Bagnara, 1998).

In fish, pigment cells are thought to be important for camouflage, courtship and communication. Studies in zebrafish, for example, have revealed a preference to form shoals with fish of identical pigment patterns as those an individual has been raised with (Engeszer, 2004). And not only male colouration, but also female colouration, has been shown to be important in mate choice in fish (Amundsen, 2001).

I.3. Patterning

The formation of pigment patterns has been a subject of scientific studies for decades. Knowledge about pigment pattern formation will not only explain how this variety arises, but a deeper understanding of pigment cell development and pigment pattern formation is medically highly relevant as a variety of human illnesses are associated

with pigment cells defects including Albinism and Piebald trait (for further examples see online Mendelian inheritence in man (OMIM), http://www.ncbi.nlm.nih.gov/entrez/query.fcgi?db¼OMIM). Strong similarities between the phenotype caused by a mutation in a gene in mouse and human can often be seen (for a list of genes involved in pigmentation in mouse and human and the phenotypes caused their mutation see: http://ifpcs.med.umn.edu/micemut.htm). But it has also been shown that, like in the example of loss of *sox10* function, humans, mouse and zebrafish can have very similar phenotypes (Kelsh, 2006 and references therein).

A large variety of different, often colourful, patterns between different genera and species exists. To fully understand how the patterning of the different genera and species occurs and what the differences in pattern formation are, it is important to answer (at least) two questions: Firstly, when are the patterns established during development? And what mechanisms are used to establish the different patterns? To answer these questions extensive research on pigment pattern mutants is done. Large collections of coat colour mutants in mouse are available thanks to mouse fancy collection, beginning in the 18th and 19th century. In addition to this a large number of coat colour mice mutants derived from mutagenesis screens are known (for a list see http://www.informatics.jax.org/). Next to mice, pattern formation has been studied most widely in amphibians and more recently extensive study of pigment cell development in zebrafish and medaka mutants, both naturally occurring pigment variants and chemically induced mutants, has started to shed light on pigment pattern development (Kelsh et al., 1996; Kelsh et al., 2004; Quigley and Parichy, 2002; Rawls et al., 2001).

Some differences in pigment pattern formation in mammals and lower animals are caused by the different behaviour of melanocytes in those groups. In mammals melanocytes transfer the melanin-containing melanosomes into the epidermis, hair or feathers colouring the organism in this way. In mouse during development melanocytes first migrate into the dermis. From here they migrate into the epidermis before populating the hair follicles leaving dermis and epidermis devoid of melanocytes. Only the epidermis of areas with little body hair such as the ears and tail still contains melanocytes. In contrast to mouse where melanocytes reside in the hair follicles they can be found in the basal layer of the epidermis in humans (Jackson, 2004). In humans, variation of skin colour of a particular region of the body between two individuals is not primarily caused by differences in melanocyte number, but differences in size, melanin content and density of melanosomes (Barsh, 2003).

The melanocytes transfer the melanosomes to the keratinocytes and the darker the skin the more numerous, larger and more pigmented are the melanosomes per keratinocyte. Thus people with European skin colour have smaller and fewer melanosomes, although melanosome number within different areas of one individual can vary.
In fish however chromatophores retain their pigment containing organelles therefore showing the true position of the pigment cell.

I.3.1. Mechanisms of pattern formation

We will now introduce three different models of how pigment pattern formation occurs with an emphasis on a possible existence of these mechanisms in embryonic and adult pigment pattern formation in zebrafish.
A model that has been suggested to be able to explain the pattern formation in all vertebrates is the reaction-diffusion (RD) mechanism. Turing first proposed such a mechanism that suggests that a prepattern is formed during early development (Turing, 1952). This prepattern is formed by the interaction of two diffusible chemical molecules -morphogens- that diffuse at different rates through the tissue (Kondo, 2002; Murray, 1981). This model has been used to explain pigment pattern formation and was further adjusted by including parameters such as cell chemotaxis (Murray, 1981; Painter et al., 2000). In the RD mechanism one of the two molecules acts as an 'activator' and the other as an 'inhibitor' (Kondo, 2002). Both morphogens are initially homogeneously distributed and a change in their distribution starts the prepattern formation. The 'activator' molecule enhances levels of the 'inhibitor' and itself, whilst the 'inhibitor' molecule inhibits production of the 'activator. Through this interaction mechanism and different rates of diffusion the two molecules create 'waves' that generate a stable, periodic pattern -the prepattern. Differences in distance between stripes as can be seen in many mammals, e.g. the striped trunk in zebras, are proposed to originate from an inactivity of the RD mechanism once the prepattern is established. Growth of the animal then leads to the slight variations in stripe width. Pigment pattern formation of a large variety of mammals such as zebra, tiger, and giraffe can be explained using the RD mechanism (Kondo, 2002; Murray, 1981). Recently, spacing between mouse hair follicles has been identified as the first *in vivo* model for the RD mechanism (Sick et al., 2006). Follicle clusters were formed when the activator WNT was suppressed whilst transgenic over expression of the inhibitor Dickkopf resulted in increase hair follicle

density. This model has also been used to describe pigment pattern formation in fish. In contrast to mammals it has been suggested that the RD mechanism remains active, resulting in even spacing between the stripes. Pigment pattern formation in the zebrafish *leopard* mutants and the angelfish can be mimicked well with the RD model (Asai et al., 1999; Kondo and Asai, 1995). A potential long range cue however has not been identified in zebrafish yet, but it has been proposed that the gene mutated in *leopard* could be a factor involved in the RD-mechanism in fish (Asai et al., 1999; Kondo, 2002). In chick, however, presence of a long-distance cue that stimulates melanoblast migration has been suggested based on tissue grafts (Tosney, 2004).

Another possibility is a prepattern, not established through long-range signals, but signals from local tissues. Such environmental cues could be expressed by tissues along the migration pathways as well as tissues close to/at the final destination of the pigment cells. Extracellular matrix molecules (ECM), for example, have been suggested to be involved in pigment pattern formation in amphibians (Epperlein et al., 1996). *Triturus alpestris* larvae have alternating melanophore xanthophore stripes. Transplantation and immunohistochemistry experiments have shown that distribution of different ECM molecules dictates the position of the different pigment cell types in *Triturus*. Melanophores preferred the areas with the more adhesive fibronectin and avoided areas with tenascin and chondroitin sulphate proteoglycan. The opposite preferences were observed for xanthophores, consistent with the characteristic pattern. It has been shown in a variety of model organisms that factors expressed in the somites are involved in regulating timing and pathway of neural crest cell migration ((Halloran and Berndt, 2003; Jesuthasan, 1996) and see below). In zebrafish defects in the horizontal myoseptum have been associated with defects in positioning of lateral stripe melanophores (Kelsh et al., 1996)(see below). Similarly, the Ambysttomatidae family of salamander possess a distinctive, horizontal yellow xanthophore containing stripe, nearly completely devoid of melanophores, positioned along the body during larval development (Parichy, 1996b). Grafting experiments resulting in loss of the lateral line organ showed that the formation of the yellow stripe is lateral line dependent. This provides further evidence, that environmental cues can be at least partly responsible for pattern formation.

A third model that has been proposed is based on local cellular interactions of pigment cells. Here local heterotypic and homotypic interactions between the different chromatophore types would lead to formation of the striped pattern (Maderspacher and

Nusslein-Volhard, 2003). Observations during the establishment of the adult pattern in zebrafish mutants (see below) suggest that these cell-cell interactions play an important role in its formation during wild-type development. Interestingly so far it looks as if only interactions between melanophores and xanthophores, but not iridophores, are important for correct stripe formation in adults (Maderspacher and Nusslein-Volhard, 2003; Parichy et al., 2000a). Recently a mathematical model, simulating the main changes from larval to adult pigment pattern, taking these findings into account has been proposed (Moreira and Deutsch, 2005). The authors show that cell-cell interactions together with specific rates of chromatophore production from stem cells can explain the early adult pattern. Even though this model simulates the pigment pattern in wild-type and some mutant fish many of the assumptions used by the authors, such as presence and strength of adhesive cell-cell interactions and cell proliferation, need to be tested.

I.3.2. Pigment pattern formation in zebrafish

An organism that has in recent years been extensively used to decipher the mechanisms involved in pigment cell patterning is the zebrafish ((Kelsh, 2004) and references therein). In both the embryonic and adult zebrafish pigment cells form a stereotypical pattern. Establishment of the pigment pattern has been shown to occur in two main phases. First a larval pattern is formed, that is then replaced by an adult pigment pattern during metamorphosis. Multiple screens have isolated a large number of embryonic and adult zebrafish mutants (Haffter et al., 1996b; Kelsh et al., 1996; Lister et al., 1999)

I.3.2.A. Embryonic pigment pattern formation in zebrafish

During early development the three types of pigment cells form a highly reproducible and recognizable pattern (Fig. 1.3 and Fig. 1.4). The main feature of this pattern are the four melanophore stripes –dorsal stripe (DS), lateral stripe (LS), ventral stripe (VS) and yolk sac stripe (YSS)- along the anterior posterior axis (Fig. 1.3 A). All except the lateral stripe also contain iridophores (Fig. 1.3 B, C). In the dorsal and ventral stripe the iridophores alternate with the melanophores. In addition to the stripes melanophores and iridophores can be found in the eye and the lateral patches. Xanthophores are mostly located more or less ubiquitously along the whole embryo (Fig. 1.3 A, green arrows). Some xanthophores can be found in the lateral stripe, but they are absent from the other

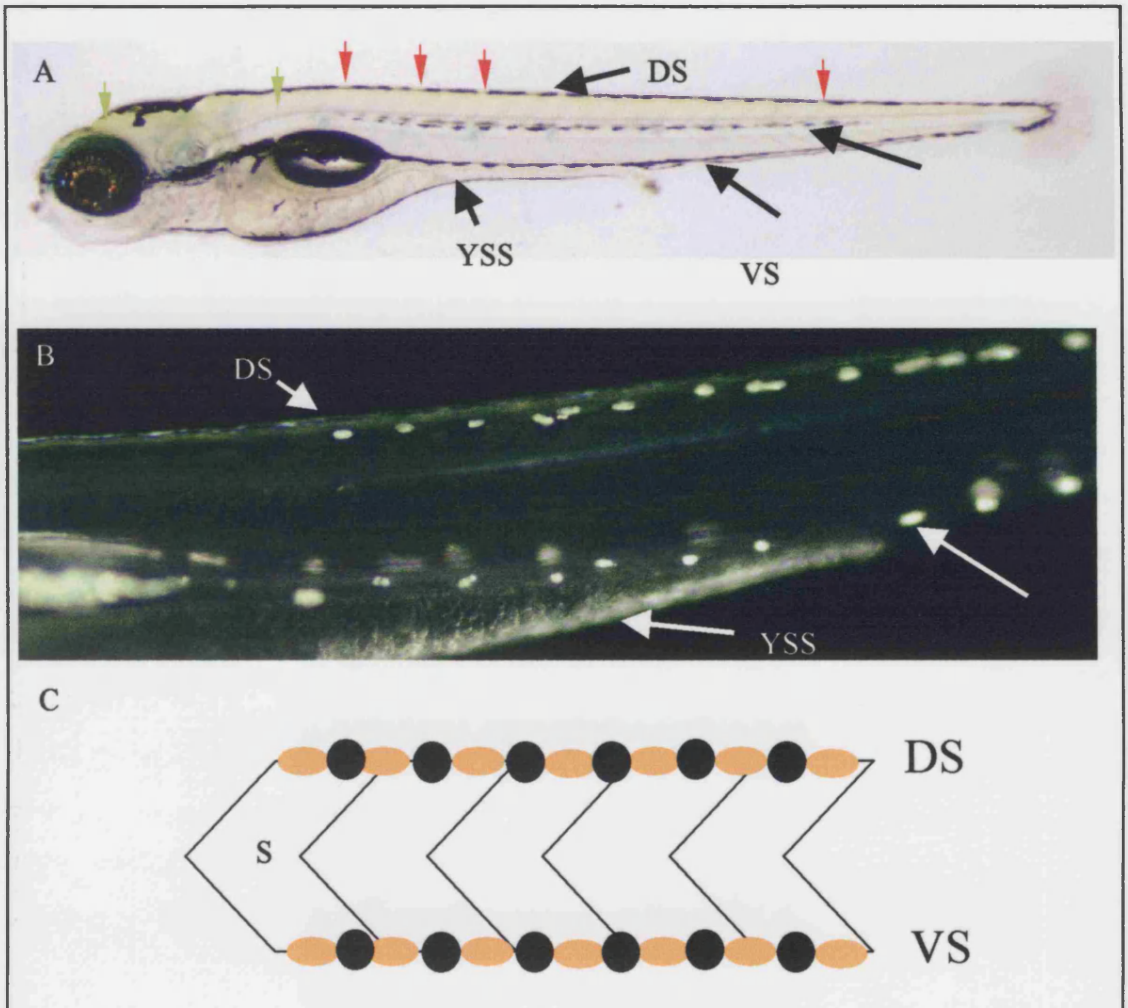

Fig. 1.3: Pigment pattern of zebrafish embryos 5 dpf
The embryonic pigment pattern in the zebrafish trunk and tail consists predominantly of 4 characteristic stripes. The dorsal (DS), lateral (LS), ventral (VS) and yolk sac stripe (YSS). With brightfield optics all four stripes containing the black melanophores can be seen (A). Xanthophores can be seen as a green/yellow shimmer in the head and dorsal half of the embryo but also extend to the VS (A, green arrows) Using incident light the iridophores present in the DS, VS and YSS are visible (B). Gaps can be seen between the melanophores (A, red arrows). These gaps are filled by iridophores which are also distributed in a spotted pattern (B). Schematic of the DS and VS in the trunk (area above the yolk sac extension) of wild-type embryos (C). Somites (S) are shown as chevrons, melanophores as black circles and iridophores as orange circles. For clarity melanophores of the LS and xanthophores are not shown.

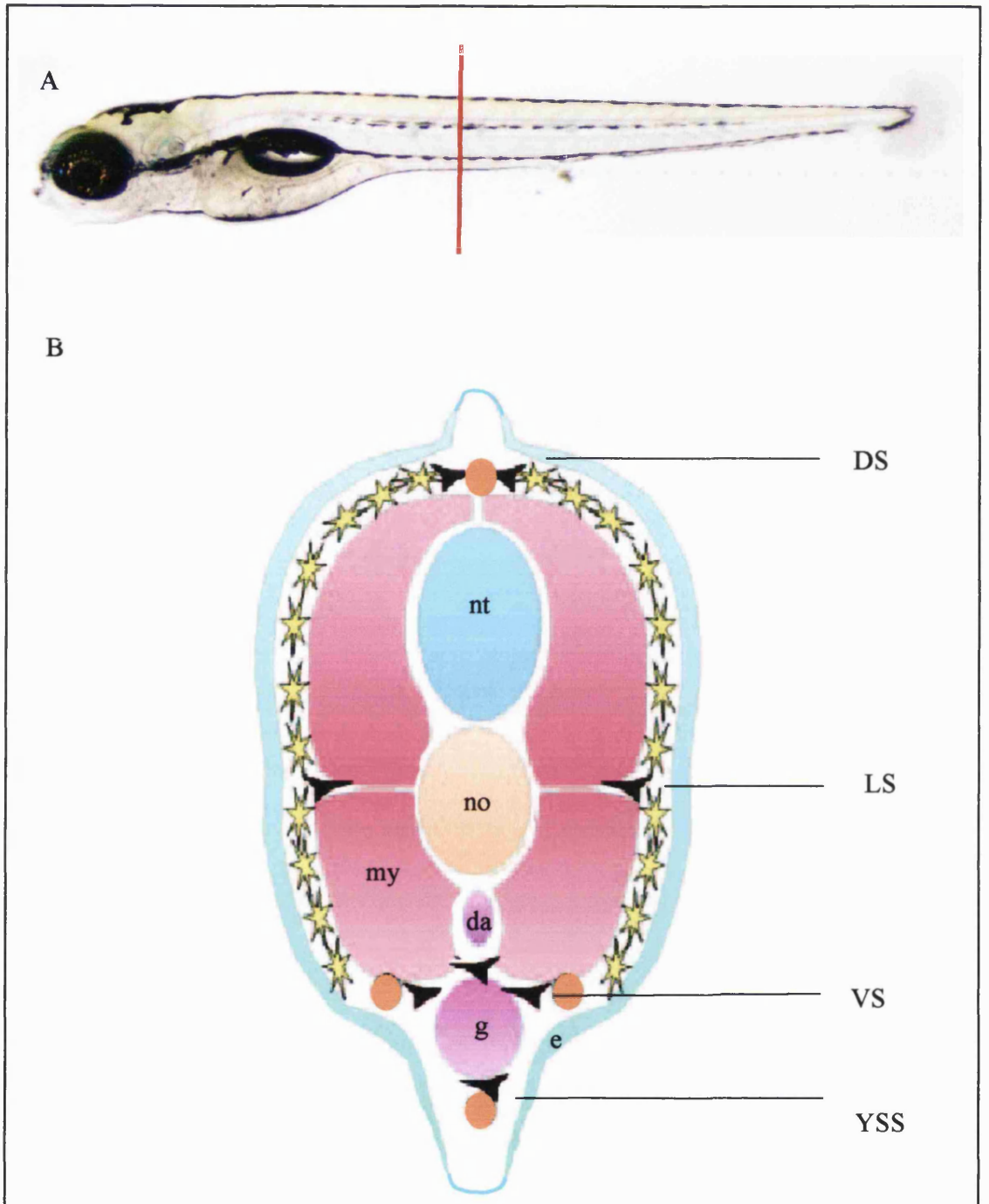

Fig. 1.4: Chromatophore distribution
Section through the trunk region of a zebrafish larvae at around 5 dpf (A, red line). In a transverse view of the zebrafish trunk melanophores (black triangles) can be seen in the DS, VS, LS and YSS. Iridophores (orange circles) are present in all but the lateral stripe. Xanthophores (yellow stars) are scattered between epidermis and myotome; nt: neural tube, no: notochord, my: myoseptum, da: dorsal aorta, g: gut, e: epidermis
Schematic drawing modified from Kelsh 2004

stripes. This early larval pattern is completely established by 5 days post fertilization (dpf) (Kelsh, 2004). The first melanophores forming the DS can be seen at about 30 hours post fertilization (hpf). About 10 hours later the first iridophores can be observed in the posterior half of the DS and very soon after in the ventral stripe (X. Yang, personal communication). The first xanthophores appear at about 42 hpf. Even though not much is known of how the striped pattern in zebrafish embryos is established, it has been suggested that environmental cues and cell-cell interactions play a role (Kelsh, 2004; Kelsh et al., 1996). Based on pigment pattern phenotypes from a genetic screen it has been proposed that both melanophores and iridophores are receptive to particular environmental cues whilst the xanthophores simply fill the remaining space. A role of environmental cues in correct pattern formation of the zebrafish embryo has been hypothesized based on findings that severe defects of the myoseptum always result in loss of the lateral stripe (Kelsh et al., 1996). A link between placement of melanophores along the lateral stripe and expression of genes has been shown in *choker* mutants (Svetic et al., 2007). Here loss of *stromal cell-derived factor 1a* (*sdf1a*) expression along the horizontal myoseptum results in a strong reduction of melanophore numbers in the lateral stripe. In addition, ectopic expression of *sdf1a* results in ectopic positioning of melanophores in *choker* mutants indicating the existence of such environmental cues in embryonic stripe formation.

Phenotypes of isolated embryonic mutants can include loss of one neural crest derived pigment cell type, loss of all three pigment cell types or misplacement of pigment cells (Haffter et al., 1996b; Kelsh et al., 1996; Lister et al., 1999). This implies that different mechanisms are necessary for correct pigment pattern formation.

I.3.2.B. Adult pigment pattern formation in zebrafish

At about two weeks post fertilisation the larval pigment pattern of zebrafish begins to be gradually replaced by the adult pigment pattern consisting of a number (4-6) horizontal black stripes and 3-5 light interstripes. The adult pigment pattern is made up of melanophores, two types of iridophores (type L and type S) and xanthophores (Hirata et al., 2003). Transmission Electron microscope (TEM) analysis of the stripes and interstripes showed a possibly more complex distribution of pigment cells than one might expect (Fig. 1.5 (Hirata et al., 2003; Hirata et al., 2005)). The interstripes are made up of a ubiquitous layer of Type S iridophores with a layer of xanthophores on

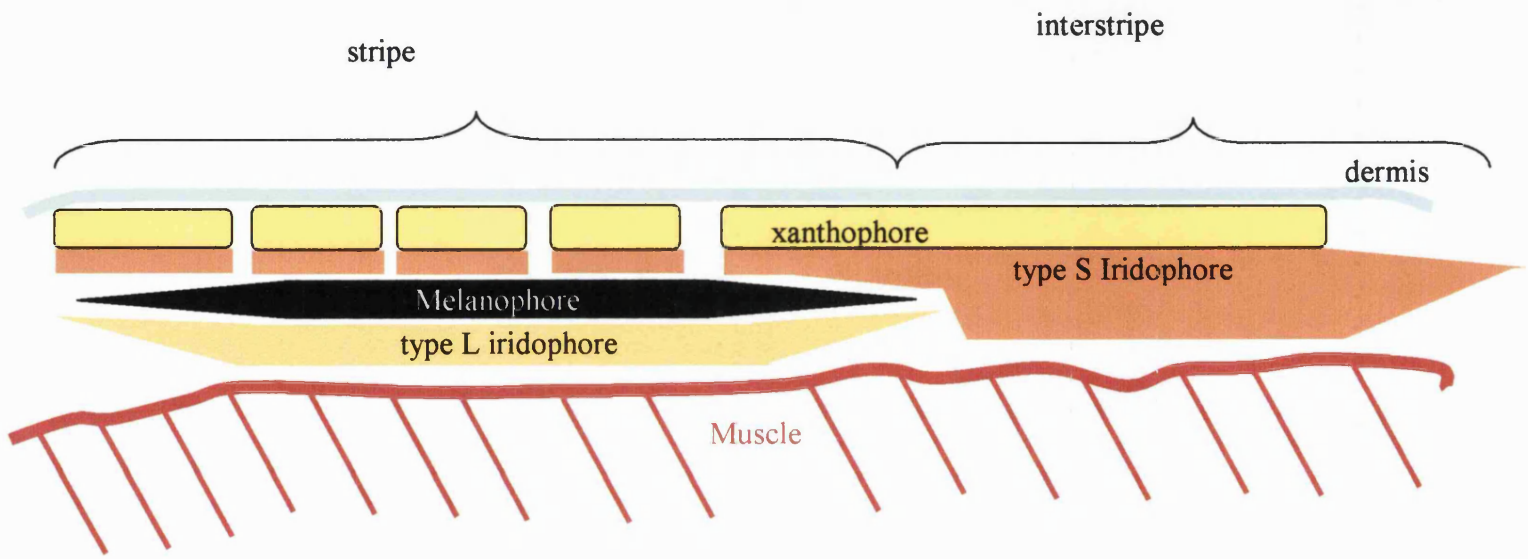

Fig. 1.5: Schematic drawing of pigment cell arrangement in the trunk stripes of adult zebrafish
The white/silver appearing interstripes are made up of a ubiquitous layer of iridophores (type S) with a layer of xanthophores directly underneath the dermis on top. The characteristic black stripes of adult zebrafish also contain this xanthophores and iridophore layer, but in addition have a ubiquitous layer of melanophores followed by a layer of type L iridophores underneath it. Modified from Hirata et al., 2003

top. The stripes also contain these two layers, but have a ubiquitous layer of melanophores underneath. This layer of melanophores, giving the stripe it characteristic black colour, has a layer of Type L iridophores underneath it. In addition to the body stripes, adult zebrafish also have horizontal stripes in the caudal and anal, but not dorsal, fin (Hirata et al., 2005). The dorsalmost region of the fish does not have stripes, but still contains all three pigment cell types (Hirata et al., 2005). During adult stripe formation some of the larval melanophores have been shown to die whilst others contribute to the adult stripes (Milos et al., 1983; Parichy et al., 2000b). Two waves of newly appearing melanophores have been observed (Johnson et al., 1995). The early stripe melanophores (ESM) appear from 2 weeks post fertilization on and can first be seen along the flank of the larvae. The late stripe melanophores (LSM) follow at 3 weeks post fertilization and together with the ESM form the first two anterior to posterior adult body stripes. A model for formation of these first two stripes has been proposed in which melanophores first appear distributed over the flank of the developing fish (Parichy et al., 2000b). Xanthophores then also arise and their presence is necessary for stripe formation as they aide the directed migration of melanophores into the prospective stripe position and thereby increases melanophore survival (Parichy et al., 2000b). Therefore the interstripe is not only formed by melanophores migrating away, but also by the melanophores remaining in the interstripe being more likely to die than those in the stripe. But in addition to this heterotypic interaction between melanophores and xanthophores and homotypic interactions of these cell types have been shown to be required for stripe formation (Maderspacher and Nusslein-Volhard, 2003). Whilst iridophores, normally populating the adult stripes, do not seem to play a role in melanophore stripe formation melanophores seem to be necessary for correct iridophore placement (Johnson et al., 1995; Parichy et al., 2000a). *rose* mutants, lacking most iridophores in the stripes, can still form melanophore stripes. Dependence of iridophores on melanophores has been suggested by adult double mutant analysis. *sparse* mutants (see I.8.3.) lack all epidermal melanophores while *leopard* mutants (see I.8.5.) possess all pigment cell types, but only about half the wild-type number of stripe-associated melanophores. In addition *leopard* mutants have a spotted instead of a stripy pattern in which iridophores can be found in the vicinity of the melanophores. The loss of the spotted iridophore distribution typical for *leopard* mutants in *sparse; leopard* double mutants shows that melanophores are necessary for iridophores to form a pattern. Without melanophores present iridophores seem to be distributed uniformly over the flank. Once the two first adult body stripes

have been established additional adult body stripes are added ventrally and dorsally to those ((Kelsh, 2004) and references therein).
Defects in pattern formation in different adults mutants have also been described and analyzed (Maderspacher and Nusslein-Volhard, 2003; Parichy et al., 2000a; Parichy et al., 2003; Rawls et al., 2001).

I.4. Patterning of the embryos

To get the expected embryonic and adult wild-type pigment cell pattern it is necessary to have the correct cell types, correct numbers of each cell type and functional patterning. The processes controlling presence of the correct cell types are mainly specification and differentiation, correct pigment cell numbers are mostly ensured by regulation of proliferation and apoptosis of pigment cells and their precursors. Patterning mechanisms are likely to include those regulating neural crest migration and cell-cell interactions. Defects in any of these mechanisms result either in loss/reduction of pigment cell numbers, increase in pigment cell numbers and/or misplacement of pigment cells.

I.4.1. Migration of trunk neural crest cells

Depending on their fate and final position in the embryo, neural crest cells have to migrate along different routes at different points in time during development to reach their final destination and generate the wild-type pattern.
In the trunk neural crest cells migrate on two major, stereotypical routes (Fig. 1.6), the lateral pathway between the ectoderm and somites (in chick the dorsolateral pathway) and the medial pathway between the myotome and neural tube (the ventromedial pathway in chick) (Halloran and Berndt, 2003; Kelsh and Raible, 2002). In contrast to fish where the neural crest cells on the medial pathway migrate between somites and notochord they migrate through the somitic mesoderm in chick (Loring and Erickson, 1987). This apparent difference in migration might be caused by the different types of sclerotome mostly present resulting in a different physiology of chick and zebrafish somites (Morin-Kensicki and Eisen, 1997). Only a very small portion of the zebrafish somite, compared to the one in chick, is sclerotome. Both pathways are only populated by specific neural crest derivatives and its precursors. Cell migrating on the ventromedial pathway give rise to melanophores, iridophores, neurons and glia of the Dorsal Root Ganglia and sympathetic ganglia while cells migrating on the dorsolateral

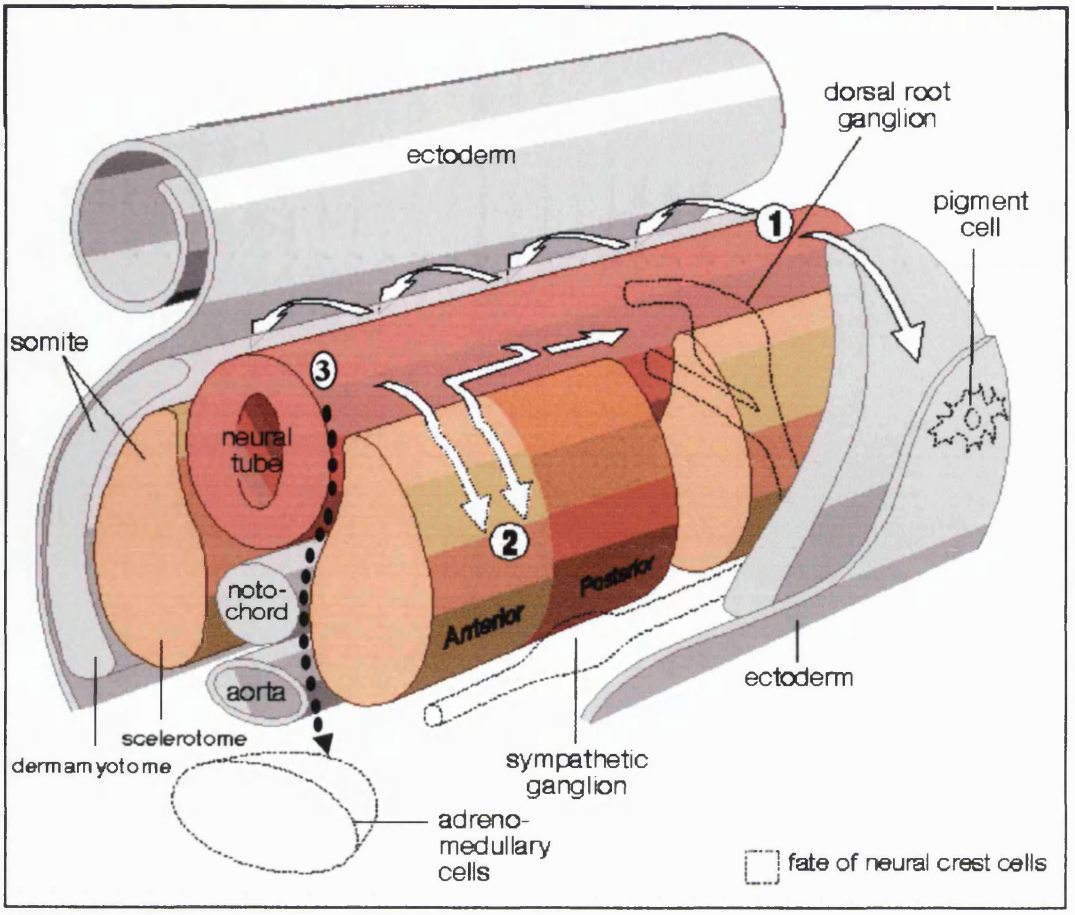

Fig.1.6: Schematic presentation of trunk neural crest migration
In chick melanophores can be seen migrating on the lateral pathway (1) whilst all other derivatives use the ventromedial pathway (2) migrating through the anterior half of the somite. In zebrafish melanophores and xanthophores migrate on the lateral pathway (1). Cells migrating on the medial pathway (3) between somites and neural tube include melanophores and iridophores.
(adapted from Wolpert et al., Principles in Development, 2006)

pathway give rise to melanophores and xanthophores only. In contrast to, for example chick, where pigment cell –melanocyte- precursors only migrate on the dorsolateral pathway, in zebrafish melanoblasts and melanophores migrate on both the lateral and medial pathway. Migration on each pathway however is only shared with one additional pigment cell type. The medial pathway is also populated by iridophores, whereas xanthophores migrate only on the lateral pathway (reviewed in (Kelsh, 2004)).

I.4.2. Pathway choice of neural crest cells

But how do neural crest cells know which pathway to choose? Both cell-cell and cell-extracellular matrix interactions have been implied in this process. Multiple attractive and inhibitory molecules have been implicated in promoting and preventing migration and regulating on which pathway the neural crest cells migrate. In fish as well as chick it has been shown that migration on the (ventro-) medial pathway precedes that on the (dorso-) lateral pathway (Erickson et al., 1992; Raible et al., 1992). The delay of population of the lateral compared to the medial pathway in zebrafish is about 5-6 hours (and about 24 h in chick). Time lapse studies of early zebrafish neural crest cells at early stages (10-12 Somites) have shown that crest cells try to extend their protrusions down both the medial and the lateral pathway (Jesuthasan, 1996). These protrusions retract as soon as they contact the medial and lateral surface of the somite. However, at around the 14 Somite stage protrusions only retract if they contact the lateral surface but not if they contact the medial surface. The author suggests that this is caused by inhibitory clues transiently present on both surfaces at early stages (10-12 Somites) but later only present on the lateral, but not medial surface of the somites. Also, the cells leaving the neural tube later might possess different properties than the early emigrating cells allowing them to migrate laterally (Erickson and Goins, 1995). Further evidence that factors on the somite surface of wild-type embryos cause the crest cell to retract their protrusions came from studies of crest cell behaviour in *spadetail* mutants. The loss of somites, and therefore all inhibitory factors potentially expressed on the outer somite surface, in *spadetail* mutants allows crest cells to populate the lateral pathway precociously.

The suggestion that inhibitory factors located on the somites could be involved in delaying the entry of neural crest cells onto the lateral pathway is corroborated by

findings from chick. Such molecules that inhibit migration have been named 'barrier molecules' (Oakley and Tosney, 1991). One of these molecules, acting as a marker for tissues that inhibit neural crest cell migration is peanut agglutinin (PNA)-binding factor. It is transiently expressed along the dorsolateral pathway, specifically the entire posterior half of each somite and the ventral part of the anterior half of each somite. In chick inability of cells to enter the dorsolateral pathway has been shown to correlate with expression of PNA-binding factor and another similarly expressed inhibitory factor, chondroitin-6-sulfate (C6S)(Oakley et al., 1994). At early stages when crest cells can only migrate down the ventromedial pathway both factors are expressed within the dorsolateral path. The decrease of the expression of PNA-binding factors and C6S coincides with the beginning of migration on the dorsolateral pathway. Premature loss of both factors by surgical removal of the dermamyotome allowed precocious migration on the dorsolateral pathway. Similar observations have been made in the Silkie fowl, a naturally occurring chick mutant, at slightly later stages (stage 28) of development (Faraco et al., 2001). Whereas in Lightbrown Leghorn embryos, with wild-type neural crest distribution, PNA-binding molecule is expressed in 2 anterior-to posterior bands – one dorsally to ventrally stretching from the neural tube to the top of the myotome and the other covering the whole myotome and perinotochordal mesenchyme- this expression is absent in the Silkie fowl. This loss of PNA-binding molecule expression in the Silkie fowl seems to lead to migration of melanoblasts along pathways not populated by neural crest cells in Lightbrown Leghorn embryos where PNA binding molecule is expressed. This apparent loss of a barrier molecule leads to melanoblasts still migrating on the ventral pathway when migration in Lightbrown Leghorn embryos has ceased; in addition, melanoblasts migrated into the somatic mesoderm and into additional ectopic locations. No direct proof for a connection between inhibition of neural crest cell migration and PNA-binding factors and C6S has been shown yet though and decrease in expression and start of migration could be coincidental. Even though there is evidence that PNA-binding factors and C6S are important factors in blocking migration neither the loss of both factors nor the physical space made by surgical removal of dermamyotome are sufficient to rescue the delay of migration completely (Oakley et al., 1994). This strongly implies that as well as the possible inhibitory factors, additional factors and mechanisms play a role in timing of migration onset. In accordance with that it has been shown that stimulating long-distance cues from the dermis might be involved in actively promoting migration (Tosney, 2004).

Transplantation of quail dermis grafts to the distal dorsal path of younger chick embryos (stage 16-17) resulted in precocious migration of melanoblasts on the dorsal path. Moreover the author showed that the degree of stimulation of neural crest migration depended on the size of the graft; the larger the graft the higher was the stimulation. Only melanoblasts seemed to respond to the stimulating signal, further suggesting that different neural crest cells might have specific properties. Additional evidence for the existence for factors specific to melanoblasts and promoting their migration on the dorsolateral pathway comes from earlier studies. Cultured quail melanoblasts when transplanted into younger chick embryos can populate the dorsolateral pathway preciously whereas other, earlier crest cell types cannot (Erickson and Goins, 1995). One factor involved in giving early and late migrating neural crest cells different properties is *Eph-B*. *ephrin-B* ligand is expressed in the dorsolateral pathway and when early neural crest cells migrate medially it blocks their entry into the dorsolateral pathway (Santiago and Erickson, 2002). However, whilst the *ephrin-B* ligands expressed by the dermomyotome prevent the migration of early neural crest cells they promote the migration of the late migrating crest cells, the melanoblasts. Blockage of the *ephrin-B/EphB* signalling by addition of soluble ligand leads to melanoblasts no longer going down the dorsolateral pathway (Santiago and Erickson, 2002). Why the melanoblasts give a different response to the *ephrin-B* expression is not known. These observations suggests that *Eph-B* might be one factor specifically helping to promote melanoblasts migration on the dorsolateral pathway. In addition, the authors showed that *Eph-B* receptors are positively promoting melanoblast migration along the dorsolateral pathway by promoting interaction of melanoblasts with the ECM fibronectin. Another receptor/ligand pair that has recently been suggested to be involved in pathway choice are *Robo* and *Slit* (Jia et al., 2005). All three *Robo* receptors are expressed in cultures of early and late stage neural crest cells. While *Robo3* expression seems identical in both groups that of *Robo1* is lightly and that of *Robo2* strongly reduced in cultures of late stages neural crest cells. Both ligands *Slit1* and *Slit2* are expressed in the dermamyotome close to the neural crest cell migratory pathway. *In vitro* assays showed that *Slit2* repels neural crest cells in what seemed to be a contact dependent manner. Further expression of a dominant-negative *Robo1* receptor allows a fraction of early stage neural crest cells to migrate dorsolaterally. The authors suggest that early high concentrations of *Slit2* in the dermamyotome repel the early crest cells and they then migrate in the medial pathway. However, Jia and colleagues (2005)

postulate that at later stages the reduced expression of *Slit2* in the somite and the *Robo* receptors in melanoblasts might promote their migration along the dorsolateral pathway. It has been suggested that *Slits* might be the long distance attractant molecule described by Toseney et al. (2004)(Harris and Erickson, 2007). These findings suggest that early and late stage migrating neural crest cells have different properties and probably in combination with changes in the properties of the pathways, direct cells into their respective migration routes. It seems that early migrating cells choose the medial pathway as they cannot migrate ventrally due their response to signals (*Eph*) or too high levels of expression of receptors (*Robo*) specific to factors expressed dorsolaterally (Harris and Erickson, 2007; Jia et al., 2005; Santiago and Erickson, 2002).

Evidence that the ventral path has similarly population specific attractive signals to the dorsal pathway has not been presented yet. It has been originally widely assumed that distance of migration in the ventromedial pathway is based on the distance the cells can travel before the somites matures (Weston and Butler, 1966). There are indications that the receptor CXCR4 and its ligand stromal cell-derived factor-1 (SDF-1) are possibly involved in instructive guidance of DRGs in mouse (Belmadani et al., 2005). CXCR4 is expressed by the sensory neural crest cells while SDF-1 is expressed along the normal pathway of DRGs. *In vitro* studies showed that in culture SDF-1 attracts CXCR4 expressing neural crest cells. Knockout of CXCR4 in mice leads to small DRGs possibly caused by many sensory crest cells not reaching the DRG (Belmadani et al., 2005). However, as knockout of CXCR4 does not lead to complete disruption of DRG formation it is probable that additional factors are involved in guidance of the sensory neurons. Further studies would be likely to reveal additional factors specific to this and other sub-populations of ventrally migrating cells and regulating their migratory properties.

I.4.3. Guidance of neural crest cells along a pathway

Once migration has begun, crest cells that entered the dorsolateral pathway travel in an unsegmented uniform fashion. However, crest cells migrating on the ventromedial pathway travel in a segmented fashion. In chick and mouse, crest cells can only occupy the rostral, but not caudal, half of each somite (Halloran and Berndt, 2003) while in zebrafish they migrate more medially (Morin-Kensicki and Eisen, 1997). That this is most likely to be caused by cues in the somitic mesoderm and not information given to the cells at the level of the neural tube has been shown by migrosurgical manipulations

(Keynes and Stern, 1988). Rotation of the neural tube by 180° did not result in any changes of neural crest migration pathways and neural crest cells were still found in the rostral half of each somite. However, when rotating the segmental plate by 180° and therefore inverting the rostral-caudal polarity of the developing somites neural crest cells migrated in the caudal half of the somite. Further studies in rodents and chick have implied a role for a variety of different factors contributing to the restriction of neural crest cells to the rostral half of the embryo. It is at least partially mediated by repulsive interaction of *Ephrin* ligands expressed in the posterior half of the somite and the corresponding Eph receptors are expressed in the neural crest cells. In rodents *Ephrin-B2* is expressed in the posteriorr somite and the neural crest cells express *EphB2* whereas in chick *Ephrin-B1* is located in the somites and the matching receptor in the neural crest cells is *EphB3* (Krull et al., 1997; Wang and Anderson, 1997). But single loss of function mutants of *Ephrin-B2* or double loss of function mutants of *EphB2* and *EphB3* display normal neural crest migration suggesting that there are functionally redundant migration cues involved in guidance of the neural crest population to the anterior half of the somite (Wang and Anderson, 1997). Other factors only expressed in the caudal half of the somites and therefore good candidates to be involved in guidance of neural crest migration include the extracellular matrix molecules F-spondin and Collagen IX (Krull, 2001). For example, disruption of F-spondin function in *in vitro* trunk explants allowed cells to populate the caudal half. Interestingly, PNA-binding molecules have been shown to be involved in guidance of neural crest migration as well. *In vitro* timelapse studies of neural crest cell migration in chick somite transplants that had been treated with PNA-binding molecule revealed a slowed rate and a changed pattern of cell migration (Krull et al., 1995). With PNA present in the whole somite, rather than as in untreated embryos the caudal half only, crest cells could be seen migrating in both halves.

In summary, the mechanisms determining pathway choice and migration along a pathway are highly complex and still incompletely understood. It is very clear however, that a host of different factors regulates these processes. As discussed above some molecules involved in guiding crest cells, opening pathways and timing of migration are known, but very little is known about factors and mechanisms necessary to stop neural crest migration.

I.5. Specification of trunk neural crest cells

I.5.1. Timing of neural crest specification

To ensure correct pattern formation it is not only important that cells migrate to the right position, but also that the correct fates are present. The establishment of such a large number of derivatives from one cell population implies a necessity for a tightly regulated schedule. Different scenarios as to when neural crest cells first become specified to specific pigment cell or other individual fates can be imagined. The two most extreme models for timing of neural crest specification would be 1) that premigratory cells are already specified before leaving the neural tube, or 2) that cells only get specified when they reach their final destination later in development. There is increasing evidence from both cell labelling and expression studies that neural crest cells at least have a strong bias towards a certain fate when they start migration indicating that specification occurs early in neural crest development.

If all crest cells were specified to a certain fate before starting migration clones of these cells should only give rise to progeny of one type of derivative. However, in zebrafish as well as in chick and mouse some crest cells that had already left the neural tube were able to give rise to clones with multiple derivatives suggesting that they are at least multipotent and arguing against a very early complete specification (Baroffio et al., 1991; Baroffio et al., 1988; Bronner-Fraser and Fraser, 1989; Bronner-Fraser and Fraser, 1988; Fraser and Bronner-Fraser, 1991; Raible and Eisen, 1994b; Stemple and Anderson, 1992). Whilst some of these cells seem to be able to only give rise to two different derivatives others can give rise to multiple different ones. Labelling of already migrating cells in chick also indicated that these cells might still be multipotent with half of the labelled crest cells contributing to multiple neural crest cell derivatives such as the dorsal root ganglion, sympathetic ganglia and cells at the adrenomedullary site (Fraser and Bronner-Fraser, 1991).

It is possible that neural crest cells giving rise to different derivatives are specified at different times. Experiments of Weston and Henion (1997), in which random crest cells from explanted quail neural tubes were labelled at different time points and their development followed when cultured with non-labelled cells, suggested that about 45% of precursors in the initial population were fate-restricted. By about 30 hours after initial emigration of cells, almost 87% were fate-restricted precursors. Similarly, single cell

labelling studies in zebrafish showed that about 80% of all clones on the medial pathway give rise to only a single derivative, suggesting that they are cell type restricted (Raible and Eisen, 1994a). Most clones giving rise to more than one derivative segregated into type-restricted precursors after the first (giving rise to 2 derivatives) or the second division (giving rise to 3 derivatives) (Raible and Eisen, 1994a).

There are strong indications that different derivatives are specified at different points during development as early and late migrating neural crest populations seem to have different properties. The early pre-migratory, emigrating and migratory crest cells in the medial pathway in chick have been shown to be able to give rise to a variety of different derivatives. However, Reedy et al. (1998) found that cultures of crest cells emigrating from the neural tube in the first 6 hours or those migrating on the ventral pathway would never contain melanocytes, even if the conditions were permissive for melanocyte development. This led to the conclusion that early migrating crest cells had a strong bias against becoming melanocytes. The opposite was true for late migrating cells. All Human Natural Killer-1 (HNK-1) positive cells (and therefore neural crest cells) migrating on the dorsolateral pathway in chick have been shown to express the melanogenic antigens Smyth line serum (SL) and MEBL-1 (Kitamura et al., 1992; Reedy et al., 1998a). Importantly these cells express SL even before they start migrating suggesting that they were strongly biased towards melanocyte fate even before migration. These observations were confirmed by Henion and Weston (1997) who also showed that appearance of melanogenic precursors was significantly delayed to that of neurogenic precursors. In zebrafish, as in chick, markers specific for melanocyte fate including *microphthalmia-associated transcription factor a* (*mitfa*), *dopachrome tautomerase* (*dct*) and *c-kit* are thought to be specific for the melanophore lineage has been shown before or at early stages of migration (Kelsh et al., 2000; Lister et al., 1999; Parichy et al., 1999). Some of the cells migrating on the medial pathway even started exhibiting pigment granules shortly after entering the pathway and then migrated into the ventral stripe demonstrates that they were not only fate-restricted but specified (Raible and Eisen, 1994a).

These observations argue against neural crest cells only being specified once they have reached their final destinations. At the same time the other extreme model -all cells being specified before they leave neural tube- does not seem to describe the timing of specification correctly either. Rather it appears that specification of the different

derivatives is asynchronous and happens at different times depending on fate and pathway.

1.5.2. Mechanism of neural crest fate specification

Originally two different models of how neural crest cells become specified have been considered. 1) progressive fate restriction and 2) direct fate restriction (Kelsh and Raible, 2002). During progressive fate restriction a pluripotent neural crest cell generates in turn cells restricted to a limited set of fates and then precursors restricted to one fate. In contrast, the direct fate restriction model proposes that postmigratory crest cells get directly specified depending on environmental cues at their final location. Even though there is evidence for both models, recent evidence favours the progressive fate restriction models. It is, however, likely that both models apply to neural crest development (reviewed in (Kelsh and Raible, 2002)).

As described above the exact timing of specification of neural crest derivatives is not (always) clear. However, cell labelling studies in zebrafish suggest that most pigment cells become specified early in or prior to the start of migration (Raible and Eisen, 1994a). Expression of melanin early on during migration as well as expression of pigment cell specific markers such as *mitfa* in melanoblasts and *GTP cyclohydrolase* 1 (*gch*) in xanthoblasts at the onset of migration argues for progressive fate restriction (Lister et al., 1999; Parichy et al., 2000a). Even though some of the expression at these early stages is overlapping between two different pigment cell types these are assumed to be restricted to the pigment cell fate (Pelletier et al., 2001). Analysis of the pigmentation mutant *colourless* suggested that ectomesenchymal fates were specified prior to start of migration and that there is a distinct population of cell giving rise to ectomesenchymal fates while another gives rise to non-ectomesenchymal fates only (Dutton et al., 2001; Schilling and Kimmel, 1994). In chick as well as zebrafish it has been shown that melanoblasts are always a population of late migrating cells, consistent with a restriction in fate prior to migration (Erickson and Goins, 1995; Henion and Weston, 1997; Reedy et al., 1998b).

Evidence of pluripotent precursors also supports the progressive fate restriction model. Isolation and culture of quail crest cells showed that very few cells were able to give rise to a large number of derivatives (neurons, glia, cartilage and pigment cells) while other crest cells under the same culture conditions were only able to give rise to one or two of these original derivatives (Baroffio et al., 1991). Recent quail *in vitro* studies in

which the fate of a differentiated glia could be reversed to a melanocyte, and vice versa, in the presence of *endothelin 3* support the existence of such restricted progenitors as this fate change produces a temporary, intermediate glial-melanogcytic precursor (Dupin et al., 2000; Dupin et al., 2003).

But there is also some evidence supporting the direct fate restriction model. Here self-renewing neural crest stem cells are instructively promoted by environmental signals to adopt a certain fate. Evidence for the existence of self-renewing neural crest stem cells comes from rat cell culture studies (Stemple and Anderson, 1992). Whilst in standard culture medium these clones gave rise to neurons and non-neuronal cells, the presence of Bone Morphogenic Protein 2 (BMP2) in the culture medium resulted in a strong bias to cultures containing neurons only (Shah et al., 1996). Consistent with a requirement of BMP2 for specification of unspecified crest cells into autonomic neurons, BMP2 is expressed and signals from the dorsal aorta close to the site of sympathetic neurons (Shah et al., 1996). Similarly, the presence of Transforming Growth factor β1 (TGFβ1) promotes smooth muscle differentiation and glial growth factor/neuregulin glia fate in expense of neuronal fate (Shah et al., 1996; Stemple and Anderson, 1992).

It thus seems possible that both direct and progressive fate restriction occur during neural crest development with a series of restrictive divisions occurring at early stages of development. At early stages of migration some neural crest cells might therefore only be able to give rise to a limited number of derivatives. Thus a certain degree of fate specification might occur early in development whilst final commitment to a fate may occur depending on environmental cues.

The observation of precursors restricted to particular sets of fates in cell culture and cell labelling studies might support a model proposed on the basis mainly of phenotypic observations of pigment cell properties in different amphibian species (see below).

1.5.3. The chromatoblast hypothesis

Occasionally, pigment cells displaying organelles of more than one pigment cell type have been observed, especially in amphibians. Likewise, some of the chromatophores in the kidney and liver of *P. danicolor* contain melanosomes, reflecting platelets and pterinosomes (Bagnara et al., 1979). Not only have single pigment cells containing the different organelles been observed, but also examples of two different types of pigment organelles contained in one single surrounding membrane have been seen. Melanosomes and reflective platelets are both within one limiting membrane in

chromatophores of *Dasyatis sabina* and some of the reflective platelets in the iris of a dove seem partially melanized.

Bagnara proposed that all three pigment cell types -melanophores, xanthophores and iridophores- contain a common primordial organelle that can give rise to all three pigment cell organelles (Bagnara et al., 1979). Bagnara and colleagues (1979) hypothesized that the final decision as to what fate a chromatophore adopts is not made at the neural crest stage and that all three pigment organelles, melanosomes, reflecting platelets and pterinosomes, are derived from the endoplasmatic reticulum (ER). A requirement for their model is that it is not irrevocably differentiated pigment cells/pigment cell precursors that are migrating but undifferentiated precursors that are free to adopt a specific fate according to the environment of their final position. In their model an ER derived primordial organelle fuses with another vesicle, containing necessary information/ingredients for the genesis of one specific pigment cell type organelle, and thereby receiving the information necessary to become a specific pigment cell organelle. Fusion of the primordial organelle containing information for different pigment cell types with more than one vesicle would then result in cells of mixed fate. Some evidence supporting this model indicates that all three pigment cell types are (at least partly) derived form ER derived vesicles.

Cell labelling studies in zebrafish could so far not show a precursor cell for all three pigment cell fates. However fate-restricted precursors giving rise to two pigment cell types -a melanized and unmelanized pigment cell type have been shown for both migratory pathways (Dutton et al., 2001; Raible and Eisen, 1994a). And at early stages during zebrafish neural crest development expression patterns of some pigment cell markers supports the idea of a common precursor. Thus the melanoblast marker *mitfa* and the xanthoblast marker *gch* are co-expressed until 30 hpf (Pelletier et al., 2001). Also *endothelin receptor B* (*ednrb1*), which from 48 hpf labels iridophores, is co-expressed in many cells with the melanophore markers *kit* and *mitfa* or the xanthophore markers *xanthene dehydrogenase* (*xdh*) and *fms* (Parichy et al., 2000a). If all pigment cells are derived from a common precursor, both cell intrinsic and environmental factors are likely to be responsible for commitment to a single fate.

I.6. Transdifferentiation

To ensure correct pigment pattern formation it is important that the correct number of pigment cells is present. A way in which a possibly already correctly formed pigment pattern can be disturbed is the presence of supernumerary chromatophores. Correct organ size is mostly regulated by limiting proliferation or apoptosis of supernumerary cells or both. When regulated through proliferation, cell number and with that organ size is limited by cells exiting the cell cycle once the correct number is achieved. The cells that have exited the cell cycle then differentiate into a specific cell type. If cells do not exit the cell cycle at the appropriate time during development, supernumerary cells are produced and cause tumours. Defects in the regulation of cell numbers can not only lead to patterning defects but also cancers.

Supernumerary chromatophores can on the one hand side arise through a defect in cell number regulation of chromatophores themselves, but on the other hand also through transdifferentiation of one chromatophore type into another or another cell type into chromatophores. Transdifferentiation has been defined as the process in which a differentiated cell type switches its fate into another differentiated cell type (Tosh and Slack, 2002). This switch is reversible and can include cell division.

Multiple studies have shown that cells of one pigment type can transdifferentiate into another. Thus Ide and colleagues generate functional melanophores by transdifferentiation from either xanthophores or iridophores from amphibian cell cultures (Ide, 1978; Ide and Hama, 1976). Further evidence comes from Thibaudeau and Holder (1998) who have monitored cells displaying xanthophore characteristics transdifferentiating into cells with melanophore characteristics in axolotl cell culture.

But non-pigment neural crest derivatives seem also to be capable of transdifferentiating into pigment cells. Interestingly, *endothelin 3* mediated transdifferentiation of quail Schwann cells into melanocytes and vive versa under cell culture conditions involves an intermediate step in which the cells possess properties of both glia and melanoblasts/melanocytes (Dupin et al., 2000; Dupin et al., 2003). Schwann cells can also transdifferentiate into melanocytes in the presence of bFGF or 12-*O*-tetradecanoyl phorbol-13-acetate (Sherman et al., 1993; Stocker et al., 1991). Although these studies indicate that *in vitro* cells of one neural crest derivative can transdifferentiate into another, no mutant or other example clearly showing this mechanism *in vivo* has been identified to date.

I.7. Genes involved in pigment cell development and patterning and corresponding mutants

Multiple genes have been shown to be important in neural crest and specifically pigment cell development. As the development from neural crest cell to a specific pigment cell fate (such as melanophore) is a lengthy process including multiple steps it is not surprising that various mutants showing defects in one of the steps necessary have been isolated. Identification of pigment mutants is relatively easy as differences in pigmentation are straightforward to detect. Pigment mutants in a variety of model organisms including zebrafish and mouse are known. A large number of zebrafish mutants with defects in melanophore development show very similar phenotypes to mammals. Differences in phenotypes could possibly be the result of presence of two copies of the gene in zebrafish as it is the case for *mitf* and *kit* (Lister et al., 2001; Mellgren and Johnson, 2004; Mellgren and Johnson, 2005). But as zebrafish have additional pigment cell types in comparison to mammals that only have melanocytes some zebrafish pigment mutants are expected to have at least partially different phenotypes. Most importantly as mentioned already possible differences in mechanisms in pigment pattern formation in mammals and fish are thought to cause these phenotypic differences (reviewed in (Kelsh, 2004)).

Here I will introduce only those pigment mutants that have a direct relevance to my work.

I.7.1. SRY-box containing gene 10 (sox 10)

sox10, a member of the Sry-related HMG box (Sox) family of transcription factors, has been implicated in neural crest formation, maintenance of neural crest stem cell multipotency and specification and differentiation of neural crest derivatives. In humans, heterozygous loss of *sox10* function leads to Waardenburg-Shah Syndrome (OMIM 277580), a neurocristopathy, which is associated with a severe reduction of enteric neurons along a variable stretch of gut, deafness and hypopigmentation of the skin (Kelsh, 2006 and references therein).

Study of *sox10* mutants in model vertebrates shows that loss of *sox10* results in severe defects of neural crest development. The phenotype of loss of *sox10* has many shared phenotypes between the different organisms studied. In zebrafish 5 different *sox10* alleles have been isolated (Kelsh et al., 1996; Malicki et al., 1996). The *sox10* mutant,

colourless, shows an almost complete loss of all neural crest derived pigment cells (some alleles have been shown to still have some iridophores) also lacks or shows strong reduction in all other non-ectomesenchymal neural crest fates (glia and enteric, sympathetic and sensory neuron fates)(Dutton et al., 2001). A mouse mutant allele is named *Dominant megacolon* (*Dom*) (Lane and Liu, 1984). *Dom* mutants have a megacolon, caused by strong reduction of myenteric ganglion cells in the colon, hypopigmentation of the skin and iris and other defects (Aoki et al., 2003; Herbarth et al., 1998; Lane and Liu, 1984; Southard-Smith et al., 1998). Homozygous mutants have much stronger defects resulting in lethality prior to 13 days of gestation (Herbarth et al., 1998; Lane and Liu, 1984). In both mouse and zebrafish *sox10* is required to drive expression of transcription factors such as *microphthalmia-associated transcription factor* (*mitfa* in zebrafish), *mammalian achaete-scute homolog 1* and *paired-like homeobox 2b* that are required for specification of melanophores, sympathetic neurons and enteric neurons respectively (Hou et al., 2006; Kelsh, 2006). The loss of *sox10* in zebrafish also results in impairment of migration, followed by cell death of most non-ectomesenchymal crest derivatives (Dutton et al., 2001).

In addition to sharing similar mutant phenotypes, zebrafish and mouse show similar, but highly dynamic *sox10* expression. *sox10* expression, using *in situ* hybridisation, has been observed in trunk and cranial premigratory as well as migrating crest cells in the trunk (Dutton et al., 2001). Cells expressing *sox10* give rise to all non-ectomesenchymal crest derivatives. *sox10* expression however is not purely limited to neural crest derivatives and can for example also be found in the otic epithelium in zebrafish. In all tissues except glia, *sox10* expression seems to be lost during differentiation to a specific fate (Dutton et al., 2001). Even though large parts of the expression pattern in mouse and zebrafish are similar, some differences can be found. The most interesting in the view of pigment development is that in contrast to zebrafish where *sox10* expression is down-regulated when pigment cell precursors start migrating along the pathway, studies in mouse have shown indicate that *Sox10* remains present during melanoblast migration (Dutton et al., 2001; Elworthy et al., 2003; Southard-Smith et al., 1998). In accordance with this, recent mouse primary neural tube explant culture studies indicate that *Sox10* may be necessary for later steps in melanocyte differentiation (Hou et al., 2006).

I.7.2. microphthalmia-associated transcription factor (mitf)

Not surprisingly as *mitf* is genetically downstream of *sox10, mitf* mutants share some phenotypic features with *sox10* mutants, the most obvious in zebrafish and mouse being the complete loss of neural-crest derived melanophores (Hodgkinson et al., 1993; Lister et al., 1999). In addition mouse *microphthalmia* mutants (*mi*) might display one or more of the following: deafness, small eyes, reduced number of mast cells and failure of secondary bone resorption (Hodgkinson et al., 1993). In humans mutations in the basic helix–loop–helix leucine zipper transcription factor MITF are associated with Albinism (OMIM 103470), Tietz syndrome (OMIM 103500) and Waardenburg syndrome (OMIM 193500/13501) and phenotypes are therefore again, like with *sox10,* similar to those in mice. In addition to lacking all melanophores the zebrafish *mitfa* mutant *nacre* shows a slight reduction in xanthophore numbers and an about 40% increase in iridophores at 3 dpf (Lister et al., 1999). Whilst a large number of these supernumerary iridophores can be found in the stripes some are located in ectopic positions mainly in the fins. Positioning of xanthophores seems wild-type. Loss of function and overexpression studies in zebrafish suggest that the activation of *mitfa* is necessary and sufficient for specification of melanocytes (Dorsky et al., 2000; Lister et al., 1999). This is different to mousse cell culture where Mitf does not seem to be sufficient to switch on all genes necessary for melanocyte development (Hou et al., 2006). Downstream targets of *mitf* in melanophore development include *dct*, *tyrosinase* (*tyr*) and *kit oncogene* (*c-kit*) (Hou et al., 2006; Kelsh, 2006).

Zebrafish *nacre* mutants have not only an embryonic but also an adult phenotype. Like in embryos, no melanophores are present, but in contrast to embryos a defect in distribution of xanthophores can be seen. Whilst some xanthophores in *nacre* mutant adults are ordered in a stripe like fashion along the horizontal myoseptum many are found in clusters. Xanthophore distribution in *nacre* adult mutants in the absence of melanophores suggests that cell-cell interactions between both are necessary to establish the correct adult pattern (Maderspacher and Nusslein-Volhard, 2003). Transplantation experiments have underlined this suggestion by showing that wild-type melanophores are necessary and sufficient to re-establish correct xanthophore stripe formation in *nacre*.

I.7.3. c-kit

c-kit the product of the gene at the *Dominant spotting* (*W*) loci in mouse has been suggested to play a role in proliferation and survival of melanoblasts (Yoshida et al., 1996). *W* mice lack all coat pigmentation and, in addition, defects in germ cell and haematopoietic precursor cell development have been observed (Geissler et al., 1988). *c -kit* is a receptor tyrosine kinase and mutations in its ligand *steel factor* have also been isolated. *Steel* (*Sl*) mice display the same phenotype (Morrison-Graham and Takahashi, 1993). Depending on the alleles the strength of the phenotype of both *W* and *Sl* mutant mice can vary. Mouse mutant studies suggest that c-kit is involved in proliferation and survival of melanoblasts (Yoshida et al., 1996).

In zebrafish a *c-kit* related gene has found to be mutated in the *sparse* mutant (Parichy et al., 1999). Unlike in mouse the isolated *c-kit* gene only affects pigment cell development. But like in mouse *c-kit* is involved in proliferation and survival of melanoblasts. Initially, normal numbers of melanoblasts are seen at early stages in development as shown by *dct* expression at 24 hpf; melanoblast numbers then declined and were visibly reduced at 36 hpf (Kelsh et al., 2000). Reduction in melanin positive cells can be seen as early as 48 hpf and by 11 days post fertilization (dpf) virtually all melanophores have disappeared (Parichy et al., 1999). Observation of melanin-positive cells during development showed that in *sparse* mutants dispersal of melanophores is defective. Even though fewer melanophores are present a greater proportion of them can be found dorsally, close to the neural tube than in wild-type siblings as kit promotes the migration of cells of the melanophore lineage. This shows that *c-kit* is involved in a multitude of mechanisms involved in proper pigment pattern formation.

I.7.4. fms

A gene that has been shown to be required for adult and embryonic xanthophore development is *c-fms* (Parichy et al., 2000b). The zebrafish *c-fms* mutants, *panther*, lack embryonic and adult xanthophores and adult stripes are formed poorly anteriorly and not formed at all posteriorly. During embryonic development *fms* is expressed in xanthophores and seems to be responsible for xanthophore migration in a fashion similar to the function of *kit* in melanophore dispersal. Loss of *fms* during adult pattern formation did not result in an impairment of overall melanophore motility. Instead loss of the wild-type pigment pattern is caused by an increased number of melanophores

dying during early adult pattern formation. The pattern of cell death also differs from wild-types in that melanophore death is non-selective whereas in wild-types mostly those in the prospective interstripe between the first two melanophore stripes die. Parichy and colleague (2000b) have proposed that this effect is caused by loss of *fms* dependent xanthophores. In addition the number of late kit-independent melanophores that are differentiating is significantly reduced.

Just as in *nacre* mutants where introduction of wild-type melanophores can rescue the stripe formation, transplantation of wild-type xanthophores into *panther* mutants can locally rescue the mutant phenotype (Maderspacher and Nusslein-Volhard, 2003). This again supports the suggestion that cell-cell interactions between melanophore and xanthophores are necessary to establish the adult stripes.

I.7.5. obelix and leopard

Two other zebrafish adult pigment pattern mutants indicating that xanthophore-melanophore interactions are necessary in adult stripe formation are *obelix* and *leopard* (Maderspacher and Nusslein-Volhard, 2003). Both mutants show only adult pigment pattern defects. It has recently been shown that the leopard phenotype is caused by a mutation in the *connexin41.8* gene (Watanabe et al., 2006). Whilst the gene mutated in *obelix* has not been isolated yet, both phenotypes and possible gene functions have been described (Maderspacher and Nusslein-Volhard, 2003). *leopard* mutants have about 50% reduction of fin and stripe-associated melanophores in the adult (Johnson et al., 1995). In wild-type adults *leopard* has been suggested to be responsible for controlling the boundary shape of the pigment stripes by regulating both homotypic and heterotypic interactions between melanophores and xanthophores (Maderspacher and Nusslein-Volhard, 2003). Loss of these interactions then results in loss of the pigment stripes and the remaining pigment cell types are grouped in spots.

Homozygous as well as heterozygous *obelix* mutants display fewer stripes than wild-type adults. Whilst heterozygous *obelix* carriers show loosely arranged wider but fewer stripes with interruptions, homozygous carriers have in addition xanthophores intermingled into the remaining melanophore stripes (Maderspacher and Nusslein-Volhard, 2003). In contrast to *leopard*, *obelix* is only required in melanophores where it is necessary to control melanophore aggregation and the boundary integrity of the stripes.

I.7.6. endothelin receptor 1b (ednrb1)

rose mutants only show an adult phenotype. Even though *rose* mutants lack most iridophores and only have a reduced number of melanophores as adults the remaining melanophores still form stripes suggesting that iridophores are not necessary for adult stripe formation (Johnson et al., 1995; Parichy et al., 2000a). The mutation in *ednrb1* results in strong reduction of melanophore and iridophore numbers in adult zebrafish. *ednrb1* is expressed in all three pigment cell types during early embryonic development before it becomes restricted to iridophores at 48 hpf. Despite this prominent embryonic expression, the *rose*$^{-/-}$ embryonic pigment pattern is wild-type. During metamorphosis *ednrb1* is expressed by lightly melanized cells as well as in cells located at the position of the developing first iridophore stripe. Despite the strong reduction of iridophore numbers and even although melanophore numbers are reduced by half in *rose* mutants adults the remaining melanophores in the dorsal trunk can form normal stripes, while those more ventrally form spots. These findings support the notion that iridophores are not required for adult stripe formation (Johnson et al., 1995; Parichy et al., 2000a).
The mouse *Ednrb* mutant *piebald lethal* (*s*) is associated with Hirschsprung's disease (OMIM 142623) (McCallion and Chakravarti, 2001; Pavan and Tilghman, 1994). *piebald lethal* mice have (with the exception of occasional spots in trunk and head) no pigmentation and die from megacolon (Hosoda et al., 1994). In mouse the initial phase of melanocyte specification and start of migration is *Ednrb* independent and a role for *Ednrb* strictly only in the final steps of melanoblast migration has been shown (Lee et al., 2003).

I.7.7. *anaplastic lympohoma kinase (alk)*

A mutant offering to shed light on the role of iridophores in pigment pattern formation is the zebrafish *alk* mutant, *shady* (Lopes et al., in prep.) . Depending on the strength of the allele *shady* mutants display either a complete loss (strong alleles like *ty82*) or strong reduction of iridophores (weak alleles like *ty9*, *trd*) (Kelsh et al., 1996). An occasional iridophore in the eye, dorsal or ventral stripe of the strong alleles can be found. Whereas strong alleles like *ty82* are embryonic lethal, *ty9* mutants are adult viable. Adult viable *shady* alleles that show an embryonic phenotype, like *ty9*, do not display an adult phenotype. However, some *alk* mutants showing an adult, but no

embryonic phenotype have been isolated (Lopes et al., in prep.). In contrast to embryonic mutants that show only a reduction of iridophore numbers, adult mutants show a strong reduction of trunk iridophores and melanophores. In *alk* mutants, the loss or strong reduction in embryonic iridophore numbers does not lead to differences in embryonic melanophore or xanthophore distribution indicating that iridophores are not necessary for embryonic stripe formation. The observations from *rose* and *alk* mutants taken together suggest that iridophores are not necessary for either embryonic or adult stripe formation (Johnson et al., 1995; Lopes et al., in prep.; Parichy et al., 2000a). Our studies in zebrafish strongly implied that *alk* is involved in specification.

As other organisms routinely used in the lab do not have iridophores it is maybe not surprising that roles in pigment cells have not been reported in other Alk mutants in mouse transgenics or *Drosophila* (Bazigou et al., 2007; Englund et al., 2003; Hurley et al., 2006; Jager et al., 2005; Pulford et al., 1997).

I.7.8. choker

In all pigment mutants described so far, change of the pigment pattern is due to loss of one or more pigment cell types. The first zebrafish pigment pattern mutant characterized where not loss, but location, of pigment cells is the obvious phenotype was *choker* (Svetic et al., 2007). *choker* mutants show a misplacement of melanophores resulting in a melanophore collar spanning the 5 anteriormost somites and a loss of melanophores in the lateral stripe. Transplantation studies have shown that these pigment phenotypes are a secondary consequence of abnormal somite development showing a role of underlying tissues in the pigment pattern formation mechanism (Svetic et al., 2007). Both loss of lateral stripe melanophores and ectopic melanophore collar formation correlate with changed *sdf1* expression. The *choker* mutant also provided an insight into the necessity of regulation of migration pathway closure in correct pattern formation. Loss of this mechanism on the lateral pathway leads to some cells leaving their normal DS and VS positions and populating the collar region.

I.7.9. Skin colour mutants in mouse

All mouse mutants described above have been identified based on their coat colour. Recently a new emphasis has been placed on identifying mouse mutants with changes in skin colour. Whilst some non-hairy areas of mice such as the skin of the tail and

external ears are often pigmented the paws of mice normally do not contain any pigmentation. Now mice with changed skin pigmentation in paws are being isolated and examined in order to identify additional genes required in pigmentation. That these phenotypes can unearth new genes has been suggested by characterization of *sooty foot*, a mutation that arouse during transgenesis experiments (Budd et al., 1997).

Whilst *sooty foot* mutants show an increase in pigmentation in the ventral feet and footpad in addition darkened skin in the ears and tail, no change in coat colour can be seen. Mapping placed the gene responsible for the *sooty foot* phenotype onto Chromosome 2, but no known genes involved in pigmentation are located in this area implicating that mutant for a new gene involved in pigment patterning has been found.

10 new dark skin (*Dsk*) mouse mutants have been identified, by dark skin colour, as part of a global screen for new dominant mouse mutants (Fitch et al., 2003). Mapping of the *Dsk* mutants shows that they all map to chromosomal regions previously not associated with pigmentation phenotypes (Table 1.1) confirming the idea that mouse skin mutants could help identify new players in pigment cell development and patterning. As well as darker skin in the ear and tail the *Dsk* mutants exhibited a varying amount of pigmentation of the footpads (Table 1.1). *Dsk2* and *Dsk5* were shown to be mutant for *Keratin 2e* and *Epidermal growth factor receptor* respectively and subsequent characterization indicated that the ectopic positioning of melanocytes seemed to be a secondary effect of hyperkeratosis (Fitch et al., 2003). However characterization of *Dsk1*, *Dsk7* and *Dsk10* revealed three gain-of function mutations directly affecting skin pigmentation (Van Raamsdonk et al., 2004). Instead of moving into the hair follicles some melanocytes remain in the dermis causing the ectopic pigmentation. Both *Dsk1* and *Dsk10* show an alteration in the G-protein α-subunit encoding gene *Gnaq* while *Dsk7* showed one in *Gna11*. By introducing a *Dct*-lacZ transgene into these mutants the authors could show that in both $Gnaq^{Dsk1/+}$ and $Gna11^{Dsk7/+}$ mice an increase in melanoblast numbers can be seen as early as lacZ positive melanoblasts can be seen. This suggests that an increase in pigment cell number rather than in pigment synthesis might be responsible for the ectopic pigmentation. Whilst at E12.5 an increase in melanoblasts in dermis and epidermis can be detected in both mutants, melanoblast numbers in the epidermis of wild-type embryos have caught up at stage E16.5 leaving only the pigment cell numbers in the dermis increased. Neither differences in proliferation nor apoptosis could be detected suggesting that the phenotype might be

caused by an increased number of neural crest cells differentiating into melanoblasts. As the phenotype is *Ednrb*-dependent the authors propose that the increase is caused by an

Locus	Timing[1]	phenotype[2]	footpad[3]	Gene[4] (chromosome)
Dsk1	3 days; fades	increase in dermal melanocytes; darker	continuous stripe	Gnaq (19)
Dsk2	6 weeks; darkens	increase in dermal melanocytes	spot-like accumulation	Keratin 2e (15)
Dsk3	2 weeks; darkens	melanin accumulation in non-hairy regions	spot-like accumulation	- (7)
Dsk4	2 weeks; darkens	melanin accumulation in non-hairy regions	spot-like accumulation	- (4)
Dsk5	8-12 weeks;	increase in dermal melanocytes	spot-like accumulation	Egfr (11)
Dsk6	3 weeks; fades	melanin accumulation in non-hairy regions	spot-like accumulation	- (3)
Dsk7	3 days; fades	increase in dermal melanocytes; darker	continuous stripe	Gna11 (10)
Dsk8	3 weeks; darkens	melanin accumulation in non-hairy regions	spot-like accumulation	- (3)
Dsk9	3 weeks; fades	increase in dermal melanocytes; darker	continuous stripe	- (11)
Dsk10	3 days; fades	increase in dermal melanocytes	continuous stripe	Gnaq (19)

Table 1.1: Summary of mouse *Dsk* phenotypes

[1]Age at first appearance of phenotype and whether phenotype darkens or fades with age

[2]Cause of skin phenotype and if hair pigmentation is affected

[3]Strength of the phenotype visible on the footpad

[4]Name of the gene where known followed by the chromosome position in parentheses

Table has been modified from (Fitch et al., 2003) and additional information been added (Van Raamsdonk et al., 2004)

enhancement of G-subunit mediated signalling downstream of *Ednrb*. The authors do not discuss why this proposed mechanism results in localized rather than general increase in pigmentation in the paws. However the mutants are a rare example of how an increased melanoblast number may lead to presence of ectopic pigment cells.

I.8. Aim

As visible from the examples described above, characterisation of various pigmentation mutants has already been able to shed light on some steps necessary for correct pigment pattern formation. We wanted to further investigate how pigment pattern formation in zebrafish occurs.

We therefore characterize *parade*, a pigment pattern mutant, that has like so many others been isolated in the large scale ENU-screen in Tübingen (Haffter et al., 1996a; Kelsh et al., 1996). *parade*, classified as a group V mutant, has ectopic chromatophores-displaying characteristics of both melanophores and iridophores-in the trunk. Dissection of its phenotype and understanding of the mechanisms involved in causing the appearance of the ectopic chromatophores should help us to get further understanding of how pigment pattern formation in zebrafish embryos occurs. Both *parade* alleles, *tj262* and *tv212*, have been described to have an accumulation of chromatophores in an ectopic position just below the notochord first apparent at 3 dpf. The authors suggest, based on observations of chromatophore position and characteristics under bright field and incident light, that some of the ectopic chromatophores contain melanosomes and reflective platelets whilst others possess only iridophore properties. To characterise *parade* we proposed 4 models- mixed cell fate, transdifferentiation, cell number and migration (see Fig. 4.1)- and asked the appropriate questions to find out which mechanism is most likely to cause the *parade* phenotype:

1) Which cell fates are possessed by the ectopic chromatophores?
2) What is the reason for the ectopic positioning of the chromatophores?
3) Are other neural crest derivatives affected in $parade^{tj262}$?
4) Which gene is mutated in $parade^{tj262}$?

To have more markers available for the study of defects in pigment cell and specifically iridophore development we decided to further define the expression patterns of *alk* (Lopes et al., in prep.), a previously described iridophore marker, *inhibitor of DNA*

binding 2 (*id2*(Chong et al., 2005)) a previously identified crest marker, and characterize expression of *sb:cb632* (Thisse et al., 2001) a newly identified crest marker.

Chapter II Materials and Methods

II.1. Fish *husbandry*

All fish strains used were grown in the fish facility of the University of Bath. Adult zebrafish and embryos were dealt with as suggested in the "Zebrafish book" by Monte Westerfield (1999). Crosses of adult fish were set up as described there, embryos collected the next morning, transferred to a Petri dish containing embryo medium (5mM NaCl, 0.17mM KCl, 0.33mM $CaCl_2$, 0.33mM $MgSO_4$, 10^{-5}% methylene blue), sorted and raised at 28.5°C. Embryos were staged according to (Kimmel et al., 1995). Embryos to be live mounted and photographed or to be fixed in 4% Paraformaldeyde (PFA, Sigma) were anaesthetised in a 0.2% solution of 3-aminobenzoic acid ethyl ester ("Tricaine", Sigma). To avoid melanization embryos were treated with 0.003% 1-phenyl-2-thiourea (PTU). After use embryos were euthanised with a lethal dose of Tricaine. Adult zebrafish were euthanised using a 1% Phenoxyethanol solution (Acros).

II.1.1. Fish strains used

wild-type: AB, WIK11 (only for map crosses)
mutant: *parade*^{tj262}, *shady*^{ty82}, *nacre*^{w2}, *colourless*^{m618}
Double mutants were generated by crossing homozygous *parade*^{tj262} carriers with homozygous *nacre*^{w2} carriers, heterozygous *shady*^{ty82} or *colourless*^{m618} carriers. The progeny were then screened for double heterogosity.

II.2. Melanophore counts

Melanophores of the ventral stripe were counted at 5 dpf in *parade*^{tj262} and wild-type embryos. To facilitate the counting of melanophores anesthetized embryos were incubated in 1 mg/ml epinephrine (Sigma, E4375) for 5 minutes. This caused the melanosomes to contract. After fixation with 4% PFA overnight melanophores were counted under a dissecting microscope (Nikon SMZ 1500).

II.3. Microinjection

Injection needles were made from borosilicate glass capillaries of the following dimensions: 1.2 mm outer diameter x 0.94 mm inner diameter (Harvard Apparatus Ltd). The needles were pulled on a model P-97 Flaming/Brown micropipette puller (Sutter Instruments Co.). The following parameters were used: heat 320, pull 240 and velocity 99. Using a pair of tweezers the tip of each needle was broken to the desired size (as small as possible).

Embryos were placed into agarose ramps and injected with a NanojectII Injector (Drummond Scientific Company) as described in the zebrafish book (Westerfield, 1999). Embryos were then transferred into Petri dishes and raised as described (II.1).

II.3.1. Morpholinos used

Morpholinos were obtained from Gene Tools. All morpholinos were kept as a 25 mg/ml stock solution at -20°C. When needed they were diluted to the desired concentration using MQ-H_20, heated for 5 minutes at 55°C and then kept at room temperature. Before injection Phenol Red was added to the working solution.

Morpholino sequences:

mdka	5'-GCCCCGCATTCTGAAAAACACACAC-3'
id2	5'-CTTATTGCCTTCATGTTGACAGCAG-3'
id2-2	5'-TCGCCTTTTTGTGTTCGAGATTCCC-3'
id2-2-mis	5'-TCcCCTTTTTcTGTTgGAcATTgCC-3'

II.4. Transplantation

Cells were transplanted from wild-type embryos of the AB strain into *parade*^{tj262} mutants and vice versa.

The day before the transplantation at least 10 identified homozygous *parade*^{tj262} carriers were set up in pairs with heterozygous *parade*^{tj262} carriers in mating boxes (II.1). The following morning all the eggs were harvested. The host embryos were cleaned, staged, and left to develop in Embryo Medium at 28.5°C until the afternoon.

At least 100 donor eggs were injected with 5% Rhodamine/5% Biotin dye at the one cell stage, using a dissecting microscope (Olympus SZ40) and a NanojectII Injector (Drummond Scientific company). Injection needles were made as described above (II.3).

The injected eggs were placed in a Petri dish containing Embryo Medium and left to develop at 28.5°C.

During cell transplantation, cells were removed from 3-4 hour old donors and transplanted into hosts of the same age. Transplantation needles were prepared initially as per injection needles. The tip was broken using a pair of tweezers; the width of the opening was slightly larger than the size of a zebrafish cell at the developmental stage at which cells were transplanted. This was achieved by situating the tip of the needle next to an embryo of the appropriate stage. The needle was then broken and the size of the opening compared to the cell diameter of the cells of the embryo next to it until the desired size was reached.

About 1 hour before transplantation both the host and donor eggs were dechorionated and the embryos hereafter kept in an agarose coated Petri dish (1.2% agarose in Embryo Medium). Seven donors and seven hosts were transferred into the transplantation plate (a Petri dish containing 2 parallel rows of 7 egg sized square cavities in 1.5% agarose in embryo medium) and covered by embryo medium. The cell transplantation was carried out on a dissecting microscope (Nikon SMZ 1500) using a Micromanipulator (Narishige, IM-50B). The 7 donor embryos were transferred into the row of cavities on the left. Host embryos were placed into the row of cavities on the right. Cells were then transplanted from the first donor embryo into the first host embryo and so on. Cells were generally transferred from one donor into one host only.

Following cell transplantation host and donor were transferred into an agarose coated Petri dish containing embryo medium and Penn/Strep (25,000 U/litre, Sigma). The embryos were then left to develop at 28.5°C, as normal. At 24 hpf the embryos were placed into new Penn/Strep Embryo Medium and PTU was added to inhibit melanization (thus preventing melanin obstruction of faintly labelled cells). Surviving embryos were examined for transplanted cells in crest positions at 24 hpf using a Leica dissecting scope (MZ FLIII) and fixed at 3 dpf for further treatment.

II.5. *In situ* hybridisation

II.5.1. Preparation of Digoxigenin (Dig) labelled in situ probes

In situ probes were synthesized using the Dig RNA Labelling kit (Boehringer).
First approximately 10 µg of plasmid containing the gene of interest were linearized at the 5`end of the gene of interest with 100 u of an appropriate restriction enzyme. To check for complete digestion an aliquot was loaded on a 1% agarose gel. The remaining sample was purified using Phenol:Chloroform:Isoamyl Alcohol (25:24:1, pH 8.0; PCI, Sigma) extraction. 1 µg of linearized plasmid was used as a template for the transcription of 5 to 10 µg of Dig labelled probe. In a 20 µl reaction mix 1 µg of DNA was combined with 2 µl of 10x Dig-NTP labelling mixture, 2 µl 10x transcription buffer, 1 µl RNAse inhibitor and 2 µl of RNA polymerase. Depending on the orientation of the gene and choice of plasmid T7, T3 or SP6 polymerase were used to create an antisense RNA probe. After incubation at 37°C for 2 hours, 2 µl of 4M LiCl and 60 µl of 100% Ethanol were added. After 30 minutes at -20°C the samples were spun down for 15 minutes at 14000 rpm. The aliquot was washed with 70% Ethanol and dried briefly. The RNA pellet was resuspended in 10 µl fresh MQ-H_2O. 1 µl was loaded on a 1% agarose gel to check the probe. 90 µl of Hyb+ (50%Formamid (Sigma), 5x SSC, 0.1% Tween20 (Sigma), 10 mg/ml yeast tRNA (Sigma), 0.1mg/ml Heparin (Sigma)) were added immediately to the remaining 9 µl and the probe stored at -20°C until needed. Usually the *in situ* probes were used at a 1:100 working dilution made up in Hyb+.

II.5.2. In situ hybridization on whole mount zebrafish embryos

Embryos were staged according to Kimmel *et al.* (1995). Embryos older than 18 somite stage were dechorionated and anesthetised before fixing overnight at 4°C in 4% PFA. Embryos younger than 18 somite stage were dechorionated after fixation.
All further procedures were carried out at room temperature and using 1 ml of solution unless stated otherwise. Embryos were washed 2x5 minutes in PBST, then dehydrated 2x5 minutes in Methanol and stored at -20°C for at least 20 minutes or until needed. After dehydration all embryos younger than 5 somite stage were transferred directly for 2x5 minutes into 200 µl Hyb- (50%Formamide (Sigma), 5x SSC, 0.1% Tween20

(Sigma)) and then into 200 µl Hyb+. All embryos older than 5 somites were digested in a proteinase K (Boehringer) solution for better penetration of probe. An incubation period of 8 minutes in 1 µg/ml proteinase K was used for embryos from 5 somite stage to 24 hpf. Embryos older than 24 hpf were incubated for 15-45 minutes in 10 µg/ml proteinase K (Roche). After a 5 minute wash in PBST embryos were refixed in 4% PFA for 20 minutes. Following a 5 minute wash in PBST, a 1 minute wash in MQ-H_2O and another 5 minute wash in PBST embryos were washed 2x5 minutes in 200µl Hyb-. Embryos were then transferred into 200 µl Hyb+ and prehybridised in a waterbath at 68°C for 1-3 hours.

Embryos were hybridised in 100 µl of 1:100 dilution of the probe and incubated at 68°C overnight. The probe was removed, saved and stored at -20°C for reuse. To wash away unbound and non-specific bound probe, embryos were washed 2x20 minute at 68°C with 2xSSCT/50% Formamide, once with 2xSSCT/25% Formamide, once with 2xSSCT followed by 2x30 minute washes in 0.2xSSCT.

Note: This wash protocol was modified halfway through my PhD to a fast wash in Hyb+, 2x30 minutes in Hyb+ and one 20 minute wash in 50% Hyb+/50% PBST.

Embryos were then washed for 5 minutes in PBST at RT and blocked for at least 1 hour in blocking solution (5% sheep serum (Sigma), 10mg/ml BSA (Sigma) in PBST). The blocking solution was replaced by 200 µl of Anti-Dig solution (1:2000 dilution of Anti-Dig-AP (Boehringer) in blocking solution) and incubated for 2 hours at RT or overnight at 4°C. The Anti-Dig solution was stored at 4°C to be reused and the embryos were washed 8x15 minutes in PBST followed by 3x5 minute washes in NTMT (10mM Tris-HCl pH 9.5, 50mM $MgCl_2$, 10mM NaCl, 0.1% Tween). For staining the embryos were transferred into 9 well glass plates and covered with 200 µl staining solution (200 µl of NBT/BCIP stock solution (Boehringer, 11681451001) in 10 ml NTMT) and stained in the dark until the desired level of staining was reached. The reaction was stopped by washing 2x5 minutes in PBST, 1x5 minutes in 0.1M Glycine pH 2.2 and 1x5 minutes in PBST. To reduce background and improve clarity of stained embryos they were washed 5 minutes in 100% Ethanol. After another 5 minute wash in PBST embryos were transferred into 4%PFA and stored at 4°C. For closer inspection under an MZ12 dissecting microscope embryos were transferred back into a Petri dish with PBST.

II.5.3. Plasmids used to generate in situ probes

alk 1.2kb: cut with SpeI; use T7 polymerase

sb:*cb632*: EcoRI, Sp6

sb:*cb321*: SalI, Sp6

II.6. Terminal deoxynucleotidyl Transferase Biotin-dUTP Nick End Labelling (TUNEL)

To identify and quantify numbers of apoptotic cells in *parade*^{tj262} embryos TUNEL staining was performed at different stages of their development using the ApopTag® Peroxidase In Situ Apoptosis Detection Kit (Chemicon, S7100). Embryos were fixed at developmental stages of interest for 2 hours at room temperature or at 4°C overnight in 4%PFA.

All further procedures were carried out at room temperature and using 1 ml of solution unless stated otherwise. Embryos were washed 2x5 minutes in PBST, then dehydrated 2x5 minutes in Methanol and stored at -20°C for 30 minutes. All embryos were digested in a proteinase K (Boehringer) solution for better penetration. An incubation period of 8 minutes in 1 µg/ml proteinase K was used for embryos 24 hpf old embryos. Embryos older than 24 hpf were incubated for 15-45 minutes depending on their age in 10 µg/µl proteinase K (Roche). After 2x5 minute washes in 2 mg/ml Glycerin (Sigma) embryos were refixed in 4% PFA for 15 minutes. This was followed by 2x5 minute washes in PBST and a 7 minute incubation in Ethanol: Acetic Acid (2:1; Fisher) at -20°C for 7 minutes. After 2 more 5 minute washes in PBST embryos were incubated for 15 minutes in 75 µl equilibration buffer. Embryos were then incubated for 1 hour in 17 µl 'working strength enzyme mix' (70% Reaction buffer, 30% TdT enzyme) on ice, followed by a 1 hour incubation at 37°C. The labelling reaction was stopped by a 5 minute wash at room temperature and a 45 minute wash at 37°C in Stop solution. After blocking the embryos for at least 1 hour at room temperature in blocking solution (2 mg/ml BSA, 5% goat serum, 1% DMSO) they were incubated in Anti-Dig solution (1:7500 dilution of Anti-Dig-AP (Boehringer) in blocking solution) at 4°C overnight.

The Anti-Dig solution was stored at 4°C to be reused and the embryos were washed 8x15 minutes in PBST followed by washes in NTMT 3x5 minute (10mM Tris-HCl pH

9.5, 50mM $MgCl_2$, 10mM NaCl, 0.1% Tween). For staining the embryos were transferred into 9 well glass plates and covered with about 200 µl staining solution (200 µl of NBT/BCIP stock solution (Boehringer, 11681451001) in 10 ml NTMT) and stained in the dark until the desired level of staining was reached. The reaction was stopped by washing 4x5 minutes in PBST and embryos were stored in 4%PFA.

For TUNEL staining combined with double Antibody staining, embryos were incubated in Anti –Dig solution (1:7500) containing also Anti-Phospho- Histone H3 antibody (see II.7.1) and/or Anti-GFP (1:200, mAb 3E6, Molecular Probes). Then the TUNEL reaction was developed as described above. After stopping the reaction with several washes of PBST embryos were incubated overnight at 4°C overnight with secondary antibody (see II.7.2) in blocking solution. The antibody was discarded and the embryos washed for 3x30 minutes in PBTX. Embryos were stored in PBST until they were examined.

II.7. Antibody staining on whole mount zebrafish embryos

Embryos were staged according to Kimmel *et al.* (1995) and fixed in 4% PFA at room temperature on a shaker for 2 hours. After 2x5 minute washes in PBTX (PBS/ 0.5% Triton-X 100, Sigma) embryos were washed 3x1 hour in MQ-H_2O to improve penetration of the probe. Embryos younger then 36 hpf were only washed for 1 hour in MQ-H_2O. After blocking for 2 hours at room temperature with blocking solution (5% horse serum (Sigma) in PBTX) embryos were incubated at 4°C overnight with the primary antibody (see II.7.1). The antibody was discarded and the embryos washed for 3x1 hour in PBTX and incubated at 4°C overnight with the secondary antibody (see II.7.2). Again, the antibody was discarded and the embryos washed for 3x30 minutes in PBTX. If a fluorescent secondary antibody was used embryos were ready for analysis at this stage. If a biotinylated secondary antibody was used embryos were incubated for 45 minutes in R.T.U Reagent (VECTASTAIN Elite) followed by 3x10 minute washes in PBTX. Embryos were then transferred into 9 well glass dishes and stained with 3,3'-Diaminobenzidine (DAB) (5 ml MQ-H_2O, 2 drops buffer, 4 drops DAB and 2 drops H_2O_2; Peroxidase Substrate Kit, VECTASTAIN). Embryos were monitored while

staining and the reaction stopped by washing 4 times in PBTX. Embryos were analysed with a Leica dissecting microscope (MZ FLIII) using fluorescence microscopy.

II.8. Antibodies used

II.8.1. Primary Antibodies

anti-Hu mouse (mouse 16A11, Molecular Probes, (Marusich et al., 1994) diluted 1:500

anit-Tyrosine Hydroxylase (mouse, Chemicon, MAB318) diluted 1:500

anti-phospho- Histone H3 (rabbit, Upstate) diluted 1:1000

II.8.2. Secondary Antibodies

Alexa Fluor 488 goat anti-mouse IgG (Molecular Probes, A11001), diluted 1:1000

Alexa Fluor 488 goat anti-rabbit IgG (Molecular Probes, A11034), diluted 1:1000

Biotinylated anti-mouse IgG (Vector Laboratories, BA-9200), diluted 1:1000

II.9. Microscopy and Photography

All embryos were cleared in a solution of 70% Glycerol in PBST for at least 30 minutes before viewing. They were then mounted either on cold (4°C) methylcellulose or in 100% glycerol and examined using a Nikon Eclipse E800. Photographs were taken both with a digital camera (SPOT or V3 Nikon). When necessary, the yolk was dissected away with dissecting needles. All digital photos were graphically adapted in Adobe Photoshop 7.0 or Adobe Photoshop CS2.

II.10. TEM Sample preparation and analysis

Samples were prepared by Ursula Potter (Centre for Electron Optical Studies, University of Bath). Sample preparation was modified from (Strmac and Braunbeck, 1999). Embryos were staged according to Kimmel *et al.* (1995) and prefixed overnight

in 4% PFA at 4°C on a shaker. Embryos were then fixed in 2.5% Glutaraldehyde, 2% PFA, 4% PVP, 0.005% $CaCl_2$ in 0.1M Sodium Cacodylate Buffer (pH 7.6) overnight at 4°C. After 3x10 minutes washes at room temperature in Sodium Cacodylate Buffer (pH 7.6) embryos were postfixed in 1% Osmium Teroxide in Sodium Cacodylate Buffer pH7.6 for 1 hour before they were rinsed again 3x10 minutes at room temperature in Sodium Cacodylate Buffer (pH 7.6). The embryos were then dehydrated for 12 minutes at 4°C in 50% Ethanol followed by a 20 minutes wash with 2 changes in 70% Ethanol at 4°C, a 20 minutes wash again with 2 changes in 90% Ethanol at 4°C, a 20 minutes wash in 95% Ethanol with 2 changes at room temperature and finally in 100% Ethanol for 30 minutes with 4 changes. For infiltration embryos incubated for an hour in 100% dry Acetone: Epoxy Resin (1:1) before they were incubated in 100% Resin overnight followed by another 1 hour incubation in 100% Resin. Embryos were finally embedded in Spurr Epoxy Resin and left for polymerization for 7 hours at 70°C.
Sections were prepared by Ursula Potter and analysed on a transmission electron microscope (JEOL JEM1200).

II.11. Molecular cloning techniques

II.11.1. Plasmid minipreps

Cultures of single colonies, picked from transformation plates, were grown in 2 ml of LB-Medium containing 50 µg/ml carbenicilin (Sigma) at 37°C on a shaker overnight. 1.5 ml of the overnight culture was transferred to an Eppendorf tube and spun at 14000 rpm for 5 minutes. The supernatant was discarded and the pellet resuspended in 80 µl Solution 1 (50mM Tris pH 8.0, 50mM Glucose, 10mM EDTA, RNAse). 160 µl of Lysis buffer (0.2M NaOH, 0.1% SDS) were added and tubes inverted until the solution was clear and viscous. Then 120 µl of Neutralizing solution (3M KAcO/ 5M HOAc, pH 5) was added and the tubes inverted again. After 5 minutes incubation at room temperature 50 µl of PCI was added and mixed by vortexing. Samples were centrifuged at 14000 rpm for 10 minutes and the supernatant was transferred to new tubes. 1 ml of 100% Ethanol was added and after 10 minutes incubation at room temperature to precipitate the plasmid DNA samples were spun for 15 minutes at 14000 rpm. The DNA was washed with 70% Ethanol, dried and resuspended in 20 µl MQ-H_20. The sample was the stored at -20°C until needed.

II.11.2. Plasmid minipreps using the Wizard Plus SV Miniprep DNA Purification System (Promega)

Cultures of single colonies, picked from transformation plates, were grown in 2 ml of LB-Medium containing 50 µg/ml carbenicilin (Sigma) at 37°C on a shaker overnight. 1.5 ml of the overnight culture was transferred to an eppendorf tube and spun at 14000 rpm for 5 minutes. The supernatant was discarded and the pellet resuspended well in 250 µl Wizard Plus Cell Resuspension Solution. 250 µl of Wizard Plus Lysis Solution was added and mixed by inverting the tubes. 10 µl Alkaline protease Solution was added and the tubes were inverted again. After 5 minutes incubation at room temperature 350 µl of Wizard Plus Neutralisation Solution was added and after inverting to mix the samples were spun at 14000 rpm for 10 minutes. The cleared lysate was transferred into a Wizard Spin Column and centrifuged at 14000 rpm for 1 minute and the flowthrough was discarded. After adding 750 µl of Wizard Plus Wash Solution samples were respun for 1 minute at top speed and the flowthrough discarded again. The wash step was repeated with 250 µl Wash Solution. The columns were transferred to a 1.5 ml microcentrifuge tubes and 100 µl of Nuclease-Free Water were added. After spinning for 1 minute at 14000 rpm the columns were discarded and the DNA stored at -20°C until needed.

II.11.3. Plasmid Midipreps using the QIAGEN Plasmid Midi Kit

A single colony was picked from a selective plate and inoculated in 50 ml LB-Medium containing 50 µg/ml carbenicilin (Sigma) on a shaker at 37°C overnight. Bacterial cells were transferred to 50 ml Falcon tubes and harvested by centrifugation at 5000 rpm for 15 minutes. The supernatant was discarded and the cells resuspended in 4 ml Buffer P1. 4 ml of Buffer P2 were added and mixed in gently by inverting the tubes 4 to 6 times. After incubating for 5 minutes at room temperature 4 ml of chilled Buffer P3 were added. The samples were mixed by inverting the tubes as before and kept on ice for 15 minutes. Samples were mixed again and centrifuged at 5000 rpm for 30 minutes. The clear supernatant was transferred to a new tube and respun for 15 minutes. During that step a QIAGEN-tip 100 was equilibrated by applying 4 ml of Buffer QBT. The cleared supernatant was then decanted into the QIAGEN-tip and allowed to enter the resin by

gravity flow. The QIAGEN-tip was then washed twice with 10 ml Buffer QC. DNA was eluted with 5 ml Buffer QF and collected in a new tube. To precipitate the DNA 3.5 ml of isopropanol were added. After mixing samples were centrifugated immediately for 30 minutes at 4°C. The supernatant was carefully decanted and the pellet washed with 2 ml of 70% Ethanol. The pellet was air dried for 5 to 10 minutes and the DNA redissolved in a suitable volume of MQ-H_2O and stored at -20°C until needed.

II.11.4. Restriction digests

Approximately 1 µg of plasmid DNA were digested in a total reaction volume varying from 20- 100 µl. The reaction mix was put together as specified by the manufacturer. Incubation was carried out at the enzyme's specific reaction temperature (usually 37°C) for 2 hours. All enzymes and their respective buffers used were purchased from Promega or New England Biolabs (NEB).

II.11.5. Gel extraction using the QIAquick Gel Extraction Kit (Quiagen)

DNA fragments of 70bp to 10kb were purified using the QIAquick Gel extraction kit (Quiagen). The desired DNA fragment was excised with a clean scalpel from a normal agarose gel and weighed in a colourless tube. 3 Volumes of Buffer QG were added to 1 Volume of gel (100mg~100 µl) and incubated at 50°C for 10 minutes or until the gel slice was completely dissolved. The sample was then applied to a QIAquick column to bind the DNA and centrifuged for 1 minute. The flow-through was discarded and the QIAquick column was placed back in the collection tube. To wash, 750 µl of Buffer PE were added and after 1 minute of centrifugation the flow-through was discarded again. After spinning the QIAquick column for another minute it was placed into a clean 1.5 ml microfuge tube. To elute the DNA, 50 µl of Buffer EB were added to the centre of the QIAquick membrane and the column spun for 1 minute. The DNA was stored at -20°C until needed.

II.11.6. Phenol-Chloroform extraction

MQ-H_2O was added until the sample volume was 100 µl. Then 10 µl of 3M NaAc and 110 µl of PCI (pH8.0, Sigma) were added. After vortexing the sample was centrifuged for 15 minutes at 14000 rpm and the resulting upper phase was transferred to a new

microfuge tube. For precipitation, 300 µl of 100% Ethanol was added and the sample stored at -20°C for at least 1 hour. Following another centrifugation for 15 minutes at top speed the sample was washed with 70% Ethanol, dried and resuspended in an appropriate volume of MQ-H_2O. The DNA was stored at -20°C until needed.

II.11.7. Ligation

Ligations were set up using 1 Unit T4-DNA Ligase and 10x Ligation buffer (Promega) in a final reaction volume of 10 µl. The final reaction contained 50-100 ng of the (digested) plasmid

The molar ratio between vector and insert was approximately 1:3. A negative control where DNA was replaced by MQ-H_2O was carried out. The ligation was incubated for 2 hours at room temperature or at 4°C overnight.

II.11.8. Preparation of Magnesium Sulphate competent cells

DH5α cells from a glycerol stock were grown in 5 ml of LB-Medium (Sigma) overnight at 37°C. on a shaker. 500 µl of overnight culture were added to 50 ml of Medium A (10mM $MgSO_4$, 0.2% Glucose in LB-Medium) and incubated on a shaker at 37°C until A578=0.55. The cells were left on ice for 10 minutes and then pelleted at 1500g for 10 minutes at 4°C. The supernatant was discarded and the cells resuspended in 500 µl ice cold Medium A. 2.5 ml of Medium B (36% Glycerol, 12% PEG, 12mM $MgSO_4$ in LB-Medium) were added and after mixing carefully aliquots of 100 µl were snap-frozen in liquid nitrogen and stored at -80°C.

II.11.9. Transformation of competent cells by heatshock

The competent cells were carefully thawed on ice. 50 µl were used per transformation. Either 5 µl ligation product or 1 µl plasmid were added and carefully mixed by flicking the tube. The tube was kept on ice for 3 to 5 minutes, heatshocked in a heat block for 90 seconds at 42°C and returned to ice for another 5 to 8 minutes. 20 –50 µl of cells were then directly spread onto an LB-agar (Sigma) plate containing carbenicilin (Sigma).

II.11.10. Agarose gel electrophoresis

To prepare an agarose gel of a certain percentage, the appropriate amount of agarose (Invitrogen) was weighed into 1xTAE buffer (0.04M Tris-acetate, 0.001M EDTA) and heated in a microwave at full power until the agarose was dissolved. The evaporated liquid was replenished with RO water, the gel solution briefly cooled under tap water. Ethidium bromide (10 mg/ml) was added for a final concentration of 0.4 mg/ml. Gels were run at 80-250 Volts for 10 minutes to 2 hours in 1xTAE buffer and examined and documented using an ultraviolet light source and a black and white camera (Alphaimager 3400, Alpha Innotech) and a video graphic thermal printer (Mitsubishi). 2% agarose gels were used for mapping (see II.12); otherwise 1% agarose gels were used.

II.12. PCR protocols used to map genes with the LN54 radiation hybrid panel

The LN54 (Loeb, NIH, 5000rad, 4000rad) collection of radiation hybrids (zebrafish in a mouse background) was kindly provided by Mike Ekker from the Loeb Research institute in Ottawa, Canada (Hukriede et al., 2001; Hukriede et al., 1999). It contains 96 samples: 93 radiation hybrid DNA samples (100ng/nl each), DNA from the two parental cell lines (zebrafish AB9 and mouse B78) and a 1:10 mixture of the latter two.

For mapping a gene on the panel, a PCR reaction with primers specific for the sequence of the gene is used. 1 µl of each of the 96 DNA samples was combined with 2 µl of 10µM of each primer, 10µl PCR Mix (Biomix Red, Bioline) and 7 µl MQ- H_2O.

PCR reactions were denatured at 94°C for 1 minute, cycled at 94°C for 30 seconds, 55°C for 1 minute, 72°C for 3 minutes for 30 cycles, followed by an extension at 72°C for 5 minutes. All 20 µl of PCR reaction were loaded on a 1% agarose gel and location of the products of the expected 500bp size was recorded. This assay was carried out in duplicate and the resulting data submitted to the mapping programme at http.//mgchd1.nichd.nih.gov:8000/zfrh/beta.cgi. Positive hybrids were scored as 1, negative hybrids as 0 and missing or unambiguous hybrids were scored as two.

Placement on a Linkage group is indicated with a LOD score (the LOD score is the logarithm of likelihood ratio for linkage). To be considered linked the best LOD score must be greater than a LOD of five. In addition the net difference between the best LOD score and the second best LOD score on another Linkage group needs to be greater than 3. The gene of interest in not only paved onto a Linkage group, but in addition the distance to the closest markers known is indicated in centiRay (1 centiRay or cR is defined as a one percent frequency of a breakage occurring between two markers after exposure to a specific radiation dose). Currently 1 cR is on average equivalent to 118 kilobases. (Hukriede et al., 2001; Hukriede et al., 1999)

II.12.1. Primers used to map cb632 and id2 on the LN54 Radiation Hybrid Panel

cb632_for 5`-GGGTCTGGGGTCAGTTGTAA-3`
cb632_rev 5`-GGCACAAAATTTCAGGAAGC-3`
id2-f 5'-TTGTGAAAAGCATTTGTTCCA-3'
id2-r 5'-TCATTTTAACTGCCGCTTCA-3'

II.13. Protocols used to map *parade^{tj262}*

II.13.1. Map crosses and bulked segregant analysis

To map *parade^{tj262}* we generated a map cross (P0, Fig. 2.1) by crossing *parade^{tj262}* heterozygous carriers (AB background) to the WIK11 (WIK) reference line (Rauch et al., 1997). Fish of the F1 generation were screened for the quarter of *parade^{tj262}*/WIK carriers. 8 pairs of carriers were identified this way and kept as separate pairs. The other F1 fish were euthanized. The 8 identified *parade^{tj262}*/WIK F1 pairs were crossed and the progeny was sorted according to their phenotype: mutant and sibling (wild-type and heterozygous carriers). Over 1000 mutant embryos from all the 8 F1 pairs were collected this way. After preparation of genomic DNA from each embryo (see II.13.1) bulked segregant analysis on pooled mutant and sibling DNA of 48 embryos was performed using a set of SSLP (Single Sequence Length Polymorphism) markers that cover the whole genome at roughly equal spacing. Agarose gel electrophoresis of the

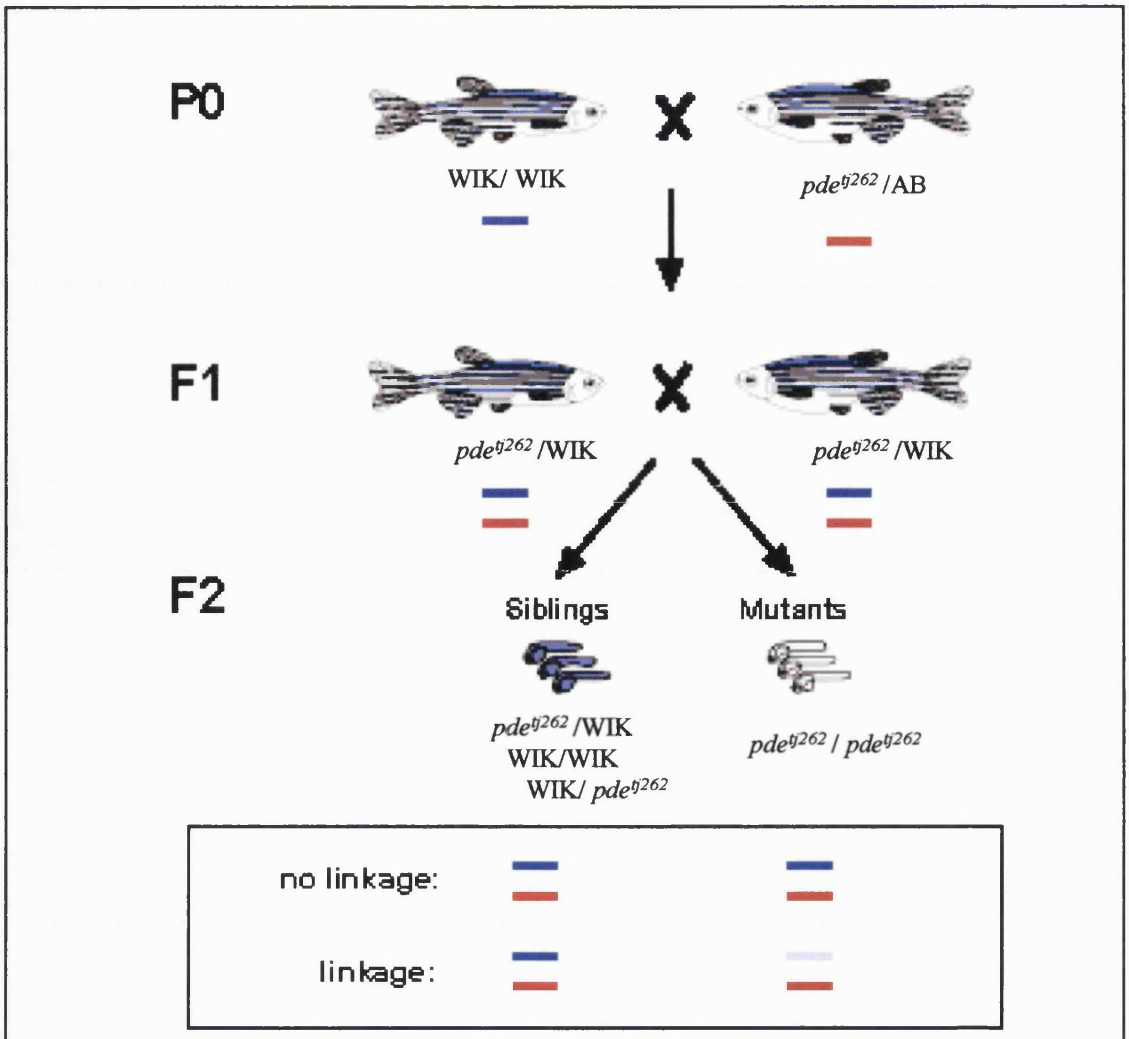

Fig.2.1 Mapping of *parade*^{tj262}
Fish of the reference lines WIK/WIK were crossed to heterozygous *parade*^{tj262} carriers (AB background). SSLP markers generate bands of different sizes in both lines (shown schematically in blue and red). Fish of the F1generation are screened for the quarter of *parade*^{tj262}/WIK carriers. These are crossed and the DNA of the resulting progeny is analysed using SSLP markers. For initial analysis pools of sibling genomic DNA and mutant genomic DNA are generated. Same intensity of the mutant and wild-type band indicates that there is no linkage between the mutation and the marker. However, a stronger AB band in the mutant pool and a stronger WIK band in the sibling pool indicate linkage between the mutation and the marker.
Figure modified from R. Geisler, 2002

SSLP fragments was used to estimate relative intensity of the WIK and AB bands. Mutant and wild-type band of the same intensity indicated that there was no linkage between the mutation and the marker. However, a stronger AB band in the mutant pool and a stronger WIK band in the sibling pool indicated linkage between the mutation and the marker. SSLP markers, that showed a linkage, were then used for further analyses on single embryos.

II.13.2. Fine mapping of parade^{tj262}

Once it had been established that a marker was linked to the mutation by bulk segregant analysis the marker was analysed on genomic DNA of single mutant F2 embryos. As an initial step, linkage of the marker was confirmed by analysing the DNA of 12 siblings and 48 mutants. The markers were then tested on further single embryos, until a consistent distance between marker and mutation could be established. To evaluate the distance between the marker and the mutation the number of embryos showing a recombination (e.g. 2) is divided by the number of embryos tested (e.g. 192). The result is multiplied by 100 to show the distance in cM e.g. 2/192 = 0.0104 x100 ~ 1 cM. The aim was to find a marker that was located only about 0.1cM away from the mutation.

II.13.3. Generation of a map

To generate a map containing the markers examined in relation to the (*parade^{tj262}*) mutation we compared the number and position of recombinants of different markers in the same embryos (Fig. 2.2). A mutation is located in the interval between two markers if the recombinants for both markers are not the same. In the event of no recombination we would expect all embryos to show the AB band. A marker is located on the same side of the mutation as another marker if it has an overlapping recombinations event in the same embryo. A marker showing the same recombination event(s) as another, but additional ones as well was on the same side of the mutation but further away than the latter. A marker showing the same recombination event(s) as another, but fewer was on the same side of the mutation but closer to the mutation than the latter.

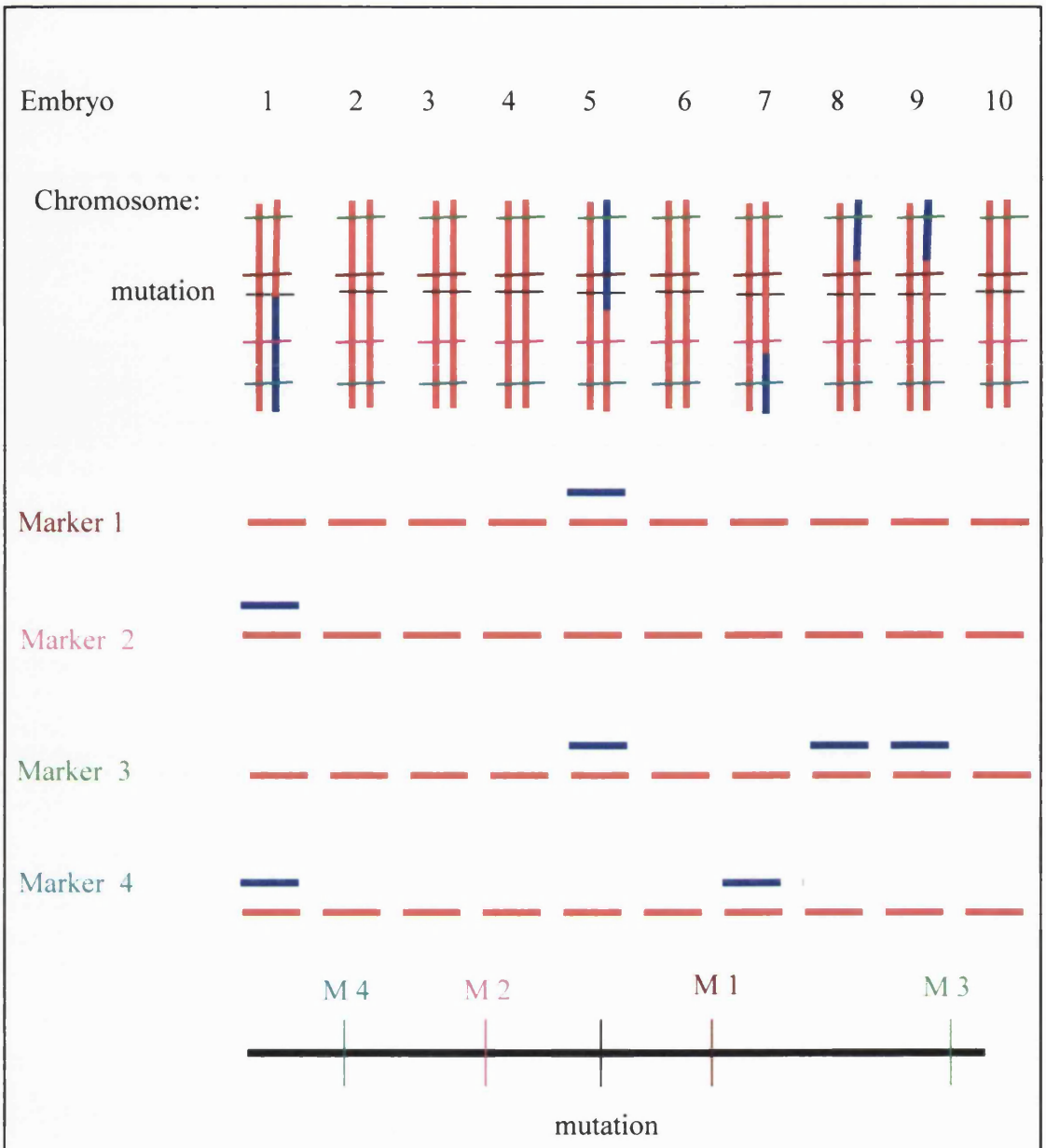

Fig.2.2 How to generate a genomic map
Panel A shows the position of the markers on the chromosome and where recombination has taken place in individual embryos. Blue indicates WIK and red indicates AB DNA. Analysis of Marker 1 (M 1) on 10 embryos shows a recombination in embryo 5. The marker is placed on one site of the mutation. Marker 2 (M 2) shows again only a recombination in one embryo, but in embryo 1. It is therefore on the other site of the mutation than M 1. Marker 3 (M 3) is like M 1 recombinant for embryo 5 and therefore on the same site of the mutation. It shows two more recombinations than M 1 mapping it further away from the mutation. Marker 4 (M 4) is recombinant for embryo 1 and 7, which puts in onto the same side of the mutation as M 2, but further away.

II.13.4. Lysis of embryos for mapping

F1 fish from the map crosses were set up, the embryos collected, sorted and grown until 5 dpf as described above. F2 embryos were then sorted by phenotype and stored in tubes in 100% Methanol at -70°C until used. For lysis, embryos were transferred into a Petri dish containing 100% Methanol. Embryos were then pipetted into a 96 well PCR plate (one embryo per well) with a glass Pasteur pipette. Plates were left in a PCR block at 70°C for approximately 10 minutes, so the Methanol could evaporate. 25 µl 1xTE (10 ml Tris-HCL, pH 8.0, 1mM EDTA) containing 17 mg/ml Proteinase K (Boehringer) were added per well, the plate covered with sealing film and heated in a Thermocycler (Techne) for 4 hours at 55°C and then for 10 minutes at 70°C to inactivate the Proteinase K. 75 µl of MQ-H_2O were added to each well. For bulk segregant analysis DNA of 25 µl of 48 sibling and mutant lysates were pooled. Plates were covered with sealing film (Starlabs) and stored at -20°C. Each plate was given a number and labelled with allele, F1 cross, mutant or siblings and the number of embryos (e.g. Plate 2, tj262, pair 1, all mutants, 75).

II.13.5. Lysis of adult fins

If necessary, fins of the P0 and F1 generation were lysed to check SSLP marker sizes. Live fish were briefly anaesthetized with Tricaine. One-half of each tail fin was cut with a scalpel and placed into a labelled (Stock number, gender, fish line) 0.2 ml tube. The fish was returned to a tank containing system water and a drop of 1% Methylene blue. After each use the blade of the scalpel was cleaned with 100% Ethanol.
40 µl 1x TE (10 ml Tris-HCL, pH8.0, 1mM EDTA) containing 17 mg/ml Proteinase K were added into each tube. These were left on a shaker at 37°C overnight. The next day, 60 µl MQ-H_2O were added and the DNA was then stored at -20°C until needed.

II.13.6. PCR protocols used to map parade (with SSLP markers)

2 µl of DNA from lysed single or pooled embryos were combined with 13 µl PCR mix [containing 1.5 µl 10x Buffer for KOD Hot Start DNA Polymerase, 1.5 µl dNTPs (2mM each), 0.6 µl 25mM MgS04, 0.3 µl DMSO, 0.5 µl forward and reverse Primer (10mM each), 8.3 µl MQ-H_2O and 0.3 µl KOD Hot Start DNA Polymerase (all Novagen)].

PCR reactions were denatured at 94°C for 2 minutes, cycled at 94°C for 30 seconds, 60°C for 30 seconds, 72°C for 1 minute for 35 cycles, followed by an extension at 72°C for 5 minutes.

2 µl of 6x Tricolour Loading dye (Promega) were added per reaction and the whole 17 µl were loaded on a 2% Agarose gel. Gels were run at 250 Volts for 2 hours in 1xTAE buffer and examined and documented using an ultraviolet light source and a black and white camera (Alphaimager 3400, Alpha Innotech) and a video graphic thermal printer (Mitsubishi).

II.13.7. Primers used to map parade^{tj262}

For initial bulk segregant mapping to place *parade^{tj262}* onto a linkage group we used two Z marker panels, G4 and H2, covering the whole genome (Geisler et al., 2007). Each panel consists of two 96 well PCR plates. For initial fine mapping the flanking Z markers showing a polymorphism and those located in between on the MGH Microsatellite Map (http://zebrafish.mgh.harvard.edu) were used. Once all the Z Markers were exhausted, markers were designed to BAC ends located in the interval between the two closest Z markers using the primer design software Primer3 (http://frodo.wi.mit.edu/cgi-bin/primer3/primer3_www.cgi). In addition candidate Simple Sequence Repeats (SSR) marker primer pairs for this work were generated using the Zebrafish SSR search website, Massachusetts General Hospital, Charlestown MA 02129; http://danio.mgh.harvard.edu/markers/ssr.html.

Sequences of markers mentioned:

P48	zK257N15SP6 -f	5'-GTGCCGAGCTCATCCCTAA-3'
	zK257N15SP6 -r	5'-TGCTAATGCAAAGCACCAAG-3'
P157	BX644371.6-f	5'-TTGGGGACTCCTTTTTCTGA-3'
	BX644371.6-f	5'-TTATTGCCGCTCTTTTTGCT-3'
P170	BX005047.5_92942-f	5'-TGCAGGAATTTCATTGGATG-3'
	BX005047.5_92942-r	5'-TGCAGGCGTACCTTCACAA-3'
P174	BX511149.9_56560-f	5'-TCGTACAGCCCTAATTCCTCT-3'
	BX511149.9_56560-r	5'-TCTCCACCTGTGGTAAAGCA-3'

Sequences of Z markers can be found on: http://zebrafish.mgh.harvard.edu

II.14. Protocol for genotyping *shady* ^{ty82} embryos

The mutation in *shady*^{ty82} generates an RFLP that allows us to identify mutants using a NheI digest.

II.14.1. Lysis of embryos for genotyping

Embryos, on which *in situ* hybridisation had been performed, were sorted for their phenotypes and then were transferred into PCR tubes (one embryo per tube) with a glass Pasteur pipette and all liquid was removed. The tubes were labelled indicating the expected genotype. 25 µl 1xTE (10 ml Tris-HCL, pH 8.0, 1mM EDTA) containing 17 mg/ml Proteinase K (Boehringer) were added per tube, the tubes were closed and heated in a Thermocycler (Techne) for 4 hours at 55°C and then for 10 minutes at 70°C to inactivate the Proteinase K. 75 µl of MQ-H_2O were added to each tube.

II.14.2. PCR protocol for genotyping shadyty82

2 µl of DNA from lysed single embryos were combined with 23 µl PCR mix [containing 2.5 µl 10x Buffer for KOD Hot Start DNA Polymerase, 2.5 µl dNTPs (2mM each), 1 µl 25mM MgS04, 0.5 µl DMSO, 0.5 µl forward and reverse Primer (10mM each), 15.5 µl MQ-H_2O and 0.5 µl KOD Hot Start DNA Polymerase (Novagen)].

A touchdown PCR was performed. PCR reactions were denatured at 94°C for 1 minute, cycled at 94°C for 30 seconds, 55-47°C for 1 minute, 72°C for 30 seconds for 30 cycles, followed by an extension at 72°C for 5 minutes.

2 µl of the resulting PCR product were used to repeat the PCR reaction as described above to increase yield.

10 µl of PCR product were digested with NheI (for volumes see II.11.4) in a total reaction volume of 100µl for 2 hours. 50 µl of the digest and 5 µl of undigested PCR product were run with the appropriate amount of 6x Tricolour Loading dye on a 1% Agarose gel. Gels were run at 120 Volts for 45 minutes in 1xTAE buffer and examined and documented using an ultraviolet light source and a black and white camera (Alphaimager 3400, Alpha Innotech) and a video graphic thermal printer (Mitsubishi).

II.14.3. Primers used for genotyping shady^{ty82}

shd intron ty82 5'-CTAACTCAAAGCAGTTTCGT-3'

shd ty82 intronR 5'-GTAACGTCATGAGCAGATAA-3'

II.14.4. Products expected for genotyping shady^{ty82}

The expected PCR product is 496bp. After NheI digest the products expected for *shady^{ty82}* homozygous mutant embryos are ~360bp and ~130bp. Heterozygous carriers are expected to show products of all three sizes.

II.15. Statistical analysis

Statistical analysis of cell counts was performed using Prism 3.0.

Chapter III Characterization of iridophore markers

III.1. Introduction

In situ hybridization is a very useful tool for the careful characterization of zebrafish mutants. Even though over the past years more and more crest markers have been found in zebrafish, only a few melanoblast/melanophore and iridophore markers have been carefully characterized (Kelsh and Raible, 2002). The knowledge of more well characterized markers will help to give further insight into the specification and migration of melanophores and iridophores.

More melanophore lineage markers than iridophore lineage markers have been characterized so far. *mitfa*, for example, is expressed in the melanophore lineage from stages before migration until melanoblasts get pigmented (Lister et al., 1999). *dct* is co-expressed with *mitfa* and can be seen in migrating cells, but its expression in the melanophore lineage starts slightly later. In addition it is maintained until the melanophores are fully pigmented (Kelsh et al., 2000; Lister et al., 1999). Another well characterized melanophore marker is c-*kit*, which is expressed in melanoblasts from pre-migratory stages on and is maintained even in fully pigmented melanophores (Parichy et al., 1999). In addition, there is obviously melanin, which enables us to identify some melanophores from as early as 27 hpf.

In contrast to melanophores, where the melanin allows an early identification of the cell type, iridophores can only be identified, by their reflecting properties, from about 40 hpf on (X. Yang, personal communication). So far, *ednrb1* is the only iridophore marker that has been published (Parichy et al., 2000). However, at early stages *ednrb1* is, consistent with the progressive fate restriction model (Kelsh, 2006), more widely expressed by melanophore, xanthophore and iridophore precursors. It becomes specific to the iridophore lineage from 48 hpf (Parichy et al., 2000a). Interestingly, even though *ednrb1* is expressed during early pigment cell development no larval pigment phenotype in mutants has been observed. However, *ednrb1/rose* mutants fail to develop normal numbers of melanophores and iridophores in adulthood and show a disrupted pigment pattern (Parichy et al., 2000a).

The only other iridophore marker, next to *ednrb1*, known when this work was started was *alk*. Whereas *ednrb1/rose* mutants show no embryonic phenotype the *alk* mutant *shady* has an early larval loss of iridophore phenotype (Kelsh et al., 1996).

As only few iridophore markers are characterized we have set out to characterize some more.

III.1.1. alk

The Receptor tyrosine kinase ALK has first been isolated as a fusion protein caused by a chromosomal translocation found in approximately one third of all non-Hodgkin's anaplastic large cell lymphoma in children mainly derived from activated T lymphocytes (Morris et al., 1994). This t(2;5)(p23;q25) translocation event fuses the amino-terminal part of the RNA-binding nucleolar protein nucleophosmin to the c-terminal cytoplasmic part of ALK resulting in an 80 kD fusion protein (p80). Expression of *Alk* in different vertebrates has been studied already, but the role(s) for *Alk* in development have not been identified. Initial Northern Blot analysis showed *Alk* transcripts in the human testis, placenta and the fetal liver, but immunostaining studies only showed expression restricted to some scattered neuron, glia and endothelial cells of the central nervous system (Morris et al., 1994; Pulford et al., 1997). In the chick ALK has been shown to be expressed in the developing PNS, more specifically cells of the sympathetic ganglia and dorsal root ganglia, as well as in subsets of motor neurons along the spinal cord and in subsets of muscles of the body wall (Hurley et al., 2006).
In mouse *Alk* expression is prominent in the nervous system and also in a variety of other tissues including skin, tongue, testis, ovary, stomach and midgut (Iwahara et al., 1997; Vernersson et al., 2006).
Whilst no endogenous in vivo *Alk* function in vertebrates is known so far a role in some invertebrates has been identified. Based on the prominent *Alk* expression in the nervous system of all organisms studied a role in regulation of neural development has been proposed. Recently *Alk* has been shown to be involved in mediating targeting of retinal axons in *Drosophila* (Bazigou et al., 2007). Together with its ligand Jelly Belly it is also necessary for correct visceral mesoderm development (Englund et al., 2003; Loren et al., 2003). In *C elegans* a role for *alk* in regulation of synapse development has been proposed (Liao et al., 2004).
The *alk/shady* locus in zebrafish was cloned and characterised by S.Lopes (Lopes et al., in prep). Different *shady* alleles have been isolated and their phenotypes range from complete loss of iridophores (strong alleles like *ty82*) to strong reduction of iridophore numbers (weak alleles like *ty9*, *trd*) during embryonic development. The strong alleles

are lethal, but this is not likely to be caused by the loss of iridophores. The weak alleles are adult viable and do not display any iridophore defects as adults. In zebrafish *alk* has been shown to work cell autonomously suggesting that it would be expressed in iridophores and/or neural crest. *alk* expression in a limited set of wild-type and *alk/shady* mutants had already been described before the start of this thesis. Comparison of iridophore distribution and *alk* expression in individual wild-type embryos at 72 hpf revealed identical patterns showing that at this stage *alk* was as expected expressed in iridophores. At 48 hpf and 30 hpf, *alk* positive cells were again described to be distributed in a pattern reminiscent of iridophore distribution at later stages in the DS and VS. At all three stages *alk* expression on the eye was also described. At 22 hpf *alk* expression in iridoblasts on the eye and in a broad ventral midbrain-hindbrain domain was observed. At all stages *alk* expression was described as absent or strongly reduced in *shady*^{ty82} mutants.

Here we have extended the expression studies of *alk* in wild-type and *shady*^{ty82} mutant embryos at early stages of development, mainly before 36 hpf.

III.1.2. Characterization of new iridophore markers

In order to identify and characterize new iridophore markers we searched the Zebrafish Information Network (ZFIN) database (http://zfin.org/cgi-bin/webdriver?MIval=aa-xpatselect.apg) for clones expressed in a pattern similar to iridoblasts/iridophores. The ZFIN database shows all expression patterns identified in a large scale *in situ* hybridization screen that has been performed by Thisse et al. (2001) in order to identify and characterize genes expressed during zebrafish development. Preliminary characterization of the expression patterns of the genes identified was posted in the ZFIN database which can be viewed publicly. cDNA clones of interest can then be ordered from the Zebrafish Resource Centre in Oregon. We found and ordered nine clones -sb:*cb632*, sb:*cb629*, sb:*cb147*, sb:*cb323*, sb:*cb356*, sb:*cb321*, sb:*cb293*, sb:*cb397*, sb:*cb293*- with iridoblast/iridophore-like expression patterns. We performed *in situ* hybridization on characterised pigmentation mutants to further characterise the expression pattern of each gene and determine in which neural crest cell type the genes were expressed.

As a first step we studied the expression patterns of each gene in 24 hpf, 48 hpf and 72 hpf wild-type embryos. The expression pattern of clones that seemed to be expressed in

pigment cells and/or their precursors was then studied in all or some of the well-characterized pigmentation mutants -*colourless*^{m618}, *nacre*^{w2} and *shady*^{ty82}- at three different developmental stages -24, 48 and 72 hpf. Comparison of the expression patterns of the markers of interest in the three mutants, based on our knowledge of specific cell types affected in these mutants, was expected to give us some information about in which pigment cell lineages they were expressed and when. Wild-type expression patterns of genes expressed in iridophores were expected to look '*alk*-like', with expression of a single row of cells along the DS at 48 hpf and 72 hpf in the typical iridophore-like fashion. In addition, we would expect expression in the lateral patches and from there leading posteriorly in a series spots on both sides of the VS. As *shady*^{ty82} mutants have no iridophores, we expected complete loss of the wild-type expression pattern at 48 and 72 hpf for iridophore markers (Kelsh et al., 1996). At 24 hpf, *shady*^{ty82} mutants cannot be distinguished from wild-type embryos based on *alk* expression (see results section below). Iridophore markers were thus expected to show either no or very low expression in *shady*^{ty82} mutants at 24 hpf. As pigment cells do not become specified in *colourless*^{m618} mutants (Dutton et al., 2001) we would expect to loose all expression of a true iridophore marker at all stages observed. Expression of an iridophore marker in *nacre*^{w2} mutants at 24 hpf is expected to be similar to that of wild-type embryos, as counts of *alk* positive cells did not show an increase in number at this early stage (E. Greenhill, unpublished). At later stages however an increase in *in situ* positive cells along the DS and VS is expected as *nacre*^{w2} mutants have an increased number in iridophores (Lister et al., 1999).

III.1.2.A. sb:*cb632*

One of the clones on the ZFIN database that had been described to be expressed in neural crest and pigment cells is *sb:cb632*. The clone named sb:*cb632* contained a 670bp long fragment of zebrafish cDNA (GenBank:CA854270). We will refer to it as *cb632.*

Since we started characterization ZFIN published a Protein sequence comparison of *cb632*, done on the Unigene site, suggesting 85.47% identity to human Guanine Monophosphate (GMP) synthetase. Furthermore high sequence similarity to GMP synthetase of *C. elegans* (56.04%), *S. cerevisiae* (39.21%), *E.coli* (35.56%) and *A.thaliana* (34.04%) is shown

(http://www.ncbi.nlm.nih.gov/UniGene/clust.cgi?ORG=Dr&CID=8251).

There are two distinct pathways, *de novo* and salvage, for the synthesis of purines. GMP synthetase is involved in the *de novo* synthesis of purines. It has been shown to be necessary to catalyze the final step which converts Xanthylate to Guanylate (Berg et al., 2002).

To our knowledge no specific involvement of GMP synthetase in pigment cell development has yet been shown. Interestingly, iridophores contain stacks of guanine platelets that are responsible for their reflecting properties (Land, 1972).

In this chapter we will describe the characterization of *cb632* expression in *nacre*^{w2} and *shady*^{ty82} mutants and will map its location within the zebrafish genome

III.1.2.B. *sb:cb321*

The second clone received from ZFIN which we will further analyse here is sb:*cb321*. The clone named sb:*cb321* contained the *inhibitor of DNA binding 2 (id2)* gene (RefSeq:NM_201291), a member of the helix-loop-helix group of transcription factors. By dimerising with basic helix-loop-helix proteins, ID proteins act as dominant negative regulators of those proteins (Norton, 2000). So far four different ID proteins have been identified in vertebrates and have been implicated in various processes during development including gastrulation, neurogenesis, angiogenesis and early crest development (Jen et al., 1997; Kee and Bronner-Fraser, 2005; Lyden et al., 1999). Even though ID proteins have been traditionally thought to be inhibitors of cellular differentiation, more recent evidence suggests that they are also involved in positive regulation of processes such as fate determination and maintenance (Neuman et al., 1993; Norton, 2000). In zebrafish the expression of *id3* and *id1* (previously known as *id6*) have been studied (Dickmeis et al., 2002; Sawai and Campos-Ortega, 1997). *id1* is expressed in a complex pattern, with expression domains including the central nervous system, notochord and brain described (Sawai and Campos-Ortega, 1997). *id3* is also expressed in a highly dynamic pattern during early zebrafish development. It expression domains include the neural crest, brain, retina and the fins (Dickmeis et al., 2002). The function of both *id1* and *id3* during zebrafish development is not known yet. When we started studying whether *id2* is expressed in neural crest and pigment cells, the only published information about its expression in zebrafish was on ZFIN. Since then (Chong et al., 2005) have published a general expression study of *id2*, concentrating

mainly on its expression in brain and nervous system. But expression in the migrating trunk neural crest at 22 hpf has also been described (Chong et al., 2005).

All four Id genes have been isolated in mouse; their expression has been studied and knockouts have been generated (Jen et al., 1997). During mouse gastrulation and neurogenesis Id2 is expressed in a variety of different domains including the neural fold and roof plate at early stages and in the dorsal root ganglia, but not sympathetic ganglia, at later stages (Jen et al., 1997). At birth Id2 null-mutant mice look wild-type but show defects in growth and generation of both natural killer cells and peripheral lymphoid organs leading increased mortality as neonates (Yokota et al., 1999). The lack of neural crest phenotype despite expression in the neural fold is probably due to redundancy of the various Id genes as both Id1 and 3 are also expressed there (Jen et al., 1997). The phenotypes of the various Id2 with Id1/3/4 double knockout combinations have not yet been described in detail but are embryonic lethal (Norton 2000).

It has been shown in chick, that Id2 has a function in neural crest fate specification. It is thought to direct ectodermal cells to neural crest and neurogenic fates rather than epidermal lineages (Martinsen and Bronner-Fraser, 1998). In both Xenopus and chick Id2 is expressed in the neural folds and areas of the heart contributed to by crest (Martinsen et al., 2004). However, involvement of Id2 in pigment cell development in Xenopus or chick has not yet been studied. In opposite to that Xenopus Id3 has been shown to have a function in proliferation and survival of neural crest progenitors with knockdown of *id3* resulting in a large decrease in melanophores (Kee and Bronner-Fraser, 2005).

In this chapter, we describe the expression of zebrafish *id2* in neural crest, specifically pigment cells, at three developmental stages in *colourless*^{m618}, *nacre*^{w2} and *shady*^{ty82} mutants, we map *id2* in the zebrafish genome and study the consequences of *id2* knockdown on pigment cell development.

III.2. Results

III.2.1 Further characterization of the alk expression pattern

In order to further establish *alk* as an iridophore marker, to specify when during development it is first specific to the iridophore lineage and to be able to use the *alk*

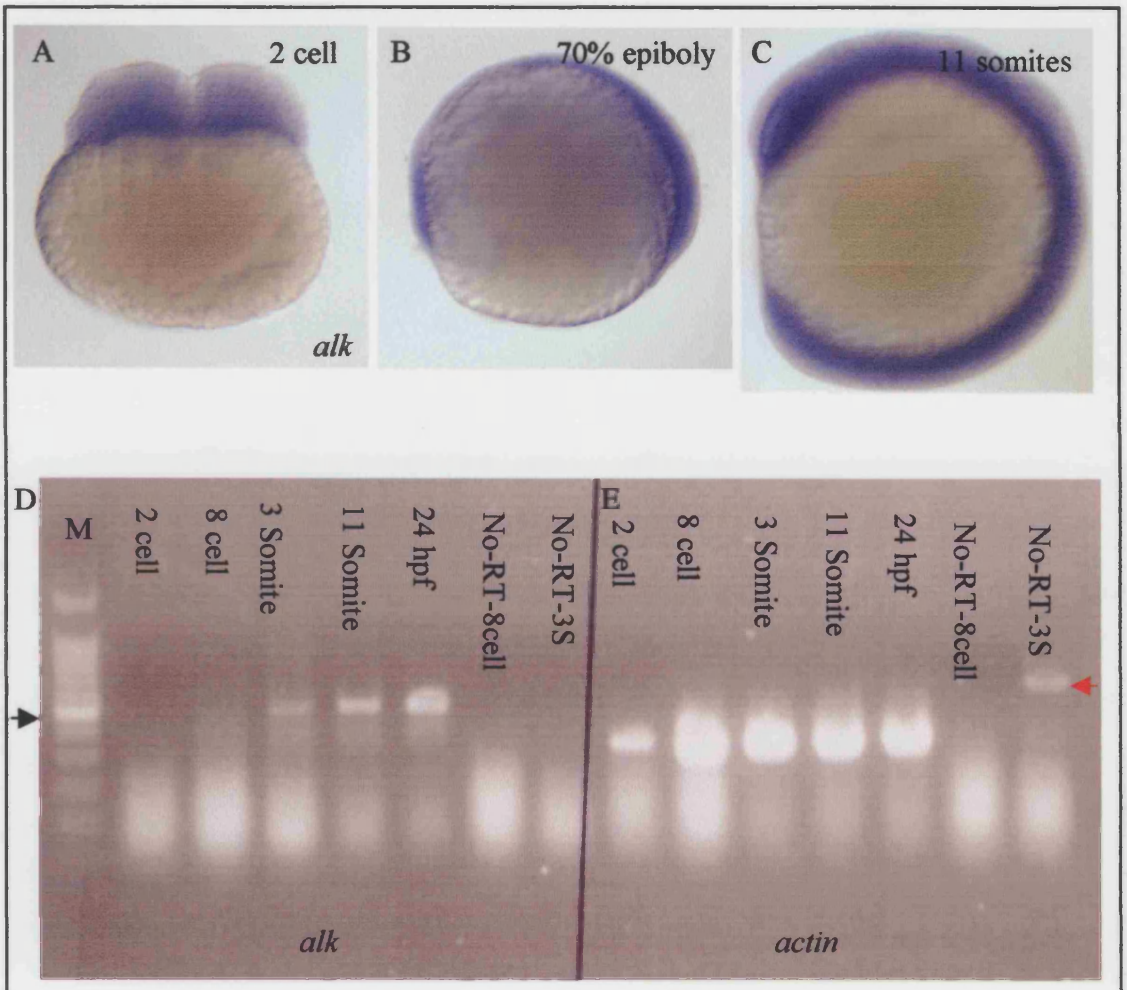

Fig. 3.1: Early *alk* expression
alk in situ hybridisation at early developmental stages (A, B) seemed ubiquitous. RT-PCR however showed, that there is no maternal *alk* transcript (D: 2 and 8 cell), suggesting that the *in situ* signal at early stages of development was background. Control RT-PCR using actin primers produced transcripts at all stages as expected (E). *alk* transcript can be detected from the 3 Somite stage on (D). Broad *alk* expression could be seen in 11 Somite old embryos (C) and RT-PCR confirmed expression at this stage (D: 11 Somite). cDNA control PCR using actin showed transcripts at all stages (E). No-RT enzyme controls were done for the 8 cell and 3 Somite stage (D, E: no RT). In the *actin* no-RT control at 3 Somites (3S) the genomic actin band can be seen (red arrow).
Size marker (M) in basepairs (bp): 1500, 1000, 900, 800 700, 600, 500, 400, 300, 200, 100; 500bp band labelled with arrow

expression pattern as a model of how iridophore markers are expressed we studied the *alk* expression pattern at various stages of wild-type and *shady*^{ty82} mutant development.

III.2.1.A. There is no maternal *alk* expression

So far, *alk* expression in developmental stages younger than 22 hpf had not been studied, we therefore began by asking when during development *alk* expression could first be seen. To analyse the expression of *alk* in embryos younger than 22 hpf *in situ* hybridization was performed on 2 cell stage, 75% epiboly and 11 Somite stage embryos (Fig. 3.1 A, B, C). To make sure the *in situ* hybridization protocol worked we also used a 24 hpf embryo where we knew the expected expression pattern. We developed all stages for three days until we could see the expected pattern in the 24 hpf control stage. Due to the long developing the expression at the 2 cell and 75% epiboly stages were slightly difficult to interpret as the whole of each embryo became purple after not having shown any specific localized expression at first. This could be caused by ubiquitous expression of *alk* at these stages or it could simply be caused by non-specific background staining. In 11 Somite stage embryos there was broad expression in the ventral part of the embryo only (Fig. 3.1 C).

To determine if there was indeed early *alk* expression and a maternal *alk* contribution we performed RT-PCR. The time points chosen were 2 and 8 cell stage to check for a maternal *alk* contribution and 3 and 8 Somite stage to examine the early expression of *alk* after midblastula transition. A sample of RNA from 8 cell stage embryos where no RT-enzyme had been used in the RT reaction was used as a negative control to exclude the possibility of genomic contamination of our samples (Fig. 3.1 D, E: no RT). As expected we could not observe a band of the size expected (~500bp) in the negative control. *actin* served as positive control and showed strong expression at all stages used (Fig. 3.1 D). The 24 hpf stage served as a positive control for the PCR as we knew from the earlier *alk* expression studies that *alk* was expressed then. A band of the expected 500bp could be clearly seen verifying that the PCR worked (Fig. 3.1 E). Using RT-PCR on cDNA of 2 and 8 cell stage wild-type embryos we detected no transcripts. This strongly indicates that there is no maternal *alk* contribution. But at the 3 and 8 Somite stages zygotic transcripts of the expected 500bp could be seen, showing *alk* is expressed at these stages (Fig. 3.1.D).

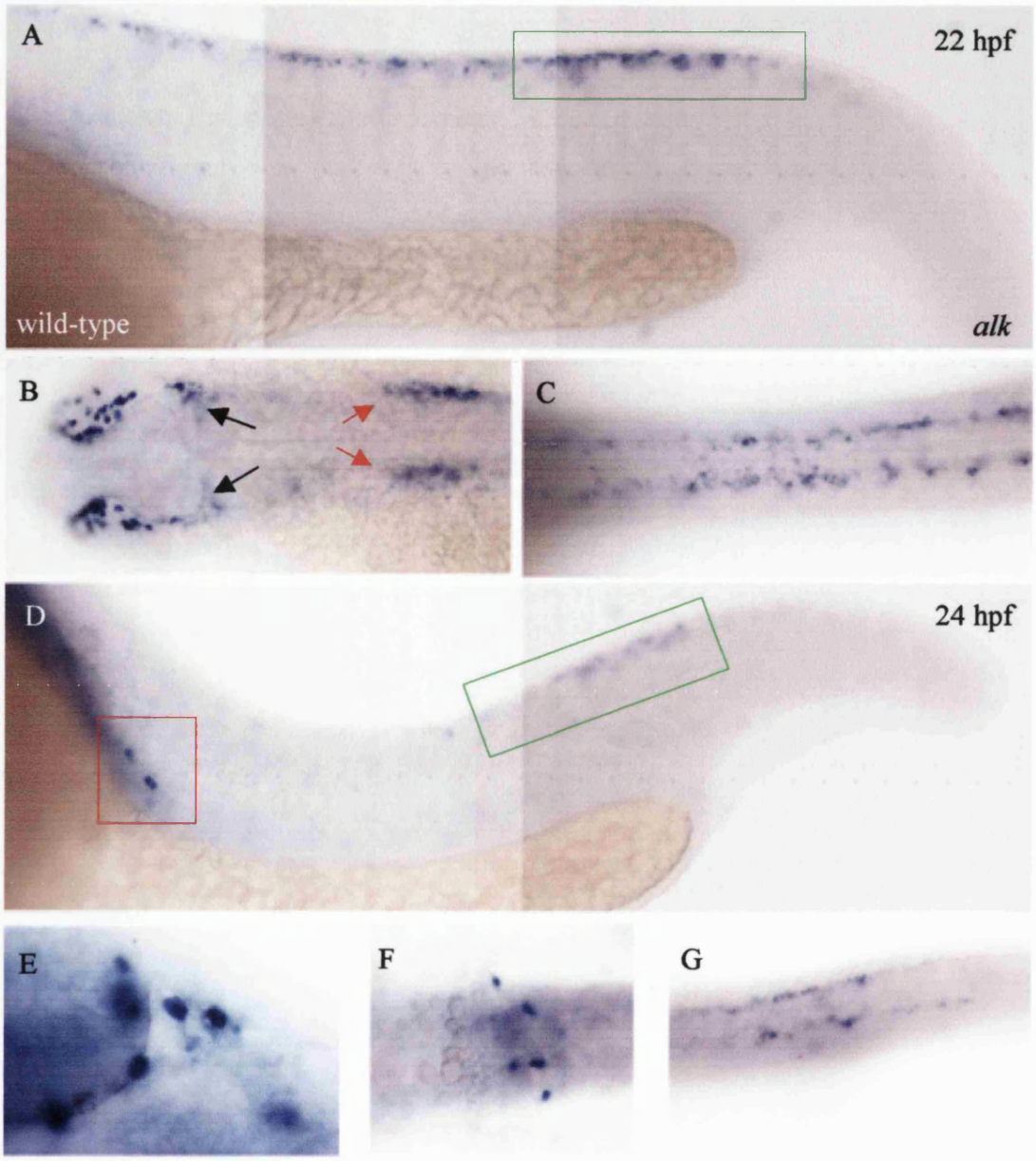

Fig. 3.2: Expression of *alk* at 22 and 24 hpf
At 22 hpf *alk* was expressed in pre-migratory crest (A) in addition to the previously described expression in the eye (B). Two additional domains of *alk* in the head could be seen. One posterior to the eye (black arrows), the other posterior to the ear (red arrows). Expression in the dorsal stripe seemed to be in two stripes. At 24 hpf levels of *alk* expression in the pre-migratory crest had gone down (D, G) while expression levels posterior to and in the eye were still strong (E). In addition, the first *alk* expressing cells in the future ventral stripe at the anterior end of the yolk sac extension could be seen (F). A, D and E lateral view; B dorsal view; C dorsal view of area in green box in A; F dorsal view of cells in red box in D and G dorsal view of *alk* positive cells in green box. In this and all subsequent figures anterior is to the left.

We therefore showed that there was no maternal *alk* expression in wild-type embryos suggesting that the staining observed at the early stages was background. Our RT-PCR results however, identified the point of first *alk* expression to be as early as 3 Somites. This result was verified by repetition of the experiment on a second set of independently made cDNA.

III.2.1.B. Detailed characterization of *alk* expression between 22hpf and 36 hpf and a brief look at later stages

Having shown that *alk* is expressed in a broad ventral domain at the 11 Somite stage, we next asked when it lost this ubiquitous expression pattern (Fig. 3.1 C), and became specific to the iridophore lineage as described by S. Lopes. For this we looked at *alk* expression between 22 hpf and 36 hpf.

At the earliest stage examined, 22 hpf, *alk* had already lost its broad expression pattern and was expressed in what seemed to be pre-migratory crest (Fig. 3.2 A, C) in a pattern similar to that of *mitfa* at 24 hpf (Lister et al., 1999) and as previously described in the eye (Lopes et al., in prep.). We could also detect *alk* expression in two additional distinct domains, one located just posterior to the ear, similar to the location where the first *dct* expression can be seen (Kelsh et al., 2000), and the other one close to the mid-hindbrain boundary, just posterior to the eye, was observed (Fig. 3.2 B). Expression in both these domains was reduced, but still present at 24 hpf. This was also true for the expression in the pre-migratory crest position (Fig. 3.2 D, G). Between 22 hpf and 30 hpf the expression in the in pre-migratory neural crest position gradually became less broad and more defined. Expression was initially seen as two stripes either side of the midline (Fig. 3.2 C) and later became a single row of expression along the midline (Fig. 3.3 E). Counts showed a steady increase in numbers of *alk* positive cells in the single DS between 26 hpf and 36 hpf (Fig. 3.3 G).

We observed the first few *alk* positive cells in the VS at 24 hpf. The cells were located anteriorly on both sides of the midline, close to the beginning of the yolk sac extension (Fig. 3.2 F). Between 24 hpf and 36 hpf *alk* expression in these two domains seemed to expand anteriorly forming the future lateral patch and posteriorly to the end of the yolk sac extension forming the rest of the VS (Fig. 3.3 A-D).

As described by S. Lopes (Lopes et al., in prep.) *alk* expression could be observed in a series of single cells along the whole length of the VS and DS at 48 hpf and 72 hpf. We extended the study to later stages and showed that at 4 dpf and 5 dpf expression

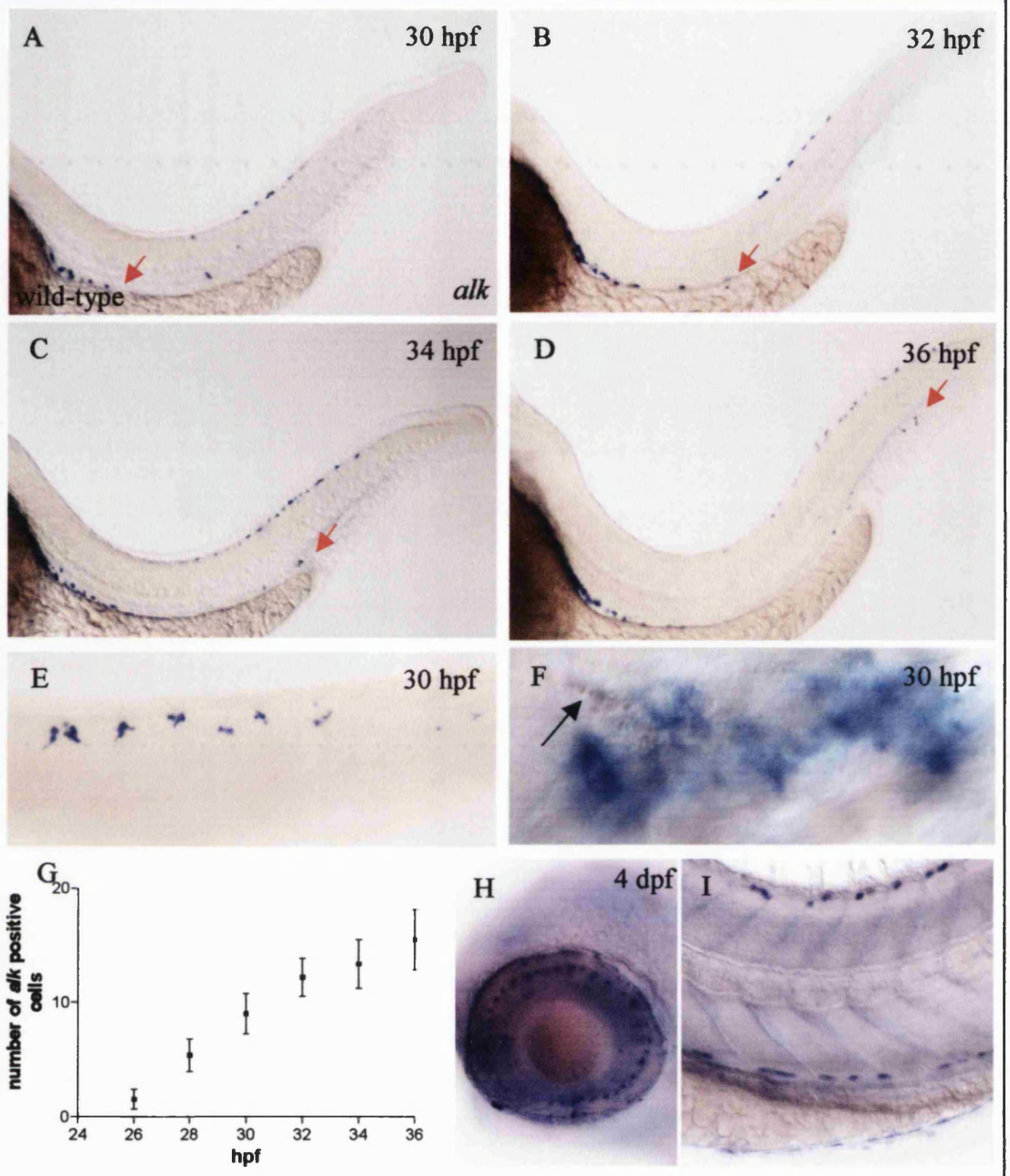

Fig. 3.3:Expression of *alk* from 30 to 36 hpf
By 30 hpf *alk* is expressed in a row of cells in the dorsal stripe (E), migrating cells and the ventral stripe (A). During further development additional cells expressing *alk* appear posterior to the previous ones in the ventral stripe (compare posterior border (red arrow) of *alk* positive cells in A-D). At the same time more *alk* expressing cells in the dorsal stripe could be observed (B-D). Melanin-expressing cells could be observed close to the *alk* expressing cells located behind the ear (F, arrow). Counts showed that the number of *alk* positive cells in a single medially located dorsal stripe increased between 26 and 36 hpf. At 4 dpf *alk* is still strongly expressed in cells in the eye (H) and in iridophores along the dorsal, ventral and yolk sac stripe (I). E dorsal view of dorsal stripe, all others lateral view

persisted in an iridophore like pattern in the DS and VS (Fig. 3.3). In addition other non pigment cell- expression domains were observed (data not shown).

We have shown here that *alk,* at early developmental stages such as 22 hpf, was expressed in a pre-migratory crest like pattern and that during later development expression became specific and was seen in an iridophore-like pattern from about 30 hpf on.

III.2.1.C. *shady*^{ty82} mutants initially express *alk*

To examine how early the iridophore lineage was affected in *shady*^{ty82} mutants we performed counts for *alk* positive cells in the progeny of a *shady*$^{ty82/+}$ in-cross and asked how early we were able to distinguish *shady*^{ty82} mutants from their wild-type siblings. We looked at 28, 31, 32, 36 and 38 hpf old embryos. *alk* positive cells in the trunk and tail, including DS and VS cells and migrating cells, but not the eye, were counted. It is of note that the counts showed quite a high variation in numbers of *alk* positive cells between wild-type siblings of the same age at these early stages (Fig. 3.4). Siblings of the embryos that were fixed for *in situ* hybridisation and counting were grown to 4 dpf to verify that all crosses used contained *shady*^{ty82} mutants.

At 31 hpf we observed that 5/20 embryos had clearly fewer *alk* positive cells than their siblings (Fig.3.4 A, D, E). This trend continued and at 32, 36 and 38 hpf we also observed 4-5 embryos having clearly less *alk* positive cells than their siblings. Roughly a quarter of the embryos seemed to have less *alk*-positive cells and since this fitted with the expected ratios of mutants in a heterozygous cross according to the Mendelian rules, we proposed that the embryos with less *alk* positive cells were the *shady*^{ty82} mutants. To test this hypothesis we utilized a RFLP caused by the mutation in *shady*^{ty82}. We genotyped the four potential *shady*^{ty82} mutants (Fig. 3.4 A, circled in red) and seven potential wild-type or heterozygous siblings at 32 hpf (see section II.14). Genotyping the embryos with less *alk* positive cells confirmed our assumption that they were *shady*^{ty82} mutants (Fig. 3.4 B, C), as we clearly detected the expected 160bp and 360bp bands. There was still some residual 520bp product visible suggesting that it was only a partial digest (Fig. 3.4). Six of the seven siblings genotyped showed the characteristic 520bp wild-type band only, whereas one of them had all three bands suggesting that it was a heterozygous carrier. As all embryos in the group with less *alk* positive cells at 32 hpf were *shady*^{ty82} mutants we assumed that this was also the case at 31, 36 and 38 hpf.

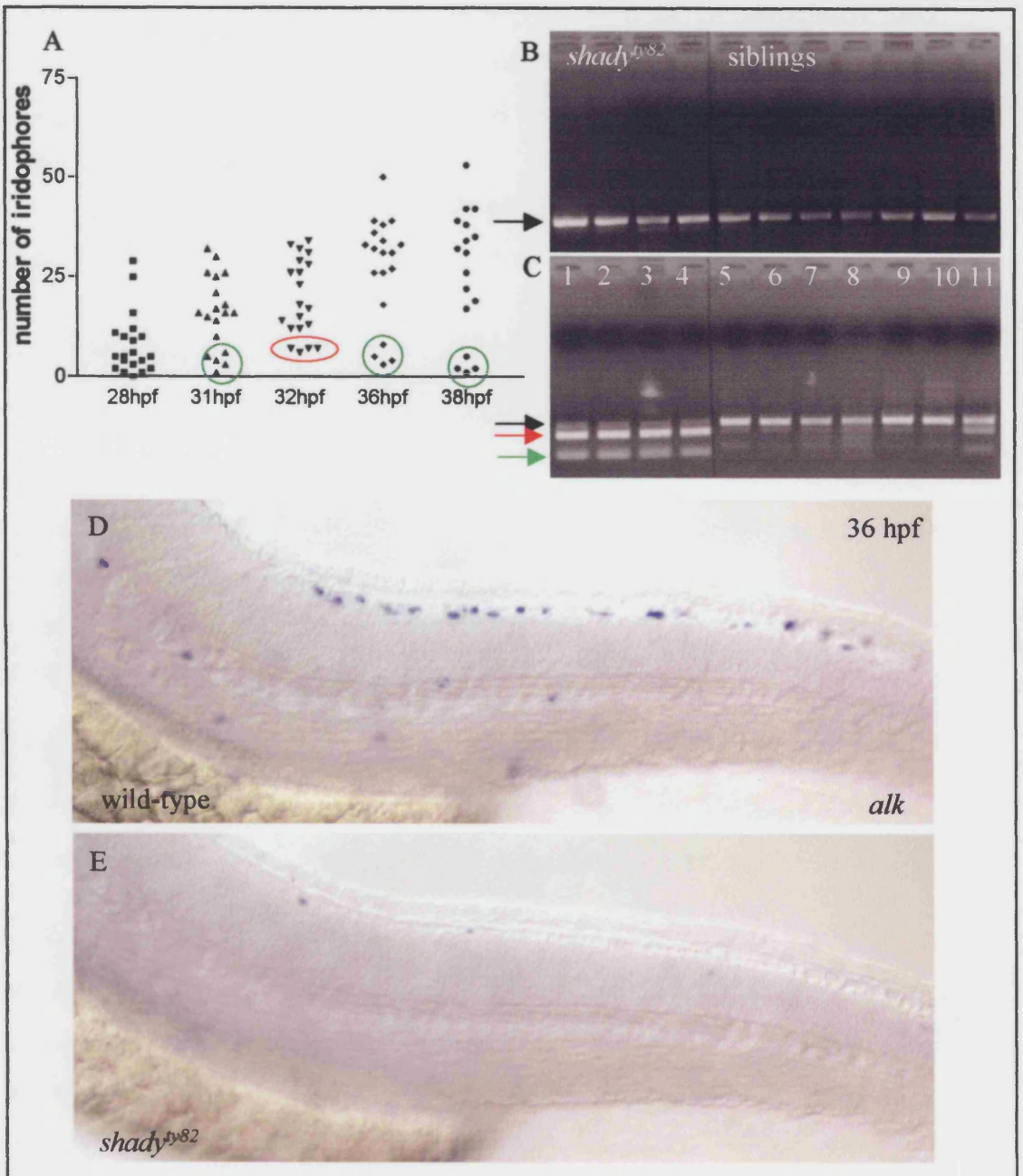

Fig. 3.4: *shady*^{ty82} mutants have reduced numbers of *alk* positive cells compared to wild-type siblings

Counts of *alk* positive cells in the progeny of a heterozygous *shady*^{ty82} in-cross showed that from 31 hpf onwards roughly a quarter of the embryos had fewer *alk* positive cells than their siblings (A, circled; green circles indicate that embryos have not been genotyped). RFLP analysis on 32 hpf embryos showed that those with less *alk* positive cells (circled in red and lane 1-4) were *shady*^{ty82} mutants (B, C). The 520bp (black arrow) PCR generated transcript was sensitive to NheI digest in *shady*^{ty82} mutants only creating a 360bp (red arrow) and 160bp (green arrow) fragment (B). At 36 hpf *shady*^{ty82} mutants (E) clearly had less *alk* positive cells than their wild-type siblings (D) in trunk and tail. E, F lateral view

Counts at an earlier stage did not give us a group of embryos with clearly fewer *alk* positive cells. At 28 hpf some embryos showed a very low number of *alk* positive cells, but the transition between those and embryos with higher numbers of *alk* positive cells was smooth.

We therefore showed that it was possible to distinguish *shady*^{ty82} mutants from their siblings based on the number of *alk* positive cells as early as 31 hpf but not yet at 28 hpf.

III.2.2. Characterization of new iridophore markers

To identify more iridophore markers we searched the ZFIN expression pattern database for genes expressed in what we assumed to be a potential iridoblast/iridophore pattern based on the expression of *alk*.

We will describe the expression of the two genes that are expressed in iridoblasts/iridophores, *cb632* and *cb321* here.

III.2.2.A.Characterization of *cb632*

One of the *in situ* hybridization markers that we were interested in characterising further after seeing its pattern described in the gene expression database on ZFIN was *cb632*.

III.2.2.A.1. Expression pattern of *cb632*

The expression pattern, described for wild-type embryos on ZFIN, for 24 hpf shows expression in the eye, tectum and pre-migratory neural crest. At roughly 48 hpf expression is described to be in pigment cells, the eye, optic tectum, pigmented epithelium retina, liver and gut. Later stages are not described. To investigate, if and in which type of pigment cells, *cb632* was expressed we examined its expression in *nacre*^{w2} and *shady*^{ty82} mutants. We concentrated our studies on expression domains likely to be iridoblasts/iridophores only.

As close examination of our wild-type expression pattern seemed identical to that described on ZFIN (Fig. 3.5 A-C) we next examined expression of *cb632* in *nacre*^{w2} and *shady*^{ty82} mutants. At 24 hpf all embryos of an in-cross of heterozygous *shady*^{ty82} carriers had expression in the pre-migratory crest (not shown). The size and extent of the *cb632* expression domain was reminiscent of that of *ednrb1* at 24hpf suggesting that it might label the same population of cells (Parichy et al., 2000a). At 48 hpf expression of *cb632* had become localised to small spots distributed in an *alk*-like pattern along the

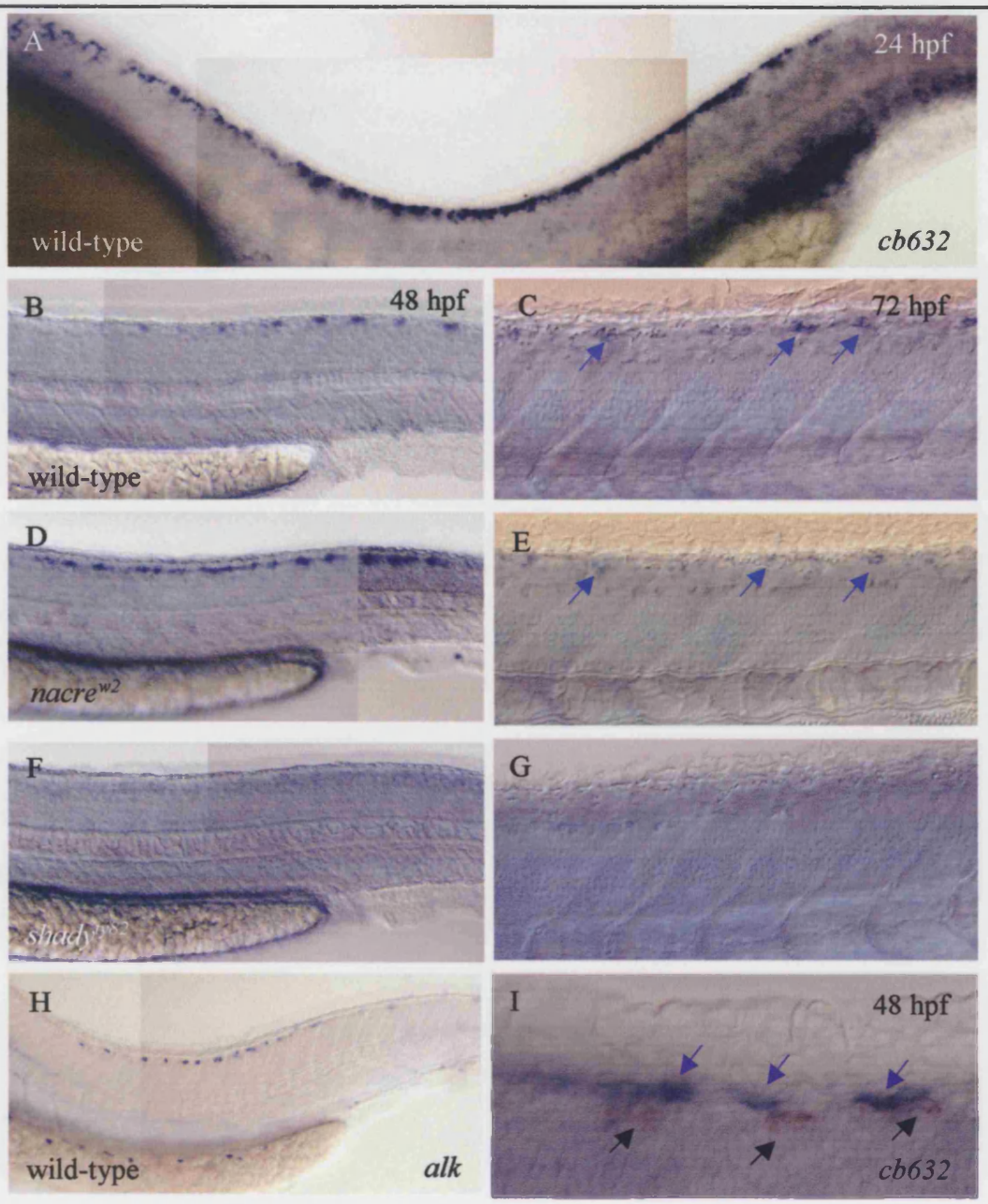

Fig. 3.5: Expression of *cb632*
At 24 hpf *cb632* expression can be seen in the pre-migratory crest (A). At 48 hpf *cb632* is expressed in a pattern reminiscent of that of *alk* (H) in the dorsal stripe of wild-type embryos (B). Higher magnification showed that *cb632* expressing cells (blue arrows) at this stage were located next to cells expressing melanin (black arrows), but did not express melanin themselves (I). At 48 hpf *nacre*^{w2} mutants show an increased number of *cb632* expressing cells in the dorsal stripe (D) compared to wild-type embryos (B). At 72 hpf *cb632* expression in iridophores was strongly reduced in both wild-type embryos (C, blue arrows) and *nacre*^{w2} mutants (E, blue arrows) compared to 48 hpf. No *cb632* expression can bee seen in *shady*^{ty82} mutants at 48 or 72 hpf (E,F). All embryos lateral view.

DS and VS in presumed wild-type embryos (compare Fig. 3.5 B, G). However 7/27 embryos, likely to be *shady*^{ty82} mutants, showed complete absence of this expression (Fig. 3.5 F). The same could be seen at 72 hpf where 3/16 embryos lacked *cb632* expression completely (Fig. 3.5, G). At 72 hpf the number of cells expressing *cb632* in the DS of wild-type embryos was reduced (Fig. 3.9 C). Only a few cells expressed *cb632* at a much lower level than at 48 hpf suggesting that *cb632* was being switched off at this stage.

We also studied expression of *cb632* in the progeny of a *nacre*^{w2} heterozygous in-cross. As described for *shady*^{ty82} all the progeny of a heterozygous *nacre*^{w2} in-cross had the wild-type expression pattern at 24 hpf and it was not possible to identify possible mutants (data not shown). However, at 48 hpf it was possible to identify embryos with an increase of *cb632* positive cells along the DS and VS (Fig. 3.5 D). As *nacre*^{w2} mutants have an increased number in iridophores it was likely that these embryos were the mutants. As expression of *cb632* was weak in wild-type embryos at 72 hpf we pre-sorted the embryos of a heterozygous *nacre*^{w2} in-cross before proceeding with the *in situ* staining in order to be certain of the genotypes. Like in wild-type embryos weak *cb632* expression in *nacre*^{w2} mutants at 72 hpf was observed (Fig. 3.5 E). We were not able to see a clear difference between expression in *nacre*^{w2} and wild-type at this stage. Repetition of this experiment produced the same expression pattern.

The comparison of the pattern of *cb632* and *alk* expression at 48 hpf in wild-type embryos suggested that both were expressed in the same cell type. Taken together with the loss of *cb632* expression in potential *shady*^{ty82} mutants and increase in potential *nacre*^{w2} mutants we suggest that *cb632* is expressed in iridophores at this stage.

To test this we carefully observed *cb632* expression in the DS of wild-type embryos, only mildly treated with PTU to allow some melanisation. It clearly showed that melanin containing cells were located next to the *cb632* expressing cells (Fig. 3.5 I) supporting our suggestion, that they were not melanophores, but iridophores.

III.2.2.A.2. *cb632* maps to linkage group 18

In view of the expression pattern it seemed likely that *cb632* might have a function in iridophore development. To determine if there was a known pigmentation mutant locus or a gene possibly involved in pigment cell development mapping close to *cb632* we mapped *cb632*. The LN54 panel is a convenient way of mapping a gene to a linkage group (see Materials and Methods). Therefore using the LN54 radiation hybrid panel

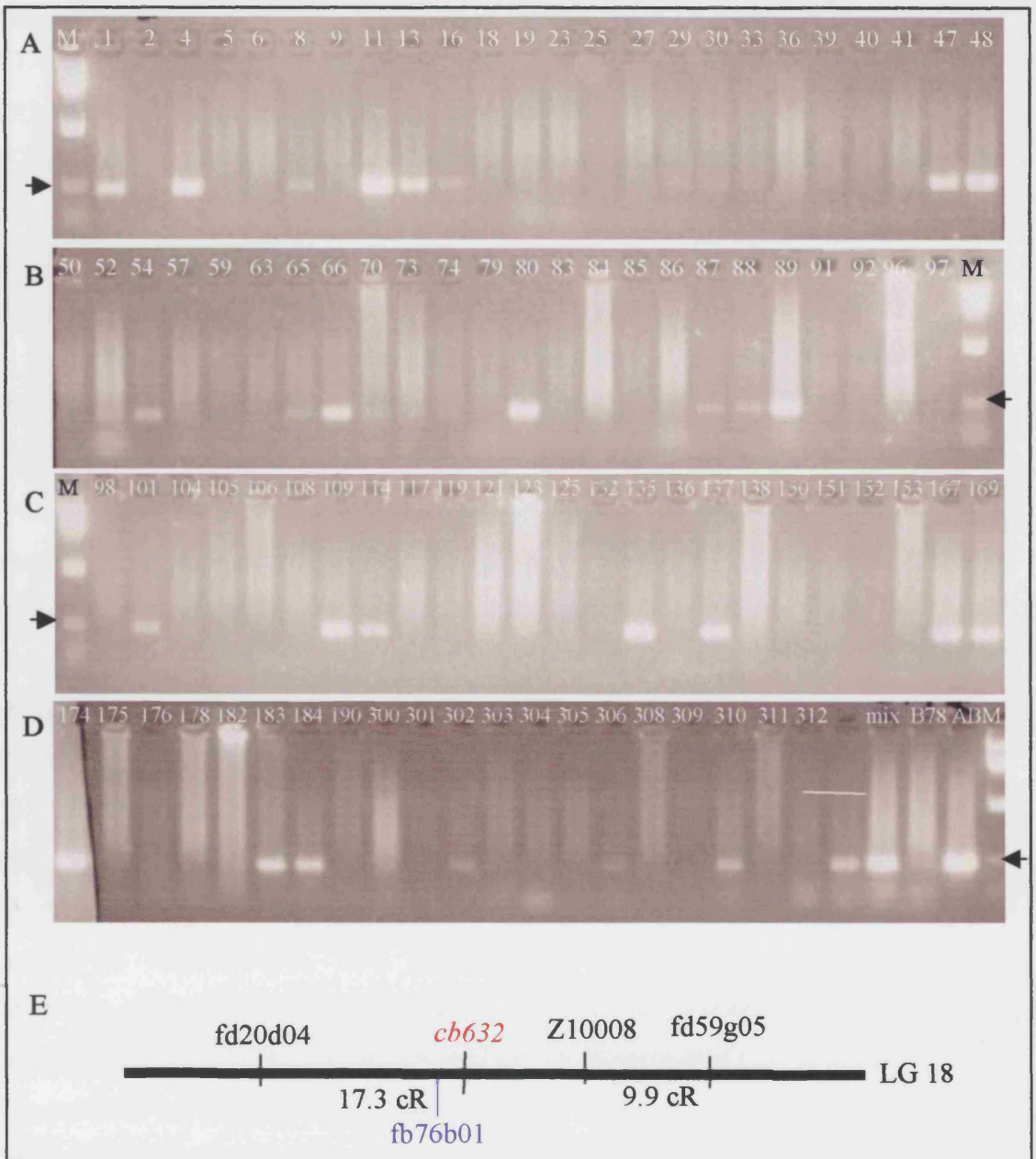

Fig.3.6: Mapping *cb632* on the LN54 Radiation Hybrid Panel

Example of the result obtained by mapping *cb632* on the LN54 Radiation hybrid panel. The control lanes showed the expected product size of ~550bp was amplified from zebrafish genomic DNA (Panel D, AB9). As expected no product was detectable from mouse genomic DNA (Panel D, B78). Radiation hybrids 1,4, 8, 11,13, 16, 47, 48, 52, 63, 65, 79, 80, 86, 87, 88, 98, 108, 109, 132, 136, 153, 167, 169, 182,183, 301, 305, 309, 312 were positive. All positives were confirmed in the duplicate screen. We mapped *cb632* on linkage group (LG) 18 17.3 cR away from fd20d04 (E). Fb76b01 mapped ~0.85 cM from *cb632* (E). Size marker (M) in bp: 1500, 1000, 900, 800 700, 600, 500, 400, 300, 200, 100; 600bp band labelled with arrow

(Hukriede *et al.,* 1999) we mapped *cb632* to linkage group 18 with a LOD of 12.6 (Fig. 3.6). The best marker in the second-best linkage group was linked to the *cb632* with a LOD of 3.8. This indicated that it was very likely that *cb632* is located on linkage group 18. *cb632* is located 17.32cR away from the closest linked marker fd20d04 at position 41.72 (Fig. 3.6 E).

The positional mapping was later confirmed by Ian Woods (http://zfin.org/cgi-bin/webdriver?MIval=aa-mappingdetail.apg&OID=ZDB-GENE-030131-9920).

No genes implicated in pigment cell, specifically iridophore, development were annotated close to the mapped position of *cb632.* We therefore BLASTED the sequence against version Zv4, Zv5 and Zv6 of the zebrafish genome project, but got no convincing hits. BLASTING the sequence against the updated version of Zv6 (whole genome) showed a predicted gene described as similar to guanine monophospate synthetase (zgc:113627). Consistent with the mapping result fb76b01, the closest marker to zgc:113627 was only located 0.85cM away from *cb632* on the radiation hybrid panel.

An overlay of the different existing mapping panels shows that that *cb632* was roughly 3.5 cM away from the closest mapped mutant –*tj266c*- with pigmentation defects. *tj266c* had been isolated during the Tübingen screen (Kelsh et al., 1996) and has been subsequently mapped to position 38.2 on the MHG panel. It has been described as having no xanthophores, dull iridophores, small eyes and a reduced jaw (http://zfin.org/cgi-bin/webdriver?MIval=aa-locusview.apg&OID=ZDB-LOCUS-030213-115).

In conclusion we mapped *cb632* to linkage group 18 close to a gene involved in guanine synthesis. A mutant with a pigmentation defect was located about 3.5 cM away.

III.2.2.B. Characterization of *cb321/id2*

One of the clones on the ZFIN database expressed in neural crest was sb:*cb321*. The clone named sb:*cb321* contained the *id2* gene (RefSeq:NM_201291).

III.2.2.B.1. Description of the neural crest specific expression pattern of *id2*

The characterization of the *id2* expression pattern was done together with Kuisoon Lee, a Masters student. As described by Chong et al. (2005) and on ZFIN, *id2* expression can be seen in cells in positions typical for pre-migratory neural crest cells along the DS and

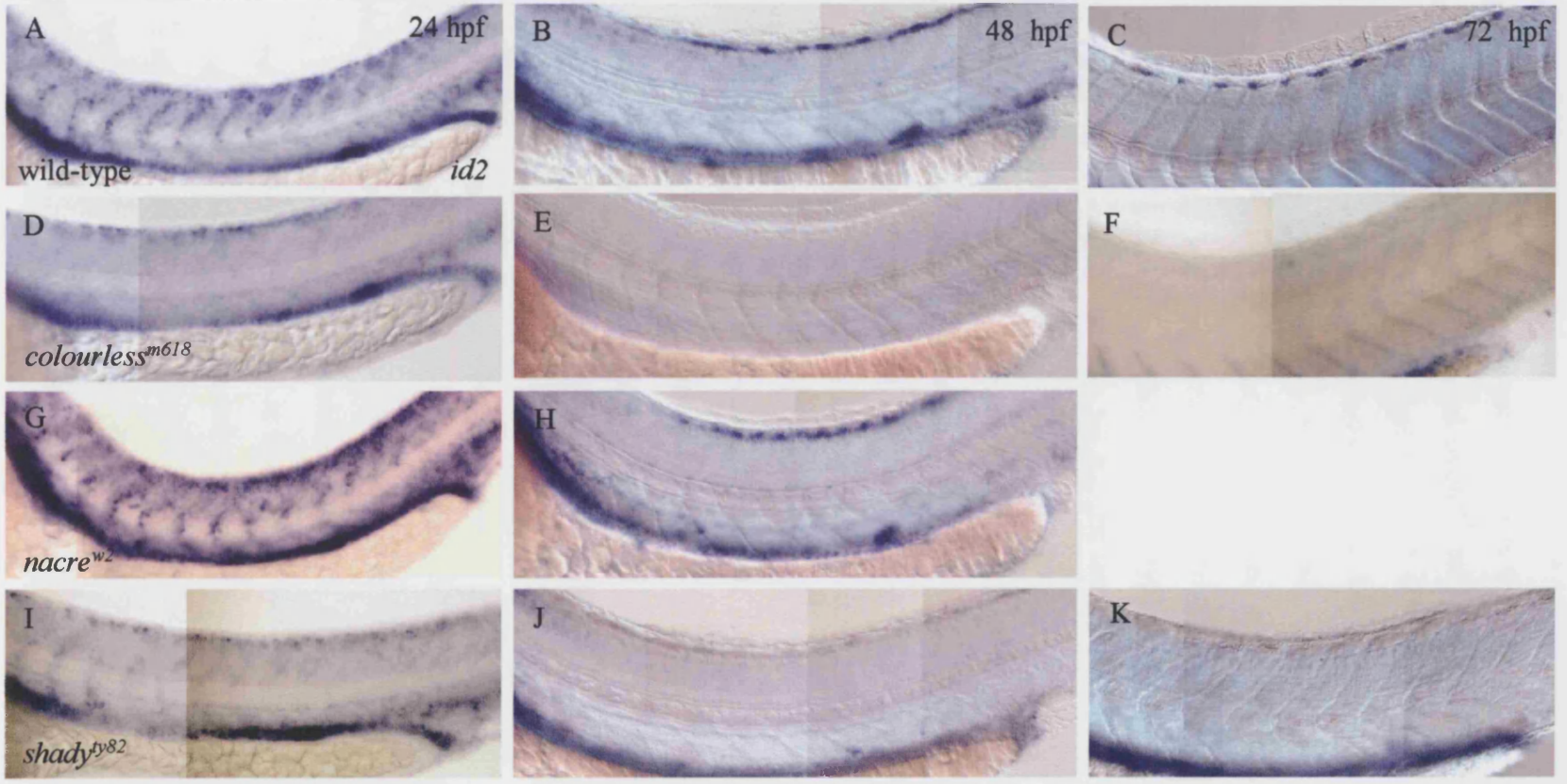

Fig. 3.7: Expression pattern of *id2*

id2 was expressed in pre-migratory and migratory crest in 24 hpf wild-type embryos (A). At 48 and 72 hpf *id2* expression in an iridophore like pattern along the dorsal and ventral stripe can be seen (B, C). *colourless*^{m618} embryos showed *id2* expression only in pre-migratory crest cells at 24 hpf (D). Complete loss of *id2* expression in the dorsal and ventral stripe could be seen at 48 and 72 hpf (E, F). *nacre*^{w2} mutants expressed *id2* in a wild-type like pattern at 24 hpf (G) and 48 hpf (H). At 24 hpf *id2* expression in *shady*^{ty82} mutants could be seen in the pre-migratory crest position and strongly reduced, compared to wild-type, in migrating crest (I). At 48 and 72 hpf no cells in a pigment cell position could be seen expressing *id2* (J, K). All embryos are lateral view.

neural crest cells migrating along the anterior half of the somites in 24 hpf wild-type embryos. Our probe showed the same expression pattern at this stage (Fig. 3.7 A). To test whether these cells were neural crest cells we looked to see whether they were present in *colourless*^{m618}, *nacre*^{w2} and *shady*^{ty82} mutants. *nacre*^{w2} mutants expressed *id2* in a wild-type like pattern at 24 hpf (Fig. 3.7 G). However, a quarter of embryos, presumably the homozygous mutants, from a heterozygous *colourless*^{m618} in-cross expressed *id2* only in pre-migratory, but not migratory, neural crest cells (Fig. 3.7 D). Presumed *shady*^{ty82} mutants had *id2* expression in the pre-migratory crest and strongly reduced, compared to wild-type embryos, in the migratory crest (Fig. 3.7 I).

At 48 hpf *id2* positive cells were detected in the typical iridophore like pattern in the DS and VS of wild-type embryos (Fig. 3.7 B). The number of *id2* positive cells in the DS of *nacre*^{w2} seemed to be increased compared to wild-type embryos (Fig. 3.7 H), consistent with the increase in iridophore number in *nacre*^{w2} mutants (Lister et al., 1999). In, the progeny of both a heterozygous *colourless*^{m618} and heterozygous *shady*^{ty82} in-cross, embryos with no *id2* expression in the DS or VS at 48 hpf was observed (Fig. 3.7 E, J).

At 72 hpf wild-type embryos still expressed *id2* along the DS and VS in an pattern identical to that of the known iridophore markers *alk* and *ednrb1* (Fig. 3.11 C). 10/38 embryos from a *shady*^{ty82} heterozygous in-cross showed loss of the iridophore-like expression (Fig. 3.7 K). Also, roughly a quarter (13/53) embryos from a heterozygous *colourless*^{m618} in-cross lacked expression in the DS and VS (Fig. 3.7 F).

At 4 dpf *id2* was not expressed in iridophores anymore (data not shown). In all potential mutants at 48 and 72 hpf strong brain expression was still present, demonstrating that the *in situ* had worked in these embryos.

The distribution of *id2* positive cells at 48 and 72 hpf in wild-type embryos suggested that it was expressed in iridophores. The loss of this expression in both *colourless*^{m618} and *shady*^{ty82} mutants was consistent with this prediction as both lack iridophores. *nacre*^{w2} mutants had an increase in *id2* positive cells consistent with the ~40% increase of iridophores in these embryos and with our predictions. We therefore conclude, that at 48 and 72 hpf *id2* labels iridophores. The broad expression pattern at 24 hpf suggested that *id2* was expressed in iridophore precursors as well as other neural crest cell precursors.

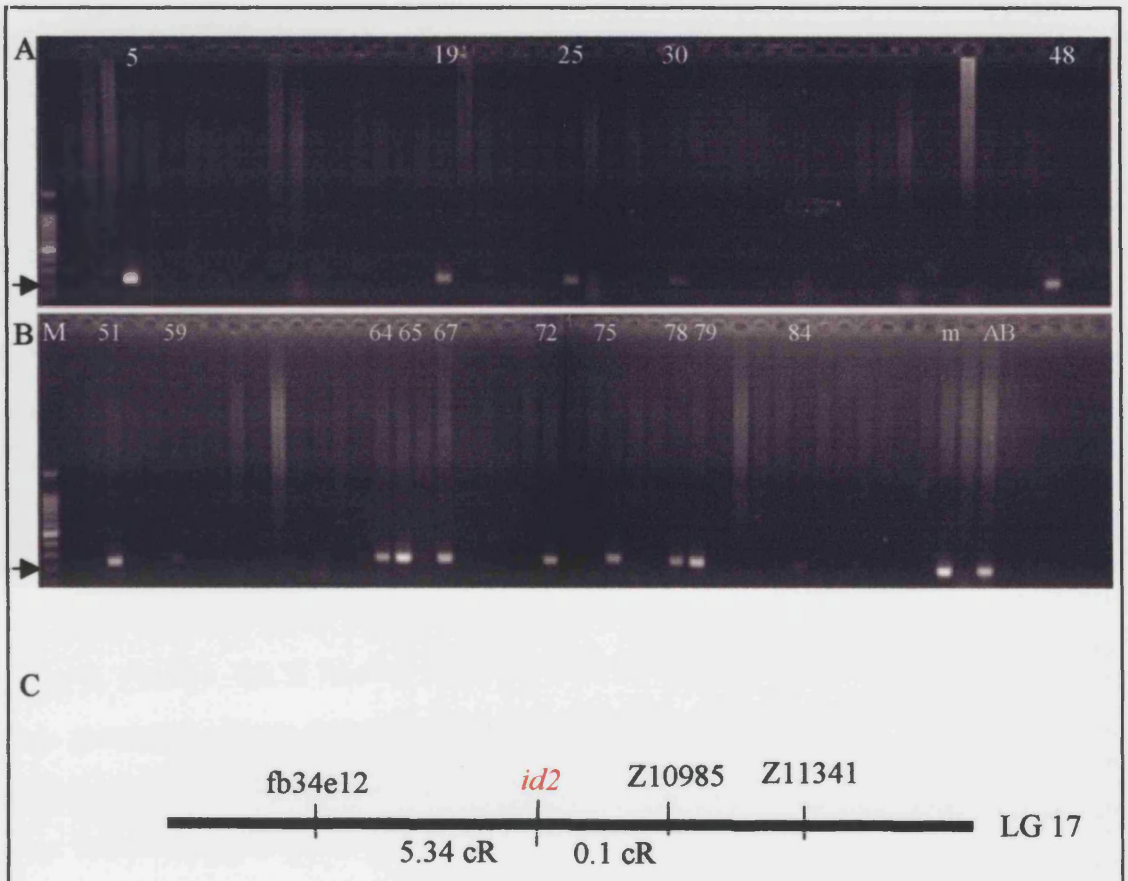

Fig. 3.8: Mapping *id2* on the LN54 Radiation Hybrid Panel
Example of the result obtained by mapping *id2* on the LN54 Radiation hybrid panel. The control lanes showed the expected product size of 250bp was amplified from zebrafish genomic DNA (Panel D, AB9). As expected no product was detectable from mouse genomic DNA (Panel D, B78). Radiation hybrids 5,19, 25 30, 48, 51, 59, 64, 65, 67, 72, 75, 78, 79 and 84 were positive. All positives were confirmed in the duplicate screen. We mapped *id2* on LG 17 5.34 cR away from fb34e12 (C).
Hybrids in panel A: 1kb, 1, 2, 4, 5, 6, 8, 9, 11, 13, 16, 18, 19, 23, 25, 27, 29, 30, 33, 36, 39, 40, 41, 47, 48, 50, 52, 54, 57, 59, 63, 65, 66, 70, 73, 74, 79, 80, 83, 84, 85, 86, 87, 88, 89, 91, 92, 96, 97
Hybrids in panel B: 1kb, 98, 101, 104, 105, 106, 108, 109, 114, 117, 119, 121, 123, 125, 132, 135, 136, 137, 138, 150, 151, 152, 153, 167, 169, 174, 175, 176, 178, 182, 183, 184, 190, 300, 301, 302, 303, 304, 305, 306, 308, 309, 310, 311, 312, mix, B78, AB9
Size marker (M) in bp: 1500, 1000, 900, 800 700, 600, 500, 400, 300, 200, 100; 200bp band labelled with arrow

III.2.2.B.2. *id2* is located on linkage group 17

In view of the expression pattern it seemed likely that *id2* has a function in iridophore development. To address the function of *id2* in zebrafish neural crest development we therefore asked if there was a zebrafish mutant for *id2* available. As no *id2* mutant had been described we decided to map *id2* on the LN54 radiation hybrid panel to identify possible pigmentation mutants close to the *id2* locus (Hukriede et al., 2001; Hukriede et al., 1999). Using the LN54 Radiation Hybrid panel we mapped *id2* to linkage group 17 with a LOD of 11.8 (Fig. 3.8). The best marker in the second best linkage group (linkage group 8) is linked to the *id2* marker with a LOD of 5.7. The low second LOD confirmed that *id2* is on linkage group 17. Unfortunately there was no (un-) characterized pigmentation mutant mapped close by. Interestingly, mapping *id2* this way put it into very close proximity (less than 0.1 cR and therefore less than 11.8 kb away) to Z10985, the Z Marker only 0.1 cM away from *alk* (S.Lopes; in prep.). This close proximity of two genes implicated in iridophore development suggests that they might be regulated together. The positional mapping was later confirmed by Ian Woods (http://zfin.org/cgi-bin/webdriver?MIval=aa-mappingdetail.apg&OID=ZDB-CDNA-040425-399).

III.2.2.B.3. Knockdown of *id2* caused reduction of iridophore number

As there was no obvious candidate pigmentation mutant close to the *id2* locus we decided to investigate its possible role in iridophore development using a morpholino knockdown approach. We designed a morpholino targeting the ATG of *id2* (Fig. 3.9 A). We tested different concentrations of *id2* morpholino and were able to see a reduction in iridophore number when injecting 46 and 92 ng of *id2* morpholino. Counts of iridophore numbers at 4 dpf in H_2O-control and 46 ng *id2*-injected wild-type embryos showed a consistent and significant reduction in iridophore number in the morphants (Fig. 3.9 D). H_2O- control injected embryos had on average 22 iridophores in the DS, whereas embryos injected with 46 ng *id2* morpholino had on average 8 iridophores. The same tendency could be seen in the VS and eye of embryos. All further experiments using *id2* morpholino were performed with 46 ng *id2* morpholino, as this dose already resulted in a significant reduction of iridophore numbers and the general morphology of the embryos was not strongly affected. The general appearance of the embryos was wild-type, although they had a tendency to develop heart oedema. Injection of higher

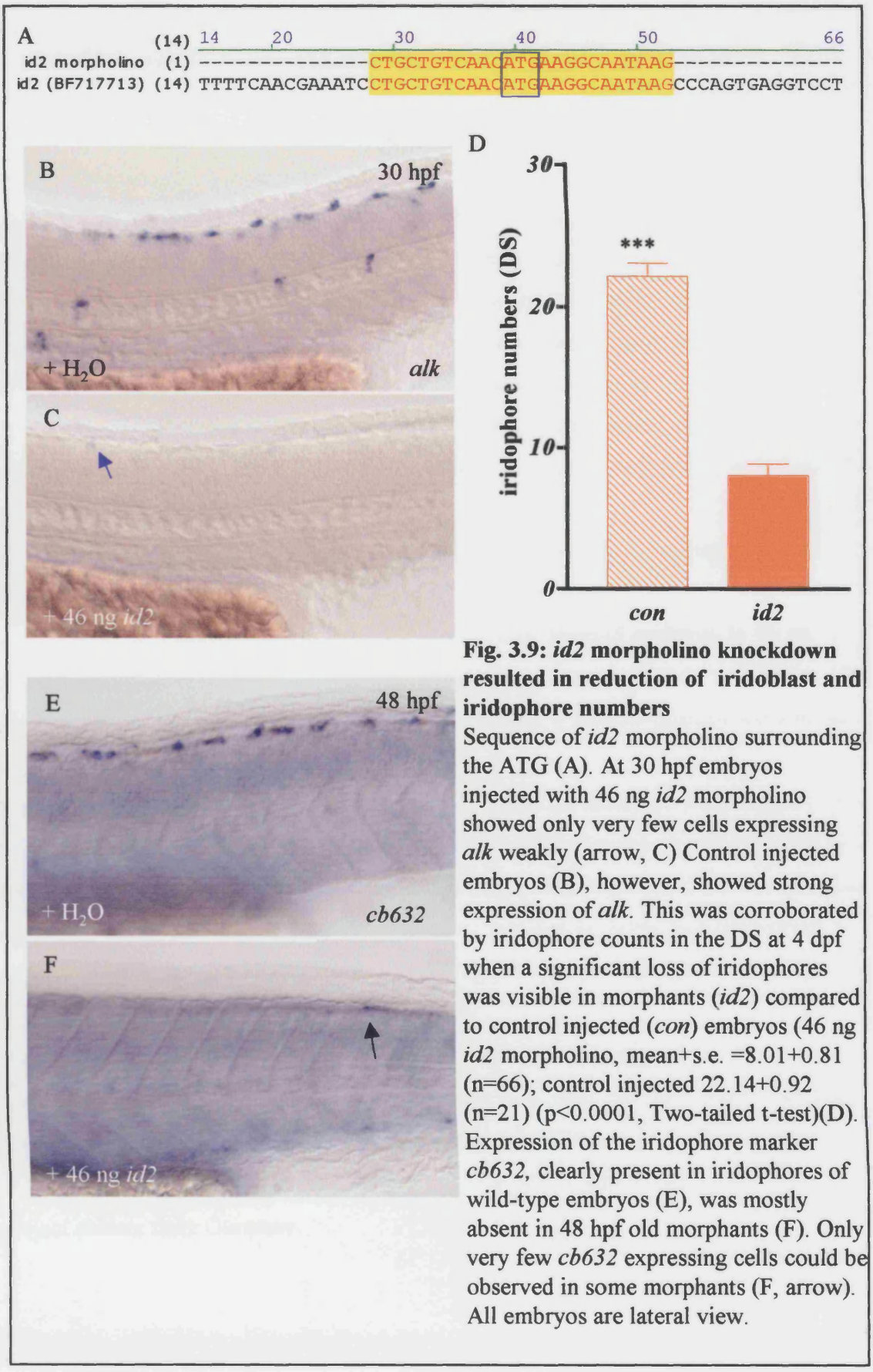

Fig. 3.9: *id2* morpholino knockdown resulted in reduction of iridoblast and iridophore numbers

Sequence of *id2* morpholino surrounding the ATG (A). At 30 hpf embryos injected with 46 ng *id2* morpholino showed only very few cells expressing *alk* weakly (arrow, C) Control injected embryos (B), however, showed strong expression of *alk*. This was corroborated by iridophore counts in the DS at 4 dpf when a significant loss of iridophores was visible in morphants (*id2*) compared to control injected (*con*) embryos (46 ng *id2* morpholino, mean+s.e. =8.01+0.81 (n=66); control injected 22.14+0.92 (n=21) ($p<0.0001$, Two-tailed t-test)(D). Expression of the iridophore marker *cb632*, clearly present in iridophores of wild-type embryos (E), was mostly absent in 48 hpf old morphants (F). Only very few *cb632* expressing cells could be observed in some morphants (F, arrow). All embryos are lateral view.

doses of *id2* morpholino did not only result in loss of iridophores, but caused morphological abnormalities like shorter body axis and smaller body. These morphological abnormalities could be the result of early broad *id2* expression or non-specific effects caused by high doses of *id2* morpholino. Using different iridoblast/iridophore *in situ* markers we next asked how soon in development iridoblast/iridophore development was disrupted. As a control for morpholino efficiency, we raised some embryos to 4 dpf and confirmed that morphants had a reduction in iridophore numbers. First of all we examined the effect of *id2* knockdown on *alk* expression. We could see a clear and strong reduction in number of *alk* positive cells –presumably iridophore precursors- 30 hpf, the earliest stage looked (Fig. 3.9 B, C). At 48 hpf expression of our newly identified iridophore marker *cb632* was nearly completely absent (Fig. 3.9 E, F). Only occasional small cells expressing *cb632* could be observed (Fig. 3.9 F, arrow).

We next examined the expression of the well characterized iridophore marker *ednrb1* in *id2* morphants (Fig. 3.10 A-C). At 3 dpf a significant reduction in the number of *ednrb1* positive cells was noted when comparing H_2O-control injected embryos to 46 ng *id2* injected embryos (Fig. 3.10 C). H_2O-control injected embryos had on average 19 *ednrb1* positive cells, whereas we counted on average 4 *ednrb1* positive cells in *id2* morpholino injected embryos.

Interestingly, injection of *id2* morpholino had no effect on melanophore numbers (Fig. 3.10 D-F). After treatment with Epinephrine we counted melanophore numbers in H_2O-control injected embryos and 46 ng *id2* injected embryos at 4 dpf and could not detect a significant difference (Fig. 3.10 F). H_2O-control injected embryos had on average 51 melanophores and embryos injected with 46 ng *id2* morpholino had on average 49 melanophores.

These results strongly suggested that knockdown of *id2* transcript has an effect only on the iridophore and not the melanophore lineage. We note that this result was fully consistent with the comparison of *id2* expression on the different pigmentation mutants.

In situ experiments on *id2* morphants were repeated and confirmed by Agnes Wyzgol, a project student from Germany.

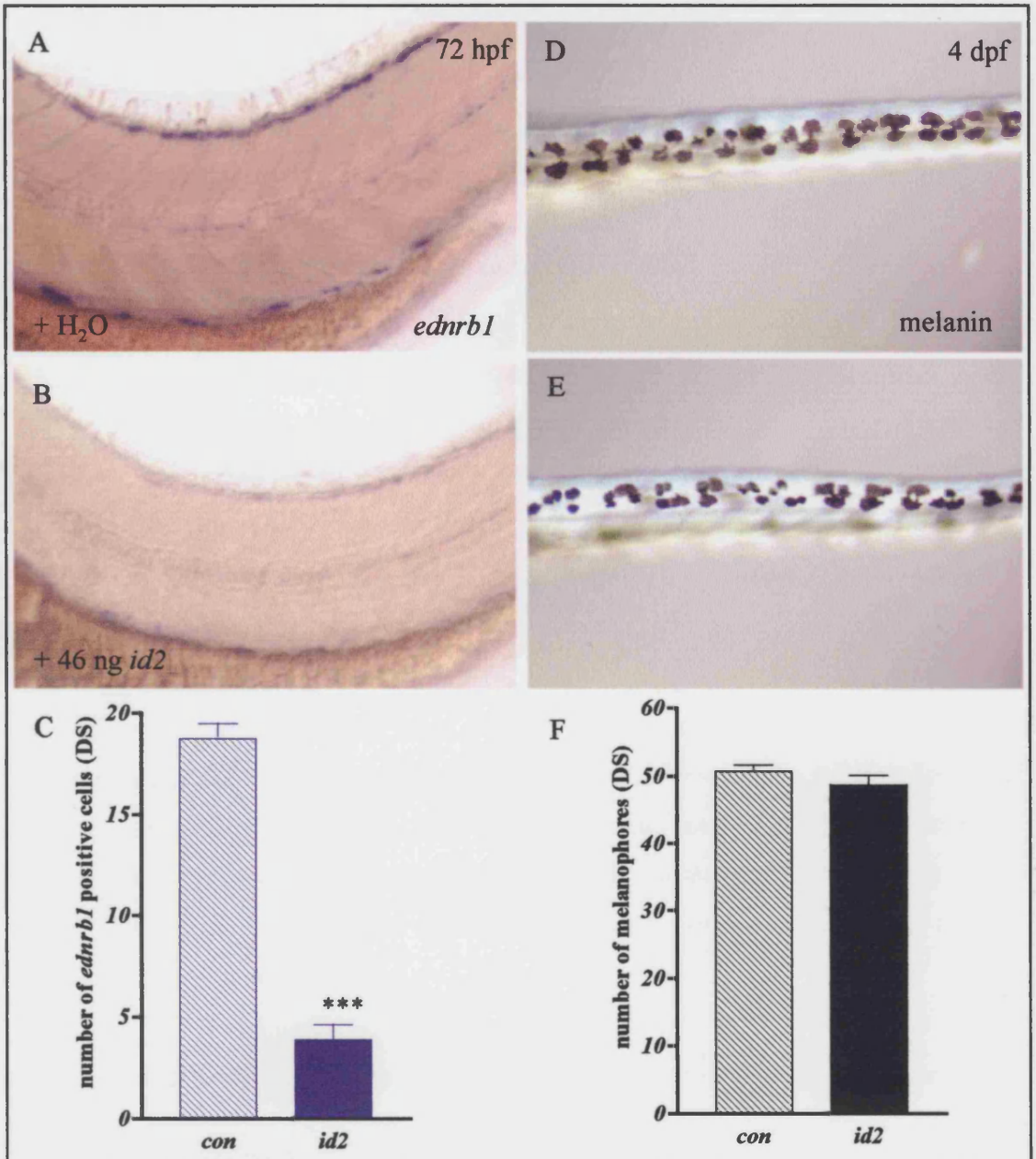

Fig. 3.10: *id2* morpholino knockdown reduced number of *ednrb1* positive cells, but not of melanophores

At 72 hpf the number of *ednrb1* positive cells was reduced in embryos injected with 46 ng *id2* morpholino (A) compared to H_2O control-injected (*con*) embryos (B). Cell counts show that this reduction is significant (C; $p<0.0001$, Two-tailed t-test). H_2O-control injected embryos had on average 19 *ednrb1* positive cells (18.74+0.75 (n=36)), whereas we counted on average 4 *ednrb1* positive cells (3.88+0.75 (n=31)) in *id2* morpholino injected embryos. However, melanophore numbers in H_2O-control injected (D) embryos and 46 ng *id2* injected embryos (E) at 4 dpf and were not significantly different (F: $p<0.05$, Two-tailed t-test). H2O- injected control embryos had on average 51 melanophores (50.70+0.89 (n=23)) and embryos injected with 46 ng *id2* morpholino had on average 49 melanophores in the dorsal stripe (48.69+1.39 (n=29)). A, B lateral view; D, E dorsal view

III.3. Discussion

In the work described here we further characterised the iridophore *in situ* marker *alk*. In addition we identified two new iridophore markers, *id2* and *cb632*.

III.3.1.Characterization of the iridoblast marker alk

To learn more about the expression of *alk* at early stages of embryonic zebrafish development and to possibly use *alk* as a model to identify further iridoblast/iridophore markers at these stages we studied the expression of *alk* up to 36 hpf.

As a first step we asked whether *alk* was expressed maternally. Using two independent sets of RT-PCR we showed that there is no maternal *alk* expression. Staining that could be seen by *in situ* hybridization at these early stages was interpreted as background caused by the long time the embryos were left to develop.

Zygotic expression was confirmed by RT-PCR from the 3 Somite stage on. As the gap between the stages studied -8 cell stage and 3 Somites- is relatively long and contains the midblastula transition, the stage at which zygotic expression starts, it is possible that zygotic *alk* expression starts soon after the midblastula transition. RT-PCR at time points nearer to the midblastula transition has to be performed to investigate this. Consistent with our RT-PCR data we could see broad expression of *alk* by *in situ* hybridisation at 11 Somites.

Having observed broad expression of *alk* at early stages in development we asked when it became specific to the neural crest lineage and iridophores as described by S. Lopes. Earlier studies had shown, by comparison of iridophore and *alk* distribution in individual embryos, that at 72 hpf *alk* was expressed in iridophores. At this stage both *alk* expression and the iridophores formed a row consisting of single spots along the DS and bilaterally along the VS. A very similar pattern, just consisting of fewer cells, had also been observed at 48 hpf, a stage at which iridophores already display their shiny properties and a correlation between iridophore pattern and *alk* expression is obvious. We here observed expression of *alk* forming a single line of spots in the DS as early as 30 hpf. At this stage iridophores do not yet display their shiny properties under incident light, but as the pattern resembles that of iridophores at a later stage we propose that they are iridoblasts. At 22 hpf expression was located in a pre-migratory crest position

and more cells than at later stages were *alk* positive. Between 24 hpf and 28 hpf *alk* positive cells in this domain became less while increasing in the single medially located DS. During further development more iridoblasts appear and populate the DS. Counts of *alk* positive cells in wild-type embryos show a constant increase in the number of *alk* positive cells between 24 and 36 hpf.

It has been proposed that multipotent neural crest cells adopt their final fate by stepwise restriction from a multipotent state to a single fate (Kelsh and Raible, 2002). Different intermediate precursors have been recorded (Baroffio et al., 1988; Le Douarin and Dupin, 1993; Shah et al., 1996). Consistent with this idea Bagnara et al. (1979) had earlier proposed that a common precursor cell can give rise to all pigment cells. A gene expressed in cells of all three pigment cell types at 22 hpf is *ednrb1* (Lister et al., 1999; Parichy et al., 2000a). *sox10* at this stage is more broadly expressed in parts of pre-migratory and migratory crest including pigment cell precursors (Dutton et al., 2001). Cells labelled with *sox10*, a transient generic marker for neural crest, at 22 hpf give rise to a variety of neural crest derivatives including all three types of pigment cells, enteric neurons and dorsal root ganglia (Dutton et al., 2001; Elworthy et al., 2003; Elworthy et al., 2005; Kelsh, 2006). The *alk* expression at 22 hpf is reminiscent of that of *ednrb1*. Considering the precedent of *ednrb1* it is therefore possible, that *alk* at 22 hpf labels a pigment cell precursor -a chromatoblast- or a precursor for iridophores and one or more other neural crest fates. This might explain why *alk* expression in the neural crest is broader at 22 hpf than 24 hpf. *alk* double *in situ* hybridisation with early known markers for other neural crest markers such as *dct* should help resolve this question. The *shady/alk* phenotype however, does not deliver any clues as to what kind of common precursor *alk* might label at 22 hpf as so far no defect in a neural crest derivative other than iridophores has been observed (Lopes et al., in prep.).

In her thesis S. Lopes (Lopes et al., in prep.) had described complete loss of *alk* expression in *shady*^{ty82} mutants at 48 hpf. We extended these studies and asked at what point in time during development it was possible to distinguish *shady*^{ty82} mutants from wild-type embryos based on *alk* expression. At 24 hpf *shady*^{ty82} mutants were indistinguishable from wild-type embryos, similar to *colourless*^{m618} mutants, that express *sox10* in a wild-type like pattern at this stage. It is conceivable that maintenance of *alk* expression might require functional *alk* protein. This would be consistent with wild-type like expression of *alk* at 24 hpf, followed by loss of expression subsequently in mutants.

In summary this suggested that *shady*^{ty82} mutants initially express *alk* and that due to the high variation of *alk* positive cells it was not possible to distinguish the *shady*^{ty82} mutants from the wild-type embryos at early stages.

Even though there was a change in number of *alk* positive cells in *shady*^{ty82} mutants, the strength of *alk* expression in the remaining cells was not reduced compared to expression in wild-type embryos. We therefore concluded that level and timing of *alk* expression within the remaining expressing cells in *shady*^{ty82} mutants was the same as in wild-type embryos. At stages later than 31 hpf *alk* expression was essentially absent with the exception of a very few cells that showed normal levels of *alk* expression.

III.3.2. cb632 and id2 are two new iridophore markers

To identify and characterize additional iridophore precursor/iridophore markers we had searched the ZFIN database for genes expressed in a pattern similar to *ednrb1* and *alk*. Two of the clones that looked interesting were *cb321/id2* and *cb632*. We concentrated on and will discuss the expression of these genes in potential iridophores and their precursors only although they were expressed elsewhere.

III.3.2.A. *cb632* is an iridophore marker

By performing *in situ* hybridisation with *cb632* on various characterized pigmentation mutants we were able to identify *cb632* as a new iridophore marker.

At 48 hpf *cb632* expression was observed in a pattern reminiscent of *alk* and *ednrb1* along the DS and VS (Parichy et al., 2000a). This spotted pattern of expression along the DS and VS is, to our knowledge, unique to iridophores. Together with the loss of cells expressing *cb632* in *shady*^{ty82} mutants and increase of cells expressing it in *nacre*^{w2} mutants this strongly suggested that *cb632* was expressed in iridophores. This is also true at 72 hpf even though the expression is weaker and fewer cells express *cb632*. Further evidence that *cb632* is an iridophore marker came from the observation that *cb632* and melanin are expressed in cells close to each other, but not in the same cells, showing that *cb632* is not expressed in melanophores. We therefore conclude that *cb632* at 48 and 72 hpf is an iridophore marker. The DS and VS are not the only places typical for iridophores where *cb632* expression can be seen. We were also able to observe

expression in the eye further supporting our theory that cb632 is expressed in iridophores.

Using the LN54 radiation hybrid panel we mapped *cb632* onto linkage group 18 and identified a gene similar to *gmp synthetase* as a candidate for *cb632*. That the identified gene was very similar to *gmp* synthetase was confirmed by protein comparison, showing 85.47% identity to human GMP synthetase, published on the Unigene site (http://www.ncbi.nlm.nih.gov/UniGene/clust.cgi?ORG=Dr&CID=8251). GMP synthetases are necessary for the *de novo* generation of guanine (Berg et al., 2002).

The expression of *cb632* seems transient as at 72 hpf its expression in iridophores was strongly reduced, but still weakly visible in wild-type embryos and *nacre*^{w2} mutants suggesting that it was in the process of being down-regulated at this stage. Iridophores first start displaying their iridescent properties weakly at about 40 hpf (X. Yang; personal communication). From 72 hpf the larval pattern of iridophore distribution does not change significantly. Reflection of light in the organelles of iridophores, the reflecting platelets, is responsible for the iridescent properties of iridophores. Reflecting platelets contain stacks of guanine discs each of which is composed of a stack of guanine crystals with intervening cytoplasmic spaces. (Bagnara, 1998) Presence of strong *gmp synthetase* expression in iridophores therefore seems plausible as large amounts of guanine crystals need to be produced. The fading of *gmp synthetase* expression at 72 hpf could indicate that the iridophores have completed there reflecting platelet assembly and maybe that the guanine crystals are very stable and do not need to be produced in the embryo anymore. This would mean that *cb632* is a marker for iridoblasts and maturing iridophores only.

At early stages of development *cb632* expression seemed not to be restricted to the iridophore lineage. At 24 hpf the pattern of *cb632* in wild-type, *nacre*^{w2} and *shady*^{ty82} mutants seemed identical and again, maybe most similar to *alk* at 22 hpf and *ednrb1* at 24 hpf. The broad expression in a pre-migratory crest position at 24 hpf suggests that *cb632* is, similarly to other neural crest markers like *alk* and *ednrb1*, expressed not only in iridophore precursors. Similarly to both other markers and in concordance with the progressive fate restriction model it is possible that it labels all pigment cell precursors at this early stage. Alternatively it could label a precursor common to iridophores and cells of one or more other non-pigment neural crest fates. Careful double *in situ* studies

of *cb632* with *alk*, xanthoblast or melanoblast markers will be able to shed more light on this question. Interestingly *cb632* is still expressed broadly in the pre-migratory crest at 24 hpf, a stage when expression of *alk* has started to become less broadly expressed.
The closest pigmentation mutant, *tj266c*, maps about 3,5 cM away from *cb632*. True estimates of the distance between *tj266c* and *cb632* are difficult to establish and could be much smaller or larger though, as it is difficult to reliably calculate distances using two different mapping panels (in this case the LN54 Radiation Hybrid panel (*cb632*) and the MGH panel (*tj266c*)). That *cb632* might be coding for the gene mutated in *tj266c* is therefore highly speculative, but attractive. The unnamed mutant *tj266c* is described as having no xanthophores, dull iridophores, small eyes and a reduced jaw (Kelsh et al., 1996). The fact that iridophores are present, but dull, in *tj266c* might well be caused by a defect in the production or maturation of the reflective platelets. As *gmp synthetase* is involved in guanine production it is a possible candidate. The described loss of xanthophores in *tj266c* would then be an indication as to what other neural crest derivative *cb632* is expressed in 24 hpf old embryos. *tj266c* has only been characterized preliminarily and it is therefore possible that the xanthophores are not completely lost, but that they are present and just lacking pigments as xanthophores require GTPs for pteridine *de novo* synthesis (Ziegler, 2003). However no *cb632* expression can be seen in the jaw. But studies at early developmental stages indicated that *cb632* might be expressed ubiquitously at low levels with increased expression in eyes, tectum and somites (Thisse et al., 2001).
A strong indication that *cb632* is a real candidate for the *tj266c* phenotype could be reached from antisense Morpholino experiments. Reproduction of the *tj266c* phenotype after *cb632* Morpholino injection would indicate that it is a strong candidate. The same would be true if a (partial) rescue of the *tj266c* phenotype could be observed by injection of full length *gmp synthetase*.
Only cloning of the gene mutant in *tj266c* and identification of the mutation would allow us to establish a definite relationship between *tj266c* and *cb632*.

III.3.2.B. *id2* is expressed in iridophores

In our search for new iridophore markers we identified the gene in clone sb:*cb321*, *id2*, as a new iridophore marker. It has been suggested previously that Id2 proteins can act as general inhibitors of cellular differentiation (Yokota et al., 2001).

Like *ednrb1* and *alk*, *id2* is expressed in an iridophore like pattern in 48 and 72 hpf wild-type embryos. Complete loss of this expression in *colourless*^{m618} and *shady*^{ty82} mutants combined with the increase of the number of cells expressing *id2* in *nacre*^{w2} embryos let us to the conclusion that it is an iridophore marker at these stages. In accordance with *id2* being expressed in iridophores we observed a strong reduction of iridophore numbers after injection of *id2* morpholino. That cells were absent, rather than just not pigmented, was indicated by significant reduction of *ednrb1* positive cells at 72 hpf. Knockdown of *id2* function showed an effect on iridophore development as early as 30 hpf with a nearly complete loss of all iridoblasts as seen by *alk in situ* hybridization. We have not studied an earlier effect of *id2* knockdown on iridophore development yet, but as *id2* is expressed in the neural crest as early as 10 Somites (Thisse et al., 2001) it may have an effect even earlier. However studies in mouse mutants have shown that *id* genes act redundantly in some tissues (Lyden et al., 1999; Norton, 2000). As *id3* is expressed in neural crest during early development (Dickmeis et al., 2002), *id2* and *id3* function might be redundant in at least most neural crest cells at this stage. That would also explain why, so far, after injection of *id2* morpholino only defects in iridophore development, but not other neural crest cell development could be observed despite *id2* being expressed in other cell types. Examination of *alk* expression at earlier stages of development, such as 24 hpf should help clarify how early during iridophore development *id2* is required.

At 24 hpf *id2* is expressed broadly in pre-migratory neural crest. The expression in the pre-migratory and migratory crest cells in trunk and tail strongly resembles that of *sox10* (Dutton et al., 2001; Parichy et al., 2000a). The broadness of its expression suggests that, analogous to the already described iridophore markers *ednrb1*, *alk* and *cb632, id2* at 24 hpf is not only a marker for iridophore precursors, but labels precursors for other neural crest cell fates as well. Even though its expression is similar to these already characterised neural crest markers it is possible that *id2* labels different combinations of crest derivatives such as melanoblasts, precursors of the glia of the lateral line nerve, sympathetic neurons or the dorsal root ganglia. Our morpholino knockdown experiments and expression studies indicate that *id2* is not expressed in melanoblasts or precursors for neurons and glia of the dorsal root ganglia. *In situ* hybridisation after *id2* morpholino knockdown with melanoblast markers, such as *dct*, and early glia marker, such as *neurogenin1*, respectively will verify this suggestion.

At 48 and 72 hpf *id2* is expressed in precursors of the glia of the posterior lateral line nerve (data not shown). Loss of an early marker such as *foxd3* could indicate a function of *id2* in the development of the glia of the lateral line nerve.

In our *id2* expression pattern studies we observed expression in nearly all the domains described by Chong et al. (2005) at 24 and 48 hpf, showing that our *in situ* probe worked. The only exception is lack of expression in the neuromasts in our studies, which is replaced by expression in the posterior lateral line nerve. We were however able to expand the number of expression domains at 48 hpf by identifying expression in iridophores. Chong et al. only describe expression in the brain, neuromasts of the lateral line and corpuscle of Stannius at this stage. In addition they describe the general expression of *id2* at 48 hpf compared to 24 hpf as relatively weak. We were not able to confirm this as our expression seems to have similar strength at both stages. We propose that this difference might be attributed to different developing times. Whereas we developed our 48 and 72 hpf old embryos longer (~3-4 days) than the 24 hpf old embryos (~1 day) Chong and colleagues might have stopped them all at the same time. That there might be a difference in length of exposure time is visible in the brain expression. Chong et al. are able to distinguish different domains, but ours have been developed so long that this is no longer possible (data not shown). But only after the long exposure time is expression in the iridophores visible suggesting that expression in iridophores compared to the brain might be low level. Alternatively, it might be more difficult to detect expression in iridophores, due to their physiology, compared to other tissues. Detection of other iridophore markers, such as *alk* or *cb632*, at 48 hpf also requires long developing times.

In putative *shady*^{ty82} mutants *alk* as well as *cb632* seem to be expressed in a wild-type pattern at 24 hpf. *id2* expression, however, is slightly reduced, but still present in some pre-migratory and migratory neural crest cells. It is possible that at this stage loss of a functional *alk* leads to loss of *id2* in iridophore precursor cells resulting in the reduced *id2* expression. This would imply a direct or indirect dependence of *id2* on *alk*.

We can only speculate about the function of *id2* in zebrafish development. But its maintenance in iridophores up to 72 hpf and its loss from most other crest derivatives suggests that it is necessary for iridophore development. Id2 has been shown to function

in different ways in different cells types and organisms (Cooper et al., 1997; Martinsen and Bronner-Fraser, 1998; Norton, 2000; Yokota et al., 2000). ID proteins have been implicated in multiple different processes during development such as proliferation, differentiation, cell cycle control and apoptosis (Yokota, 2001). ID proteins often function as general inhibitors of differentiation and are therefore highly expressed in undifferentiated cells. Once ID is down-regulated, cells can differentiate. But ID proteins can also adopt the opposite function, as positive regulators. ID is then required for determination and maintenance of a differentiated state.

Maintenance of *id2* expression in iridophores once they already possess reflecting properties suggests that *id2* might act as a positive regulator in iridophores. To determine the function of *id2* in development of iridophores further studies are necessary. As we were not able to identify a mutant, with defects in iridophores or other neural crest defects, mapping closely to *id2* loss of function studies will have to be done using morpholino knockdown. Alternatively an *id2* mutant might be identified through TILLING (Targeting Induced Local Lesions in Genomes). Observation of the effects of *id2* knockdown on cell proliferation and cell death will help explain the role of *id2* in iridophore development. Reduction of cell proliferation or apoptosis of iridoblasts/iridophores, detectable with PH3-antibody and TUNEL staining respectively, after reduction/loss of *id2* function would indicate an active role of *id2* in regulation of these processes. Determination of when expression of iridoblast/iridophore markers is first lost should help clarify when *id2* is first necessary in iridophore development. In addition over-expression studies should contribute to our understanding of *id2* function.

Chapter IV Preliminary characterization of *parade*^{tj262}

IV.1. Introduction

Understanding neural crest development can help us understand complex key steps during development such as patterning, regulation of cell number through proliferation and apoptosis, fate choice and cell migration. A light could already be shone on some of the different key aspects of neural crest development by looking at zebrafish pigmentation mutants.

During wild-type embryonic development zebrafish embryos/larvae form a characteristic, highly conserved and reproducible, pigment pattern comprising of four body stripes: DS, VS, LS and YSS (Fig. 1.1.A). All stripes except the LS, that contains only melanophores, are made up of melanophores and iridophores (Fig. 1.1.A, B). Xanthophores are distributed over the whole body of the zebrafish embryo with higher numbers located in the dorsal half. During a large scale screen in Tübingen 285 mutants with pigment pattern defects were isolated (Kelsh et al., 1996). Only a few of those mutants have been characterised so far and the focus has been on ones that have a defect in patterning mostly due to lack of one or more pigment cell types. *shady* mutants for example lack iridophores, but no difference in the patterning of the remaining pigment cell types has been shown (Lopes et al., in prep.). The almost complete loss of pigment pattern in *colourless* mutants is due to the almost complete loss of all pigment cell types (Dutton et al., 2001). In both cases the few escaping pigment cells that can be found are in wild-type positions (Kelsh and Eisen, 2000). Considering these phenotypes it is not surprising that the roles suggested for *sox10* and *alk* lie in different specification steps during neural crest development (Dutton et al., 2001; Elworthy et al., 2003; Kelsh and Eisen, 2000)(Lopes et al., unpub.). The *mitfa* mutant *nacre* couples complete loss of melanophores with a 40% increase of iridophores (Lister et al., 1999). Generally all iridophores can be found in their wild-type location in the stripes and only some of the supernumerary iridophores are, for so far not discovered reasons, in ectopic positions (Lister et al., 1999).

As the mechanisms determining how the embryonic pigment pattern develops are not revealed by mutants clearly lacking one or more chromatophore types, examination of mutants with misplaced pigment cells and identifying the mechanisms behind the misplacement might help us identify mechanisms of early pigment pattern formation. During the Tübingen mutagenesis screen in 1996 some mutants with ectopic pigment

cells leading to "abnormal chromatophore distribution", such as *moonshine, tiger, floating head, momo* and *parade* have been isolated (Kelsh et al., 1996). These have either not been characterised yet or the focus during their characterization has been mostly on phenotypes other than pigmentation (*moonshine* (Ransom et al., 2004), *floating head* (Melby et al., 1997)). One of the mutants isolated that has not been characterised yet was *parade*. Two *parade* alleles with identical strength of phenotype, *tj262* and *tv212*, were isolated. The prominent feature of the *parade* mutant phenotype are the 'mixed chromatophores' (Kelsh et al., 1996), pigment cells appearing to contain organelles of iridophores and melanophores, positioned just below the notochord. The chromatophores can be observed as early as 3 dpf and show characteristics of both melanophores and iridophores.

The only embryonic zebrafish mutant with misplaced pigment cells characterised so far is *choker* (Svetic et al., 2007). *choker* mutants show not only a complete absence of lateral stripe melanophores, but also a melanophore collar spanning the first five trunk somites. By studying *choker;nacre* double mutants it has been shown that a concurrent loss of xanthophores in the collar area of *choker* mutants is independent of the accumulation of melanophores. The melanophore collar starts forming by abnormal migration of melanophores from both the DS and VS between 36- 48 hpf. Ectopic expression of *sdf1a* in the region of the forming collar has been linked to the collar appearance (Svetic et al., 2007). Taking together the results from the studies on *choker*, other pigment mutants and insights from studies on amphibians and medaka it has been suggested that local environmental cues as well as chromatophore interactions are important for embryonic pigment pattern formation (Kelsh, 2004).

Xanthophore-melanophore interactions have been shown to be necessary and sufficient in establishing the adult pigment pattern (Maderspacher and Nusslein-Volhard, 2003; Parichy et al., 2003). Thus loss of xanthophores in *panther/fms* mutants results in loss of the melanophore stripe organization (Parichy et al., 2003). Melanophore intrinsic *obelix* function has been shown to be important for boundary formation of the melanophore stripes. While the number of chromatophores is thought not to be affected, lack of *obelix* results in fewer, undulating and wider stripes (Maderspacher and Nusslein-Volhard, 2003). Iridophores, however, seem not to be necessary for adult stripe formation (Kelsh, 2004). In addition to the chromatophore interactions there are indications that pre-patterning of the embryo might be important for the position of the stripes (Kelsh, 2004). A reaction-diffusion mechanism of morphogens has been

suggested to establish a pre-pattern (Turing, 1952). Formation of the pigment pattern in the zebrafish mutant leopard has been shown to correlate with a model based on a pre-pattern (Asai et al., 1999).

Not only is the overall pigment pattern organised but there also seems to be local organisation of pigment cells. Careful, recurrent arrangement of melanophores, iridophores and xanthophores has been described by Bagnara as the 'dermal chromatophore unit' (Bagnara et al., 1968). In the dermis of anurans the melanophores form the lowest layer with an iridophore on top followed by a xanthophore. The melanophore has been described to extend 'fingers' around the iridophore and xanthophore. Even though there is a close association between all the three chromatophore types present Bagnara and colleagues at the time did not find any indications of a 'communicating mechanism' between the melanophores and iridophores (Bagnara et al., 1968).

Formation of pigmentation patterns have not only been studied in zebrafish and amphibians. Some studies of pigmentation mutants in other species where pigment cells in ectopic positions have been described show that these can help us discover new genes involved in neural crest development. A large number of the mouse mutants characterised so far show changes in their coat colour caused by reduction of a pigment cell type (Baxter et al., 2004; Nakamura et al., 2002). However, recent screens in mice have opened up a whole new group of pigmentation mutants to look at. Whereas traditional screens have generally focused on coat colour i.e. hair, the focus was now also on mouse skin colour (Fitch et al., 2003; Hrabe de Angelis et al., 2000; Nolan et al., 2000; Shiroishi, 2001). During a global screen for chemically induced dominant phenotypes 10 heterozygous phenotypic dark skin (*Dsk*) mutants, with increase in pigmentation of the non hairy body areas such as the footpad, have been isolated and described (see Table 1.1 in introduction)(Fitch et al., 2003). In addition an increase in skin pigmentation can be seen in the ears and tails and sometimes a slightly darker coat colour. The increase in dermal melanocytes in *Dsk1*, *Dsk7* and *Dsk10*, however, has been shown to be a primary, *Ednrb*-dependent, effect caused by an increased melanoblast number in the dermis. All three mutations are in G-protein α-subunits with *Dsk1* and *Dsk10* being gain-of-function mutations in *Gnaq* and *Dsk7* in *Gna11* (Van Raamsdonk et al., 2004) van Raamsdonk et al. suggest, that as no difference in proliferation, apoptosis and dorsoventral migration could be seen in mutants compared

to wild-types the increased number of dermal melanoblasts is caused by an increase in melanoblasts caused by increased Gq signalling.

Another mouse mutant that has been described as having increased pigmentation, more specifically increased amounts of melanin in epidermal keratinocytes, in the ventral feet, footpad and all nonhairy skin is sooty foot (Budd et al., 1997). Even though it has been mapped to Chromosome 2 no candidate gene responsible for the increase of melanin within the epidermal keratinocytes could be identified. The authors propose two scenarios to explain the phenotype. Firstly, a defect in melanoblast migration could lead to an increase in melanin secreting melanocytes in the footpads causing the dark foot phenotype. Or else a change in rate of melanin production of melanocytes normally producing low levels or no melanin present in the footpad could cause the sooty foot phenotype. (Budd et al., 1997)

A pigmentation mutant where presence of ectopic melanocytes has been associated partly with a defect in regulation of migration is the Silkie fowl (Faraco et al., 2001; Reedy et al., 1998b). Even though in comparison to Lightbrown Leghorn the Silkie fowl has a delay in melanocyte development they show an increased number of ventral pathway melanoblasts at later stages. These melanocytes are located in areas such as the connective tissues, mesenteries, peritoneum and the meninges of the brain and spinal cord, which normally do not contain any melanocytes (Faraco et al., 2001). This ectopic positioning is due to melanoblasts populating the normally not used ventral pathway and probably also to continued cell proliferation of the ventral melanoblasts. A correlation has been shown between the appearance of melanoblasts/cytes and the loss of lectin peanut agglutinin (PNA), known to label tissues that act as migration barriers, in Silkie fowl (Faraco et al., 2001).

While the mutants described above seem to mostly have ectopic and supernumerary pigment cells the ectopic chromatophores distinguishing *parade* mutants from their wild-type siblings have not only been described to be ectopic, but it has been suggested that they are of mixed chromatophore fate. Cells of mosaic chromatophore fate have been shown in multiple species.

Described examples of pigment cells containing organelles of two or more pigment cell organelles within one chromatophores include the erythrophores of the red-backed salamander (*Plethedeon cinereus*) that contain melanosomes, reflective platelets and pterinosomes (Bagnara, 1991). Pterinosomes and reflective platelets have been found in

the garter snake (*Thamnophis sp.*) (Bagnara, 1999). Many similar examples have been described for other amphibians, fish and reptiles ((Bagnara, 1991; Bagnara, 1998). Not only have pigment cells with mosaic organelles been described, but there are also cases of pigment cells where the organelles themselves are mosaic. One such example are some of the iridophores in the iris of the dove that contain partly melanized reflective platelets (Bagnara et al., 1979). Similarly chromatophores in the kidney and liver of the leaf frog (*P.danicolor*) contain elements of all three organelles, melanosomes, reflective platelets and pterinosomes, within one limiting membrane (Bagnara et al., 1979).

The above described examples of pigment cells and organelles of mixed fate led Bagnara to propose the model of a 'Common origin of pigment cells' – where a stem cell contains a primordial organelle that possesses the ability to differentiate into any pigment cell organelle (Bagnara et al., 1979). Problems in the differentiation process could then lead to pigment cells with organelles characteristic of different fates. It has been shown that some totipotent neural crest cells are under the right conditions able to give rise to neuronal, glial, pigment and mesenchymal derivatives (Le Douarin and Dupin, 2003). More commonly though multipotent precursors have been observed to give rise to restricted groups of progenitors such as glia and melanocytes or glia and neurons (Le Douarin and Dupin, 2003; Raible and Eisen, 1994a). It is therefore possible that a precursor giving rise to all different pigment cells exists as well. Evidence for the possible existence of such a common chromatoblast precursor comes from knowledge of gene expression patterns. *ednrb1* for example may be expressed in cells able to give rise to melanophores, iridophores and xanthophores in zebrafish at early stages in development as has been shown by overlap with markers specific for the different fates (Parichy et al., 2000a). Also *gch*, a xanthoblast marker, and *mitfa*, a melanoblast marker, have been shown to be expressed in the same cell (Pelletier et al., 2001). The existence of a partially restricted neural crest precursor cell, such as a chromatoblast, might help explain why neural crest cells in culture have the ability to transdifferentiate into another pigment cell type. In amphibian cell culture studies xanthophores and iridophores transdifferentiated into melanophores (Ide, 1978; Ide and Hama, 1976). Video recording of axolotl cell cultures also showed xanthophores differentiating into melanophores (Thibaudeau and Holder, 1998).

These examples all focus on transdifferentiation between pigment cells. But there are also examples of non-pigment neural crest derivatives differentiating into pigment cells. In the presence of bFGF, Schwann cells can transdifferentiate into melanocytes

(Sherman et al., 1993). Another example is the quail mutant *silver* where loss of *mitfa* leads to retinal pigment epithelium cells transdifferentiating into neural retina (Mochii et al., 1998). These last observations lead to the proposal that the increase of iridophore numbers in *nacre* mutants might be caused by a fate switch from melanoblasts to iridoblasts (Lister et al., 1999). If, as it has been suggested, the ectopic pigment cells in *parade* are of mixed fate, characterization of *parade* will shed further light on the regulation of differentiation of pigment cells (Kelsh et al., 1996).

Here we characterize the pigmentation mutant *parade*^{tj262} that has previously remained uncharacterized. The ectopic cells of potentially mixed fate might help us identify an important key player in cell specification and/or migration.

In this thesis we will consider 4 different models as to why chromatophores, described as having characteristics of both melanophores and iridophores, appear in the ectopic position in *parade*^{tj262} mutants (Fig. 4.1).

One possibility is that the ectopic cells, as proposed by Kelsh et al. (1996), are of mixed melanophore-iridophore fate (Fig. 4.1 B) like, for example, the pigment cells of mosaic fate that have been reported in the red-backed salamander (Bagnara, 1999). Lack of a certain factor during development could result in some pigment cell precursors adopting one fate but not fully repressing another one and consequently displaying characteristics of both in this case melanophores and iridophores. Such failure of specification to a single fate might then lead to aberrant migration and the mixed fate chromatophores in the ectopic position. That adaptation of a specific fate can be necessary for migration along a certain path was shown by Erickson and Goins. With elegant transplantation experiments they showed that only cells displaying properties of melanoblasts or melanocytes were able to enter the dorsolateral pathway (Erickson, 1995). Just as cells that are not specified as melanocytes in chick are unable to enter a specific pathway, cells having adopted a mixed fate might not be able to exit a pathway or get stuck (Fig. 4.1 B3).

Another possible explanation for chromatophores appearance in the ectopic position could be that they adopt a single fate, but that there are more pigment cells in *parade*^{tj262} mutants than in wild-type embryos similar to the Silkie fowl or the *Dsk1*, *Dsk7* and *Dsk10* mutants (Faraco et al., 2001; Van Raamsdonk et al., 2004). It is imaginable that each stripe has the ability to hold only a certain number of chromatophores. Once this capacity is reached cells would then be repelled from the stripe. The area of the VS,

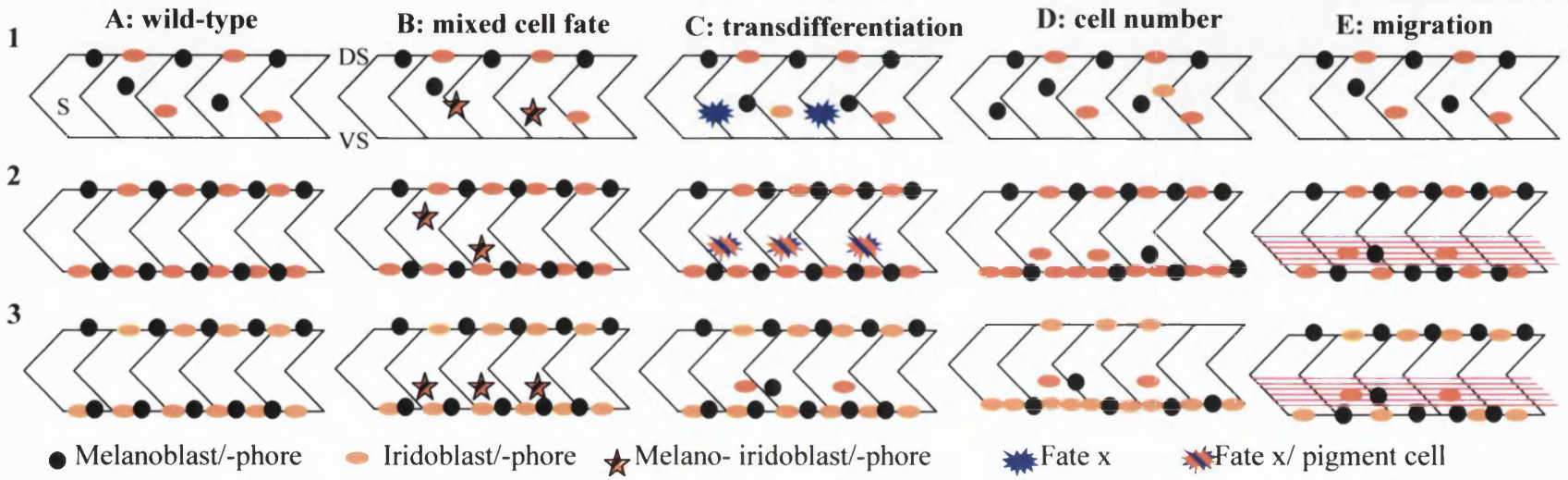

Fig. 4.1: Models for the appearance of the *parade*^{tj262} phenotype

A)In **wild-type stripe formation** during early development iridoblasts/iridophores and melanoblasts/melanophores migrate (A1) along specific pathways in the trunk to form the VS. B) **Mixed fate cells** might start migration normally (B1) and then get stuck in an ectopic position (B2, B3). C) **Transdifferentiation** of a cell type x (C1) into pigment cells (C2) could lead to these transdifferentiated cells occupying the ectopic position (C3). D) An increase in migrating pigment cell number (D1) could lead to an increase in ventral stripe pigment cells with supernumerary cells being repelled into the ectopic position (D3). E) **Aberrant migration of pigment cells** caused by over-expression or loss of expression of a factor extrinsic or intrinsic to pigment cells (symbolized here in red in ventral half of embryo) could lead to pigment cells migtating back into or getting stuck in the ectopic position.

For ease of illustration this model only considers pigment cells in the DS, VS and ectopic position. Somites are shown as chevrons (S)

above the yolk sac extension, near which the ectopic cells are appearing, is generally quite packed with chromatophores. It is therefore possible that there would be no space for additional chromatophores and with lack of other possibilities they would adopt an ectopic position, similar to *nacre* mutants, where some supernumerary cells can be found in the fins (Lister et al., 1999). Alternatively, loss of expression (or increased expression) of a localised environmental signal could lead to some pigment cells adopting an ectopic position. Similar to *choker* mutants where loss of *sdf1a* along the mysoseptum leads to loss of melanophores in the LS (Svetic et al., 2007). Reasons for the appearance of supernumerary chromatophores could be defects in regulation of cell proliferation or cell death mechanisms of chromatophores (Fig. 4.1 D) or transdifferentiation of cells of other neural crest fates e.g. enteric or sympathetic neurons into chromatophores (Fig. 4.1 C).

Alternatively it is possible that the appearance of the ectopic chromatophores is caused by migration defects (Fig. 4.1 E). As described above, effects in migration control have been suggested to be responsible for melanocytes populating atypical areas (Faraco et al., 2001). The position of the ectopic chromatophores strongly suggests that these cells have migrated on the medial pathway, but that some aspect of migration control might be defective. At least two possible scenarios can be imagined. On the one hand side it is possible that the ectopic chromatophores are cells originally intended to be in the VS, still trying to move down to the VS, but are stuck in their position. On the other hand it is possible that they had reached their final destination, e.g. the VS, already but could not stay there and migrated backwards on the medial pathway. These changes in behaviour of pigment cells could be caused by mutation of a gene encoding a factor expressed within the chromatophores itself or in the tissue, e.g. the somites, close to the ectopic cells.

The aim of this chapter is to gain more understanding of the *parade*^{tj262} phenotype and take first steps towards explaining the appearance of the ectopic chromatophores.

IV.2. Results

IV.2.1. Initial phenotypic characterization

As an initial step in characterization of *parade*^{tj262} we carefully observed mutant embryos by light microscopy.

Ectopic chromatophores could be seen in the ectopic position ventral to the notochord (Fig. 4.2) as previously reported (Kelsh *et al.*, 1996) as early as 3 dpf. It was not possible to determine ectopic cells in younger embryos as melanophores were still migrating on the medial pathway towards the VS at these stages and some of those are temporarily located in positions similar to the one in which the ectopic cells appear. Daily examination of the phenotype showed that the phenotype persist until at least 14 dpf. Older larvae have not been examined yet. *parade*^{tj262} mutants are homozygous viable and show no obvious adult pigmentation phenotype.

IV.2.1.A. Location of the ectopic chromatophores

The strength of the pigmentation phenotype of *parade*^{tj262} mutants was quite variable. To document this, we studied the distribution of ectopic pigment cells in *parade*^{tj262} mutants. A high level of variation in the number and position of ectopic cells could be seen between and within different batches of embryos. Generally the accumulation of ectopic chromatophores was mostly restricted to the posterior trunk region between the anterior end of the swim bladder and the anus (Fig. 4.2 D, E and Fig. 4.3). The anterior border was mostly about 2-3 somites posterior to the posterior end of the swim bladder and ectopic cells in *parade*^{tj262} could never be seen anterior to the swim bladder. However in some batches ectopic cells were visible in the anterior tail mainly, but not exclusively, in the somites just posterior to the anus. In addition, ectopic iridophores could be seen in the ventral tail fin. Note that ectopic cells in the fin were present in the first 5 somites posterior to the anus only (Fig.4.3). In general the ectopic cells tended to be in adjacent somites.

Although dorsal to the VS, the ectopic chromatophores often showed protrusions reaching to the VS. These protrusions were reminiscent of those in wild-type embryos than can be seen by migrating pigment cells at earlier stages, such as 48 hpf, when they pass the position in which the ectopic cells can be found. Transverse sections of 5 dpf

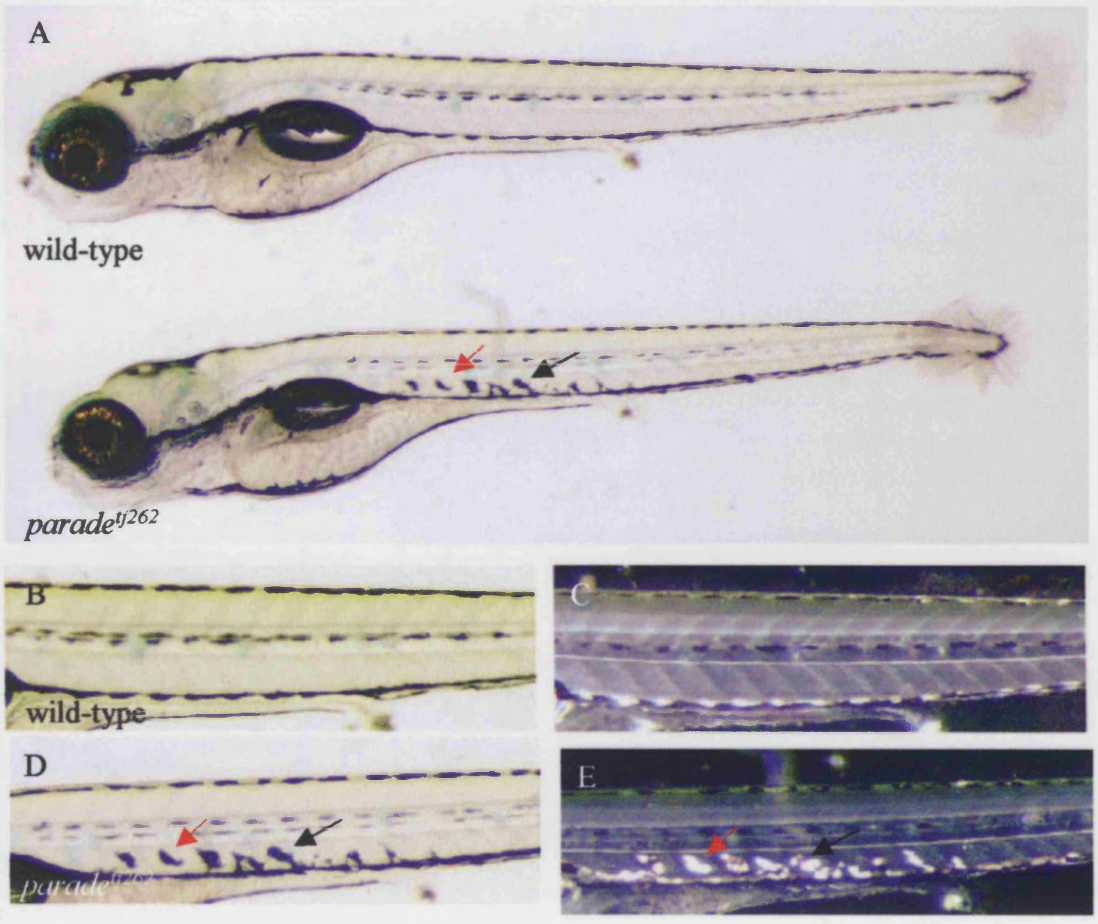

Fig. 4.2: Phenotype of *parade*^{tj262} mutants
In 5 dpf old wild-type embryos the embryonic pigment pattern is established and the four stripes- DS, VS, LS and YSS- are visible (A, B, C). In comparison to their wild-type siblings *parade*^{tj262} mutants showed an accumulation of ectopic chromatophores in the trunk region between the lateral and ventral stripe in addition to the four stripes (A, D, E; arrows).
With bright-field optics, these ectopic cells showed melanophore characteristics (D, arrows), but with incident lighting these cells also displayed iridophore fate (E, arrows). Note that some of the ectopic cells shared a very similar shape (red arrows, D, E).

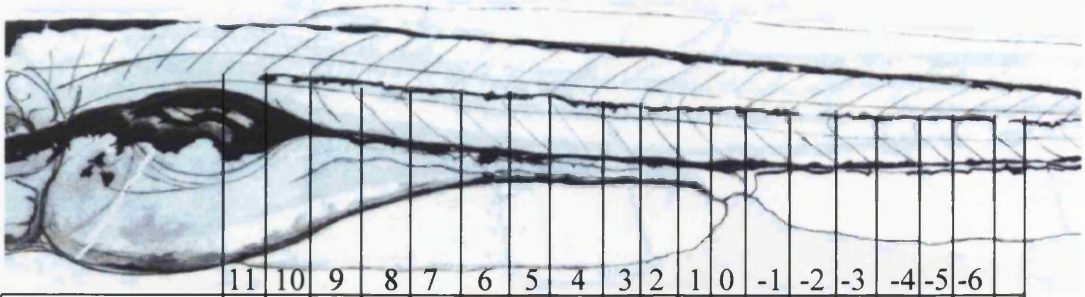

	11	10	9	8	7	6	5	4	3	2	1	0	-1	-2	-3	-4	-5	-6
Embryo 1			●	●		★	●		★	●						●		
2					★	★	●	●	●	●	●							
3				●	●	★	★		●	●	●							
4				●	●		●	●	●	●	●							
5							★		●	●	●							
6							★	●	★	●								
7			★	●	●	●	●	★	●									
8			●	●	●		●	●										
10				●	●													
11				●	● ●	●	● ●	●	●	●								
12						● ●	●	★	●	●								
13					★ ●	●	●	★	●	●								
14				●	●	●	★	●	★									
15						●	●											
16				★		●												
17			●	●	●	●	★	●	●	★	●							
18							●	●	● ●	★	●		●	●	●	●		
19							●	●	★	●	●			●				
20				●	★	★	★	★	●	●						●	●	
21					●	●	●	●		●								
22						★		●		●								
23				●	●	★	★	●				★						
24				●			●		★	●		●	●	●	●	●		
25				●	★	★	★	★	★	★	★					●		
26						●												
%			3	8	11	14	16	12	13	11	5	2	1	2	1	2	1	

Fig. 4.3: Distribution of ectopic pigment cells in *parade*^{tj262}
Observation of pigmentation in 5 dpf old *parade*^{tj262} embryos showed that melanophores (black circle), iridophores (orange circle) and chromatophores that seemed to display melanophore and iridophore fate (red and orange striped stars) could be found ectopically in the trunk. Whereas ectopic iridophores were found in trunk and tail (in the somites) other ectopic chromatophores were only found in the trunk. Ectopic chromatophores were never observed anterior to the posterior end of the swim bladder. The average percentage of ectopic cells per somite (bottom row) was highest from somite 8 to somite 1 in the trunk lying above the yolk sac extension (cells appearing to display both chromatophore fates were counted as two; percentage rounded to the nearest full number)

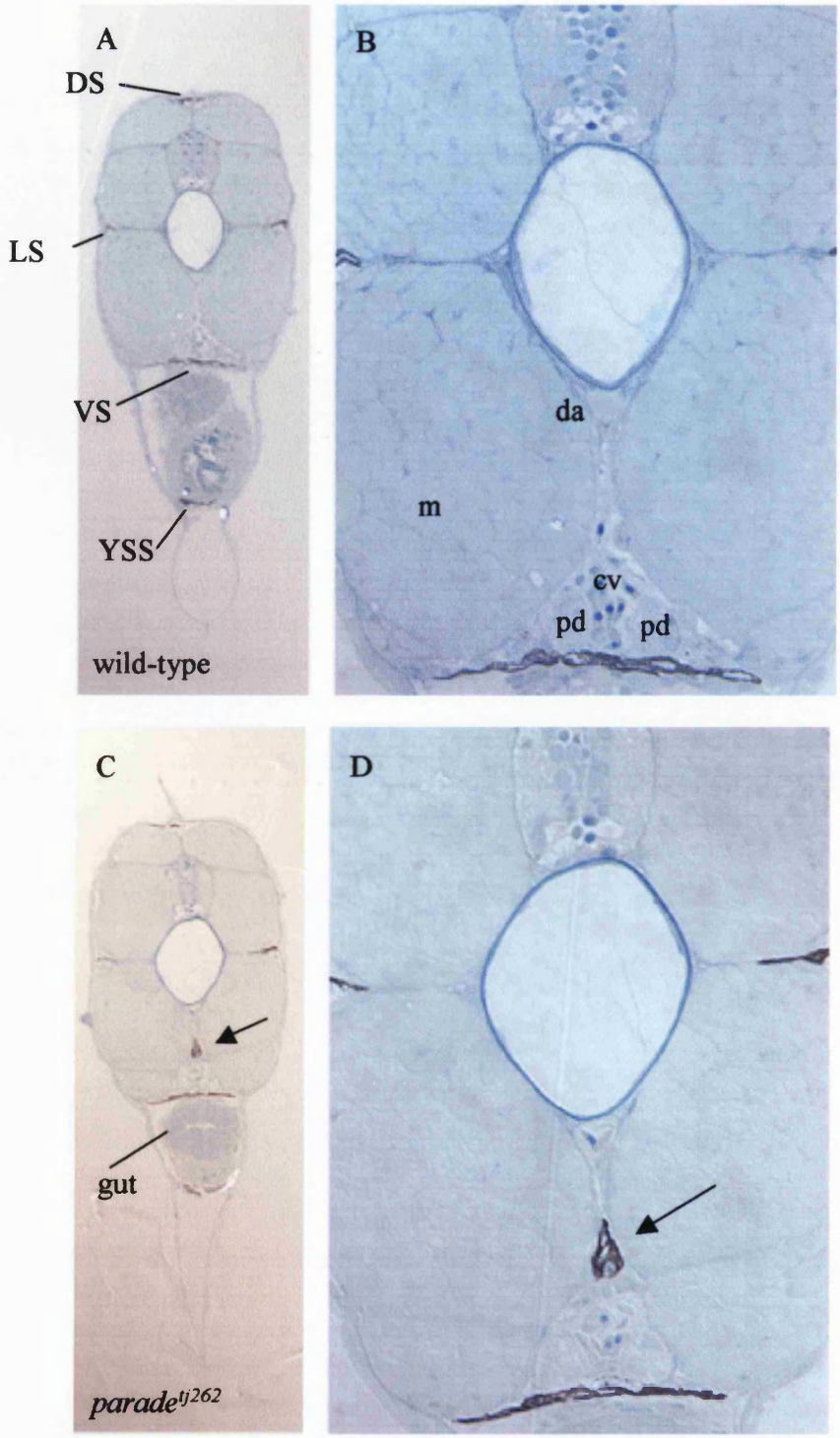

Fig. 4.4: Transverse trunk sections of 5 dpf wild-type and *parade*^{tj262} embryos. In plastic sections of wild-type embryos (A, B) melanophores could be seen in the DS, VS and YSS and on both sides of the embryo in the LS. In *parade*^{tj262} embryos additional melanin expressing cells can be seen ventral to the dorsal aorta (da), dorsal to the caudal vein (cv) and pronephric ducts (pd) and medial to the myotomes (m) (C, D arrow).

old *parade*^{tj262} clearly showed that the ectopic chromatophores occupy a very medial position, directly beneath the notochord and dorsal aorta in a position between the myotomes and above the caudal vein (Fig. 4.4 C, D). In all further studies we will only defined cells as ectopic if they were situated above the caudal vein.

IV.2.1.B. Cell fate of ectopic chromatophores

Once we had established the distribution of the ectopic chromatophores we addressed the question of their cell fate. As previously reported by Kelsh et al. (1996) most of the ectopic chromatophores under transmitted and incident light showed characteristics of melanophores as well as iridophores (Fig. 4.2 D, E). Characteristics typical for xanthophores could not be observed. However, this was hard to see as xanthophore characteristics can be obscured by melanophores and iridophores. To address if the ectopic chromatophores expressed genes typical for all three chromatophores fates whole mount mRNA *in situ* hybridisation, using known markers for the three pigment cell types, was performed.

The expression of melanin, clearly visible in some of the ectopic chromatophores, strongly suggested that they were melanophores (Fig. 4.2 D). This was confirmed by *in situ* hybridization using *dct* as molecular marker for the melanophore lineage (Kelsh et al., 2000). *dct* has been shown to be expressed in undifferentiated cells (5 hours before melanisation) as well as differentiated (melanised) melanophores. To avoid melanin obscuring the *in situ* signal we treated the embryos with PTU, which inhibits melanin synthesis (Pietzsch-Rohrschneider, 1977; Westerfield, 1995). *In situs* at 5 dpf using the progeny of heterozygous *parade*^{tj262} in-cross showed expression of *dct* in 10/45 embryos in cells situated at the location of the supernumerary chromatophores (Fig. 4.5 A, B) in addition to expression in the wild-type positions of melanophores. This ratio is as expected for a recessive mutation (Chi-square= 0.09, degrees of freedom: 1, $p \leq 1$). We therefore concluded that all embryos with ectopic *dct* expression were homozygous *parade*^{tj262} mutants confirming the melanophore fate of these cells.

As a lineage marker for iridophores we used *ednrb1* (Parichy et al., 2000a). 7/40 embryos of a heterozygous *parade*^{tj262} in-cross showed expression of *ednrb1* at the location of the ectopic chromatophores (Fig. 4.5 C, D). Again the ratio was consistent with the conclusion that the ectopic cells in *parade*^{tj262} express this marker and thus

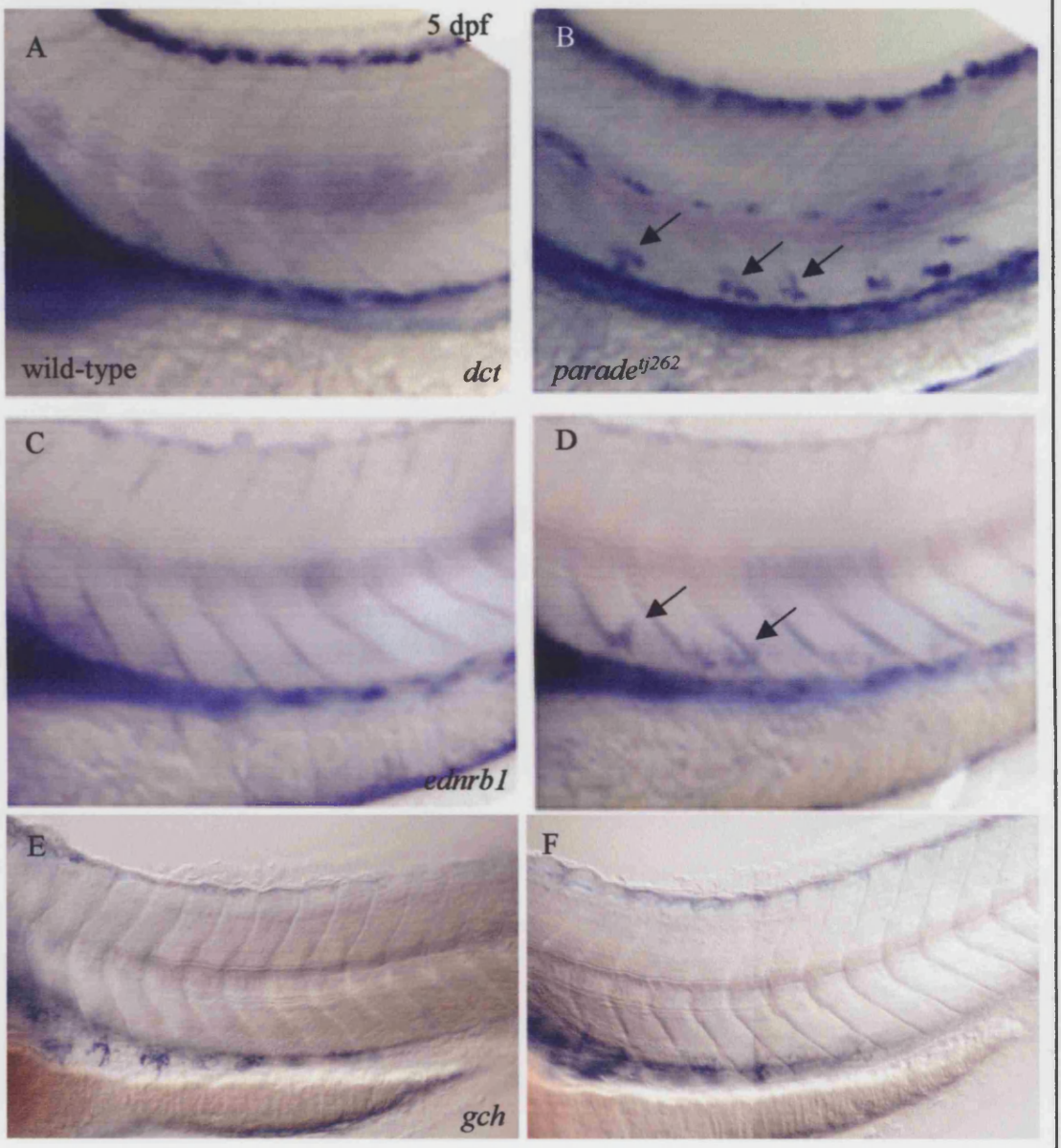

Fig. 4.5: Ectopic chromatophores express melanophore and iridophore, but not xanthophore lineage markers

Unlike wild-type siblings (A) *parade*^{tj262} mutants express the melanophore lineage marker *dct* in cells located at the position of the ectopic cells (B, arrows) in the trunk at 5 dpf. The iridophore marker *ednrb1* is also expressed in ectopic cells in *parade*^{tj262} (D, arrow) but not in their wild-type siblings (C). No difference can be seen in the expression of the xanthophore marker *gch* in the trunk of 3 dpf old wild-type (E) and *parade*^{tj262} embryos (F). Embryos in E and F were sorted based on presence/absence of ectopic cells prior to the *in situ*. All pictures lateral view.

have iridophore fate (Chi-square= 0.7, degrees of freedom: 1, $p \leq 1$). Having confirmed our microscopic observations that the ectopic chromatophores display indeed iridophore as well as melanophore fate we checked for xanthophore markers. Two markers for xanthophore lineage, *gch* and *xdh*, have been characterized (Parichy et al., 2000b; Pelletier et al., 2001)). In an initial experiment we could not identify embryos expressing *gch* or *xdh* in an ectopic position. To verify that there was no *gch* phenotype in *parade*^{tj262} mutants we pre-sorted live embryos of a heterozygous *parade*^{tj262} in-cross by their iridophore phenotype. But again *in situ* hybridization with *gch* at 3 dpf did not show any positively stained cells in the area of interest in *parade*^{tj262} mutants but stained numerous cells elsewhere in the expected wild-type pattern (Fig. 4.5 E, F). We therefore concluded that as the ectopic chromatophores did not show expression of xanthophore fate markers they were restricted to melanophore and iridophore fate only.

IV.2.2. Ectopic pigmentation consisted of clustered chromatophores

As *in situ* hybridisation confirmed the results of DIC and bright field microscopy that the ectopic cells displayed characteristics of both iridophores as well as melanophores, we next asked whether these ectopic chromatophores were of mixed iridophore melanophore fate as proposed by Kelsh *et al.* (1996) or if they consisted of closely associated clusters of melanophores and iridophores (Fig. 4.6 and 4.7). We chose a direct test to answer this aspect and examined the phenotype of the ectopic cells in sections with both light and an electron microscopy. Studies in the leaf frog (*P.danicolor*) have shown that organelles of the different pigment cell types can be seen intermingled in cells of potentially mixed fate using TEM microscopy (Bagnara, 1998). Mixed cell fate of the ectopic chromatophores in *parade*^{tj262} could, as described earlier, be a reason for the ectopic positioning of the chromatophores.

Sagittal sections of *parade*^{tj262} examined by bright field microscopy showed that the ectopic cells consisted of distinct but intimately associated areas containing melanosomes and reflecting platelets respectively (Fig. 4.7 B, C).

To examine if the compartmentalization of melanosomes and reflecting platelets was due to their being clustered separately within one cell or in adjacent melanophores and iridophores, we looked whether they were separated by cell membranes using TEM. Embryos were embedded, sectioned and photographed by Ursula Potter in the Centre for Electron Optical Studies at the University of Bath. The closely associated

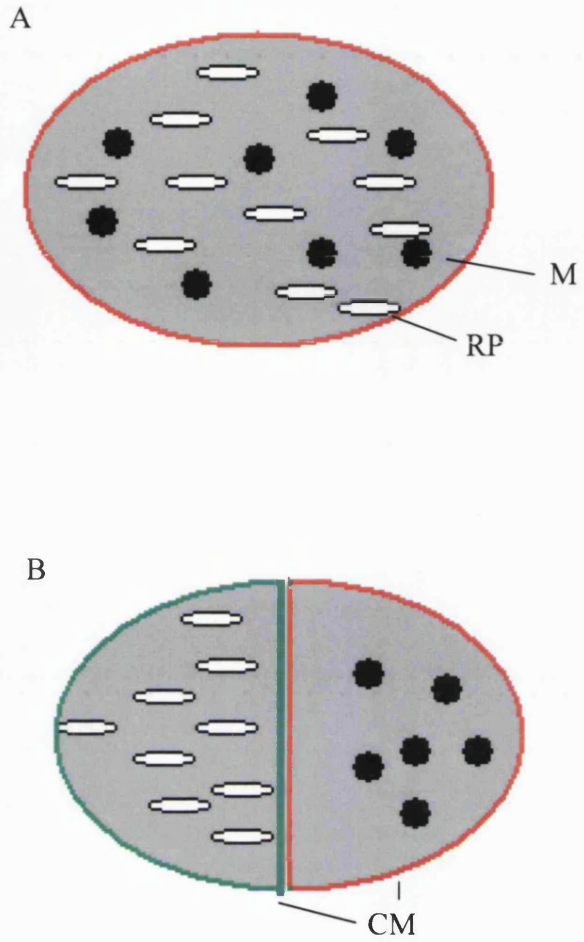

Fig. 4.6: Possible organisations of melanosomes and reflective platelets in the ectopic chromatophores

Schematics for cells of mixed melanophore iridophore fate (A) and cell clusters of closely associated melanophores and iridophores (B). Chromatophores of mixed cell fate are expected to have melanosomes and reflective platelets intermingled without separating cell membranes (A). Closely associated clusters of melanophores and iridophores however are expected to have separating cell membranes (CM) between the reflective platelets (RP) and melanosomes (M)(B).

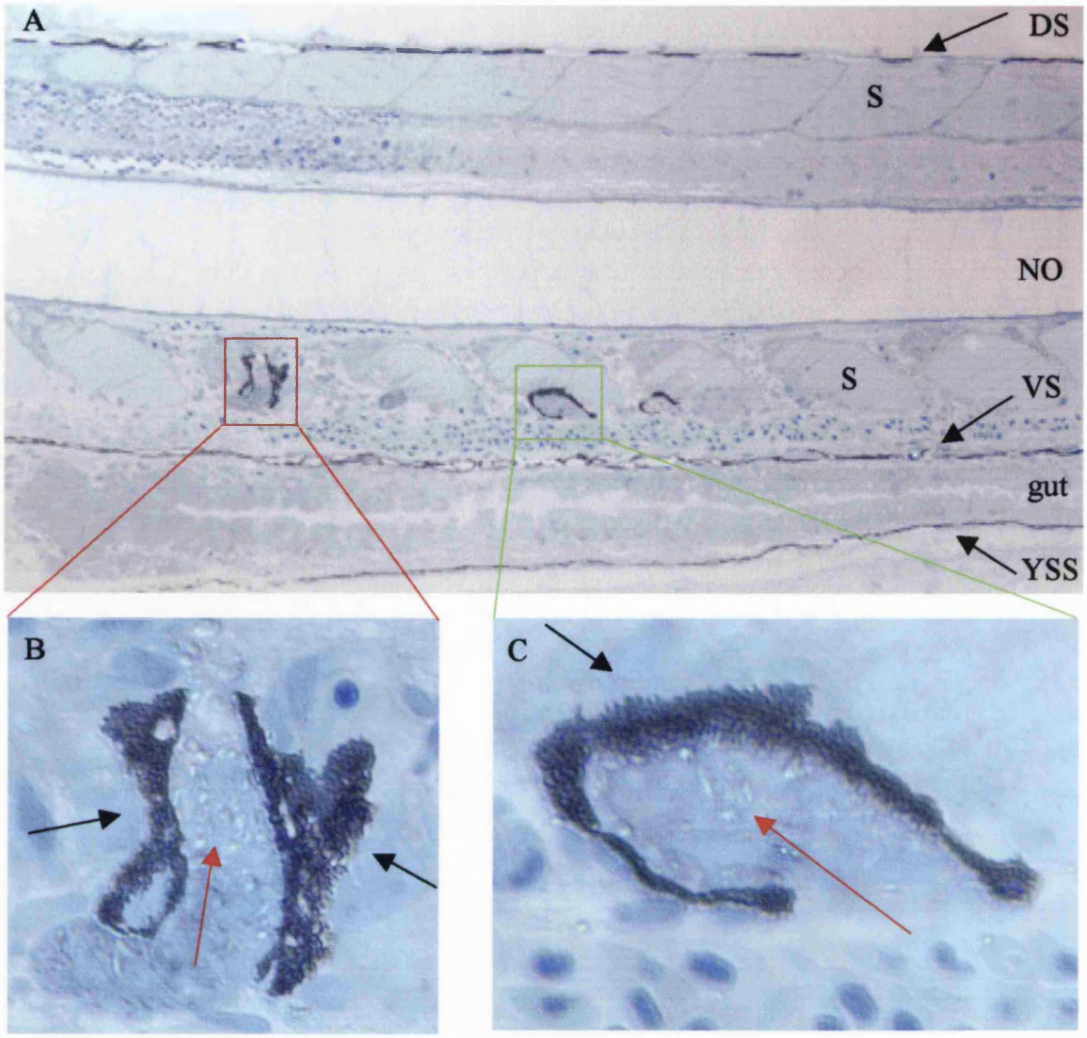

Fig. 4.7: Reflecting platelets and melanosomes are clustered
Longitudinal sections of the trunk of *parade*^{tj262} mutants clearly showed melanophores in the DS, VS and YSS visible by the black melanin (A). In addition, distinct areas containing melanin were in the ectopic position (A, boxed areas). Higher magnification of these areas of ectopic melanin (B, C, black arrows) showed that they were next to areas containing reflective platelets organelles (red arrow). The organelles of the chromatophores in the ectopic position therefore seemed compartmentalized but intimately associated (NO: Notochord, S: somite)

melanophores and iridophores of the YSS were used as a control. TEM examination of melanophores and iridophores of the YSS in 5 dpf *parade*^{tj262} embryos showed that both cells types, clearly distinguishable by distinct areas of melanosomes and reflective platelets, were separated by double membranes (Fig. 4.8 E, F). Some interruptions, likely to be an artefact from sectioning, of the double membrane around the distinct clusters of melanosomes and reflective platelets were visible.

As expected from low power overviews of ectopic chromatophores of a 5 dpf *parade*^{tj262} TEM showed distinct areas of melanosomes and reflecting platelets (Fig. 4.8 A). No pterinosomes could be seen strengthening the view that the ectopic cells did not have xanthophore fate. Higher magnification of the boundary of these areas showed double membranes between the clusters of melanosomes and reflective platelets (Fig. 4.8 B-D). More than one distinct area of reflective platelets surrounded by double membranes could be observed. Double membranes could also be seen in between areas of melanosomes suggesting that a cluster contained more than one melanophore or that one melanophore folds around the iridophores of the cluster. To verify that what we saw represented close association of melanophores and iridophores, we compared the appearance of the melanosomes, reflective platelets and double membranes of the closely associated melanophores and iridophores in the YSS. The general appearance of the double membranes observed in the ectopic cluster was very similar to the ones observed between melanophores and iridophores of the YSS. Again interruptions in the double membrane could be observed. They seemed to be somewhat more frequent than in the yolk sac stripe. The similar nature of the membranes of melanophores and iridophores in the YSS and the ectopic chromatophores strongly suggested that the latter contain individual melanophores and iridophores in close association and not cells of mixed melanophore iridophore fate.

These findings strongly conflicted with the theory that the ectopic positioning of the chromatophores was the result of them being of mixed cell fate. Consequently we focused on testing our other models.

IV.2.3. parade^{tj262} *mutants have supernumerary iridophores*

Having shown that appearance of the ectopic chromatophores was not caused by the cells having adopted a mixed fate, we next asked whether the primary cause was an increased number of melanophores and iridophores in *parade*^{tj262}. The ectopic

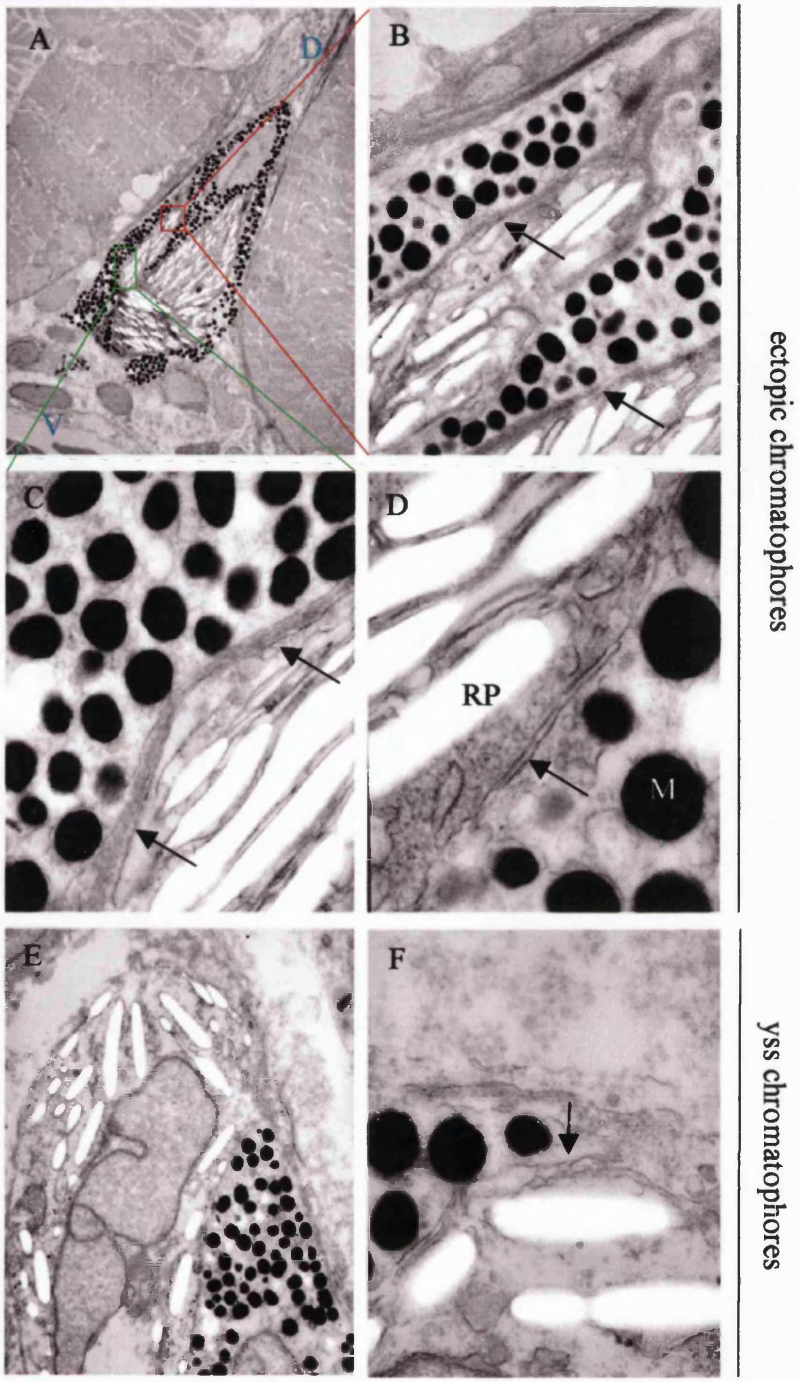

Fig. 4.8: Clustered melanosomes and reflecting platelets are separated by cell membranes

TEM photomicrographs show overview of ectopic cells in *parade*^{tj262} (A) enlarged in B-D, and compared with chromatophores in the yolk sac stripe (E, F). Note the prominent cell membranes (arrow) between clustered melanosomes (M) and reflecting platelets (RP) both in ectopic chromatophores and cells of the YSS suggesting that the ectopic chromatophores are cell clusters and not one cell of mixed fate. A-D dorsal is to the top right corner (D) and ventral to the bottom left (V), E, F anterior is to the top.

positioning of the chromatophores could then be a secondary effect, possibly caused by a limit in capacity for chromatophores in the VS.

To see if *parade*^{tj262} mutants had not only ectopic but supernumerary chromatophores we counted the melanophores and iridophores in the DS and VS of wild-type siblings and *parade*^{tj262} mutants. Pigment cell counts were done at 4 dpf as *parade*^{tj262} mutants can be clearly distinguished from wild-type embryos at this stage, but the swim bladder has not inflated yet allowing easier handling of the embryos. To make counting easier and clearer to interpret the individual embryos where split into four areas (Fig. 4.9 A): the DS (outlined in blue), the area of ectopic cells (yellow), the anterior ventral stripe (AVS, green) and the posterior ventral stripe (PVS, red). Melanophores and iridophores of 49 wild-type and 43 *parade*^{tj262} embryos were counted. At 4 dpf melanophores within the stripes form a more or less continuous stripe. Embryos were therefore treated with epinephrine and then fixed to allow easier counting of melanophores. Iridophores were counted in live embryos under incident lighting.

VI.2.3.A. There was no increase in melanophore and iridophore numbers in the DS of *parade*^{tj262} mutants

To see if there was an effect on pigment cell number in the DS or VS we looked at both stripes to see if the number changed. We first ask if there was a change in melanophores and iridophore numbers in the DS of *parade*^{tj262} mutants.

Counts of melanophores and iridophores in the DS of 4 dpf old *parade*^{tj262} mutants showed no significant difference to wild-type numbers (Fig. 4.9 B, C).

IV.2.3.B Iridophore, but not melanophore, numbers in the VS were increased

After having seen no difference in melanophore and iridophore number in the DS we went on to look at the VS. As the phenotype so far had been associated with the trunk region of embryos we decided to split the VS into two regions. The AVS reaching from the posterior end of the swim bladder to the anus and the PVS extending from the anus to the tip of the tail. In contrast to the DS of *parade*^{tj262} which phenotypically looked identical to that of wild-type embryos we often observed iridophores, but not melanophores, situated in an ectopic position in the PVS. These ectopic iridophores

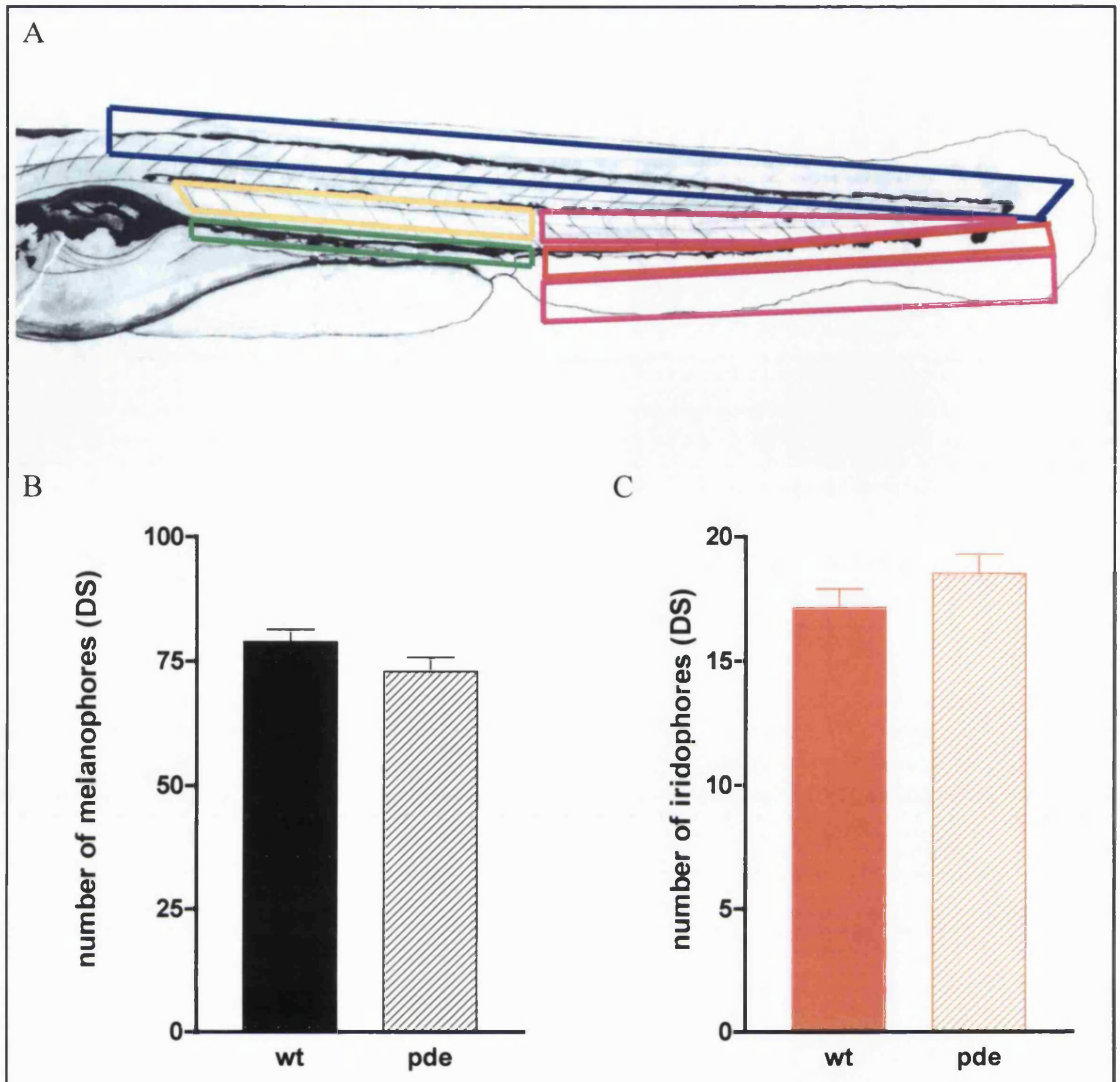

Fig. 4.9: Counts of melanophores and iridophores in *parade* ^{tj262}
Areas of chromatophore counts in the trunk and tail of 4 dpf embryos (A): dorsal stripe (blue box, DS), posterior ventral stripe (red box , PVS) , ectopic cells (EC, trunk: yellow box, tail: pink boxes) and anterior ventral stripe (green box, AVS). There is no significant difference in melanophore numbers in the DS of *parade*^{tj262} compared to wild-type embryos (B; $p>0.05$, Two-tailed t-test; (wild-type: mean +s.e. 78.8+ 2.5 (n=20); *parade*^{tj262} : 72.8+2.8 (n=20)). Similarly no significant difference between iridophore numbers in the DS could be observed (C; $p>0.05$, Two-tailed t-test; (wild-type: mean + s.e. 22.9+ 0.9 (n=29); *parade* ^{tj262}: 20.4+1.1 (n=22)).

were located either in the ventral fin or in their typical position in the stripe. We counted ectopic iridophores separately from those along the VS. We first looked at melanophores. Counts in the PVS showed no significant increase (or decrease) of melanophore numbers in *parade*^{tj262} compared to wild-type embryos (Fig. 4.10 A).
Having shown that there was no increase in melanophore numbers in the PVS we next looked at iridophores. Counts revealed a significant increase, of about 47%, in the number of iridophores in *parade*^{tj262} mutants compared to wild-type embryos. By taking the ectopic cells into account the number of iridophores in *parade*^{tj262} increased even more, by 52%, compared to wild-type embryos (Fig.4.10 B).
To find increased number of iridophores, but not melanophores, in the PVS was very interesting, as so far no phenotype for the PVS had been described.

IV.2.3.C. Iridophore numbers in the AVS were increased

To see if the increase of iridophores was consistent along the whole VS we next looked at the chromatophore numbers in the AVS. Again, we counted the chromatophores found in wild-type like positions (green box, Fig. 4.9.A) separately from the ectopic ones (yellow box, Fig. 4.9 A).
In contrast to the DS, epinephrine treatment was not helpful for the AVS and the melanophore morphology there remained unchanged. The reason for that might be difficulties with the penetration of epinephrine or differences in melanophore morphology compared to the DS. Therefore, we could only examine iridophore numbers in the AVS.
We first looked at the iridophores located in the wild-type positions along the AVS. Interestingly, the number of these did not differ significantly when comparing counts of *parade*^{tj262} mutants to wild-type embryos (Fig. 4.10 D, compare wt and pde-AVS). However, including the ectopic iridophores into our calculations resulted in a significant increase of iridophores in *parade*^{tj262} compared to wild-type (Fig. 4.10 C, compare wt and pde-all). Thus, in contrast to the PVS, where supernumerary iridophores could be found, in the AVS of *parade*^{tj262} mutants only the ectopic cells were supernumerary.
The overall increase of iridophores in the VS of *parade*^{tj262} mutants was ~58% (Fig. 4.10 D). Therefore, our counts showed a clear increase of iridophore numbers in the VS, but not the DS of *parade*^{tj262} embryos. Even though it was not possible to count

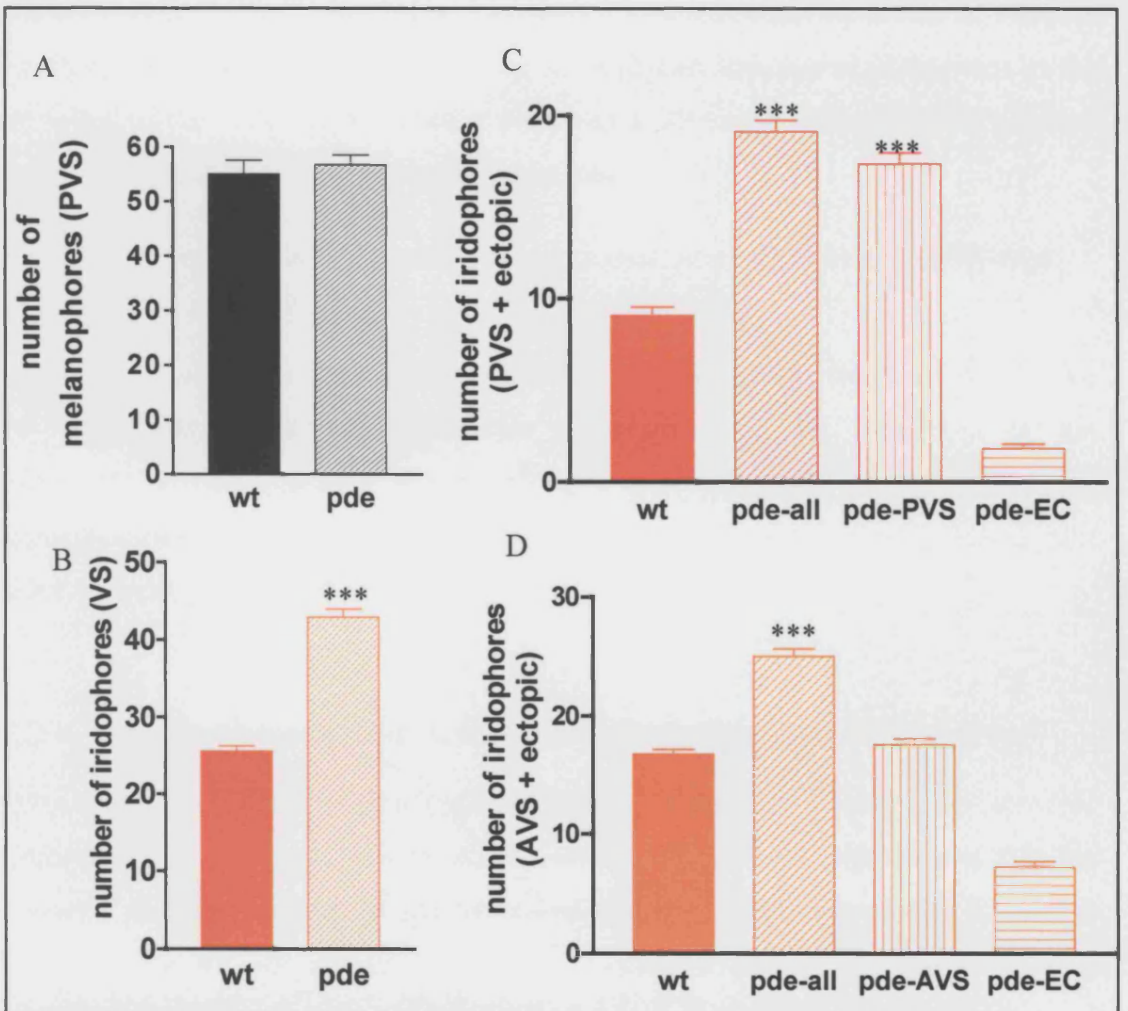

Fig. 4.10: Iridophores but not melanophores were increased in the VS in *parade^{tj262}*

Counts showed that there is no significant difference in melanophore numbers in the PVS (A; $p>0.05$, Two-tailed t-test; (wild-type: mean +s.e. 55.0+ 2.5 (n=20); *parade^{tj262}* : 56.6+1.8 (n=17)). Iridophore numbers in the VS however were increased by ~58% in mutant compared to wild-type embryos (B; $p<0.0001$, Two-tailed t-test; (wild-type: mean +s.e. 25.5+ 0.6 (n=49); *parade^{tj262}* : 42.8+1.0 (n=43)). Division of the VS into AVS and PVS showed that the number of iridophores is increased in both parts (C, D). The overall number of iridophores in the PVS (including all ectopic cells) were significantly increased in *parade^{tj262}* (pde-all) compared to wild-type (wt) (C; $p<0.0001$, Two-tailed t-test; (wild-type: mean +s.e. 9.0+ 0.4 (n=49); *parade^{tj262}* : 21.7+0.7 (n=43)) . Even without taking the ectopic cells into consideration and looking only at the iridophores in the PVS (pde-PVS) the increase was significant compared to wild-type (wt) C; $p<0.0001$, Two-tailed t-test; (wild-type: mean +s.e. 9.0+ 0.4 (n=49); *parade^{tj262}* : 17.3+0.6 (n=43)). Like in the PVS the number of all iridophores (including ectopic cells) were significantly increased (C, pde-all; $p<0.0001$, Two-tailed t-test; (wild-type: mean +s.e. 16.7+ 0.3 (n=50); *parade^{tj262}* :24.9+0.6 (n=45)). In contrast to the PVS, however, comparison of counts in the AVS (excluding ectopic cells) between wild-type (wt) and *parade^{tj262}* (pde-AVS) showed no significant difference (C; $p<0.05$, Two-tailed t-test; (wild-type: mean +s.e. 16.76+ 0.3944 (n=50); *parade^{tj262}* : 17.55+0.5125(n=45)).

melanophores in the AVS, the counts from the PVS indicated that there was no increase in melanophore number in the VS. Having identified an increase of iridophores in the ventral half of the embryos, we asked if there was a difference in xanthophore numbers even though no ectopic xanthophores were present.

IV.2.3.D. *gch* expression in *parade*^{tj262} mutants showed no difference to wild-type embryos

Having already seen that there was no difference in melanophore numbers at 4 dpf we next looked at xanthophore expression. Comparison of the expression of the xanthophore marker *gch* at 3 dpf in wild-type and *parade*^{tj262} mutants showed no detectable differences either (Fig.4.5 E, F). Embryos had been separated based on their phenotype before *in situ* hybridisation.

IV.2.4. Do other neural crest cells transdifferentiate into iridophores?

Having established that the number of iridophores but not melanophores was increased in *parade*^{tj262}, even though both could be found in the ectopic position, and that the phenotype was restricted to the VS, we asked what caused the increase in iridophore number in the VS of *parade*^{tj262}embryos. Possible scenarios, that we considered included over-proliferation of iridophores in the ventral half of the embryo, failure of regulation of iridophore number by cell death or trans-differentiation of cells of other neural crest fates (Fig.4.1).

A possible explanation for the increase in iridophore number in *parade*^{tj262} mutants could be that cells usually giving rise to another neural crest fate (e.g. sensory or enteric neurons) located close to the ectopic position transdifferentiate into iridophores from their original fate or differentiate into iridophores straightaway from a common progenitor (Fig. 4.1 C). If trans-differentiation from a 'fate x' to iridophores occurs late during development of 'x' we might be able to see a decrease or complete loss in number of these cells. On the other hand an early trans-differentiation of only a few cells of a 'fate x' would be a lot harder to track as subsequent rounds of proliferation combined with regulatory mechanisms might be able to make up for the loss of some progenitors.

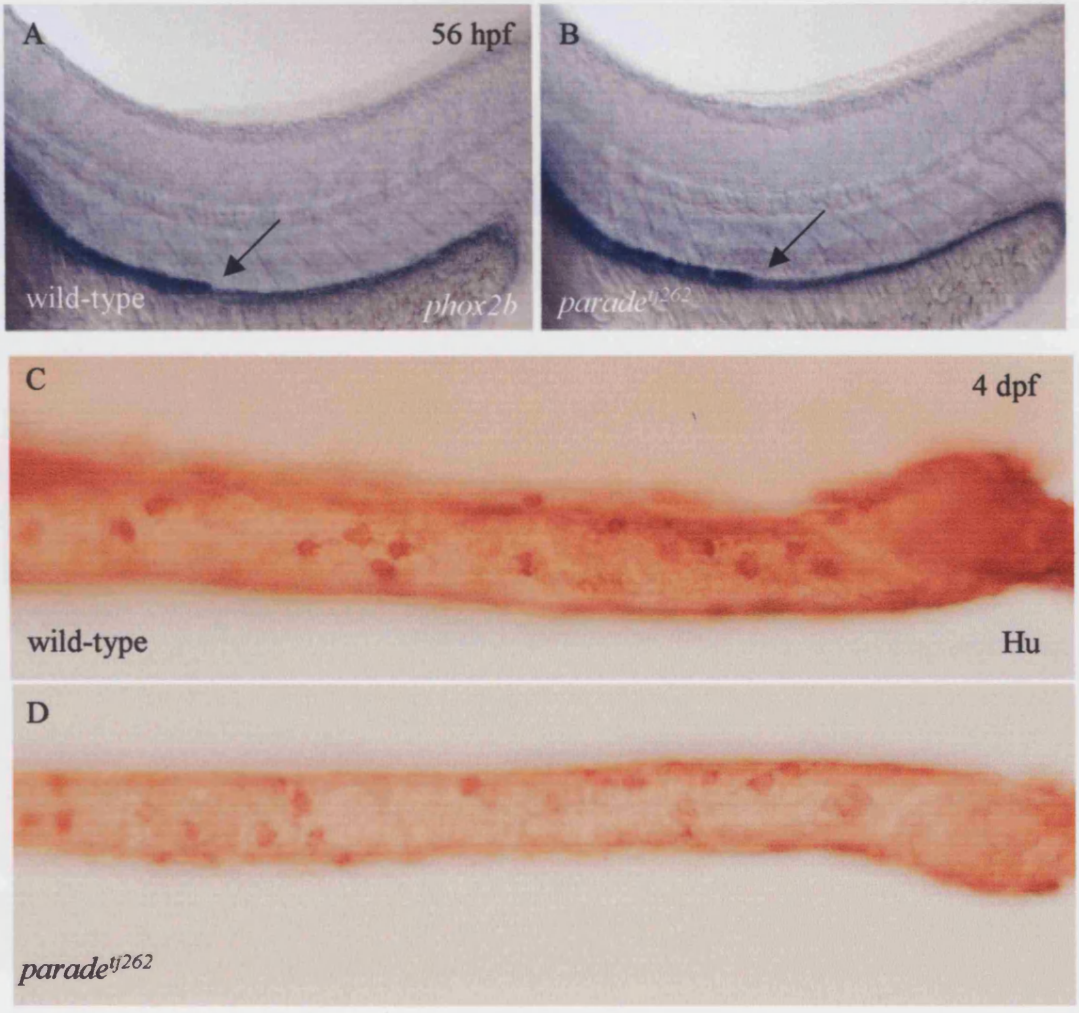

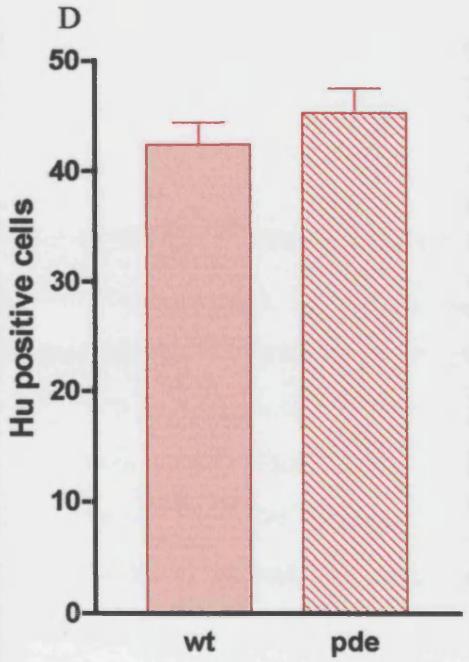

Fig. 4.11: There is no decrease in *phox2* and Hu positive cells in *parade*^{tj262}

There is no difference in the signal intensity or anterior posterior extension (arrows) of *phox2b*, a marker for differentiating enteric neurons and their precursors in wild-type and *parade*^{tj262} mutants (A, B). Counts showed that, at 4 dpf there was no significant difference between the number of Hu stained enteric neurons in mutant and wild-type embryos ($p<0.05$, Two-tailed t-test; D). wild-type embryos had an average of 42 Hu positive cells in the posterior end of the gut (mean = s.e. 42.4+ 1.9 (n=10); A) and *parade*^{tj262} mutants had 45 (45.2+ 2.2 (n=10); B). In both images the anterior end of the gut tube is to the left.

IV.2.4.A. *parade*^{tj262} mutants showed no difference in enteric neuron numbers

Enteric neurons along the gut are a neural crest derivative (Elworthy et al., 2005). The position of enteric neurons along the gut tube next to the VS made them a candidate for our studies (for position of gut tube in relation to the ectopic cells see Fig. 4.4. C). To see whether there were any differences in the number of enteric neurons in *parade*^{tj262} compared to wild-type embryos indicating that enteric neurons or their precursors transdifferentiate into iridophores we examined expression of Hu antigen and *phox2b* in *parade*^{tj262}. *phox2b* has been shown to label differentiating enteric neurons and their precursors (Elworthy et al., 2005). To establish if there was a difference in the number of differentiating enteric neurons between *parade*^{tj262} and wild-type embryos we examined expression of *phox2b* at 56 hpf. We observed no differences in strength and size of *phox2b* expression domains and therefore concluded that there is no loss of early differentiating neurons in *parade*^{tj262} (Fig. 4.11 A, B). While *phox2b* labels precursor cells Hu is not expressed in neurons until about 3 dpf. It is an ideal marker for enteric neurons at 4 and 5 dpf. To see if *parade*^{tj262} lacked differentiated enteric neurons we examined the expression of Hu antigen (Fig. 4.11 C, D). No significant difference between numbers of enteric neurons in dissected guts of wild-type and *parade*^{tj262} embryos could be detected (Fig. 4.11 E).

Our results showed no differences in the number of differentiating or differentiated enteric neurons. It was therefore unlikely that trans-fating enteric neurons were the reason for the increase in iridophore numbers in the VS of *parade*^{tj262} mutants.

IV.2.4.B. *parade*^{tj262} mutants have a decreased number of sympathetic neurons

Another neural crest derivative located closely to the position of the ectopic chromatophores are sympathetic neurons. At 7 dpf differentiated sympathetic neurons can be seen in a position similar or just dorsal to the ectopic pigment cells (Fig. 4.12 C-E)(An et al., 2002). This single, irregular row stretching to the anus and located just below the aorta can be detected with Hu antibody. The position of the sympathetic neurons close to the ectopic cells would make them a good candidate for cells that might transdifferentiate into iridophores. If sympathetic neurons transdifferentiate into iridophores we would expect to see a reduction in/or complete loss of sympathetic neurons in *parade*^{tj262} mutants.

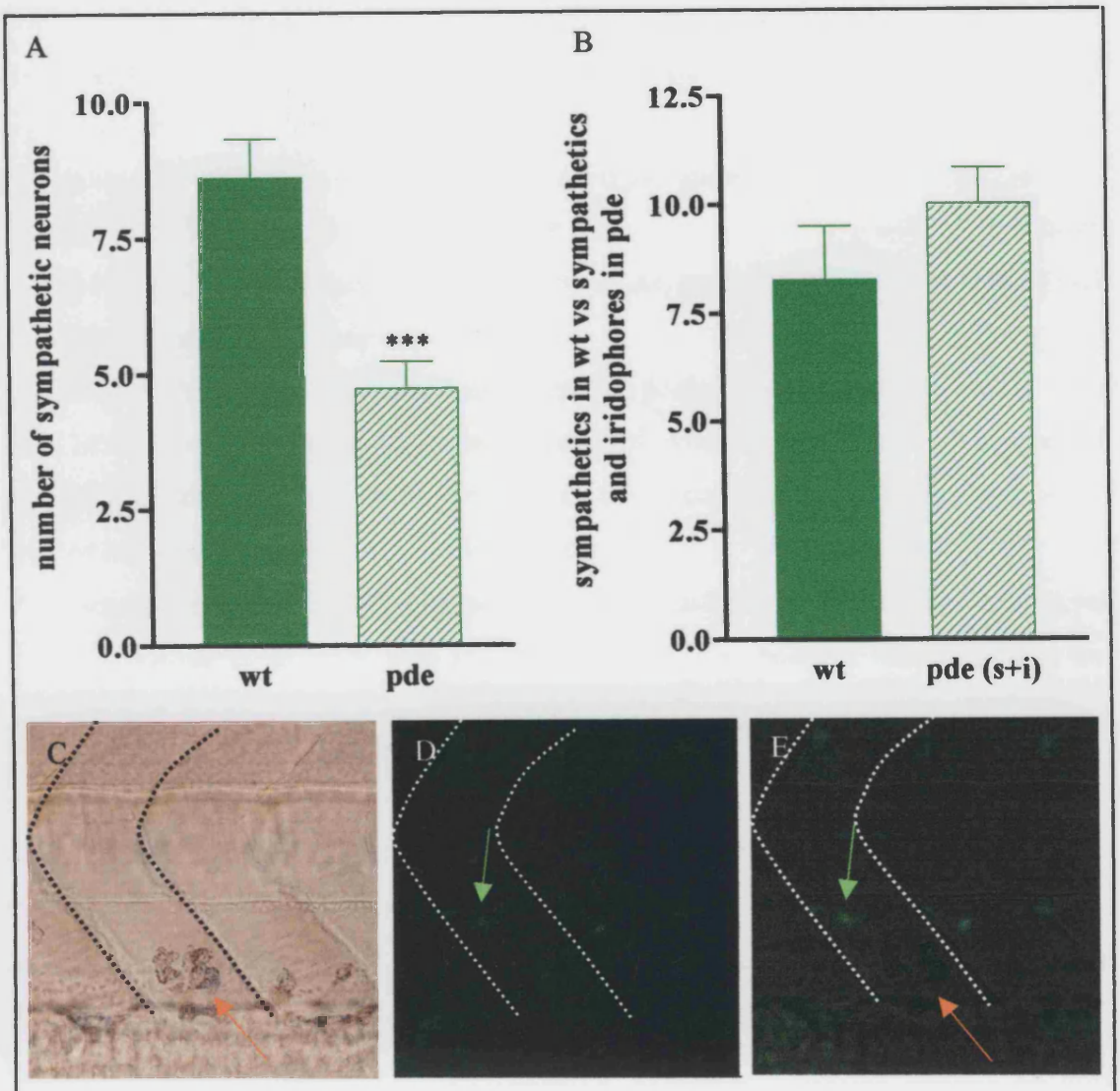

Fig. 4.12: Sympathetic neuron numbers were decreased in *parade*^{tj262}
Counts of Hu antibody labelled sympathetic neurons in the AVS showed a significant reduction in *parade*^{tj262} mutants compared to wild-type siblings (A; $p<0.0001$, Two-tailed t-test; (wild-type: mean +s.e. 8.6 + 0.7 (n=23); *parade*^{tj262} : 4.7 +0.4 (n=40)). However, when comparing the number of sympathetic neurons in wild-type against the number of sympathetic neurons and iridophores in *parade*^{tj262} no significant difference could be observed (B; $p>0.05$, Two-tailed t-test; (wild-type: mean +s.e. 8.2 + 1.2 (n=8); *parade*^{tj262} : 10 +0.8 (n=25)). Comparison of iridophore position (C, E; orange arrow) and sympathetic neuron position (B, E; green arrow) showed that sympathetic neurons and ectopic iridophores could be found in the same somite in *parade*^{tj262} mutants.
A: bright field optics, B: fluorescent light, C: overlay of A and B; somite boundaries are shown as dashed lines

Counts of sympathetic neurons in the area where ectopic chromatophores occur (between the posterior end of the swim bladder and the anus) at 7 dpf showed a significant reduction in their number (Fig. 4.12 A). At 8 dpf the decrease was still detectable ($p<0.05$, Two-tailed t-test; (wild-type: mean + s.e. 9.3+ 0.6 (n=18); *parade*^{tj262}: 7.3+0.6 (n=13)). No difference in Hu antibody staining of enteric neurons or DRG could be seen in *parade*^{tj262} compared to wild-type indicating that the staining had worked well and the decrease was specific.

Counts at earlier stages (5 dpf and 6 dpf) were not performed as at these stages the only cells labelled with Hu antibody were the cervical sympathetic neurons located at the anterior end of the swim bladder. An obvious difference between the staining in wild-type embryos and mutants could not be seen though.

We therefore showed a significant decrease in sympathetic neuron numbers in larval stages in *parade*^{tj262} mutants. This reduction could be dependent or independent of the increase in iridophore numbers.

IV.2.4.C. Presence of ectopic iridophores was not correlated with loss of sympathetic neurons within a somite

In a straightforward model of one cell type transdifferentiating into another reduction of the original cell type by one cell should result in the increase in cell number of the final fate by one. As we had observed a reduction in sympathetic neurons number we next asked if the number of sympathetic neurons and ectopic iridophores in *parade*^{tj262} mutants equalled the number of sympathetic neurons in wild-type embryos in the AVS. We only looked at the number of iridophores as this was the cell population for which we had detected an increase. Our counts revealed that the difference in the AVS between the number of sympathetic neurons alone in wild-type embryos compared to the number of sympathetic neurons and ectopic iridophores together in *parade*^{tj262} mutants was not significantly different (Fig. 4.12 B). Thus, conceivably the loss of sympathetic neurons might be compensated by a gain in iridophores. In principle, of course, this result was consistent with a direct transdifferentiation between these cell types.

If sympathetic neurons transdifferentiate into iridophores a reduction of sympathetic neuron number in close proximity to the ectopic iridophore should be detectable. We therefore studied the distribution of ectopic iridophores in connection with

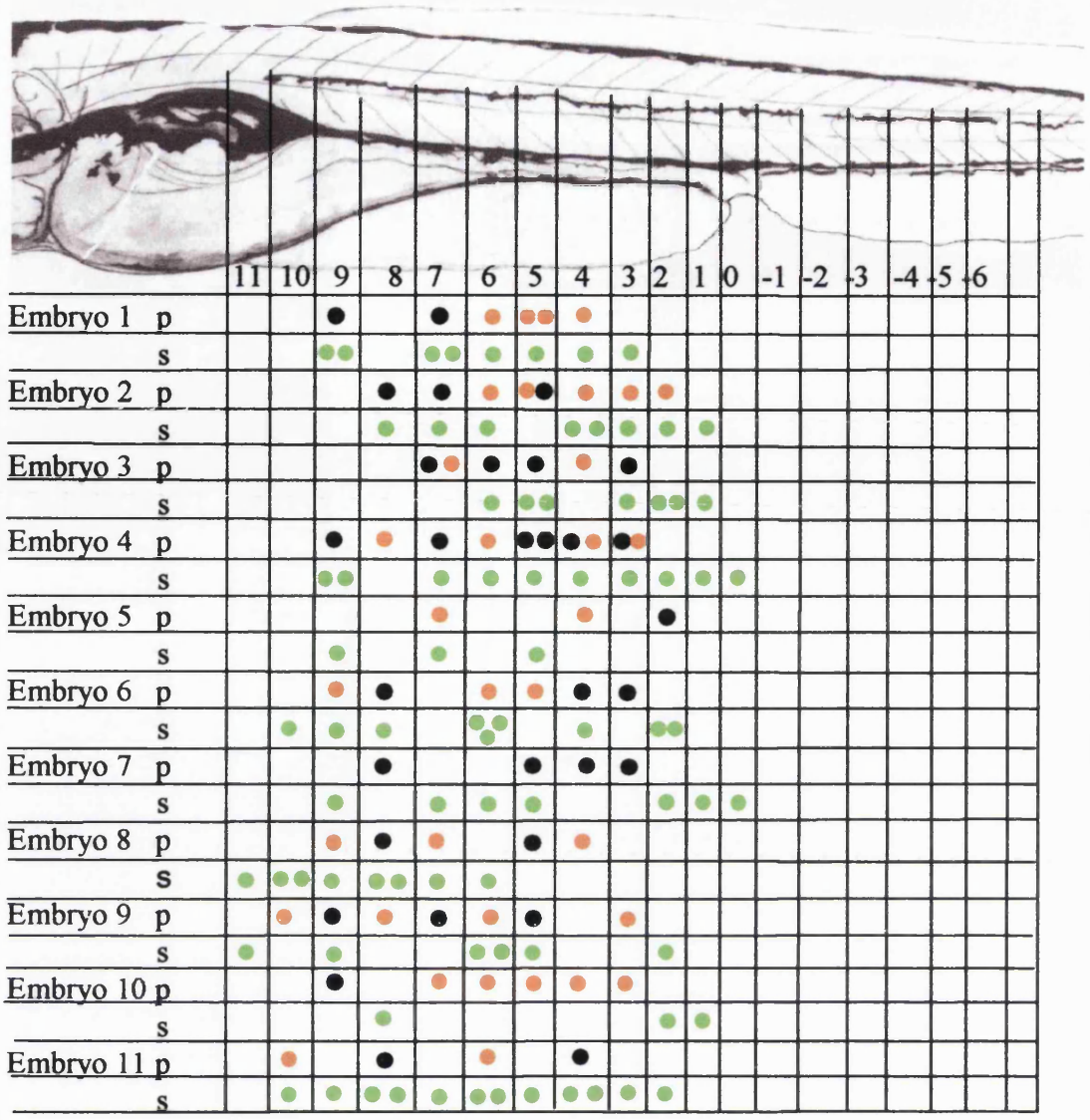

Fig. 4.13: Ectopic iridophores and sympathetic neurons could be found in he same somite

Observation of presence of sympathetic neurons and chromatophores at 7 dpf in the ectopic position per somite showed that presence of ectopic chromatophores in a somite did not necessarily correlate with loss of sympathetic neurons. Each embryo was observed using DIC optics ad fluorescent light and the presence of pigment cells (p) and sympathetic neurons (s) was noted for each somite.

presence/absence of sympathetic neurons within each somite. In both wild-type siblings and *parade*^{tj262} mutants the distribution of sympathetic neurons was similar and not in a regular pattern. Some somites contained up to 3 sympathetic neurons while others contained none. Our observations showed, however, that presence of ectopic iridophores did not consistently result in a complete loss of sympathetic neurons in this somite (Fig. 4.12 C-E and Fig. 4.13). Of the 32 somites observed that contained one or more ectopic iridophore 14 still had 1 sympathetic neuron, 1 had 2 sympathetic neurons and 1 somite even had three sympathetic neurons. 15 somites containing iridophores showed no sympathetic neurons. As the numbers of sympathetic neurons per somite were so irregular it was not possible to conclude from our observations that the loss of a sympathetic neuron in a somite resulted in a gain of an iridophore. Even though the decrease in sympathetic neuron number in *parade*^{tj262} mutants could be connected to the increase in iridophore numbers, it could also be an independent second phenotype. Ideally, we would look at earlier developmental stages to see when loss of sympathetic neurons and increase of iridophores first occurs. But unfortunately no early markers for sympathetic neurons in the trunk have been characterised in zebrafish so far. We therefore focused on when the increase in iridophores can first be detected to see if it is only late and tightly correlated with the described sympathetic neuron phenotype.

IV.2.5. Iridoblast numbers were increased as early as 36 hpf

To see if a transdifferentiation from sympathetic neurons into iridophores was a likely scenario we investigated how early an increase in iridophore and iridoblast numbers could be seen in *parade*^{tj262} mutants. In addition, we asked whether the ectopic appearance of iridophores could be seen as early as the increase in iridophores was visible or later.

Iridophores can be seen displaying their shiny characteristics weakly from about 40 hpf on. However, as they were only just starting to display their characteristics, the number of cells visible seemed quite variable between siblings. At 48 hpf iridophores were clearly and easily visible with incident light and we therefore decided to look at this stage. We first asked if it was possible to establish a clear correlation between presence or lack of iridophores in the ectopic position at 48 hpf and an embryo being *parade*^{tj262}. Thus, embryos were sorted according to presence or lack of iridophores in the ectopic position and grown to 4 dpf in two separate dishes, labelled putative siblings and

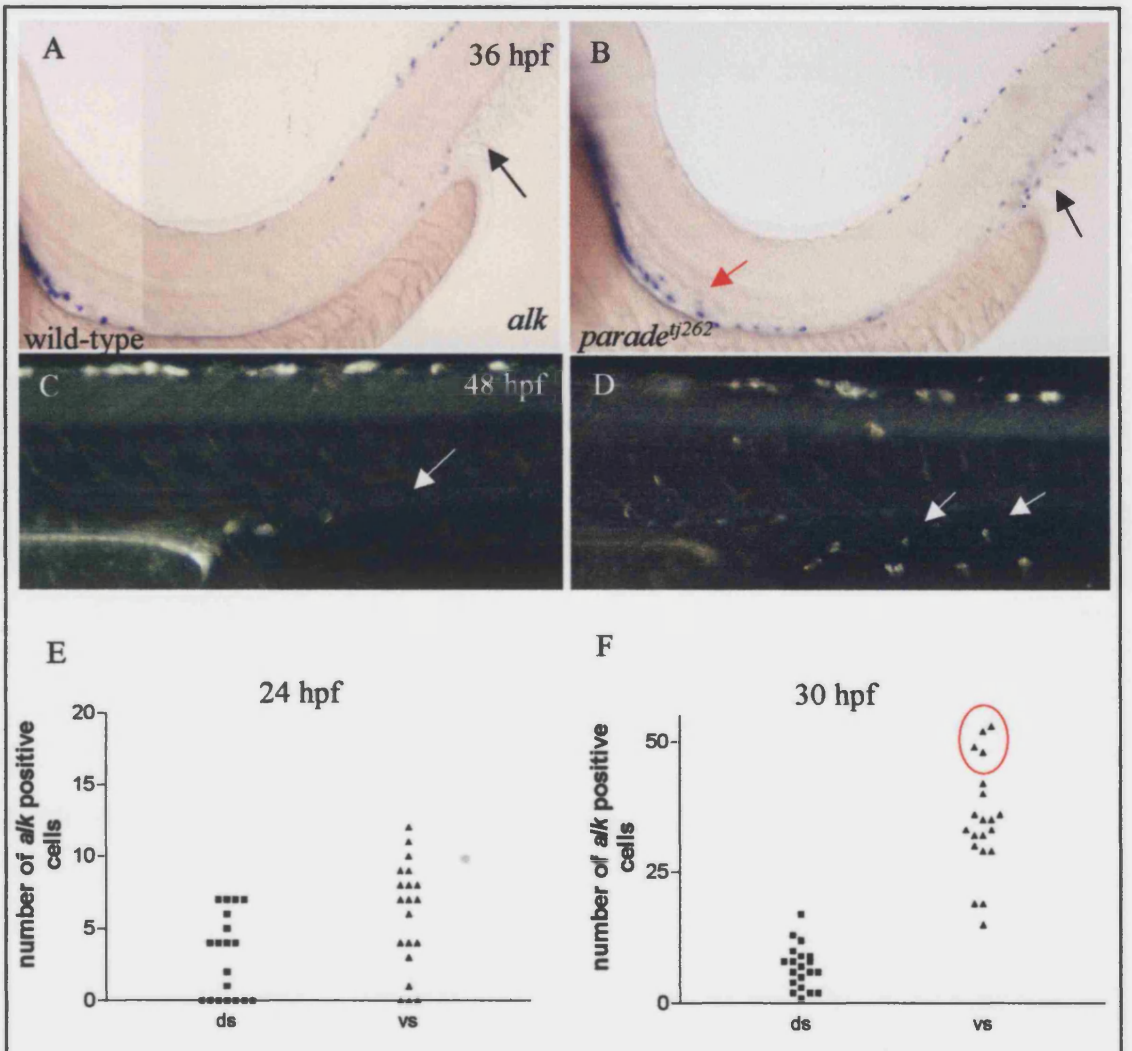

Fig. 4.14: Early increase of iridoblasts and iridophores in *parade*^{tj262} mutants
At 36 hpf *alk*-positive cells can be seen in the DS and VS in wild-type embryos (A). An increase of *alk* positive cells in the VS of *parade*^{tj262} mutants could clearly be seen at 36 hpf (B). Ectopic cells can already be seen in both the trunk (B, red arrow) and the ventral fin. (A, B compare area with black arrow). A few iridophores could be seen in the PVS of wild-type embryos at 48 hpf (C, arrow). The number of iridophores in the PVS of *parade*^{tj262} mutants seemed increased in both the ventral stripe and fin (D, arrows). To observe how early we could see an increase in iridophore precursors we looked at alk expression at 24 and 30 hpf in the progeny of a heterozygous *parade*^{tj262} in-cross. The number of *alk* positive cells in the DS and VS in the progeny of an in-cross was quite variable at both stages as seen by counts in the DS of wild-type and *parade* mutants (DS; E, F)). Counts of *alk* positive cells in the ventral stripe at 24 and 30 hpf also showed high variability (E, F). However at 30 hpf 4/20 embryos appeared to show an increased number of *alk* positive cells (VS, F, red circle)

mutants. But we found roughly the same percentage of *parade*^{tj262} embryos in the sibling and mutants dish at 4 dpf suggesting that at 48 hpf iridophores in the ectopic position were not a feature by which *parade*^{tj262} mutants could be identified. It was, however, possible to distinguish *parade*^{tj262} mutants from their siblings definitively by taking the number of iridophores in the PVS into account. At 48 hpf roughly a quarter of the progeny from a *parade*^{tj262} heterozygous in-cross had more iridophores in the posterior VS and ventral fin (Fig. 4.14 C, D). We again separated the potential *parade*^{tj262} mutants and their siblings and raised them to 4 dpf. Using this criterion, the increased number of iridophores in the PVS, all embryos (25/25) that had been sorted into the 'mutant' Petri dish at 48 hpf were *parade*^{tj262} mutants. Taken together these observations suggest that the increase in iridophore numbers was visible and happened before the appearance of ectopic cells in *parade*^{tj262} mutants, suggesting that the latter might be an effect of the earlier.

We were unable to distinguish *parade*^{tj262} mutants from wild-type siblings based on the iridophore phenotype prior to 48 hpf

Therefore, to determine the earliest time point at which we could see an increase in iridoblast/iridophore number we used the iridophore/-blast marker *alk*. To verify that both the supernumerary and ectopic cells expressed *alk* we first looked at 3 dpf. We could see *alk* expression in the ectopic positions and, as expected, counts showed a significant increase of *alk* positive cells in the PVS of *parade*^{tj262} mutants compared to wild-type embryos (Fig. 4.15).

A clear difference in distribution and number of *alk* positive cells could be seen in roughly a quarter of embryos of a *parade*^{tj262} heterozygous in-cross at 36hpf. In addition to having more *alk* positive cells above the yolk sac extension these embryos had an increase of *alk* positive cells in the PVS, especially ectopically in the ventral fin (Fig.4.14 A, B). Some of the supernumerary *alk* positive cells in the trunk area seemed to be ectopic. As the pattern of *alk* expressing cells in this quarter of the embryos was identical to that of iridophores at 48 hpf we assumed that the embryos with an increase in *alk* positive cells were *parade*^{tj262} mutants. The increase in *alk* positive cells in both these areas can also be seen at all later stages observed.

Counting *alk* positive cells in the DS and VS of a *parade*^{tj262} heterozygous in-cross at 30 hpf indicated that it might be possible to already distinguish mutants from their siblings at this stage. Even though there was slight variation in the number of *alk* positive cells in the DS at this stage it was not possible to identify a group of embryos that had a

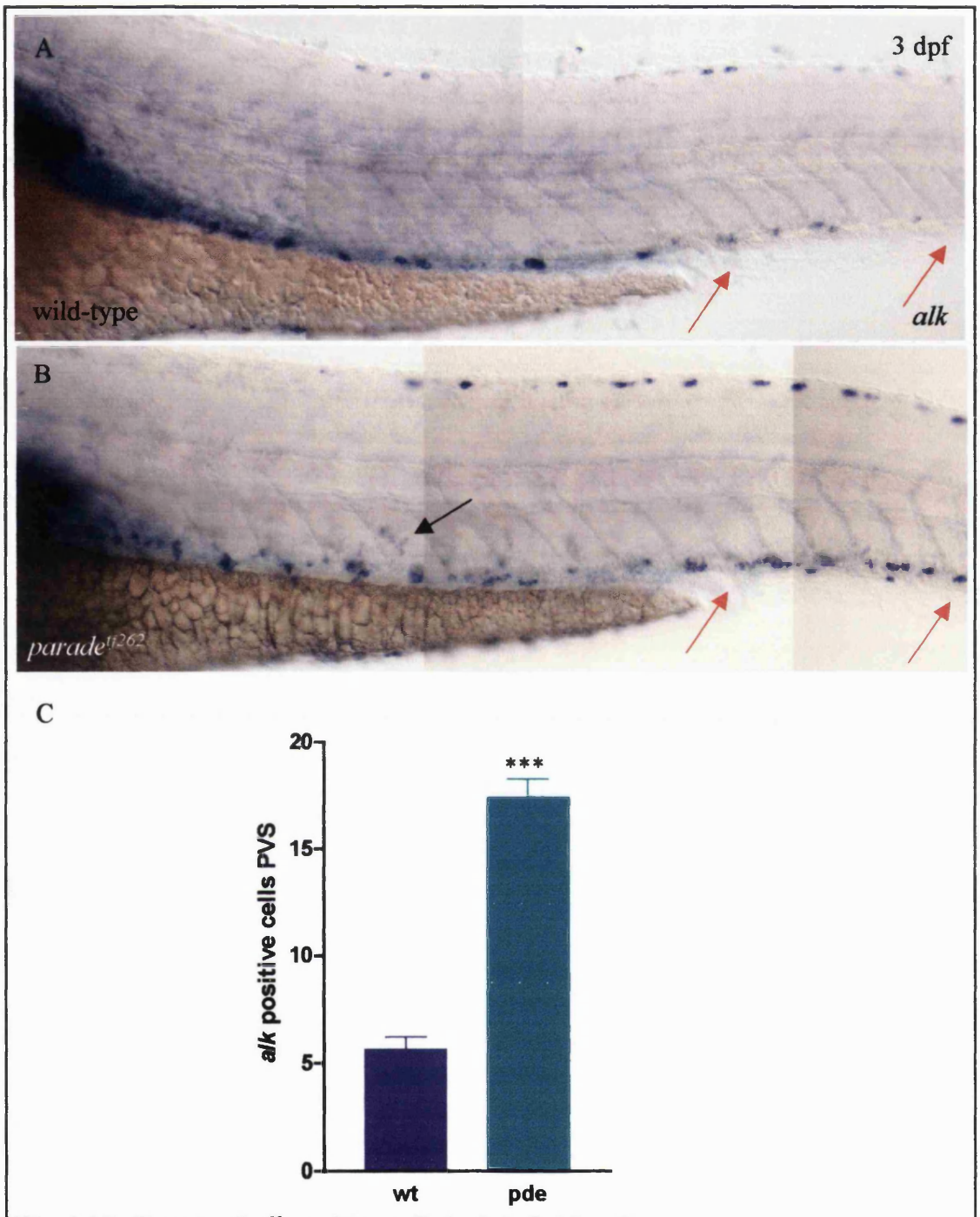

Fig. 4.15: Counts of *alk* positive cells in 3 dpf old embryos
At 3 dpf alk positive cells can be seen in a typical iridophore-like pattern in the dorsal and ventral stripe in wild-type embryos (A). In addition to the wild-type expression domains ectopic, *alk* expressing cells were observed in *parade* ^{tj262} mutants (B, black arrow). As expected from our observations at earlier stages more *alk* positive cells could be seen in the PVS (compared expression between two red arrows in A and B). Counts of *alk* positive cells in the PVS of *parade*^{tj262} mutants showed a significant increase compared to wild-type embryos ($p<0.0001$, Two-tailed t-test; C). (wild-type: mean = s.e. 5.64+ 0.57 (n=17); *parade*^{tj262}: 17.04+0.85 (n=20); C).

strong increase compared to their siblings (Fig. 4.14 F). VS counts however revealed a different picture, with 4/20 embryos appearing to have more *alk* positive cells in the VS than their siblings (Fig. 4.14 F). It seems likely that these 4 embryos were *parade*^{tj262} mutants. Isolation of the gene affected in *parade* allowing genotyping of the embryos would verify this prediction. Interestingly counts of *alk* positive cells in the DS and VS at 24 hpf showed no embryos with an obvious increase in those cells. We therefore speculate that the increase might happen between 24 and 30 hpf (Fig. 4.14 E).

In summary we showed, using *alk* as a marker for iridoblasts, that it was possible to distinguish *parade*^{tj262} mutants from their siblings as early as 36 (and perhaps 30) hpf by an increase in iridophore numbers. Our findings have pushed the point at which it is possible to identify *parade*^{tj262} from 3 dpf to 36 hpf in fixed and to 48 hpf in living embryos. In addition we showed that this increase is the first visible phenotype in parade. The ectopic appearance of the chromatophores the main phenotype so far appears at a later stage (between 48 and 72 hpf).

IV.3. Discussion

In this chapter we have examined the phenotype of the pigmentation mutant *parade*^{tj262} and began to test hypotheses as to how its phenotype might be caused.

At the beginning of this chapter we have introduced multiple scenarios as to how and why chromatophores might appear in the ectopic position. The first scenario we suggested was that some chromatophores during development adopted a mixed chromatophore fate which subsequently led to them being ectopic (Fig. 4.2.B).

To test this hypothesis we investigated which potential pigment cell fates these ectopic chromatophores have and showed that they were both melanophores and iridophores. We excluded that the ectopic cells had xanthophore fate as TEM examination of the organelles of the ectopic cells, but also *in situ* analysis with cell-type specific markers, confirmed that the cells were only of melanophore and iridophore and not xanthophore fate. The position of the cells strongly suggests that these cells have migrated on the medial pathway. It was therefore not necessarily surprising that these cells did not display xanthophore fate as it has been shown that only melanophores and iridophores can be seen on this pathway. Xanthophores migrate on the lateral pathway (reviewed in (Kelsh, 2004)).

Using TEM microscopy we excluded the possibility that the ectopic chromatophores were of mixed melanophore- iridophore cell fate. Various examples of pigment cells with mixed cell fate have been described, but these cells had in all cases the different pigment cell organelles randomly mixed (Bagnara et al., 1979). However, the ectopic chromatophores in *parade*^{tj262} mutants showed distinct areas of reflective platelets and melanosomes separated by cell membranes. Even though the separating cell membranes were slightly harder to detect between areas of reflective platelets and melanosomes in the ectopic cells than in the closely associated cells of the YSS they seemed clearly separated by membranes. In addition, the observation in live embryos that some of the ectopic pigment cells only displayed characteristics of one pigment cell type strengthened the view that the ectopic cells were not of mixed fate.

During the close observations of the *parade*^{tj262} mutant phenotype we however observed a localised increase of iridophores in the VS. The increase in iridophore, but not melanophore, numbers could be observed along the whole length of the VS (including the ectopic cells). Different reasons for an increase in iridophore numbers can be imagined (Fig. 4.2. C, D). Transdifferentiation of cells of another fate into iridophores would lead to and increase in iridophore numbers (Fig. 4.2. C) as would a defect in the regulation of iridophore cell numbers (Fig. 4.2. D).

Cells of one chromatophore type could transdifferentiate into another. In amphibian cell culture experiments both xanthophores and iridophores could be transformed into melanophores. In both cases it resulted in a decrease of the former pigment cell types (Ide, 1978; Ide and Hama, 1976). Transdifferentiation of one chromatophore type would be more plausible easier by the proven existence of a common precursor. Common fate-restricted precursors have been shown giving rise to a melanized and unmelanized pigment cells on the medial pathway in single cell labelling studies in fish (Dutton et al., 2001; Raible and Eisen, 1994a). And a common precursor for all three pigment cell fates has been proposed (Bagnara et al., 1979). We could, however, not see a difference in the numbers of melanophores in the PVS in *parade*^{tj262} mutants at 4 dpf. We also observed no differences in *gch* expression at 3 dpf, indicating that xanthophore numbers were unaffected in *parade*^{tj262} as well. These results suggest that neither differentiated melanophores nor xanthophores transdifferentiate into iridophores. However, we cannot exclude the possibility that a common precursor (for two or potentially all three pigment cell fates) gives in *parade*^{tj262} mutants rise to more iridoblasts than the other two chromatoblasts resulting in increased numbers of iridophores later.

Transdifferentiation of both non-pigmented and pigmented neural crest cell types has been shown *in vitro*. Quail Schwann cells have been shown to be able to transdifferentiate into melanocytes and vice versa in crest culture studies (Dupin et al., 2000; Dupin et al., 2003). Also common fate precursors for pigmented and non-pigmented neural crest cells, e.g. glia and melanocyte, fates have been shown in single cell labelling and culture studies (Dupin et al., 2003; Dutton et al., 2001; Harris and Erickson, 2007). As transdifferentiation of one cell type into another should result in decrease in cell number of the former we checked numbers of possible candidates. Possible non-pigment neural crest derivates transdifferentiating into chromatoblasts could be enteric and sympathetic neurons. We showed that no difference in enteric neuron number could be observed in *parade*^{tj262} tending to exclude transdifferentiation of this fate as a candidate. Secondly, we looked at sympathetic neurons which are in a position similar to the ectopic chromatophores. We could observe a decrease in sympathetic neuron number at 7 dpf. The earliest appearance of ectopic chromatophores can be seen sometime between 48 and 72 hpf. This is about 4 days before we detected the decrease in sympathetic neuron number making it difficult to link the ectopic appearance of chromatophores to the decrease in sympathetic neuron number. Reduction of sympathetic neurons numbers in the tail at stages when they are differentiated could indicate a connection between increase and decrease of iridophores and sympathetic neurons respectively. After all iridophore numbers in the tail are also increased. However, the observation that an increase in putative *parade*^{tj262} mutants can be already seen as early as 36 hpf, long before sympathetic neurons are differentiated, makes it unlikely that transdifferentiation from sympathetic neuron to iridophore fate is responsible for the increase in iridophore numbers. As so far no markers labelling sympathetic neuron precursors in the zebrafish trunk have been isolated, we cannot test if sympathetic neuron precursor numbers are reduced due to them becoming iridoblasts. A recent screen for *sox10* targets might however unearth some markers making it testable (T. Chipperfield and R. Kelsh, pers. communication). Neural crest cells, at least partly assumed to be sympathetic precursors, have been described populating the region just ventral to the dorsal aorta much earlier leaving the possibility that these precursors become chromatophores instead of neurons (Raible and Eisen, 1994a; Raible et al., 1992). Speculative models linking these two phenotypes can be proposed. For example, Bmp2 signalling from the dorsal aorta has been implied in specification of sympathetic neurons (Shah et al., 1996). Another similar signal could be normally responsible to

help regulate the fate choice of a potential iridophore/sympathetic neuron precursor. Loss of this signal could then lead to some cells adopting iridophore instead of sympathetic neuron fate.
Alternatively, the decrease in sympathetic numbers could be independent of the chromatophore phenotype possibly caused by a defect in regulation of cell numbers of both. Sympathetic neurons have been shown to still proliferate up to 4 weeks post fertilization (An et al., 2002). So could loss of a signal responsible for regulating numbers of both cell types result in over-proliferation of iridophores and reduced proliferation of sympathetic neurons?

The large time gap between the first presence of increased *alk* positive cells at 36 hpf and the differentiation of sympathetic neurons suggests that a mechanism, other than transdifferentiation, might be responsible for the *parade*^{tj262} phenotype. This early increase could be a result of defects in the regulation of cell proliferation or apoptosis directly or indirectly affecting VS iridophores. Alternatively, a higher number of neural crest cells than in wild-type embryos could differentiate into iridoblasts.
As we can already detect an increase in the number of *alk* positive cells at 36 hpf we looked for an increase of proliferating or decrease of apoptosing cells between 24 and 36 hpf in *parade*^{tj262} mutants. Unfortunately, we were not able to identify potential *parade*^{tj262} embryos before 40 hpf, other than by *alk* expression, as the ectopic positioning of the pigment cells seemed to occur later and iridophores did not display their reflective properties yet. As we were not able to pre-sort the embryos into *parade*^{tj262} mutants and siblings we needed to perform double staining, labelling the iridoblasts/iridophores with *alk* to be able to identify the mutants by an increase in this specific population.
To test if *parade*^{tj262} mutants have increased proliferation we therefore planned to count the number of cells positive for *alk* and Phospho-Histone 3 (PH3) Antibody, which is highly specific for cells in mitosis. Even though PH3 Antibody worked well as a single staining, it did not work with a standard *in situ* hybridisation-Antibody double protocol. Possible reasons for this could be steps in the *in situ* protocol such as treatment with Methanol or washing at high temperatures. Treatment with Methanol is often incompatible with preservation of antigens. But omission of the Methanol step did not lead to visible Antibody staining. To avoid high temperature affecting the protein configuration and therefore binding capacity we incubated with primary PH3 Antibody

before moving on to the *in situ* protocol, but this did not improve the Antibody staining either. Further careful adjustments to both protocols such as change in concentration of Antibody, hybridisation temperature or incubation times will hopefully overcome these difficulties, allowing us to test this idea.

An alternative mechanism leading to an increase in iridophore number is a defect in regulation of apoptosis. Cells undergoing apoptosis can be labelled using TUNEL. We combined the TUNEL staining with *alk* to label the iridophore precursors to be able to see if less cell death occurs in iridophore precursors in *parade*^{tj262} mutants. Unfortunately, even though both protocols work separately, the double staining has not worked so far. One of the key steps during the TUNEL protocol is the transfer of a biotin-dUTP by a terminal deoxynucleotidyl transferase to the strands breaks in the DNA caused by endonucleases. As the *in situ* staining was performed first, again sensitivity in this step might be lost by the effects of Formamide or high temperatures during hybridization. By integrating the TUNEL protocol into the *in situ* protocol we brought this step forward and did it before the hybridisation. This increased the TUNEL signal, even though it was not perfect, but probably due to degradation of the mRNA in the meantime resulted in loss of the *in situ* signal. Further modifications to the protocols, such as reduction of hybridization temperature, to improve the staining have to be tested.

Another reason for the early appearance of supernumerary iridophores could be that a higher number of neural crest cells differentiate into iridoblasts/iridophores. *parade*^{tj262} is not the only mutant that has an early increase in iridophore numbers. Counts have shown that in *nacre* mutants the increase in iridophores is an early event as well. Loss of *mitfa* results in an early loss of melanophore precursors and at 30 hpf, the earliest time point looked so far, *nacre* mutants already have more *alk* positive cells than wild-type siblings (E, Greenhill, personal communication). Here, like in *parade*^{tj262}, the increase of iridophore numbers can be attributed to an early phase of development before circa 30/36 hpf. In contrast to *parade*^{tj262} mutants though, the increase of iridophores in *nacre* is coupled to a loss of melanophores. It has been suggested that in *nacre* the increase in iridophore numbers could be a secondary effect caused by direct or indirect regulation of their numbers by melanophores or that instead of becoming melanoblasts cells adopt iridophore fate and these are maintained subsequently (Lister et al., 1999). Similar to *parade*^{tj262} mutants the medaka mutant *ml-3* has a localized increase of leucophores in the DS and head only showing that an increase of one cell

type can be localised (Kelsh et al., 2004). Preliminary characterisation of *ml-3* mutants revealed that they also lack xanthophores suggesting that the increase in leucophores could possibly be connected to the loss of xanthophores. A fate switch scenario similar to that proposed in *nacre* could take place in *ml-3* mutants. This would be also analogous to the increased melanoblast phenotype in *Dsk1* and *Dsk7* mice. Heterozygous *Gnaq* (*Dsk1*) and *Gna11* (*Dsk7*) mutants have an increased number of melanocytes suggested to result from more neural crest cells differentiating into melanoblasts (Van Raamsdonk et al., 2004). Whilst the increase can be initially seen in epidermis and dermis, melanocyte numbers in the epidermis at later stages are wild-type also illustrating that a mechanism for regulation of supernumerary cell number can be spatially restricted. Thus it would be possible that in *parade*^{tj262} mutants an increase in iridoblasts in other areas such as the DS could be regulated very fast. The finding that *nacre* mutants have increased iridophore numbers in both stripes however argues somewhat against this possibility. Testing of an early increase in iridoblast number is however slightly difficult as all iridoblast markers so far for stages such as 24 hpf seem to label more than one neural crest cell/ chromatophore type.

The observation that the increase of iridophores in the VS of *parade*^{tj262} mutants, and not as previously thought the appearance of ectopic iridophores, is the first phenotype suggests that the ectopic positioning may be a secondary effect.
Consistent with this proposal, the increase of iridophore numbers in the PVS was actually higher (an increase of 32% in the AVS compared to 52 % in the PVS) although not associated with ectopic cells. A significant increase in the AVS could only be reported when taking the ectopic iridophores into account, suggesting that the number of iridophores in the wild-type AVS position was not increased compared to wild-type. In the PVS most of the supernumerary iridophores were located within the PVS itself revealing a difference in the behaviour of supernumerary cells and explaining why this increase had not been spotted earlier. Iridophores in an ectopic position could sometimes be observed in the PVS though.

A first step in discovering the mechanism responsible for the ectopic positioning is to see when they first appear. The ectopic chromatophores in the trunk had been reported to be present and clearly visible at 3 dpf (Kelsh et al., 1996) and our observations confirmed this. At 36 hpf when the first supernumerary *alk* positive cells can be seen in

the trunk some of these cells were also in the ectopic position. But some embryos without an increased number of *alk* positive cells sometimes had cells in the ectopic position. This indicated that even though some of the ectopic cells in the potential *parade*^{tj262} embryos might be future ectopic cells, it is likely that some of these cells are only temporarily in the ectopic position while migrating down the ventral pathway. At 48 hpf *parade*^{tj262} mutants could not yet be distinguished by presence of ectopic iridophores, although chromatophores in the position later occupied by the ectopic cells were visible in both wild-type and mutant embryos. From simple observations at different time points it was not possible to say which of these cells would be ectopic. Time-lapse studies monitoring the behaviour of the chromatophores between 30 and 72 hpf would help solve this question. At this stage melanophores can be easily tracked as at least a large majority of them melanized already. Iridophores will be harder to track as they only start displaying their reflecting properties from 40 hpf on. We have now an established system to do time-lapse studies in the laboratory and are hoping to perform them soon.

Even though something is known about the regulation of the start of migration and during migration of pigment cells nothing is known of mechanisms involved in maintenance of the established embryonic stripe pattern. Our observations that we cannot see ectopic iridophores in some of the *parade*^{tj262} embryos could indicate that cells that are in the ectopic position at 3 dpf originate in the VS, but then supernumerary cells are expelled. This would imply a mechanism regulating cell numbers in the stripes. Cell-cell interactions of chromatophores could be responsible for regulation of cell numbers in the stripes in zebrafish. Homotypic and heterotypic interactions between melanophores and xanthophores have been shown to be necessary for stripe formation in adults (Maderspacher and Nusslein-Volhard, 2003). Even though complete loss of melanophores or iridophores does not result in failure of stripe formation in zebrafish embryos, a role for cell-cell interactions in embryonic stripe formation has been widely assumed from observations (Kelsh, 2004). For example, xanthophores occupy the spaces resulting from loss of some DS melanophores in *sparse* mutants (Kelsh et al., 1996). And positioning of melanoblasts invading the LS in a second wave is negatively influenced by melanoblasts of the first wave (Milos et al., 1983). In addition our TEM observations show very close association of melanophores and iridophores in the stripes. Therefore, an initial hypothesis was that each stripe has the ability to

accommodate a certain number of pigment cells –a holding capacity. Supernumerary pigment cells will then be expelled from the stripe. Loss of one pigment cell type allows more cells of another pigment cell type to accommodate the stripe as seen in *nacre* (Lister et al., 1999).

This hypothesis fits nicely with our observation of iridophore behaviour in the AVS where most (all) supernumerary iridophores are ectopic. In the PVS however only some ectopic iridophores were found ectopically between the somites or in the fins of *parade*^{tj262} mutants whereas the majority of (sometimes all) supernumerary iridophores can be found in the VS itself. The different behaviour of the supernumerary iridophores in the AVS and PVS might be caused by different limits to holding capacity depending on the amounts of space available for the pigment cells in the different areas of the stripe. While the VS above the yolk sac in wild-type embryos is covered with tightly packed melanophores and iridophores, gaps between the pigment cells can be seen in the PVS. These gaps might allow the PVS to accommodate a greater increase in pigment cell numbers. This would explain why most of the supernumerary cells in the PVS stay in the stripe. The numbers of iridophores in the stripe might be regulated by cell-cell interaction between iridophores or between iridophores and another pigment cell type e.g. melanophores. From our observations so far it looks though as if only iridophores and not melanophores in the VS are supernumerary. Close interactions of iridophores and melanophores in the VS of wild-type and *parade*^{tj262} embryos might lead to some melanophores leaving the VS with the iridophores. Melanophores in the ectopic position are however not always associated with iridophores making this scenario less compelling. It seems therefore more likely that the holding capacity of the VS is reached by presence of a few supernumerary iridophores in the VS which subsequently leads to a highly variable small number of melanophores being expelled. Close physical presence of both cell types in the ectopic position might then lead to interaction and close association.

Alternatively, an environmental cue from a tissue close to the VS, for example the gut, could be necessary to form or maintain the (A)VS. Similarly to the involvement of environmental cues in LS formation in *choker* mutants, where *sdf1a* along the myospetum is necessary for correct stripe formation (Svetic et al., 2007). A change in the expression of an environmental signal in *parade*^{tj262} mutants would then lead to some cells leaving the VS. This scenario would also explain why mostly cells in the area we defined as the AVS are ectopic as this is the stretch of VS dorsal to the gut.

Diffusion of the environmental cue into the first few somites of the PVS could then lead to cells appearing, as observed, in the ectopic position in the first few somites of the PVS.

We will investigate and discuss the (in-) dependence of melanophores on iridophores and vice versa to appear in the ectopic position in the next chapter using double mutants.

Factors other than cell-cell interactions have been implicated in regulation of pigment cell patterning. Likewise, factors within the pigment cell as well as in the tissue they are migrating through appear to be important (Harris and Erickson, 2007). Both changes within the migrating chromatophores and the environment they are migrating through seem necessary to allow wild-type patterns and timing of migration. Expression of EphB receptors in melanoblasts and ephrinB ligands along the dorsolateral migration pathway in chick, for example, are responsible for timing and pathway choice of melanoblasts along one pathway while preventing them from entering the other (reviewed in (Halloran and Berndt, 2003)). On the other hand factors such as PNA-binding protein, expressed in a dynamic manner in both pathways, have been suggested to block crest cell migration along the dorsolateral pathway in chick (Oakley et al., 1994). In the Silkie fowl loss of the barrier molecule PNA causes supernumerary melanoblasts to migrate into normally unpopulated tissues (Faraco et al., 2001; Reedy et al., 1998b). At the same time no changes in melanocyte appearance in dermis and epidermis have been reported. This scenario is reminiscent of that we describe here in *parade*^{tj262} mutants, where an increase in a pigment cell type coincides with ectopic appearance of pigment cells. In zebrafish *choker* mutants, ectopic expression of *sdf1a* leads to a limited number of melanophores leaving the DS and VS and forming an ectopic collar of melanophores (Svetic et al., 2007). Similarly loss of a molecule, normally creating a barrier to prohibit chromatophores from migrating up the medial pathway once they have reached the VS and expressed by a tissue lying above the VS, in *parade*^{tj262} could lead to cells moving out of the VS into the ectopic position. The reduced number of supernumerary pigment cells in the PVS might, as above, be due to differences in the density of chromatophores in the AVS and PVS. This model suggests that before moving into the ectopic position all cells should be located in the VS. This might possibly explain why we cannot correlate presence of ectopic iridophores at 48 hpf with presence at 5 dpf. At 48 hpf these cells might be in the VS and only migrate

dorsally again a bit later. As mentioned above careful time-lapse studies will help solve this problem.

As an alternative to loss of a factor expressed in e.g. the myotomes, differences in timing of expression of such a factor in *parade*^{tj262} might lead to ectopic positioning of the cells. It is possible that a migration barrier is put up earlier in *parade*^{tj262} mutants than in wild-type embryos. Only late migrating cells would be caught in the ectopic position. That could explain the variability in the number of ectopic cells as a slight difference in timing either of the late migrating cells or the erection of the barrier could lead to more or less cells getting stuck.

The increase of iridophores without an observed loss of another pigment cell fate makes *parade*^{tj262} different to all so far observed embryonic zebrafish mutants and the first pigment pattern mutant that has an increase in one pigment cell type without loss of another whilst showing a difference in pigment pattern from wild-types. As *parade*^{tj262} adults show no easily detectable phenotype *parade* might not play a function in late development.

Chapter V Characterization of *colourless*^{m618}; *parade*^{tj262} (*cls*^{m618}; *pde*^{tj262}), *shady*^{ty82}; *parade*^{tj262}(*shd*^{ty82}; *pde*^{tj262}) and *nacre*^{w2}; *parade*^{tj262} (*nac*^{w2}; *pde*^{tj262}) double mutants

V.1. Introduction

The outstanding phenotype of *parade*^{tj262} mutants is the appearance of ectopic chromatophores located above the VS. In the previous chapter we have shown that the ectopic cells are melanophores and iridophores which in some cases are closely associated. In addition there is also an increase in iridophore numbers in the VS. The localized appearance of both ectopic and supernumerary iridophores raises the possibility that one is dependent on the other. In addition, the close association of some of the melanophores and iridophores could indicate that their ectopic appearance is dependent on each other.

To begin to investigate the reason for the appearance of the ectopic chromatophores we utilized the characterised pigment specification mutants *colourless*^{m618}, *shady*^{ty82} and *nacre*^{w2} (Dutton et al., 2001; Kelsh and Eisen, 2000; Lister et al., 1999; Lopes et al., in prep.). Lack of *sox10* function in *colourless*^{m618} mutants leads to loss of all non-ectomesenchymal crest fates (Dutton et al., 2001; Kelsh and Eisen, 2000). Even though progenitors of these cells are present in *colourless*^{m618} mutants, they fail to become specified and differentiate and die by apoptosis between 35 and 45 hpf. *mitfa/nacre*^{w2} mutants lack all neural crest-derived melanophores and have an ~40% increase in iridophores (Lister et al., 1999).. Loss of *alk* function results in loss of all iridophores in *shady*^{ty82} mutants (Lopes et al., in prep.). However, an 'escaper iridophore' can be found from time to time. No changes in other neural crest derivatives have been observed so far in *shady*^{ty82} mutants.

By combining these mutations with *parade*^{tj262} in double mutant embryos, we can test specific models for the mechanism generating ectopic pigment cells in *parade*^{tj262} mutants.

V.1.1. Models for presence of ectopic cells

V.1.1.A. Transdifferentiation

We have previously suggested and investigated different models as to how these ectopic cells appear. One possibility for the appearance of the supernumerary iridophores is transdifferentiation of cells of another fate into chromatophores (Table 5.1, Model 1). These cells could then be ectopic due to space restrictions in the VS or they might not

be fully or correctly differentiated. As described previously, cells transdifferentiating into iridophores could either be cells of another neural crest

Models	**mechanism**	***cls*^{m618}; *pde*^{tj262}** (no non-ectomesenchymal crest derivatives)	***nac*^{w2};*pde*^{tj262}** (no melanophores)	***shd*^{ty82};*pde*^{tj262}** (no iridophores)
1) Transdifferentiation Cells of another fate transdifferentiate into the ectopic melanophores and iridophores	neural crest derivative	No ectopic melanophores or iridophores	Ectopic iridophores or no iridophores	Ectopic melano-phores
	non neural crest derivative	ectopic melanophores or iridophores	Ectopic iridophores and possibly melanophores	Ectopic melano-phores and possibly irido-phores
2) Capacity Loss of *parade* leads to a defect in regulation of cell numbers resulting in a localised increase in iridophore numbers. Ectopic iridophores appear due to a mechanism limiting cell numbers in the VS.	Appearance of ectopic melanophores dependent on iridophores	No ectopic melanophores or iridophores	Ectopic iridophores	No ectopic melano-phores
	Appearance of ectopic melanophores independent of iridophores	No ectopic melanophores or iridophores	No ectopic iridophores	Ectopic melano-phores and no ectopic irido-phores
3) Migration Loss of *parade* leads to an increase in iridophore numbers and a defect in maintenance/ establishment of the stripe	Appearance of ectopic chromatophores dependent on loss of 'migration factor'	No ectopic melanophores	Ectopic iridophores	Ectopic melano-phores

Table 5.1: Predicted phenotypes of pigment double mutants under different models of *parade* function

derivative or of a non-neural crest fate. Cells have been shown to be able to transdifferentiate from one neural crest fate into another in cell culture studies. Ide and colleagues transdifferentiated xanthophores and iridophores into functional melanophores in amphibian cell cultures (Ide, 1978; Ide and Hama, 1976). Further evidence came from Thibaudeau and Holder (1998) who have monitored cells displaying xanthophores characteristics transdifferentiating into cells with melanophore characteristics in axolotl cell culture. Examples of non-pigment neural crest derivatives differentiating into pigment cells are also known. In the presence of bFGF or 12-*O*-tetradecanoyl phorbol-13-acetate, Schwann cells can transdifferentiate into melanocytes (Sherman et al., 1993; Stocker et al., 1991). Our observations in the previous chapter suggest that neither enteric neurons nor melanophores or xanthophores transdifferentiate into iridophores. We have shown a strong reduction in sympathetic neuron numbers in *parade*^{tj262} mutants but were not able to establish a definitive link to the presence of the ectopic iridophores. This can be tested by observing pigmentation in *colourless*^{m618}; *parade*^{tj262} double mutants. Presence of ectopic iridophores in *colourless*^{m618}; *parade*^{tj262} would clearly show that there is no link as no sympathetic neurons can be detected in *colourless*^{m618} mutants (Kelsh and Eisen, 2000).

If cells from a non-neural crest derivative transdifferentiate into melanophores and iridophores, we should observe ectopic chromatophores in *colourless*^{m618}; *parade*^{tj262} double mutants (given that their transdifferentiation is *sox10* independent (Table 5.1, Model 1 and Fig.5.1)). In *shady*^{ty82}; *parade*^{tj262} double mutants we would expect to get ectopic melanophores and possibly ectopic iridophores. In contrast to that *nacre*^{w2}; *parade*^{tj262} double mutants should display ectopic iridophores and possibly melanophores (Table 5.1, Model 1). However, if the ectopic cells are derived through transdifferentiation of a non-ectomesenchymal crest derivative we would expect to see no ectopic chromatophores in *colourless*^{m618}; *parade*^{tj262} double mutants as all pigment cells are lost. *shady*^{ty82}; *parade*^{tj262} and *nacre*^{w2}; *parade*^{tj262} double mutants would be expected to have only ectopic melanophores and iridophores respectively.

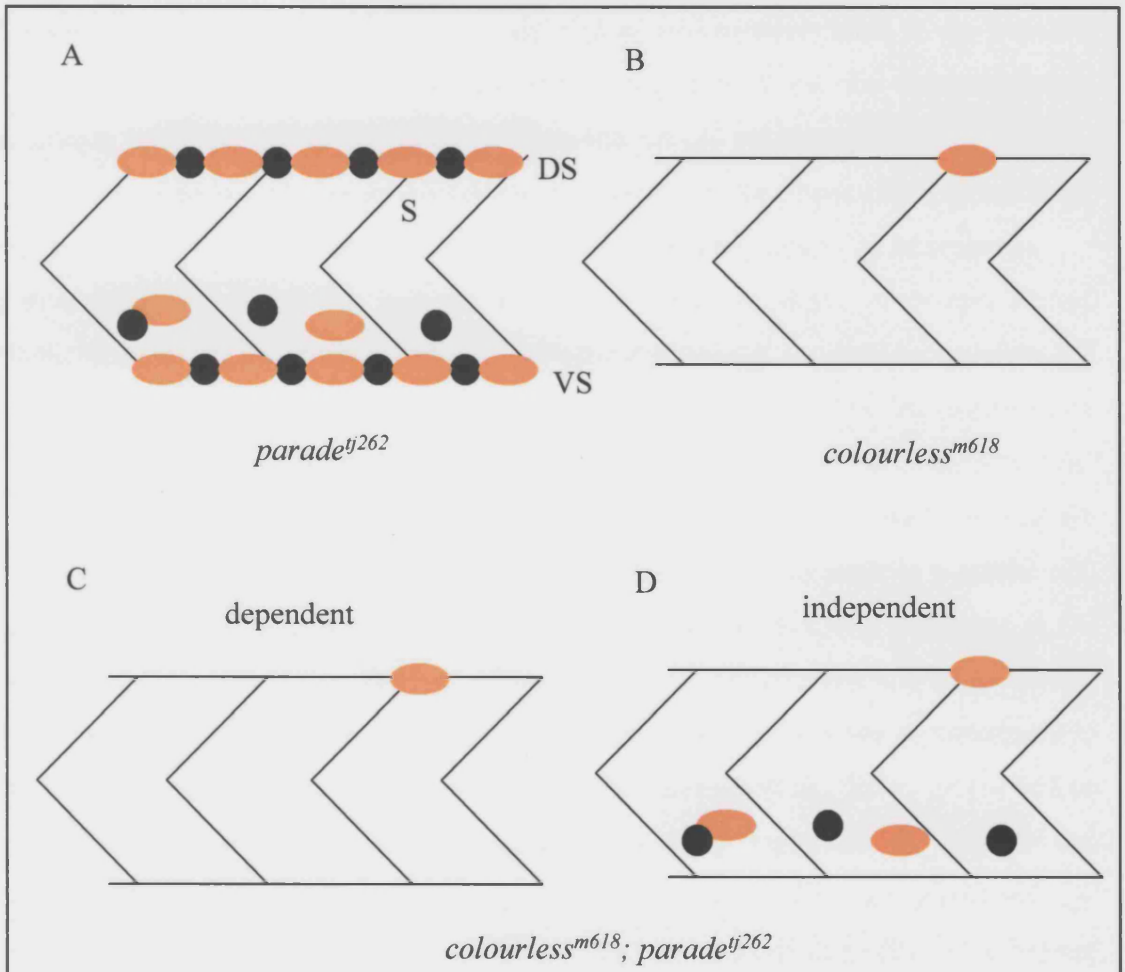

Fig . 5.1: Model for possible *colourless*^{m618}; *parade*^{tj262} phenotypes
parade^{tj262} mutants display melanophores (black circles) and iridophores (orange circles) in the dorsal and ventral stripe and the ectopic position (A). *colourless*^{m618} mutants have no melanophores and only very few iridophores (B). If appearance of ectopic chromatophores is dependent on *sox10*, *colourless*^{m618}; *parade*^{tj262} mutants should not have any ectopic chromatophores (C). If however, the ectopic cells are independent of *sox10*, for example through trans-differentiation from a non neural crest cell type, *colourless*^{m618}; *parade*^{tj262} double mutants should have ectopic pigment cells (D).

V.1.1.B. Limit in capacity

An alternative model is that a defect in regulation of cell numbers leads to the increase in iridophore numbers. Due to chromatophore capacity limits the supernumerary iridophores would be subsequently repelled into the ectopic position (Table 5.1, Model 2). Presence of melanophores in the ectopic position could be physically dependent on the ectopic iridophores e.g. they are dragged into the ectopic position by iridophores.

To investigate the possibility that the increase in chromatophore, more specifically iridophore, numbers is responsible for the ectopic positioning we need to correlate the presence of supernumerary and ectopic pigment cells in the VS. Only a few examples of mutants with ectopic chromatophores are known. Most of these mutants possess only one pigment cell type- melanocytes. Interestingly, in most of these mutants the ectopic positioning of a pigment cell type goes hand in hand with an increase in pigment cell numbers. But even though it has been shown that the gain-of-function mutations in G-protein subunits result in an increased melanocyte number in hair and non-hairy skin in the mouse *Dsk 1, 7* and *10* mutants it has not been examined how the supernumerary, ectopic melanocytes get into their position (Van Raamsdonk et al., 2004). In the Silkie fowl continued proliferation of melanoblasts has been suggested to lead to the supernumerary melanocytes. These migrate into areas usually not populated by melanocytes. Loss of PNA-binding molecules and subsequent reduction of a barrier against melanoblasts migrating medially from the dorsolateral pathway and late ventral migration has been suggested to be responsible for the ectopic appearance. (Faraco et al., 2001). But again it has not been shown if the ectopic positioning is (in-) dependent of the increase in melanoblast number or vice versa. Some zebrafish mutants with ectopic pigment cells have been studied already. The zebrafish *nacre* mutant shows an increase and ectopic positioning of iridophores (Lister et al., 1999). Here, in contrast to *parade*^{tj262}, the increase is visible in both the DS and VS and the ectopic cells are located (mostly) in the fins. The reason for the ectopic positioning of the iridophores in *nacre* mutants has not been determined yet. However, it is unlikely to be caused by a general chromatophore overcrowding of the DS and VS as ample space should be available in the stripes after the loss of the melanophores. It is possible though that an unknown regulatory mechanism puts an upper limit to the number of iridophores per stripe. This could be similar to the situation in the PVS of *parade*^{tj262} mutants where only some of the supernumerary iridophores are ectopic.

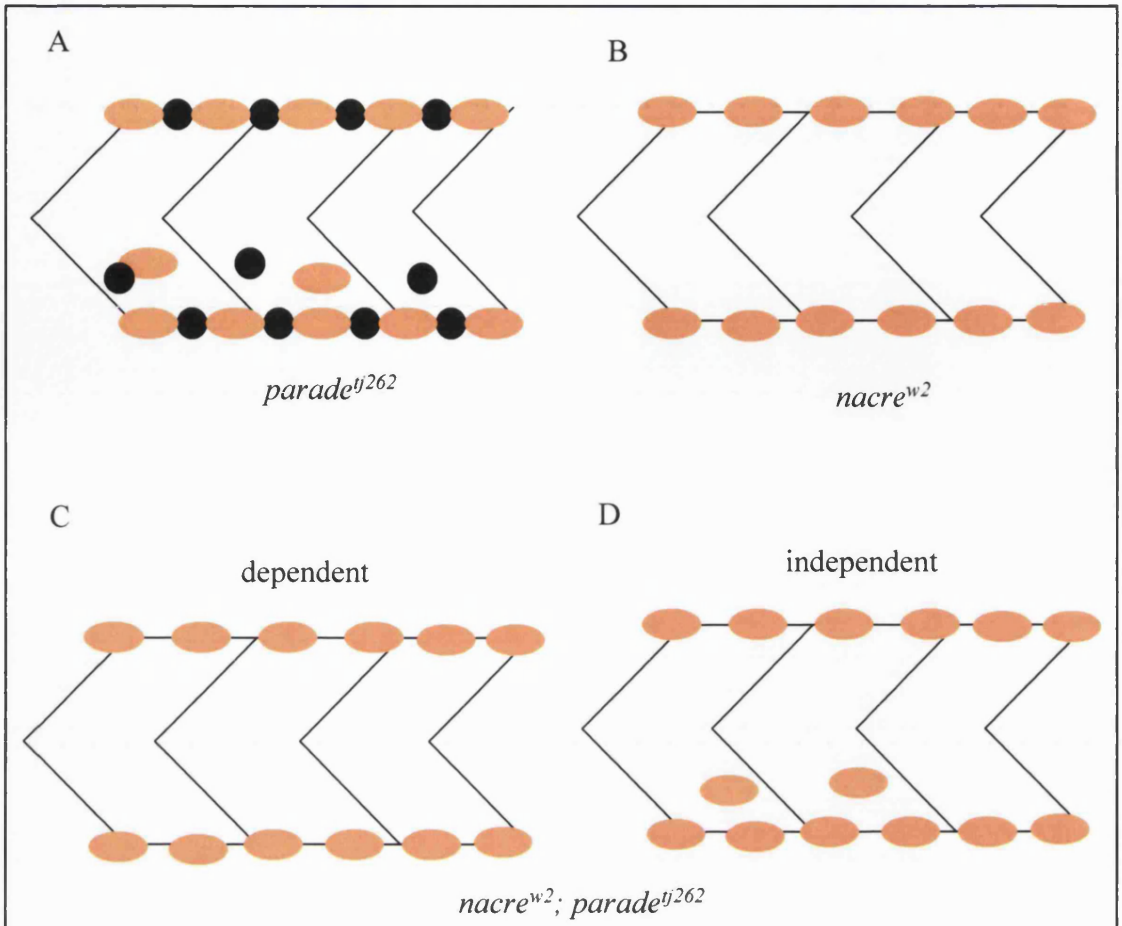

Fig. 5.2: Model for possible *nacre^{w2}; parade^{tj262}* phenotypes
parade^{tj262} mutants display melanophores (black circles) and iridophores (orange circles) in the dorsal and ventral stripe and the ectopic position (A). *nacre^{w2}* mutants do not have any neural crest derived melanophores, but have an increased number of iridophores in the dorsal and ventral stripe (B). In addition ectopic iridophores can be found in the fins (not shown). If appearance of ectopic iridophores in dependent on melanophores we would expect to lose the ectopic iridophores in *nacre^{w2}; parade^{tj262}* double mutants (C). However, we would expect to still see ectopic iridophores if their ectopic appearance was independent of that of melanophores (D).

If, as proposed, close association of melanophores and iridophores is responsible for the ectopic positioning of melanophores the loss of iridophores in *shady*^{ty82}; *parade*^{tj262} double mutants should also result in loss of ectopic melanophores (Table 5.1; Model 2 and Fig.5.2). Alternatively if the ectopic localisation of the melanophores is independent of their interaction with iridophores, *shady*^{ty82}; *parade*^{tj262} double mutants should still display ectopic melanophores (Table 5.1, Model 2 and Fig.5.2). Similarly the dependence of iridophore appearance on presence of melanophores in the ectopic position can be tested showing if a loss of melanophores could overcome a possible overcrowding effect in the VS caused by the increased number of iridophores. Loss of the ectopic iridophores in *nacre*^{w2}; *parade*^{tj262} mutants would indicate that presence of melanophores in the VS is necessary for iridophores appearance in the ectopic position (Table 5.1, Model 2 and Fig.5.3). As *nacre*^{w2} mutants lack all melanophores, dependence of iridophores on melanophore should result in loss of ectopic cells, whereas independence should result in ectopic iridophores in *nacre*^{w2}; *parade*^{tj262} double mutants (Fig.5.3).

V.1.1.C. Migration

Thirdly, if appearance of ectopic chromatophores is independent of each other, a defect in establishment or maintenance of the VS, such as loss of a barrier molecule that normally inhibits pigment cells from re-entering the medial pathway once they reached their final destination, could lead to ectopic positioning of some melanophores and iridophores (Table 5.1, Model 3).

Timing, as well as pathfinding, of neural crest cells has been studied extensively, especially in chicken (Krull, 2001; Oakley et al., 1994). Multiple attractive and inhibitory molecules have been suggested to be implicated in promoting and preventing migration and regulating on which pathway the neural crest cells migrate. Time lapse microscopy of early migrating neural crest cells in zebrafish suggested that inhibitory signals from the somites along the lateral pathway lead to collapse of cell protrusions including filopodia of neural crest cells trying to venture down the pathway and the cells then using the medial pathway instead (Jesuthasan, 1996). In chicken expression of both peanut agglutinin lectin (PNA)-binding activity and chondroitin-6-sulfate (C6S) has been shown to correlate with this inhibition of entry into the dorsolateral path (Oakley et al., 1994). In comparison very little is known about signals that stop neural

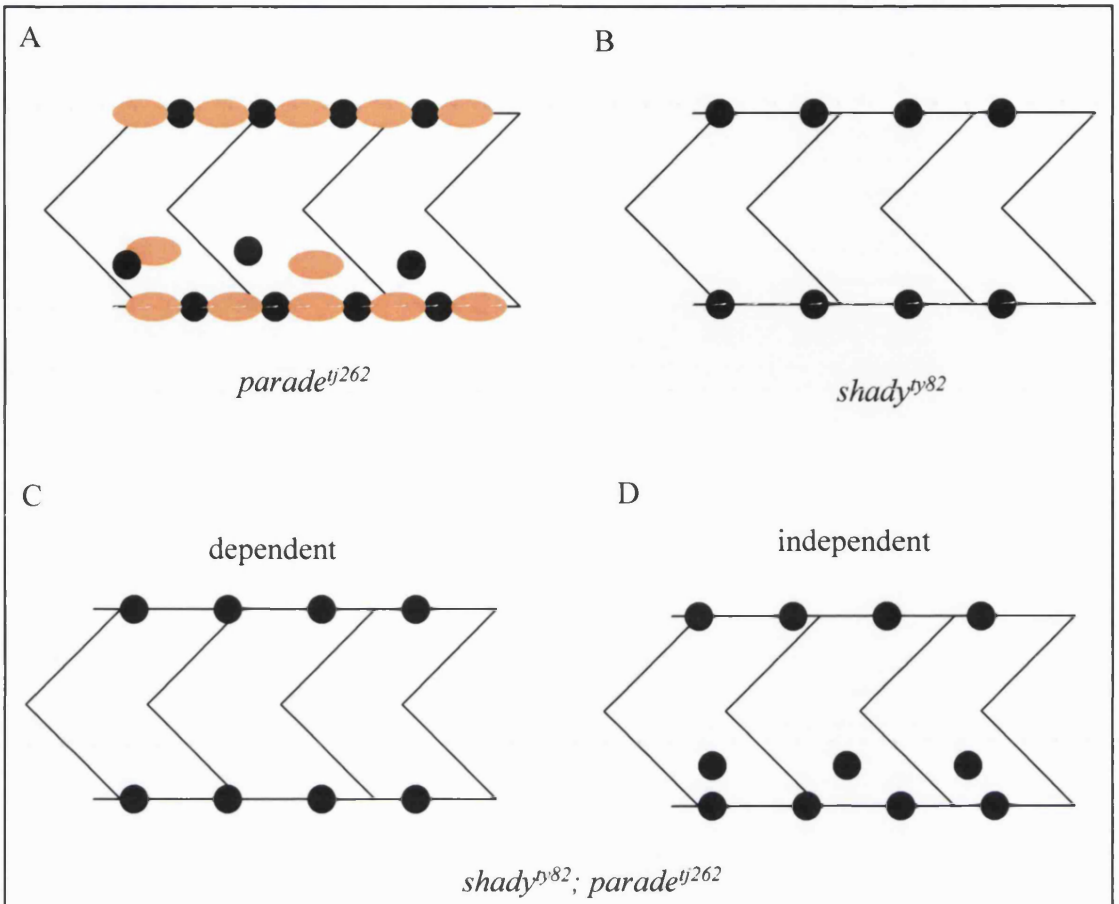

Fig. 5.3: Model for possible *shady*^{ty82}; *parade*^{tj262} phenotypes
parade^{tj262} mutants display melanophores (black circles) and iridophores (orange circles) in the dorsal and ventral stripe and the ectopic position (A). *shady*^{ty82} mutants do not have any iridophores (B). If appearance of ectopic melanophores is dependent on iridophores we would expect to loose the ectopic melanophores in *shady*^{ty82}; *parade*^{tj262} double mutants (C). However, we would expect to still see ectopic melanophores if their ectopic appearance was independent of that of iridophores (D).

crest migration and aide neural crest cells to remain in their final location. But loss of PNA-binding protein has been shown to correlate with abnormal melanoblast migration in the Silkie fowl (Faraco et al., 2001). While melanoblast migration on the ventral pathway in White Leghorn embryos has ceased at Hamburger-Hamilton stage 22, melanoblasts in the Silkie fowl continue to migrate on this pathway and populate the sclerotome.

Therefore, lack of closure of the ventral pathway for melanoblasts results in the melanoblasts being in ectopic positions. First indications of similar mechanisms playing a role in the closure of the neural crest migration pathways in zebrafish comes from timelapse studies of wild-type embryos and *choker* mutants. *choker* mutants have an ectopic collar of melanophores coinciding with an area of ectopic *sdf1a* expression (Svetic et al., 2007). Whereas in wild-types melanophores of the lateral pathway start evacuating the collar region at around 36 hpf, possibly indicating the shut down of this pathway, some melanophores in this area remain in *choker* mutants. At 48 hpf most melanophores are in their positions in the VS and DS. Even though these cells are highly active and extend protrusions they remain in their position. In *choker* mutants cell of the VS and DS displaying protrusive behaviour often migrated on the lateral pathway towards the collar (Svetic et al., 2007). Interestingly, only a restricted number of melanophores seem to migrate to the collar. On average the collar contains 15 melanophores at 60 hpf (Svetic et al., 2007). This is similar to *parade*^{tj26} mutants where only a few chromatophores can be observed in the ectopic position. If ectopic appearance of the melanophores and iridophores is caused by a defect in establishment or maintenance of the VS then each cell type should be independent of the other and loss of one of the chromatophore types in *shady*^{ty82}; *parade*^{tj262} and *nacre*^{w2}; *parade*^{tj262} double mutants respectively should should not affect ectopic presence of the other chromatophore type (Table 5.1, Model 3 and Fig. 5.2, Fig. 5.3).

By careful observation using bright field optics and incident lighting we observed the progeny of heterozygous *colourless*^{m618}; *parade*^{tj262}, *shady*^{ty82}; *parade*^{tj262} and *nacre*^{w2}; *parade*^{tj262} for potential double mutants to establish whether appearance of ectopic melanophores and iridophores was dependent on each other and for the presence of non-ectomesenchymal crest.

V.2. Results

V.2.1. colourless^{m618}; parade^{tj262}

V.2.1.A. *colourless^{m618}; parade^{tj262}* had no ectopic chromatophores

To check if complete loss of crest derived pigment cells resulted in *sox10*-dependent loss of ectopic pigment cells we studied *colourless^{m618}*; *parade^{tj262}* double mutants (Fig. 5.1).

colourless^{m618}; *parade^{tj262}* were generated by crossing heterozygous *colourless^{m618}* carriers to homozygous *parade^{tj262}* carriers. The progeny were screened for heterozygous *colourless^{m618}*; *parade^{tj262}* embryos. In subsequent analysis of the progeny (387 embryos) of in-crosses of *colourless^{m618}*; *parade^{tj262}* double heterozygotes we were able to identify 202 embryos with the wild-type phenotype (expected number according to Mendel: 216) (Fig. 5.4.A) and 80 embryos with the *parade^{tj262}* phenotype (Fig. 5.4.B). All 105 remaining embryos clearly showed loss of all neural crest derived melanophores and (nearly) all iridophores (Fig. 5.4.C) suggesting that they were homozygous for *colourless^{m618}*. Some of the embryos still had iridophores (Fig. 5.5.A). None of these 105 embryos had any ectopic cells, even if they had iridophores in the VS. We were therefore not able to distinguish *colourless^{m618}*; *parade^{tj262}* and *parade^{tj262}* mutants. A chi-square test showed that our counts matched the expected distribution according to Mendel (Chi-square= 1.281, degrees of freedom: 2, $p \leq 1$). We therefore concluded that loss of all crest derived pigment cells resulted in loss of all ectopic chromatophores suggesting that the presence of ectopic chromatophores was *sox10*-dependent.

V.2.1.B. *colourless^{m618}; parade^{tj262}* had no increased number of iridophores

As we were unable to distinguish *colourless^{m618}* mutants from *colourless^{m618}; parade^{tj262}* double mutants in the progeny of a heterozygous *colourless^{m618}*; *parade^{tj262}* in-cross based on the presence of ectopic cells, we asked if it was possible to distinguish them based on the number of iridophores in the VS. As *parade^{tj262}* mutants have an increased number of iridophores this increase might be detectable in *colourless^{m618}*; *parade^{tj262}* double mutants. Previous observations had revealed that while the number of iridophores in the DS and VS of *colourless^{m618}* mutants was always strongly reduced

Fig. 5.4: *colourless*^{m618}; *parade*^{tj262} double mutants have no ectopic chromatophores

5 dpf wild-type embryos (A) show neither melanophores nor iridophores located in the ectopic position whereas *parade*^{tj262} mutants do (B). Both *colourless*^{m618} and *colourless*^{m618}; *parade*^{tj262} have no or very few iridophores in the dorsal and ventral stripe (C). None of these embryos showed ectopic iridophores or melanophores.

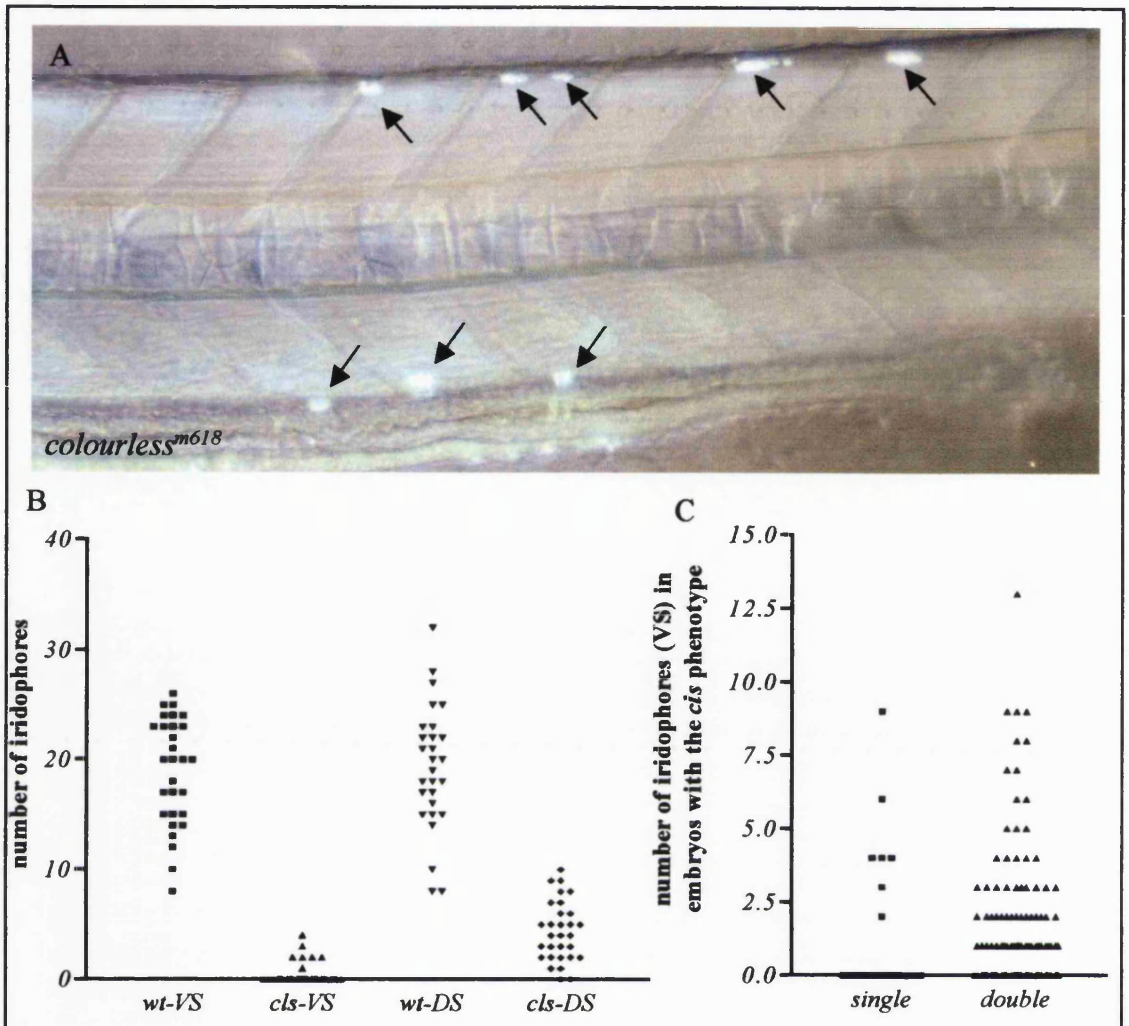

Fig. 5.5: *colourless*^{m618} and *colourless*^{m618}; *parade*^{tj262} mutants could not be distinguished

colourless^{m618} mutants had iridophores in the DS and VS (A, arrows). However counts showed that *colourless*^{m618} (*cls*) mutants had significantly less iridophores then wild-type (*wt*) embryos in both the DS and VS at 5 dpf (B). Comparison of the spread of iridophore numbers in the progeny of a heterozygous *colourless*^{m618} in-cross displaying the *colourless*^{m618} phenotype (*single*) to embryos with the phenotype from a *colouress*^{m618}; *parade*^{tj262} double mutant cross (*double*) showed no significant difference (C; $p>0.05$, Two-tailed t-test; (*single* : mean +s.e. 1.10+0.41 (n=29); *double*: 1.56+0.20 (n=134)). As the latter embryos also did not have ectopic iridophores it was not possible to distinguish *colourless*^{m618} mutants from *colourless*^{m618};*parade*^{tj262} embryos based on iridophores.

compared to wild-type embryos it was very rarely zero (Fig. 5.5 B). In the progeny of a *colourless*^{m618} heterozygous in-cross 28/30 observed embryos had between 1 to 10 iridophores in the DS. Out of the 28 embryos with iridophores in the DS 7 had also iridophores in the VS (Fig. 5.5 B). Comparison of the distribution of iridophores in the VS of *colourless*^{m618} mutants and the progeny of heterozygous *colourless*^{m618}; *parade*^{tj262} in-cross, that displayed the *colourless*^{m618} phenotype, showed no obvious difference in the number of cells present in the VS (Fig.5.5 C). As we were not able to distinguish *colourless*^{m618} mutants from *colourless*^{m618}; *parade*^{tj262} double mutants based on an increase in VS iridophore number we suggest that in the absence of *sox10* absence of *parade* does not lead to an increased number of VS iridophores.

V.2.2. shady^{ty82}*; parade*^{tj262}

To see if the appearance of melanophores in the ectopic position is dependent or independent on the presence of iridophores in the ectopic position we studied *shady*^{ty82}; *parade*^{tj262} double mutants.

V.2.2.A. *shady*^{ty82}; *parade*^{tj262} double mutants have ectopic melanophores

We generated *shady*^{ty82}; *parade*^{tj262} double mutants by crossing homozygous *parade*^{tj262} mutants with heterozygous carriers for *shady*^{ty82}. The progeny was raised and in-crossed. As all fish were *parade*^{tj262} carriers the progeny was screened for *shady*^{ty82} carriers. Identified heterozygous carriers of both mutations were then in-crossed, the progeny examined for their phenotypes and sorted into different groups depending on their phenotype. According to the Mendelian rules we expected to potentially get, in the case of presence of ectopic melanophores being independent of iridophores, four different phenotypes. We expected 1/16 to be double *shady*^{ty82}; *parade*^{tj262}, 3/16 to have a *parade*^{tj262} phenotype, 3/16 to have a *shady*^{ty82} phenotype and 9/16 to show a wild-type phenotype. Careful phenotypic examination at 5 dpf showed that we were able to group the progeny of an in-cross of heterozygous *shady*^{ty82}; *parade*^{tj262} carriers into these four categories. Out of the 1415 embryos examined 796, exactly 9/16, showed a wild-type phenotype (Fig. 5.6 A- C). 262/1415 showed the *parade*^{tj262} phenotype (wild-type pattern of melanophores and iridophore and ectopic melanophores and iridophores; Fig. 6 D- F) and 253/1415 the *shady*^{ty82} phenotype (wild-type distribution of melanophores,

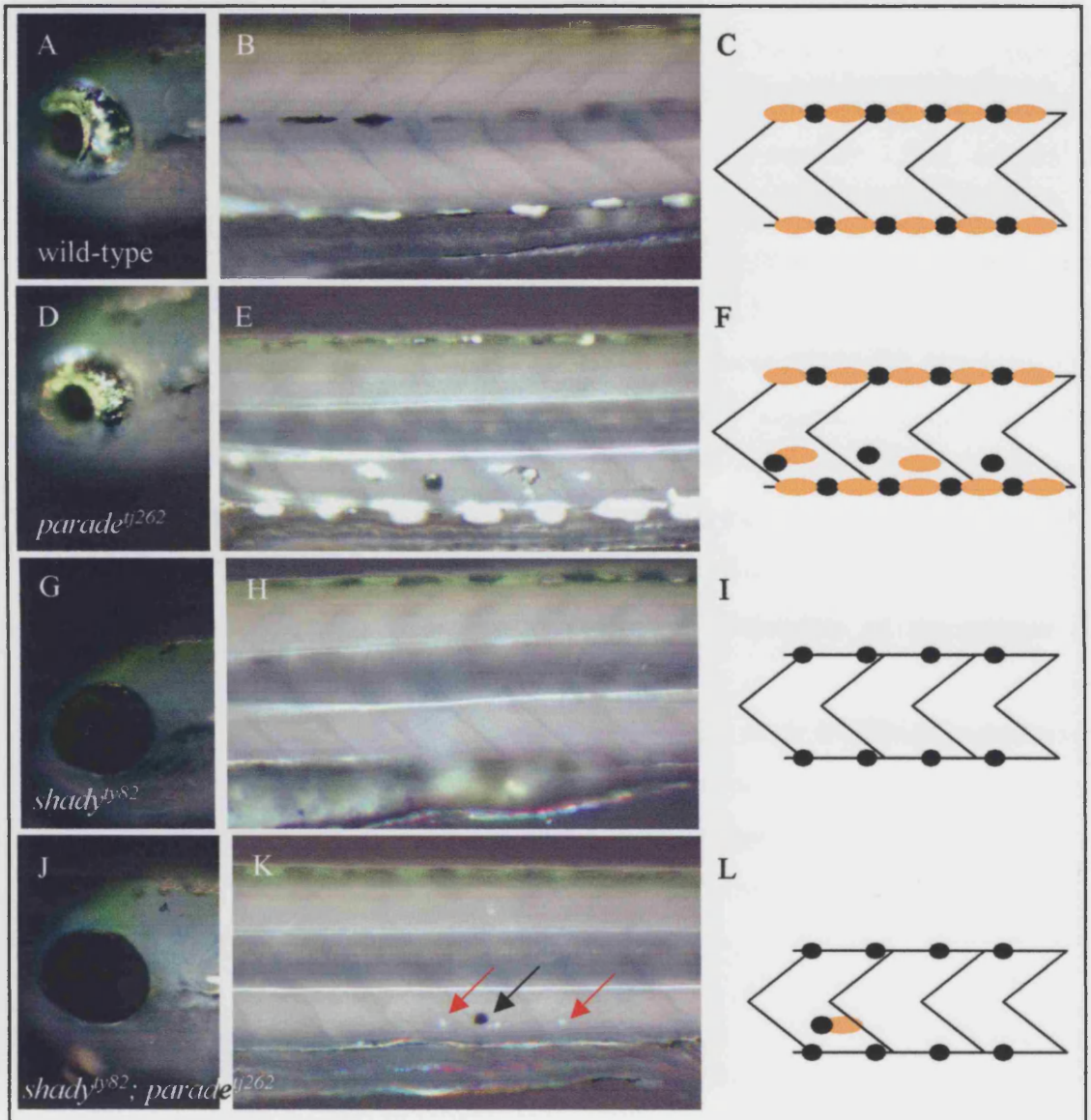

Fig. 5.6: Double mutant analysis showed iridophore –independent appearance of ectopic melanophores

5 dpf wild-type embryos (A, B, C) and *shady*^{ty82} mutants (E, F, G) showed neither melanophores (A, E) nor iridophores (B, F) located in the ectopic position. *shady*^{ty82} mutants could be easily identified by loss of iridophores in the eye (compare A to D). In contrast *parade*^{tj262} mutants had melanophores (B) and iridophores (D) in this position. Revealingly *shady*^{ty82};*parade*^{tj262} mutants continued to have ectopic melanophores (K, black arrow) like *parade*^{tj262} mutants. Surprisingly they also had ectopic iridophores even though they clearly lacked iridophores in the eye (J, K, red arrow). All pictures are incident lighting and lateral view of the trunk except A, D, G, J which are a lateral view of head ; C, F, I, L schematic drawings of the phenotype.

but complete loss of iridophores; Fig. 5.6 G- I). The fourth group, 104/1400 embryos, were clearly *shady*^{ty82} mutants showing general lack of iridophores in the eye, lateral patches and stripes, but had ectopic melanophores (Fig. 5.6 J- L). A chi-square test showed that the difference between the real and expected Mendelian distribution of embryos into these four groups was not significant (Chi-square= 1.520, degrees of freedom: 3, $p \leq 1$).

Surprisingly, most of the embryos we grouped as *shady*^{ty82}; *parade*^{tj262} did not only have ectopic melanophores, but also ectopic iridophores (Fig. 5.6 J- L; Fig. 5.7 A). Even though the double mutants did have ectopic iridophores they did not have any iridophores in the DS or the eye (except an assumed 'escaper' iridophore). Most embryos had at least one iridophore in the VS and some of the batches observed even showed a strongly increased number of iridophores in the VS compared to *shady*^{ty82} mutants. Irrespective of these iridophores our observations so far suggest that the ectopic positioning of the melanophores could be independent of the number of iridophores in the VS.

However, the rather unexpected appearance of iridophores made it difficult to determine if the ectopic appearance of melanophores was dependent or independent of iridophores. Therefore, we decided to count the number of melanophores and iridophores to see if we could observe a change in numbers and to see if there was a close correlation between the presence of iridophores and melanophores.

V.2.2.B. Numbers of ectopic melanophores and iridophores are reduced in *shady*^{ty82}; *parade*^{tj262} double mutants

To see if the ectopic appearance of melanophores in *shady*^{ty82}; *parade*^{tj262} mutants was completely dependent on iridophores we counted the ectopic chromatophores in *shady*^{ty82}; *parade*^{tj262} double mutants. In order to have less variables we used double mutants derived from two crosses that had no iridophores in the VS for our counts. The number of ectopic melanophores in *shady*^{ty82}; *parade*^{tj262} double mutants was on average reduced by 50% compared to *parade*^{tj262} mutants (Fig. 5.7 B). Surprisingly, the number of ectopic iridophores was reduced less, only by about 37%, compared to melanophores (Fig. 5.7 C). 27% of all *shady*^{ty82}; *parade*^{tj262} double mutants observed had no ectopic melanophores, but iridophores, while 25% had no ectopic iridophores.

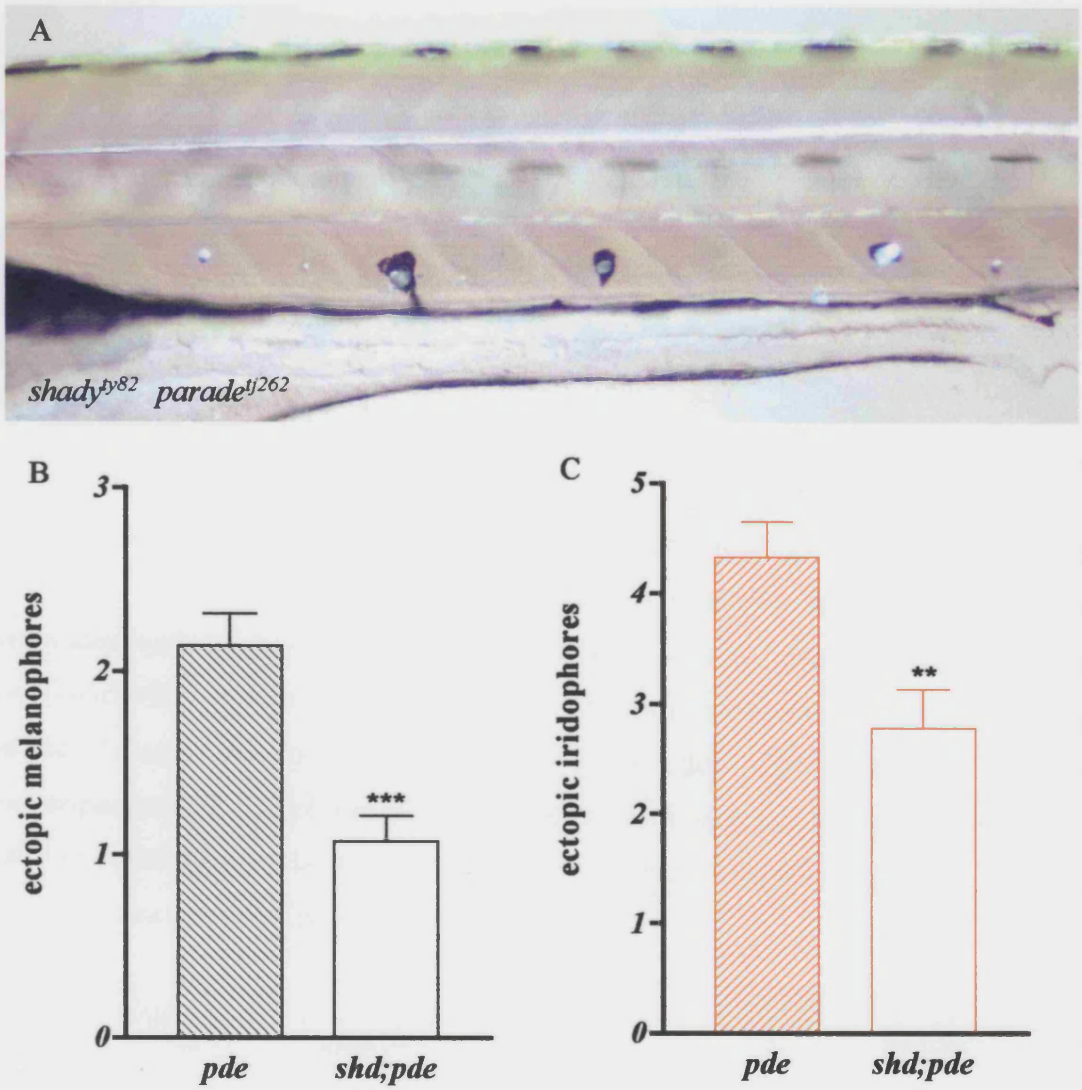

Fig. 5.7: *shady*^{ty82}; *parade*^{tj262} double mutants had reduced numbers of melanophores and iridophores

A close up of the trunk area of a *shady*^{ty82}; *parade*^{tj262} (*shd;pde*) double mutant showed both melanophores and iridophores in the ectopic position (A). Counts showed that the number of melanophores in *shady*^{ty82}; *parade*^{tj262} mutants was significantly decreased compared to *parade*^{tj262} mutants (B; $p<0.001$, Two-tailed t-test; (*parade*^{tj262}: mean +s.e. 2.14+ 0.17 (n=86); *shady*^{ty82}; *parade*^{tj262}: 1.075+0.1383 (n=67)). The number of ectopic iridophores that could be found in *shady*^{ty82}; *parade*^{tj262} mutants was also significantly reduced (C; $p<0.0017$, Two-tailed t-test; (*parade*^{tj262}: mean +s.e. 4.32+0.32 (n=86); *shady*^{ty82}; *parade*^{tj262}: 2.77+0.35 (n=67)).

Finding double mutants with ectopic melanophores but without ectopic iridophores suggested that appearance of melanophores in the ectopic position was at least partly independent of iridophores. But presence of the remaining ectopic melanophores could be dependent on the remaining ectopic iridophores. We therefore examined whether the ectopic melanophores were often associated with iridophores.

V.2.2.C. Presence of iridophores did not correlate with that of melanophores

As double mutants very surprisingly had iridophores in the ectopic position we asked if their presence mostly correlated with the presence of melanophores. Close association of both could indicate that the appearance of these melanophores is dependent on iridophores. We carefully observed the ectopic chromatophores in *shady*^{ty82}; *parade*^{tj262} mutants from both lateral sides (left and right) and recorded their fate (Fig. 5.8). Interestingly in only very few cases could melanophores and iridophores be observed associated with each other. Out of the 42 melanophores observed 5 (~12%) were associated with iridophores. 1 melanophore (~2%) was positioned in the same somite as an iridophore and other 86% were completely independent of iridophores. In most cases melanophores and iridophores in the ectopic position were not located closely to each other or appeared associated. These observations imply that the ectopic positioning of melanophores might be independent of iridophores.

V.2.3. nacre^{w2}*; parade*^{tj262}

To see if loss of melanophores resulted in loss of ectopic iridophores, indicating dependence of the ectopic iridophores on the melanophores we generated *nacre*^{w2}; *parade*^{tj262} double mutants. Lack of *mitfa*, as seen in *nacre* mutants, results in complete loss of crest derived melanophores, but a 40% increase in iridophore numbers (Lister et al., 1999).

V.2.3.A. *nacre*^{w2}*; parade*^{tj262} double mutants have ectopic iridophores

As both *nacre*^{w2} and *parade*^{tj262} were adult viable crossing them created embryos all heterozygous mutant for *nacre*^{w2} and *parade*^{tj262}. When in-crossing these we expected 1/16 to be double *nacre*^{w2}; *parade*^{tj262}, 3/16 to have a *parade*^{tj262} phenotype, 3/16 to

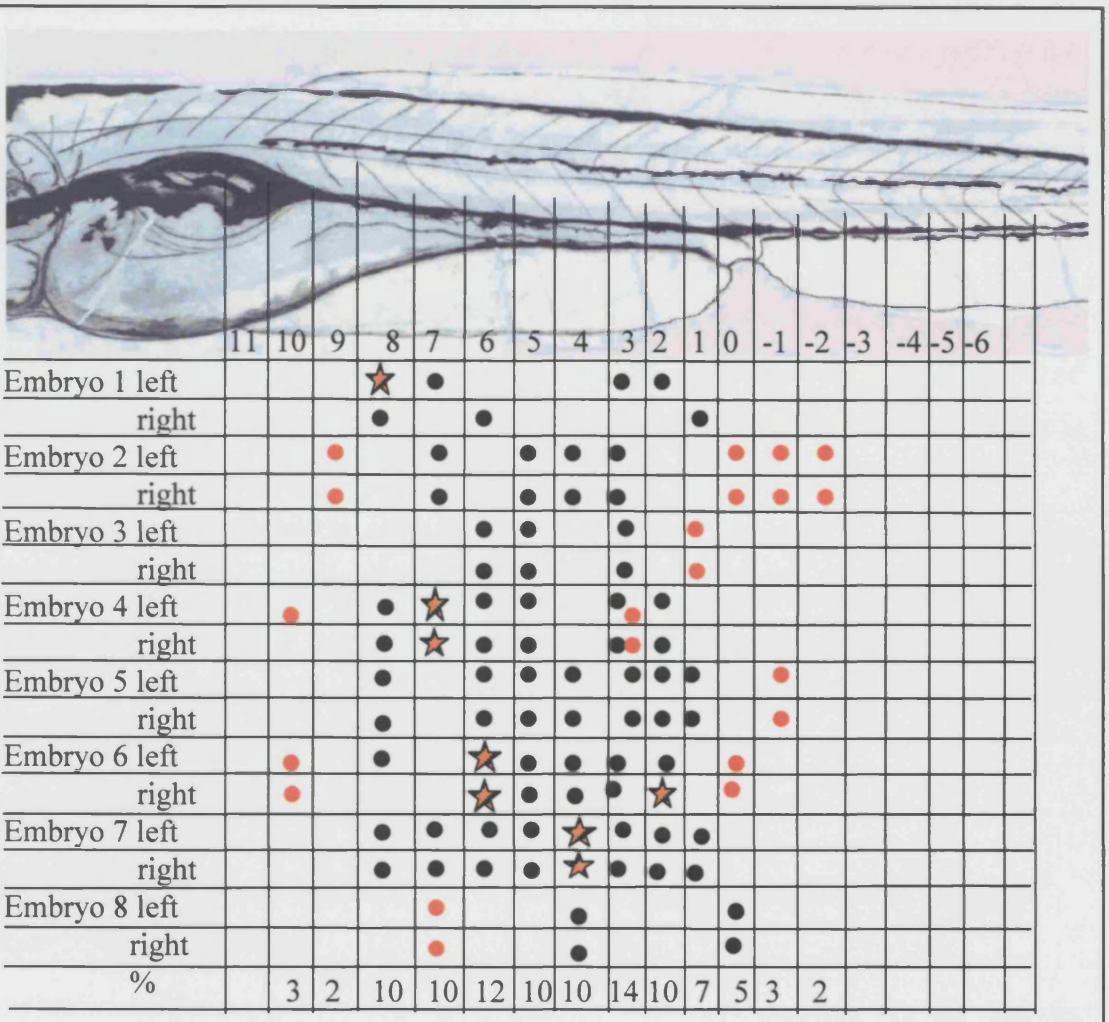

Fig. 5.8: Distribution of ectopic chromatophores in *shady^{ty82};parade^{tj262}* double mutants

Close examination of the ectopic cells of *8 shady^{ty82}; parade^{tj262}* double mutants from both sides reveals that most of the ectopic melanophores were not associated with iridophores. orange circle: iridophore, black circle: melanophore: black and orange striped star: closely associated melanophore and iridophore. Embryos were observed from both sides at 5 dpf. The average percentage of ectopic cells per somite (bottom row) was highest from somite 8 to somite 1 in the trunk above the yolk sac extension (cells appearing to display both fates were counted as two; percentage rounded to the nearest full number)

have a *nacre*^{w2} phenotype and 9/16 to show a wild-type phenotype. Examination at 5 dpf showed that as expected 873/1484 embryos displayed the wild-type (Fig. 5.9. A- C), 247/1484 the *parade*^{tj262} (Fig. 5.9 D- F) and 285/1484 the *nacre*^{w2} phenotype (Fig. 5.9 G- I). 79/1484 showed a phenotype not falling into these three categories and were assumed to be *nacre*^{w2}; *parade*^{tj262} double mutants (Fig. 5.9. J- L). In addition to lack of all melanophores they showed ectopic iridophores above the caudal vein, the location of the ectopic chromatophore in *parade*^{tj262}.

Chi- square analysis showed again that the distribution of embryos into the four groups was not significant from the expected Mendelian ratios (Chi-square= 3.947, degrees of freedom: 3, $p \leq 1$) and therefore suggested that the ectopic appearance of iridophores is independent of melanophores.

We noted that iridophores in both *nacre*^{w2} and *nacre*^{w2}; *parade*^{tj262} did not always display the typical nugget shaped and quite flat wild-type shape of iridophores, but often looked like small "contracted" balls. The ectopic iridophores in *nacre*^{w2}; *parade*^{tj262} are small and contracted suggesting that iridophores need to interact with melanophores to display their wild-type shape.

V.2.3.B. Numbers of ectopic iridophores were not significantly reduced in *nacre*^{w2}; *parade*^{tj262} double mutants

Our results so far suggested that melanophores were not required for the ectopic positioning of supernumerary iridophores. We counted the ectopic chromatophores in *nacre*^{w2}; *parade*^{tj262} double mutants to see if they were reduced as in *shady*^{ty82}; *parade*^{tj262} mutants indicating a partial dependence. Counts of iridophores in the ectopic position revealed that they were not significantly reduced in *nacre*^{w2}; *parade*^{tj262} double mutants compared to *parade*^{tj262} mutants (Fig. 5.10) suggesting that the ectopic positioning of iridophores was independent of melanophores.

V.2.3.C. The increase of iridophores in *nacre*^{w2}; *parade*^{tj262} double mutants was not additive

As previously mentioned Lister et al. (1999) showed that the number of iridophores in *nacre* is increased by approximately 40% in the DS at 3 dpf. It has been suggested that the overall increase in iridophore number in *nacre*^{w2} mutants might be caused by

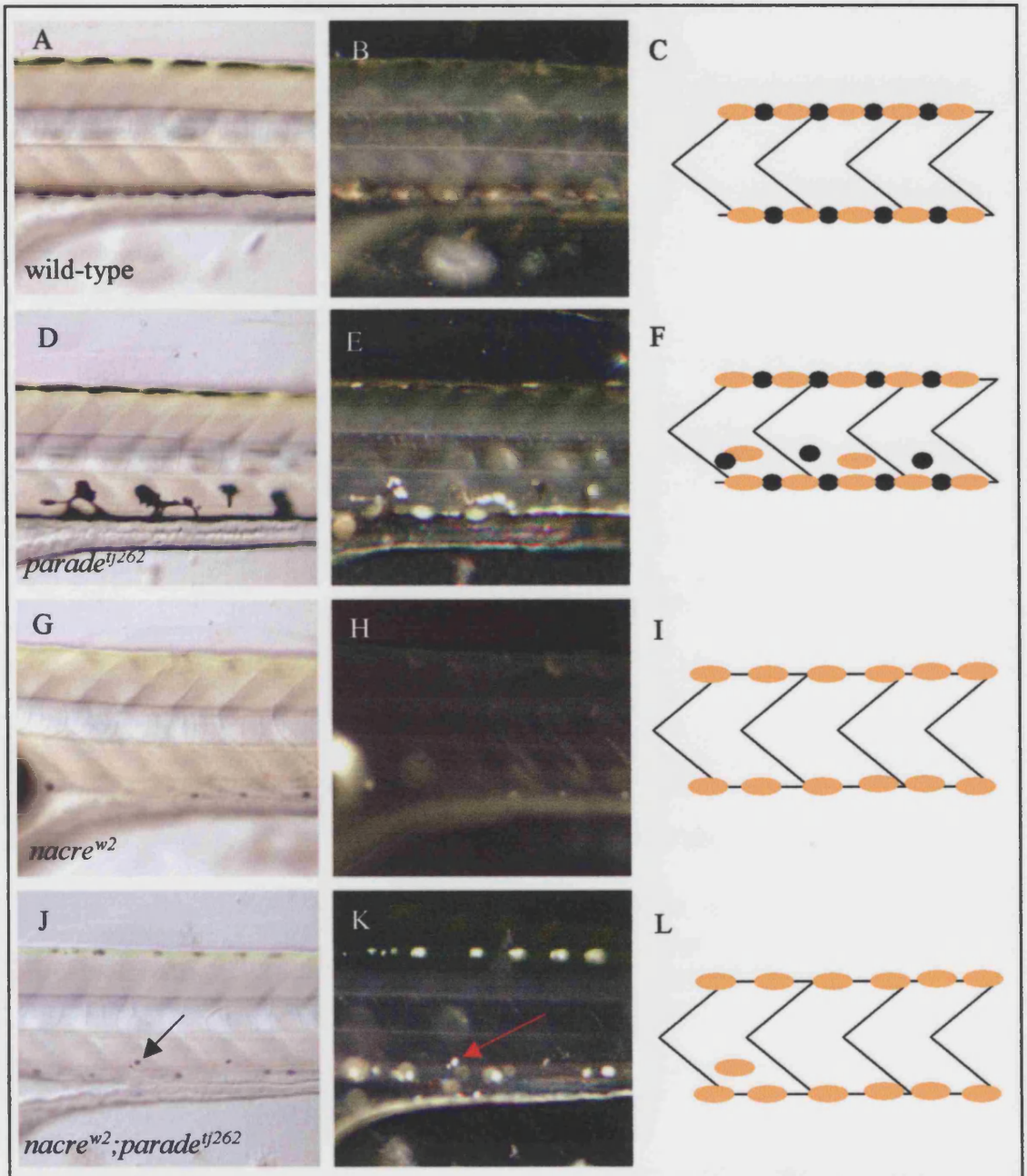

Fig. 5.9: Double mutant analysis shows melanophore –independent appearance of ectopic iridophores

5 dpf wild-type embryos (A, B, C) and *nacre*^{w2} mutants (E, F, G) showed neither melanophores (A, E) nor iridophores (B, F) located between the medial and ventral stripe. In contrast *parade*^{tj262} mutants had melanophores (B) and iridophores (D) in this position. Revealingly *nacre*^{w2};*parade*^{tj262} continued to have ectopic iridophores (G, H, arrows) like *parade*^{tj262} mutants. All pictures lateral view of the trunk. A, D, G, J Normaski optics; B, E, H, K incident lighting and C, F, I, L schematic drawings of the phenotype.

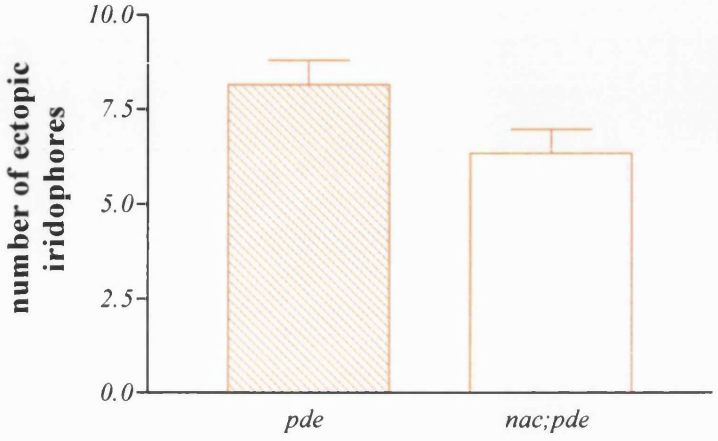

Fig. 5.10: Number of ectopic iridophores were not significantly reduced in *nacre^{w2}; parade^{tj262}* double mutants

Counts of ectopic iridophores at 5 dpf showed that the number of ectopic iridophores in *nacre^{w2}; parade^{tj262}* mutants was not significantly different to that of *parade^{tj262}* mutants (p=0.05, Two-tailed t-test; (*parade^{tj262}*: mean +s.e. 8.15+0.64 (n=46); *nacre^{w2}*; *parade^{tj262}*: 6.34+0.63 (n=41)).

melanoblasts switching fate. If the increase in *parade*^{tj262} is caused by a defect in regulation of cell numbers we might expect to see an additive effect of both phenotypes. This would be visible in an increase of iridophore numbers in *parade*^{tj262} single mutants compared to *nacre*^{w2}; *parade*^{tj262} double mutants unless there is a stripe dependent mechanism regulating its maximum capacity (Table 5.1, Model 2).

Similarly to Lister's counts our counts at 5 dpf showed that the number of iridophores in the DS of *nacre*^{w2} and *nacre*^{w2}; *parade*^{tj262} mutants was increased by about 45% compared to both wild-type and *parade*^{tj262}mutants (Fig. 5.11 A). The increased number of iridophores in the DS of *nacre*^{w2}; *parade*^{tj262} double mutants seemed therefore to be caused by loss of *mitfa*.

In the VS the number of iridophores in *nacre*^{w2} and *parade*^{tj262} and *nacre*^{w2}; *parade*^{tj262} was increased compared to wild-type embryos independent if the ectopic iridophores were included or not (Fig. 5.11 B, C). But the situation here was different to the DS where *nacre*^{w2} and *nacre*^{w2}; *parade*^{tj262} had roughly the same increase in iridophore numbers. In the VS *nacre*^{w2}; *parade*^{tj262} mutants had a significant increase in iridophores in the VS when the ectopic iridophores were included in our counts compared to *nacre*^{w2} mutants (Fig.5.11 C). This increase was only caused by the ectopic iridophores as without them no significant difference was detectable. There was no difference though between iridophore numbers in *parade*^{tj262} and *nacre*^{w2}; *parade*^{tj262} in the VS.

These observations show that the effects of *mitfa* and *parade* on iridophores are not additive.

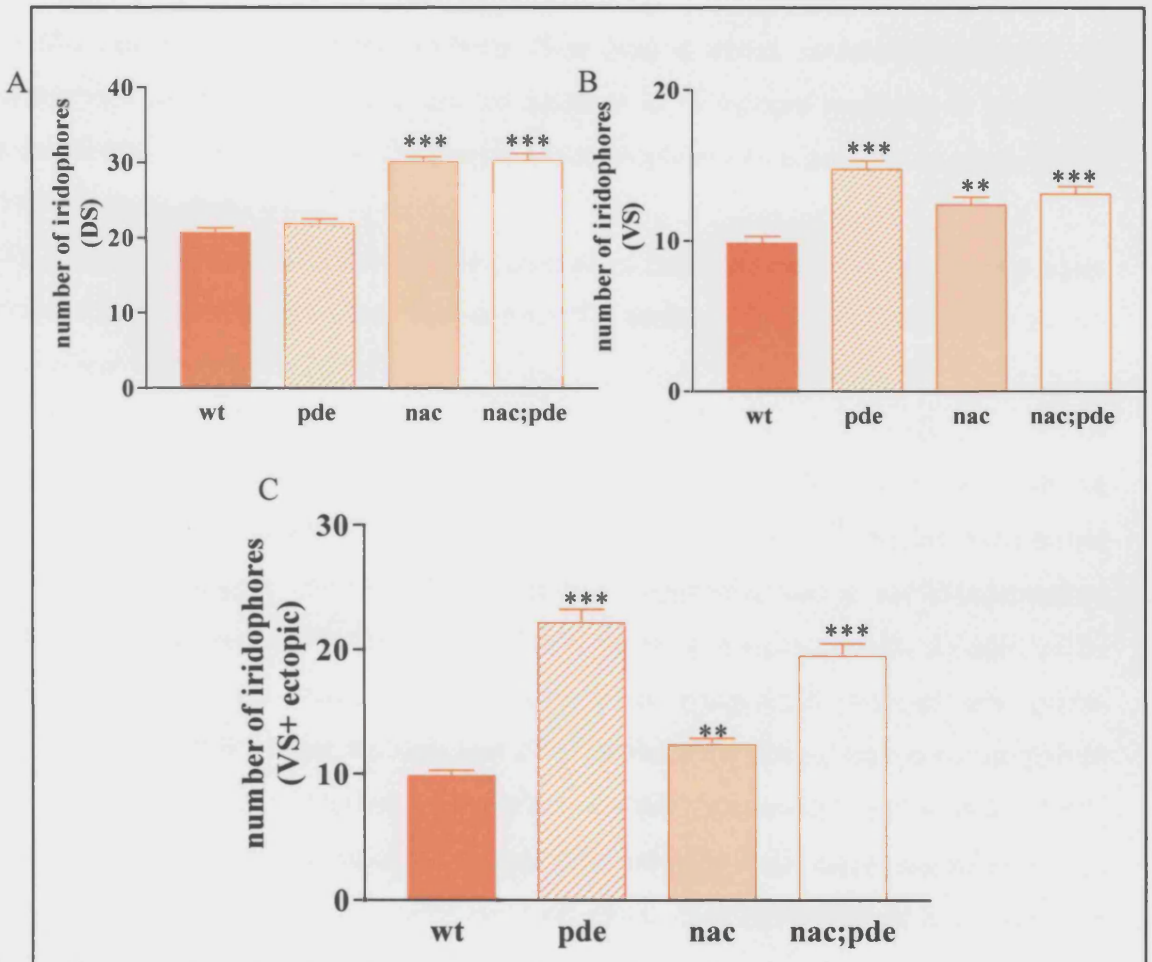

Fig. 5.11: The increase of iridophores in the ventral stripe of *nacre*^{w2} and *parade*^{tj262} mutants was not additive

As shown previously the number of iridophores in the DS of *parade*^{tj262} mutants was not significantly different than in wild-type embryos (A). Compared to these the number of iridophores in the DS of *nacre*^{w2} and *nacre*^{w2}*; parade*^{tj262} mutants was significantly increased (A, ANOVA; $P<0.001$) compared to wild-type. In the VS (AVS + PVS) the number of iridophores was increased in *nacre*^{w2} (B, ANOVA, $P<0.01$) and *parade*^{tj262} and *nacre*^{w2}*; parade*^{tj262} mutants (B, ANOVA, $P<0.001$) compared to wild-type. In addition the number of iridophores in the ventral stripe of *parade*^{tj262} was increased compared to *nacre*^{w2} (B, ANOVA, $P<0.01$) but not *nacre*^{w2}*; parade*^{tj262} (B, $P>0.05$). There was no significant difference in the number of iridophores between *nacre*^{w2} and *nacre*^{w2}*; parade*^{tj262} mutants either (B, ANOVA, $P>0.05$). The only change when taking the ectopic iridophores into account was that the difference between *nacre*^{w2} and *nacre*^{w2}*; parade*^{tj262} became significant (C, ANOVA, $P<0.001$).

V.3. Discussion

In this chapter we examined whether there was a direct connection between the appearance of the ectopic cells and the increase in iridophore numbers in *parade*^{tj262} mutants and if appearance of the ectopic chromatophores is dependent on none, one or both chromatophore types.

We proposed 3 models for the ectopic presence of melanophores and iridophores based on our previous observations that *parade*^{tj262} mutants showed an increase in VS iridophore numbers (Table 5.1).

First we investigated, using *colourless*^{m618}; *parade*^{tj262} double mutants, if a *sox10*-independent transdifferentiation event might be responsible for the presence of the ectopic iridophores (Table 5.1; Fig. 5.1). *colourless*^{m618}; *parade*^{tj262} double mutants did not have any ectopic chromatophores strongly suggesting that a *sox10*-independent transdifferentiation event is not responsible for the ectopic pigment cells. As most of the prime candidates for transdifferentiation such as sympathetic neurons are *sox10*-dependent, we still cannot exclude that cells transdifferentiating into chromatophores cause the increase in iridophore numbers and ectopic positioning (Dutton et al., 2001; Kelsh and Eisen, 2000). Loss of the ectopic pigment cells is not surprising as *sox10* has been shown to be involved in early steps of neural crest development and *colourless* mutants lack non-ectomesenchymal neural crest derivatives (Dutton et al., 2001). However, we also showed that the increase in iridophore numbers observed in *parade*^{tj262} mutants could not be observed within the remaining iridophores in *colourless*^{m618}; *parade*^{tj262} double mutants. If loss of *parade* would lead to over-proliferation of iridophores an increase in the numbers of remaining iridophores could have been expected. This observation therefore indicates that a mechanism other than over-proliferation might be responsible for the increase in iridophores.

To explore if a limit in capacity for pigment cells of the VS is the reason for the ectopic positioning of melanophores and iridophores in *parade*^{tj262} mutants we generated double mutants lacking only one of the pigment cell types (Table 5.1; Model 2). The limit in capacity could be for all pigment cells together or for each pigment cell type individually. Loss of melanophores in *nacre*^{w2};*parade*^{tj262} double mutants however did not result in a significant reduction in iridophore numbers in the ectopic position

demonstrating that simply reduction of overall pigment cell numbers in the VS is not sufficient to loose the ectopic iridophores. However, in *nacre*^{w2} mutants the increase of iridophores in the VS seems to be evenly distributed throughout trunk and tail and generally no ectopic iridophores can be found in the ventral trunk (Lister et al., 1999). These observations suggested that generally loss of one pigment type in the stripe allows the increase of the other without cells having to leave the AVS. It could therefore be possible that each stripe does not only have a limit in capacity for chromatophores in general, but for each cell type in particular. After all the increase in iridophore numbers in *parade*^{tj262} (58%) is greater than the increase in *nacre*^{w2} mutants (40%)(Fig. 5.11). Thus loss of melanophores in *nacre*^{w2};*parade*^{tj262} might not be enough to make up for this extra increase in iridophore numbers and would therefore not result in loss of the ectopic iridophores.

As none of the supernumerary cells in *parade*^{tj262} are located in the AVS, even though the AVS seems to be able to accommodate some supernumerary iridophores, it is possible that a mechanism regulating cells numbers in the VS is not, or not solely, responsible for the ectopic positioning of the iridophores.

As the loss of melanophores does not result in a loss of the ectopic cells it also shows that the ectopic positioning of the iridophores is independent of presence of melanophores in *parade*^{tj262}. This observation is not necessarily surprising as the number of melanophores in the VS did not seem to be increased .

Given that restriction of overall chromatophore numbers is not responsible for the appearance of iridophores in the ectopic position, the phenomenon might be the result of restriction of number of each chromatophore type. Even though we cannot count the melanophores in the AVS we have, from our observations in the PVS, no reason to believe that melanophore numbers are increased. The significant decrease, but not complete loss, in melanophore numbers in the ectopic position in *shady*^{ty82}; *parade*^{tj262} double mutants therefore suggests that not simply a restriction of chromatophore type number in the VS is responsible for the ectopic presence of pigment cells. Also the presence of ectopic melanophores in the absence of supernumerary iridophores indicates that the melanophores are not solely ectopic because of the presence of higher numbers of iridophores. Taken together with the fact that the melanophores were hardly ever associated with the iridophores we suggest that the appearance of the melanophores in the ectopic position is independent of iridophores.

If an increase in iridophore numbers would be solely responsible for the ectopic positioning we would expect to see the iridophores present in *shady*^{ty82}; *parade*^{tj262} double mutants in the VS not the ectopic position. Rescue experiments in *shady*^{ty82} embryos have shown that iridophores can be located in the VS of *shady*^{ty82} embryos (Lopes et al., in prep.). The finding that the few iridophores in *shady*^{ty82};*parade*^{tj262} mutants are ectopic and not in the VS further supports the theory that the increase in iridophore number is not solely responsible for the ectopic positioning of the chromatophores.

Our observations from the double mutant studies so far suggest that a mechanism involving establishment or maintenance of the VS might play a role in causing the *parade*^{tj26} phenotype (Table 5.1, Model 3). Factors expressed either in tissues above or below the VS or in the chromatophores could be responsible for maintenance of the VS. The mis-expression of *sdf1a* has been suggested to be responsible for appearance of the ectopic collar in *choker* mutants (Svetic et al., 2007). Here, as in *parade*^{tj26}, only a few chromatophores migrate out of their natural position and populate the ectopic position. Mispositioning of an increased number of pigment cells combined with an increase in their number has been described in the Silkie fowl (Faraco et al., 2001). Loss of the barrier molecule PNA has been suggested to be responsible for the misplacement although, as in *parade*^{tj262}, the connection between the increase of pigment cell number and defect in migration is not known. As suggested in the previous chapter a environmental factor, possibly expressed in the gut, could cause some chromatophores to move into the ectopic position. This could explain why in *shady*^{ty82};*parade*^{tj262} and *nacre*^{w2};*parade*^{tj262} mutants chromatophores are found in the ectopic position. Ectopic positioning and increase in cell number would then be completely independent of each other. Identification of the gene responsible for the *parade*^{tj262} phenotype may help us resolve the mechanism underlying this phenotype.

A puzzling finding in the *shady*^{ty82}; *parade*^{tj262} mutants was the higher number of iridophores in comparison to single *shady*^{ty82} mutants and that these iridophores were in the ectopic position. Both transdifferentiation of another cell type into (possibly *alk*-independent) iridophores or over-proliferation combined with a defect in maintenance/establishment of the VS caused by a loss of *parade* could lead to the increase. Given that *shady*^{ty82} mutants have occasional iridophores in the trunk it is

conceivable that these undergo increased proliferation in absence of *parade*. These cells would then appear ectopically because of defects in stripe formation/ maintenance. It is surprising however that none of the iridophores are located in the VS itself.
Another possibility is that even in the absence of *alk* another neural crest derivative is able to transdifferentiate into iridophores. Presence of the occasional 'escaper' iridophore in *shady*^{ty82} mutants again suggests that it is generally possible to become an iridophore in this genetic background.

Our double mutant studies show that it is unlikely that a limit in chromatophore numbers in the VS solely leads to the melanophores and iridophores in the ectopic position. We cannot determine however if a *sox10*-dependent transdifferentiation event or an increase in iridophore number combined with a defect in VS establishment/ maintenance is responsible for the increase in iridophore numbers and ectopic positioning of the cells.

Chapter VI Mapping of *parade*

VI.1. Introduction

It has been estimated that a mutation in 1400-2400 genes in zebrafish will give an embryonic or early larval detectable phenotype (Amsterdam et al., 2004; Haffter et al., 1996a). Multiple screens have been performed and a large number of zebrafish mutants, amongst them the one described in this thesis, *parade*^{tj262}, has been obtained (Haffter et al., 1996a; Haffter et al., 1996b; Kelsh et al., 1996). An important step in characterising the isolated mutants is identifying the mutation responsible for causing the phenotype. Generally two approaches are used to identify the mutated genes. Some genes have been identified using a candidate gene approach. As the name implies this approach requires a candidate gene, usually identified by a strong similarity of the mutant phenotype to a phenotype in another organism, where the mutated gene responsible is known. Various different zebrafish mutants including *colourless/sox10*, *parachute/n-cadherin* and *nacre/mitfa* have been mapped and cloned using the candidate gene approach (Dutton et al., 2001; Lele et al., 2002; Lister et al., 1999). However, for a large number of mutants no candidate genes are available. In this case a positional cloning approach (Fig. 6.1) is taken to identify the mutated gene (Collins, 1992). Positional cloning requires genome scanning for an initial rough positioning of the gene followed by fine mapping of the gene to a genomic clone. Afterwards steps necessary for cloning the gene such as chromosome walk, screening for genomic clones and BAC/PAC rescue experiments have to be performed to identify the transcript (Geisler, 2002). Again multiple zebrafish mutants have been mapped this way including *mont blanc/tfap2a*, *somitabun/smad5*, *shady/alk*, *mother superior/foxd3*, *fading vision/silver* and *one-eyed pinhead/EGF-related protein* (Barrallo-Gimeno et al., 2004; Hild et al., 1999; Lopes et al., in prep.; Montero-Balaguer et al., 2006; Schonthaler et al., 2005; Woods et al., 2006; Zhang et al., 1998).

As the characterisation of *parade*^{tj262} did not suggest any strong candidates we employed a positional cloning approach to identify the gene mutated in *parade*^{tj262}.
A requirement for genome scanning, the first step of the positional cloning approach, as well as fine mapping of a gene of interest later is a genetic map containing a high number of markers (Knapik et al., 1996). In a genetic map the distance between two markers is established based on the probability of meiotic recombination between them. To generate a genetic map around a mutation in zebrafish a high number of

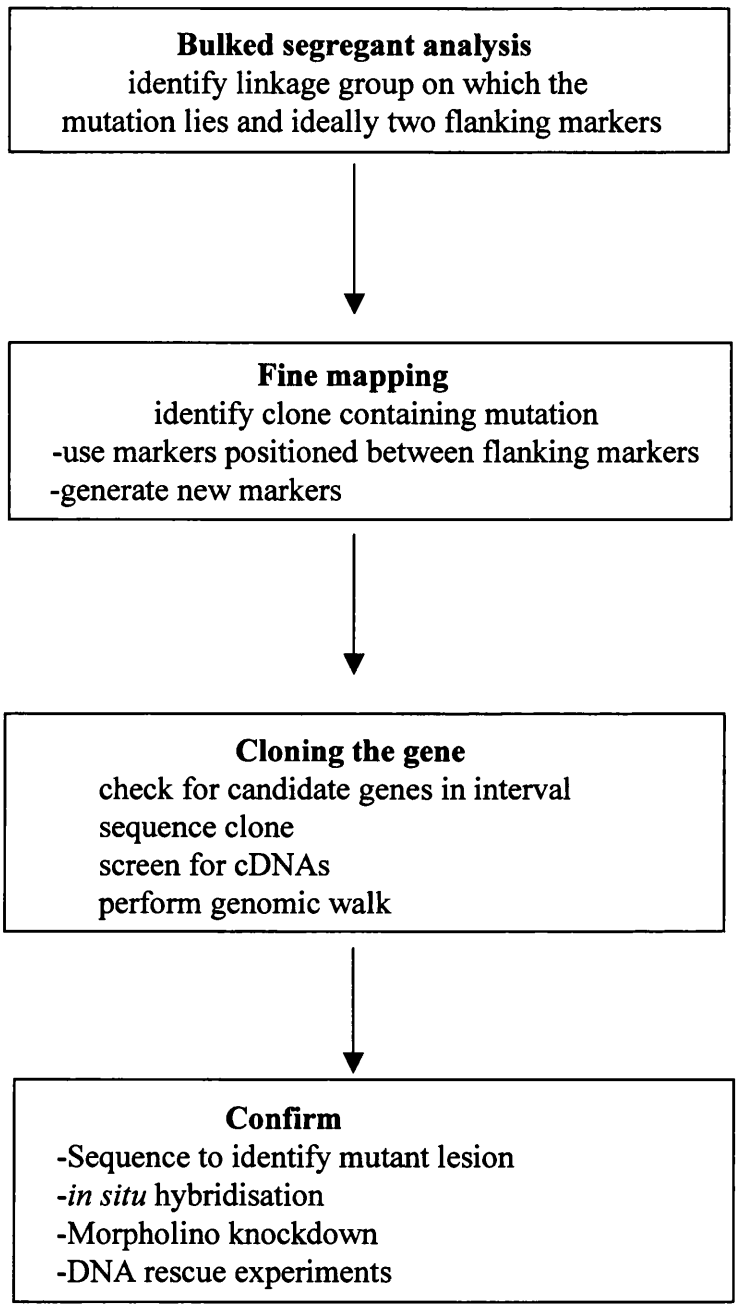

Adapted from Geisler, 2002

Fig. 6.1: Strategy for positional cloning approach

polymorphic markers is scored on the F2 generation. To establish the F2 generation the zebrafish line carrying the mutation (here *parade* with AB background) is crossed to a reference line (here WIK (Rauch et al., 1997))(Fig. 2.1). The resulting F1 generation is in-crossed to produce the F2 generation which is sorted into two groups: those displaying the mutant phenotype (mutants) and those that are not (siblings). One type of markers used are SSLPs (Single Sequence Length Polymorphisms, also called microsatellites). SSLPs are CA repeats flanked by two primers. These polymorphic CA repeats are highly variable in length and abundant in zebrafish (Rauch et al., 1997). Importantly, they are also co-dominant, which means that both alleles of a diploid embryo can be scored on an agarose gel (Geisler, 2002).

Multiple mapping panels, containing a large number of markers that can be used, have been generated (Geisler, 2002). The first and most established is the MGH panel (Knapik et al., 1996; Knapik et al., 1998). It contains 3842 SSLPs that were scored on 48 diploid F2 embryos of an AB x India map cross. The MGH panel covers the genome with a resolution of 1.2 cM. As a result 1 cM represents approximately 660 kb (Geisler, 2002). Another more recently established map containing over 3900 marker is the Heat shock (HS) panel (Amores et al., 1998; Kelly et al., 2000; Postlethwait et al., 2000; Woods et al., 2000). It has been produced using 47 haploid embryos. In opposite to the MGH panel where nearly all markers are SSLPs, the HS panel uses mostly ESTs (Expressed Sequence Tags), SNPs (Single Nucleotide Polymorphism), cDNA and genes. Some other panels with smaller numbers of scored markers are the GAT (W.S. Talbot unpub.) and MOP panel (Amores et al., 1998). An integrated map of the zebrafish genome containing over 34000 markers produced by J.H. Postlethwait can be found on ZFIN. It contains amongst others all markers from the panels mentioned above and two Radiation Hybrid panels (LN54 and T51) (Geisler et al., 1999; Hukriede et al., 2001; Hukriede et al., 1999; Kwok et al., 1998).

To obtain a rough map position in a positional cloning approach, bulked segregant analysis (see II.13.1) on F2 embryos is performed (Geisler et al., 2007). Comparison of the intensities of the different sized allele bands on a gel can then show a potential linkage (see Materials and Methods Fig. 2.1). Recently two different set of markers covering the whole genome have been generated to ensure that genes can be placed as quickly and cost efficiently as possible on the genome (Geisler et al., 2007). All markers

used in the sets are from the MGH panel. We used these two sets of 192 microsatellite markers, G4 and H2, that have been developed to reliably position genes on Linkage groups of Tübingen x WIK map crosses (Geisler et al., 2007). The markers picked cover the genome with an average distance of 11.6 cM for the G4 and 11.5 cM for the H2 panel. As the two sets of markers were chosen because of their polymorphisms between the Tübingen and WIK and not the AB and WIK lines and in addition because none of these lines are isogenic, it is possible that some markers will not show polymorphism in the progeny of all of the F2 pairs used. Ideally two linked markers flanking the mutation are identified, thus defining an interval containing the gene of interest. If that is not possible, two markers on one side should be isolated to confirm linkage.

Once two flanking markers have been identified, further fine mapping is required in a positional cloning approach to identify a genomic clone to which the mutation is localized. Here, as a first step, markers from all panels suggested to be located between the two markers flanking the mutation are used to find more closely linked markers. The aim is to find a clone with a marker located about 0.1 cM away from the mutation. Generally if this is not possible with the markers present, new markers have to be generated. To generate new markers, genomic libraries can be screened for the known markers. Different genomic libraries, such as Yeast Artificial Chromosomes (YACs), P1 artificial chromosomes (PACs) and Bacterial Artificial Chromosomes (BACs) have been generated (Geisler, 2002). A high coverage of the genome and inserts of large size are desirable for the individual clones of such a library. Traditionally, when no sequence information for clones was available, the genomic libraries were screened either with the nearest known marker or a nearby cDNA clone. This was done by two methods: 1) pools of genomic clones were screened by PCR. Once a positive pool is identified the single clones in this pool are screened or 2) gridded library filters of bacterial colonies each containing a clone were screened by hybridization. Positive clones could then be ordered and the DNA isolated (Geisler, 2002). Identified clones can then be used to start a genomic walk by sequencing the ends of the clones, designing primers against them and again screening for further overlapping clones containing this sequence. Ideally the PCR product thus generated is polymorphic and can also be used to determine the distance to the mutation. Otherwise further markers have to be generated after sequencing additional parts of the clone of interest.

Another possibility to identify new markers is to identify the position of the known markers on the sequenced zebrafish genome. Then the sequencing and assembly of the zebrafish genome allows us to easily obtain the sequence of the region between two markers. With more and more of the zebrafish genome being sequenced this is a very attractive alternative, especially as large numbers of the markers of the MGH panel are being annotated from the outset. BAC libraries from the Tübingen line have been fingerprinted by restriction digests to produce contigs of overlapping clones that are then sequenced and assembled to produce a physical map of the zebrafish genome (Geisler, 2002). By now a large number of the BACs (over 7600 with the sequencing of about 6000 clones completely finished) known are integrated into the assembly of the zebrafish genome (http://www.ensembl.org/Danio_rerio/index.html).

A good way of creating new markers is to develop primers against the sequence of BAC ends annotated in ENSEMBL between the two closest known markers. Newly designed pairs of primers designed against BAC end sequences can then be tested for polymorphisms. Alternatively new candidate SSR (Single Sequence Repeat) marker can be obtained by entering the scaffold or BAC accession number on a webpage designed by the MGH (http://danio.mgh.harvard.edu/markers/ssr.html). Again the markers obtained this way have to be tested. On average 1 of 5 markers is polymorphic.

Difficulties with fine mapping can occur in centromeric regions where the recombination rate is particularly low and in areas not covered by many markers (e.g. Linkage group 21) (Geisler et al., 2007).

The assembly of the zebrafish genome containing known markers can make the generation of new markers and identification of genes a lot easier. Time consuming identification of clones within the interval of interest is not necessary anymore as they can be looked up in the assembly. In addition new markers can be generated easily as the sequence of the clones is readily available. However, for this approach to be useful it is necessary that the contig between the two original flanking markers is complete and correct. Where this it is not the case and patchy areas only seem to be complete, generating primers against clones which turn out to be wrongly placed only costs time and money. If gaps are present and visible on ENSEMBL, genomic clones in the gaps can be found by screening with markers against the ends of the last known clone (see above).

Once a clone containing the mutation has been identified the next step is to identify the gene carrying the mutation. Injection of BACs or PACs to see if the clone can partially rescue the mutant phenotype can help confirm that the gene of interest is on the clone. Injection of three PACs containing the marker, z10985, that linked closest to the *shady* mutation showed that only one of the three PACs injected, named PAC 3, could partially rescue the *shady* phenotype (Lopes et al., in prep.). Closer analysis of the PACs showed that while PAC 1 and 2 were mostly overlapping PAC 3 had a large piece of unique DNA containing the gene *alk.*

Although most clones have been sequenced and annotated by now, if the sequence of the clone is not known yet it can be sequenced and then software (such as Genescan) can be used to predict transcripts. However, gene and protein prediction software is not always completely reliable (Geisler, 2002) and it might therefore be necessary to search manually for cDNAs. Candidate genes can then be cloned using common approaches such as PCR and Rapid Amplification of cDNA Ends (RACE).

Once a candidate gene has been identified and cloned there are several experiments that can be done to verify that it is the gene containing the mutation (Geisler, 2002). The most direct approach is to identify the lesion in the mutated gene. Other possibilities are knockdown of the candidate gene by morpholino injection, rescue of the phenotype by DNA injection and *in situ* hybridisation experiments. Often a number of these experiments are performed.

In this chapter we describe our progress in mapping *parade* and the difficulties we encountered. The mapping was done in collaboration with Elisabeth Busch-Nentwich and Derek Stemple (Cambridge).

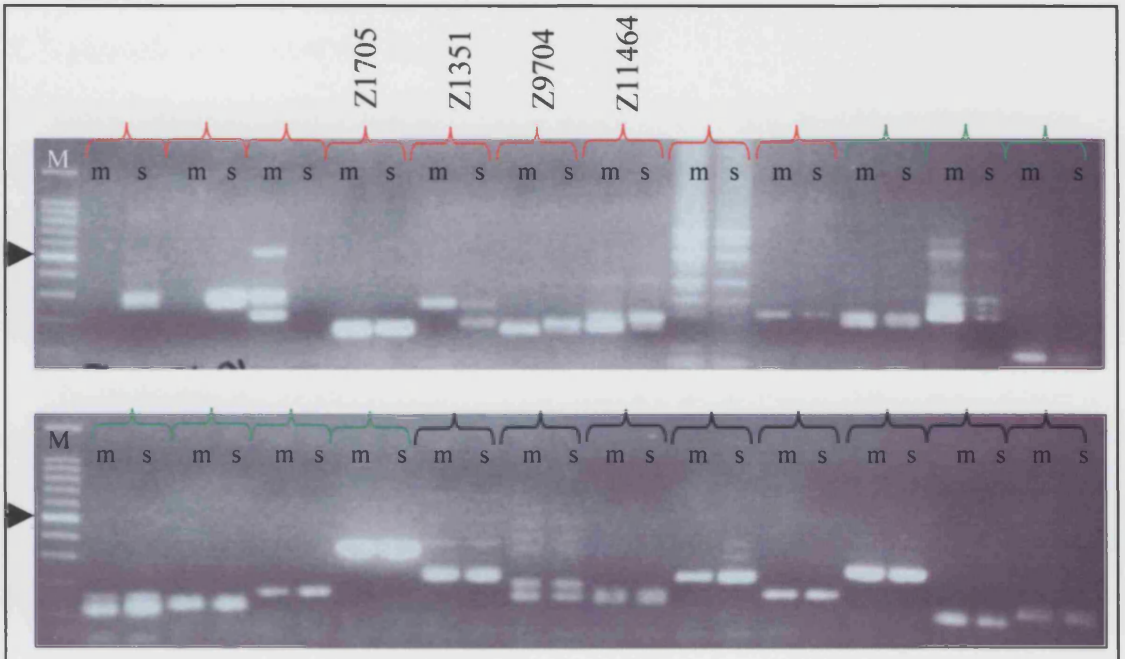

Fig. 6.2: *parade* was mapped to linkage group 1
Example of a pooled PCR gel. The gel only shows markers against Linkage Group 1 (red bracket), 2 (green) and 3 (black).

The bulked segregant analysis on DNA of 48 pooled mutant (m) and siblings (s) showed the mutation was located on Linkage group 1. To be able to detect linkage the sibling and mutant band need to be of different size. Presence of only one band of the same size in mutant and sibling lane indicates that the marker used is not polymorphic (for example marker Z1705). In lanes where no bands were visible the PCR did not work. Different intensities of this single band were most likely due to pipetting mistakes when loading the gel. A stronger AB band in the mutant pool and a stronger WIK band in the sibling pool indicate linkage between the mutation and the marker (see Fig. 2.1; and difference in intensities of bands for marker Z11464). Complete loss of one band indicated very tight linkage (see Z1351where complete loss of the lower band representing the WIK allele has occurred). Markers Z1351, ZZ9704 and Z11464 (all placed on Linkage group 1) showed recombination. The *parade*^{tj262} mutation had a strong potential linkage to Z1351 as the mutant DNA showed only one band while the sibling DNA showed two. Weakest linkage was to marker Z11464 where bands of both alleles were visible but showed different strength. Size marker (M) in bp: 1500, 1000, 900, 800 700, 600, 500, 400, 300, 200, 100; 500bp band labelled with arrow.

V.I.2 Results

VI.2.2. parade is located on linkage group 1

A first step in mapping *parade* was to identify which linkage group is the mutated locus lies on. For this we performed bulked segregant analysis on pooled DNA of 48 *parade* mutant embryos and 48 siblings (Fig. 6.2). All embryos used were progeny of Pair 2 of the F1 generation. To locate *parade* on a linkage group we used the G4 and H2 panels of SSLP markers, each covering the whole zebrafish genome (Geisler et al., 2007).
Using this approach we mapped the mutation on Linkage group 1 with the G4 panel. Three markers showed recombination Z1351, Z9704 and Z11464 (Fig. 6.2). We confirmed the location of the mutation by mapping it on the H2 panel. Again two markers situated on Linkage group 1, Z10978 and Z11618, were recombinant. The next step in the mapping process was to establish on which side of the mutation these markers lay in order to find flanking markers.

VI.2.2.A Fine mapping of *parade*

VI.2.2.A.1. Z1351 and Z9704

As of the three markers, Z1351, Z9704 and Z11464, isolated Z1351 seemed to have the strongest potential linkage and Z11464 the weakest we started by testing if Z1351 and Z9704 were flanking the mutation (Fig. 6.3). Scoring Z1351 and Z9704 on the 48 mutant embryos showed no overlapping recombination events, suggesting that they were each on different sides of the mutation. A first estimate of the distance of the two flanking markers Z1351 and Z9704 to parade was 4 cM for Z1351 and 26 cM for Z9704 (Fig. 6.3). By scoring them on the same embryos we placed Z10978 on the same side as Z1351. Z11618 and Z11464 were placed on the same side of the mutation as Z9704 (Fig. 6.4). Z10978 and Z11618 were the two closest flanking markers.

VI.2.2.A.2. P174 mapped ~0.2 cM away from the mutation

From the 50 markers that were suggested to be between Z1351 and Z11464 on the MGH panel (http://cvrc-barracuda.mgh.harvard.edu/zebrafish/MapViewer.aspx), the sequence for 33 markers was available and 16 of those were polymorphic for one or

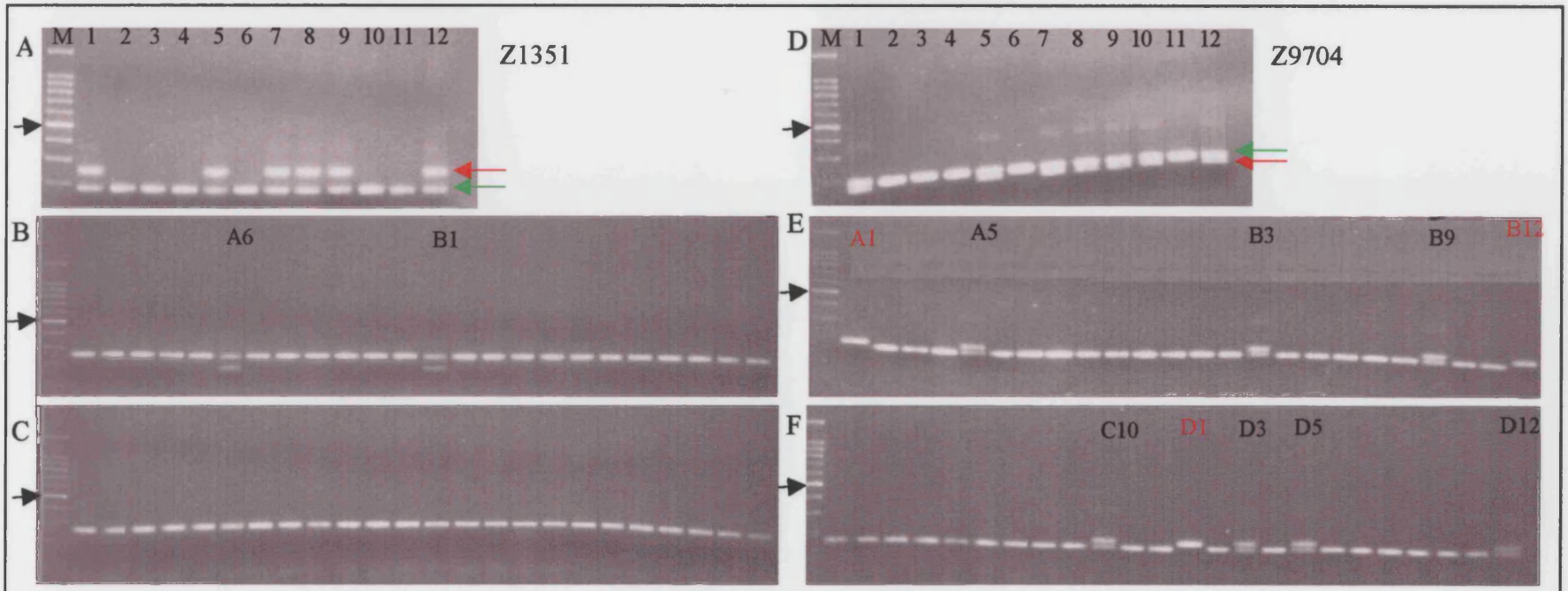

Fig. 6.3: Z1351 and Z9704 flanked the interval containing the mutation

Analysis of Z1351 on 12 sibling embryos confirmed that it was polymorphic (A). All embryos had the lower band representing the WIK allele (green arrow) while only embryo 1, 5, 7, 8, 9 and 12 had the AB band (red arrow) as well. Single embryo PCR with the mutant embryos used for pooled DNA in bulked segregant analysis showed that Z1351 had 2 recombinants, A6 and B1, in 48 embryos (B, C). Testing of Z9704 on the 12 siblings also confirmed that it was polymorphic (D). Here the lower band represented the AB allele (red arrow) while the larger band was the WIK allele (green arrow). PCR on the same 48 mutant embryos as Z1531 with Z9704 showed no overlap in recombinants indicating that the two markers were positioned on either side of the mutation (E, F). Three embryos - A1, B12 and D1 (red) - showed a double recombination event. While A5, B3, B9, C10, D3, D5 and D12 only have a single recombination event.A first rough estimate placed Z1351 4 cM and Z9704 26 cM 7 single and 3 double recombinants in 48 embryos) away from the mutation.

Size marker (M) in bp: 1500, 1000, 900, 800 700, 600, 500, 400, 300, 200, 100; 500bp band labelled with arrow

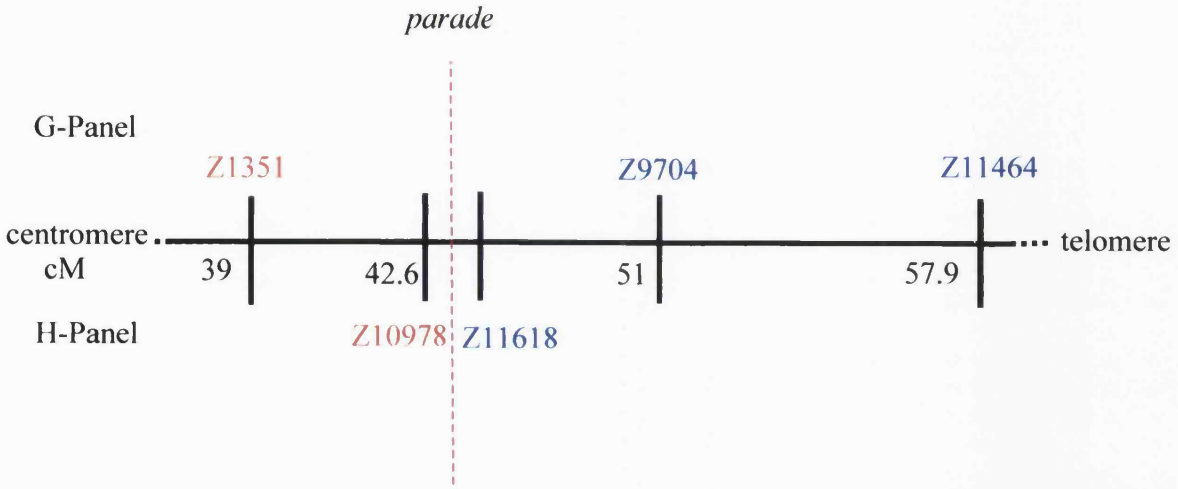

Fig. 6.4: Diagram showing the results of the first stage of mapping *parade*^{tj262}
The mutant locus was placed on linkage group 1 between the markers Z1351 on the 'right side' (here and in all future figures markers on this side of the mutation are shown in red) and Z9704 and Z11464 on the 'left' side (shown in blue) comprising an interval of 18.9 cM when using markers of the G panel. The two polymorphic markers, Z10978 and Z11618, from the H panel also framed the mutation, but were mapped to the same position on the MGH panel.
The centromere was located further to the left of the set of markers. Distances in cM as suggested by the MGH panel and not to scale.

more of our F2 pairs. The two closest markers were Z15424 with 9/579 recombinants (~1.5cM; thus ~990 kb) on the 'left' side and Z23059 with 22/576 recombinants (~3.8 cM; ~2510 kb) on the 'right' side of the gene of interest (Fig. 6.5). Both markers were mapped on Zv4. Z15424 was located on clone BX324156.5 and Z23059 about 500 kb away on clone BX000460.5 (Fig.6.6 A). However gaps in the assembly suggested that the area of interest on ENSEMBL was not completed yet and explains why the distance estimated from the mapping (990 kb + 2510 kb = 3500 kb) and on ENSEMBL did not match.

One other marker, fe24c01.x1, was annotated in the interval, but was not polymorphic on any of our F2 embryos. As no other known markers had been mapped between Z15424 and Z23059 we generated new markers by testing primers designed against BAC ends located in the interval. One marker created this way was zK257N15SP6 P48). It mapped onto the same side as Z15424, but only ~1.2 cM (3 recombinations in 248 embryos) away from *parade*. Consistent with this, the BAC end sequence it was generated against had been mapped onto clone BX511037.9 located in the interval between our two previous markers (Fig. 6.6 A).

At the time we narrowed the interval down slightly on the left hand side the 5th version of the zebrafish assembly (Zv5) was released (Fig. 6.6 B). The gap in the assembly remained and Zv_scaffold71 was replaced by Zv_scaffold41. By using potential SSR markers designed against repeats on Zv_scaffold41 we were not able to reduce the interval. Moreover our mapping data suggested that Zv_scaffold41 was not located within our interval. Markers designed against Zv_scaffold41 showed not only a higher number of recombinants than the two closest markers so far, Z15424 and P48, suggesting that it was located outside the interval but also showed recombination events in completely different embryos suggesting that it was most likely placed on a different linkage group.

In the light of our analysis, it was reassuring to see that Zv_scaffold41 had been removed from this region in version 6 of the zebrafish assembly (Zv6) and 4 new clones (CT573100.1, Zv_scaffold95, BX649371.6 and Zv_scaffold97) were added in the interval between our two closest markers, P48 and Z23059 (Fig. 6.7 A). In addition the gap between the clones of the left and right half of our interval seemed to be closed. Unfortunately, of the four new markers located on these newly added clones, none were polymorphic in our mapping cross. We therefore developed our own markers against

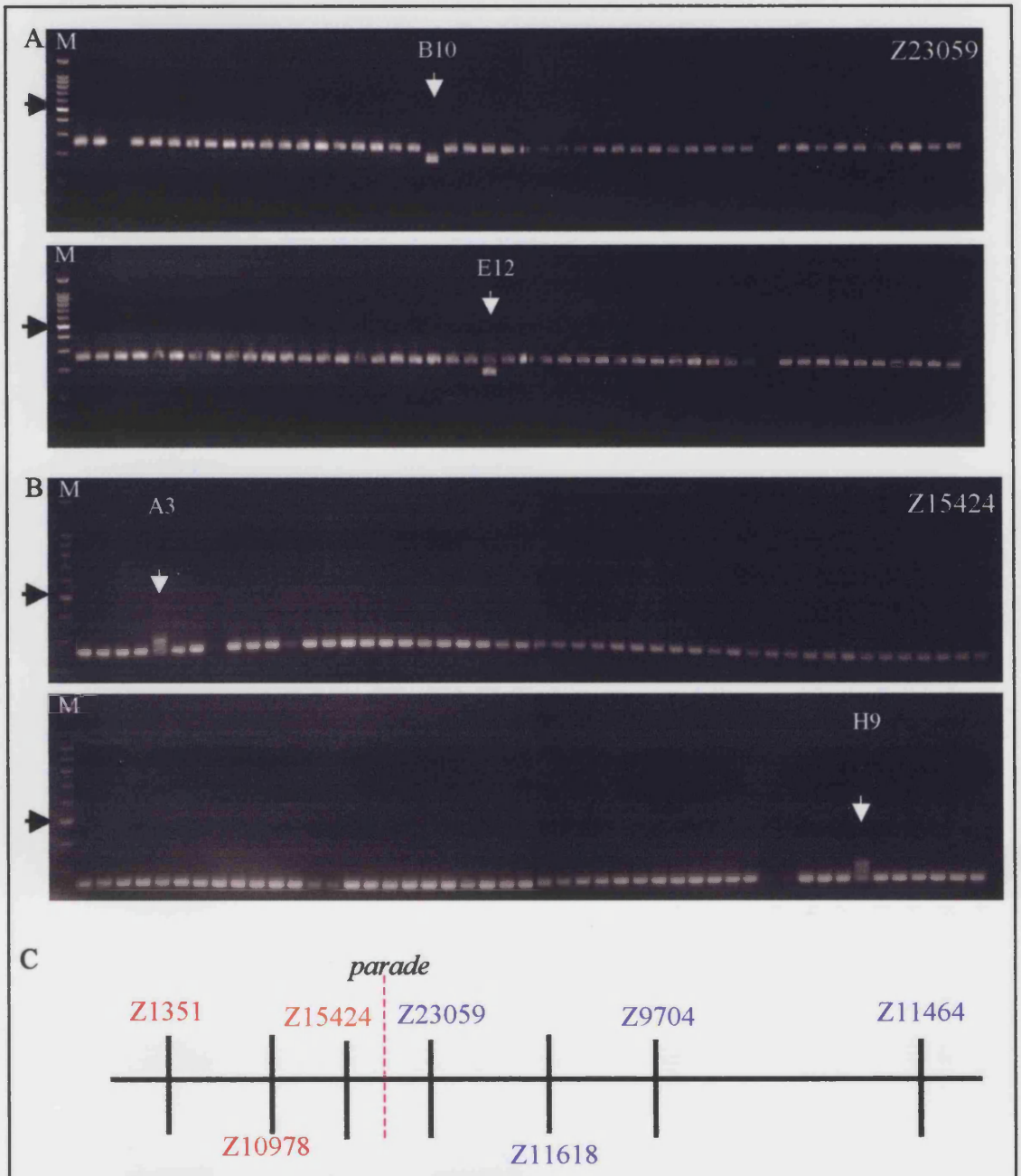

Fig. 6.5: Z15424 and Z23059 flanked the mutation
Comparison of the recombination events seen with two different markers, Z23059 (A) and Z15424 (B), after PCR on the same 96 individual mutants showed that they had no recombinants in common and were therefore located on different sites of the mutation (see Fig. 2.2). Z23059 was recombinant for B10 and E12 (A, white arrows) while Z15424 was recombinant for A3 and H9 (B, white arrows). Analysis on additional embryos placed Z15424 ~1.5 cM and Z23059 ~3.8 cM away from the mutation within the previously defined interval (C).
Size marker (M) in bp: 1500, 1000, 900, 800 700, 600, 500, 400, 300, 200, 100; 500bp band labelled with arrow

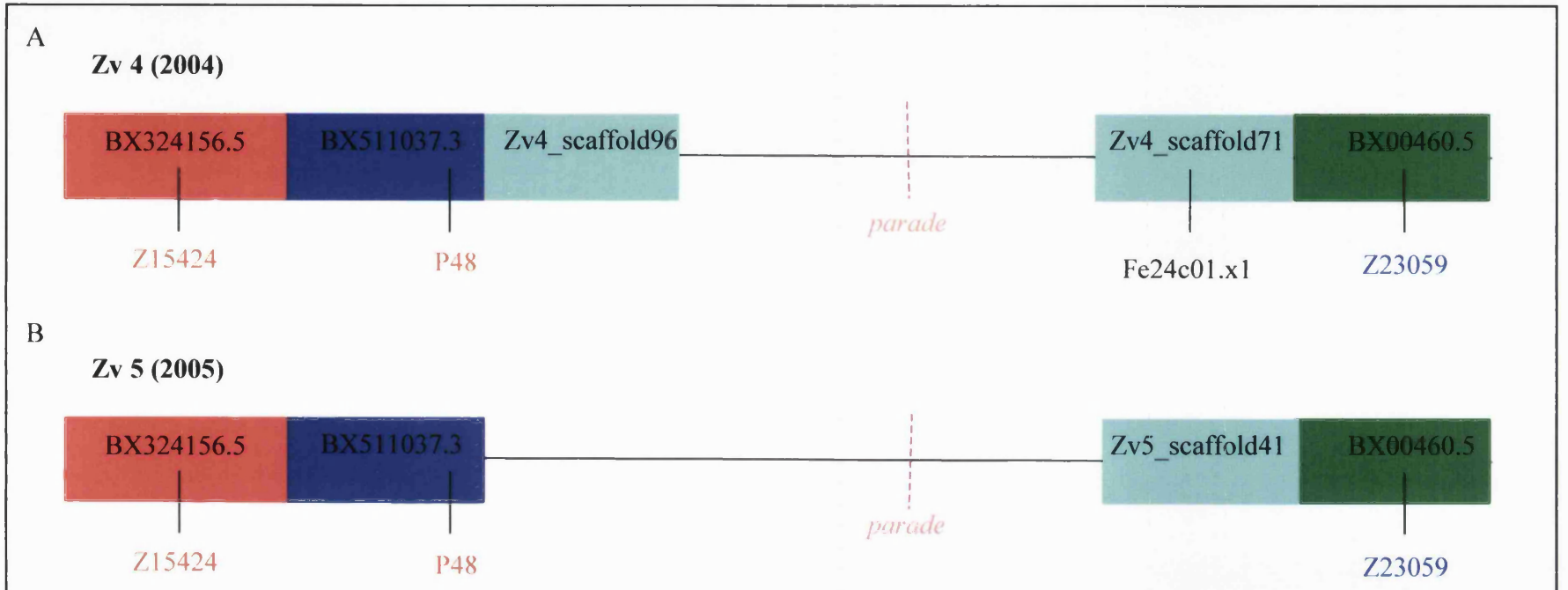

Fig. 6.6: Schematic presentation of the interval between Z15424 and Z23059 in Zv4 and Zv5
In the 4th assembly of the zebrafish genome, Zv4 (A), 3 clones had been suggested to be located between Z15424 on BX324156.6 and Z23059 on BX00460.5. A marker, P48, designed against sequence of BX5110373 mapped to the same side as Z15424, but was ~1.2 cM closer to the mutation than Z15424. Markers generated against both Zv4_scaffold 96 and 71 did not show linkage to *parade* and therefore suggested that they were placed wrongly. Consistent with this observation both had been removed from Zv5 (B). However, testing of markers generated against Zv5_scaffold41 suggested that it also was misplaced and located outside the interval of interest Each coloured box represents one clone while the single black line represents a gap in the assembly. Here and in the next figure each colour represents one clone in all different assemblies except clones in light blue. Clone shown in light blue indicate that they are clones that were removed from later assemblies. Sizes of clones and 'gaps' are not to scale. The potential position of the mutation is shown in pink.

the new clones by again using the SSR marker search tool on the MGH webpage. Using these markers we determined that Zv_scaffold97, like Zv-scaffold41 earlier, was not located in the interval of interest. But we were also able to narrow down the interval on the left hand side further from 1.2 cM to 1 cM (2 recombinants in 192 embryos) using a marker on clone BX644371.6 (P157) (Fig. 6.7 A).

The distance between the two markers framing the interval (P157 and Z23059) was estimated to be 4.8 cM from our mapping data. However, the distance suggested by the assembly between BX649371.6.1 and Z23059 49cM was only about 0.2 cM.

We therefore contacted Mario Caccamo at the Sanger to check if the assembly of this area was finished. They informed us that on the assembly available clone BX64371.6.1 was located left of a gap that was not shown in ENSEMBL. However unpublished assembly data suggested 3 clones (DKEY-68P1, BX511149 and BX005047) that were closing the gap (Fig. 6.7 B). Using SSR primers designed against the sequence of clones BX511149 and BX005047, we were able to get within 0.22 cM (4 recombinants in 1795 embryos) of the mutation (Fig. 6.7 B) suggesting that, if the assembly is final this time, the mutation would lie on DKEY-68P1. Unfortunately, DKEY-68P1 has not been sequenced yet. Primers designed against the sequenced ends were not polymorphic. Sequencing of this clone has now been prioritized by the Sanger and the first sequence data is expected for the middle of April 2007.

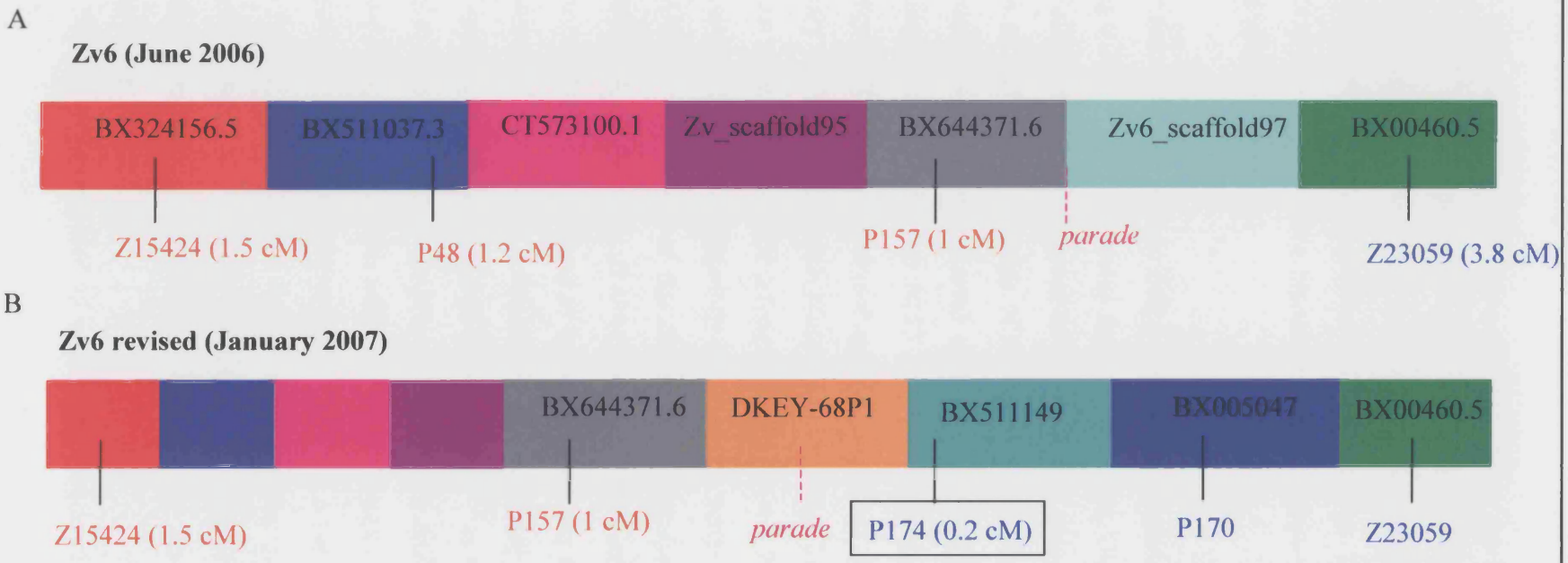

Fig. 6.7: Schematic presentation of the interval between Z15424 and Z23059 in Zv6 and a yet unpublished version
In the 6th version of the assembly of the zebrafish genome the gap between clone BX511037.3 and BX00460.5 was closed with 4 new clones (CT573100.1, Zv_scaffold95, BX649371.6 and Zv_scaffold97) (A). Markers located on Zv6_scffold97 showed no linkage to the mutation suggesting that it was not located in the interval. The closest marker at this stage was P157 mapping about 1 cM (1 recombinant in 192 embryos) away from the mutation on the left side. Our mapping data showed that P157 was ~660 kb (= 1 cM) and Z23059 ~2510 kb away from our mutation and the only clone suggested to be within this interval Zv_scaffold97 was not. This suggested that additional clones had to be in our interval of interest.
We received upon personal communication with M. Caccamo (Sanger centre) a revised version of Zv6 which had additional clones in our interval (B). A marker, P174 (black box), generated to BX51149 mapped only 0.2 cM (4 recombinants in 1795 embryos) away from the mutation. As this places P174 about 132 kb away from the mutation and the average size of a clone is 130 kb we suggest that the mutation is located on DKEY-68P1. All sizes not to scale.

IV.3. Discussion

As no candidate genes were available from the phenotypic characterization of the *parade*^{tj262} phenotype we adopted a positional cloning approach. Even though it was straightforward to map the mutation to Linkage group 1 it proved more difficult to narrow down the exact position of the mutation. This was mostly due to the initially poor coverage of the area, containing multiple gaps and clones that were wrongly placed and removed later.

We were however able to find a closely linked marker (P174) we estimate to be located only 0.22cM (~ 132 kb) away from the mutation. Our second flanking marker (P157) on the other side of the interval is ~ 1 cM away. Our interval has therefore an estimated size of ~792 kb. It consists of the ends of the two clones on which our markers are located and the unsequenced clone DKEY-68P1. The size of the interval could potentially be smaller as P157 has only been tested on a small number (192) of embryos. However, as the average size of a BAC clone from the DanioKey Pilot BAC library is 130 kb (Zebrafish library details, Sanger) and the distance from P174 is ~132 kb we suggest that *parade* is located on DKRY-68-P1.

An approach that has frequently been used to verify if a gene of interest is located on a BAC/PAC is injection of this clone. DNA injection however results in highly mosaic individuals. In the case of *shady*, where PAC mediated rescue of the phenotype has been performed, the success of the experiment was easily scorable by presence of a few localized iridophores in embryos otherwise lacking them (Lopes et al., in prep.). This approach is however not suitable for parade^{tj262} as the phenotype is highly variable. If only a few ectopic cells are present it would be difficult to determine if a few cells got rescued or if this embryo only had a few ectopic cells. Similarly a reduction of the increase in iridophore numbers in the AVS in a very small localized area would not be possible to detect. Parallel injection of the clone and a constitutively expressing GFP construct could help indicate the possible location of the clone, but as we do not know if *parade* functions cell autonomously or not it would still be difficult to make any conclusions.

We have therefore decided to wait for the sequence of DKEY-68P1. We do expect to get the first sequence data from the Sanger centre shortly and will then be able to test our prediction that the mutation is located on it. Generation of new polymorphic

markers as well as sequence analysis should help us close in on the mutation and identify the gene affected by it. Our characterisation so far has not uncovered a clear function for *parade* but comparison of the function of known genes in DKEY-68P1 to their homologues in other organisms could give us some candidates to concentrate on.

Chapter VII Final Discussion

Coat colour patterns of animals have fascinated scientists and laypersons for decades. To achieve the correct pigment pattern, regulation of pigment cell fates, numbers and position is necessary. Therefore a large variety of different mechanisms including regulation of cell number, specification, differentiation and migration is involved in correct patterning. Much work to understand these mechanisms has been done, mainly in chick and mouse but also in zebrafish. It is now known that, depending on the organism, pre-pattern by morphogens as well as environmental cues and cell-cell interactions play a role in pigment pattern formation. Mutants displaying ectopic pigment cells can help to make further progress in understanding how pattern formation occurs. Only a few mutants with ectopic pigment cells have been isolated and studied so far, perhaps because the defects leading to the ectopic cells, such as migration defects, affect earlier cell migration steps, for example during gastrulation already, and in many cases embryos die before ectopic pigment cells could be observed.

parade^{tj262} is one of few zebrafish pigment pattern mutants known that has ectopic pigment cells. To learn more about the establishment of the pigment pattern in zebrafish we studied *parade*^{tj262} which had been isolated during a large scale screen based on the appearance of ectopic chromatophores in the trunk. In addition, as a second study partly aimed at allowing us further study of the *parade*^{tj262} phenotype, we further characterised the known iridophore marker *alk* and identified in *gmp synthetase* and *id2* two new iridophore markers.

We have shown using *alk* that the first detectable phenotype in *parade*^{tj262} mutants is an increase in *alk*-positive iridoblasts in the VS clearly detectable as early as 36 hpf. This increase can still be seen in the PVS, at a stage when ectopic pigment cells can be observed mainly in the trunk. Nearly all of the supernumerary iridophores in the trunk are located in the ectopic position. Even though we observed melanophores and iridophores -sometimes closely associated- in the ectopic position we did not observe an increase in melanophore numbers in the PVS. Our studies suggest that the ectopic iridophores first move into the VS before adopting an ectopic position in the trunk as we are not able to distinguish *parade*^{tj262} mutants and wild-type embryos on the basis of cells in the ectopic position at 48 hpf. Using *colourless*^{m618};*parade*^{tj262} double mutants we showed that the presence of ectopic chromatophores is *sox10*-dependent. Our *nacre*^{w2};*parade*^{tj262} and *shady*^{ty82};*parade*^{tj262} double mutants studies suggest that the presence of each pigment cell type is (at least partly) independent of each other. It furthermore suggests that, as loss of one pigment cell type is not enough to lose all

ectopic cells of the other type, increase of iridophore numbers is not (solely) responsible for chromatophores appearing in the ectopic position. We also show that whilst the number of enteric neurons is wild-type in *parade*^{tj262} mutants, a decrease in sympathetic neuron number at 7dpf is detectable. This decrease might be present earlier, but so far no earlier markers for differentiated sympathetic neurons or its precursors in zebrafish have been isolated. The decrease of sympathetic neuron number could be dependent or independent of the increase in iridophore numbers.
In addition, by mapping *parade* to linkage group 1 and isolating a BAC that possibly contains our gene of interest we have made an important step towards its cloning.

From our studies so far we propose that the *parade*^{tj262} phenotype is hyper-proliferation and ectopic appearance of pigment cells. No other pigment (pattern) mutant characterised so far shows this combination of phenotypes.
nacre mutants, like *parade*^{tj262} mutants show an increase in iridophore numbers (Lister et al., 1999). The increase of iridophores in *nacre* has been proposed to result from a fate switch from melanophore to iridophore fate, explaining the loss of melanophores in *nacre*. We have not observed a loss of another neural crest derivative in *parade*^{tj262} mutants suggesting that a different mechanism causes the increase in iridophore numbers. In contrast to *parade*^{tj262} mutants, the increase of iridophore numbers in *nacre* is not restricted to the VS but can be seen in the DS and VS. In addition the increase in VS iridophores in *nacre* mutants does not lead to cells being present in the typical ectopic position in the trunk of *parade*^{tj262} mutants. Only very few supernumerary cells are ectopic in *nacre* and then they are located in the fins, showing a clear difference to *parade*^{tj262}.
Other characterised mutants displaying ectopic pigment cells are the mouse *Dsk* mutants (Fitch et al., 2003; Van Raamsdonk et al., 2004). Like in *parade*^{tj262} the *Dsk7*, *Dsk1* and *Dsk10* mutants have supernumerary and ectopic pigment cells. The supernumerary cells are thought to arise due to more neural crest cells differentiating into melanoblasts. It is unlikely that this is the case in *parade*^{tj262} as we would predict seeing an increase in iridophores in all stripes, similar to *nacre* mutants, then. Unlike in wild-type mice where all melanocytes move into the hair follicles, in *Dsk1*, *Dsk7* and *Dsk10* mutants some cells remain in the epidermis of the non-hairy region. Even though little is known about the mechanisms by which melanocytes move into the hair follicles *cadherins* have been associated with the migration process (Nishimura et al., 1999). It has not been shown

why the melanocytes in *Dsk* mice remain ectopic. However, the phenotype of *Dsk* mice is different compared to *parade*^{tj262} as the cells remain in a tissue, the epidermis, that they populate during normal development for a short period of time. In *parade*^{tj262}, even though the ectopic cells are in a position along the medial pathway through which they migrate at some stage, our observations suggest that the ectopic cells seem to first join the ventral stripe before moving into the ectopic position.

The Silkie Fowl is another partly characterised pigmentation mutant that has an increased number of pigment cells combined with the appearance of these supernumerary cells in the ectopic position. Why an increase in melanoblasts/melanocytes occurs in the Silkie Fowl is not known. Loss of the barrier molecule PNA-binding factor has been linked to melanocytes invading tissues usually not populated by them, suggesting that one defect in the Silkie Fowl lies in the restriction of melanocytes to a specific pathway. This is different to *parade*^{tj262} where the all pigment cells seem to migrate along the wild-type pathways.

In contrast to the *Dsk* mouse mutants and the Silkie fowl, but similar to *parade*^{tj262} mutants *ml-3* medaka mutants a localised increase in a pigment cell type unlikely to be caused by migration defects (Kelsh et al., 2004). The supernumerary leucophores can be observed in the DS and head only. VS leucophore numbers seem wild-type. Like *nacre*, but unlike *parade*^{tj262} mutants, *ml-3* mutants seem to have a decrease in a pigment cell type as cells displaying xanthophore characteristics could not be observed. This could indicate a 'fate switch' mechanism similar to the one in *nacre* is responsible for the increase in leucophores. But as the *ml-3* mutant has not been characterised yet, this is purely speculative. In contrast to *parade*^{tj262} nearly all *ml-3* leucophores – supernumerary and normal ones- can be found in an ectopic position lateral to the dorsal stripe. However, this might indicate that an environmental signal normally directing the leucophores into the DS is missing or a signal repelling the leucophores is over-expressed. This potential environmental signal miss-expression would be along the whole DS and not like we will propose for *parade*^{tj262} only in parts of the stripe.

The only other true zebrafish embryonic pigment pattern mutant characterised so far is *choker* (Svetic et al., 2007). *sdf1a* expression in the myoseptum that normally acts as an environmental cue to position melanophores along the lateral stripe is lost resulting in loss of the lateral stripe melanophores. Unfortunately, in *choker* mutants it is not known if the number of melanophores is increased in *choker* mutants. It has been shown though that some cells normally located in the DS and VS migrate to a patch of ectopic *sdf1a*

expression creating a melanophore collar. The collar area is also devoid of xanthophores normally located in this region. As we suggest for *parade*^{tj262} mutants, the ectopic pigment cells are first located in the stripe before some cells move into the ectopic position. However, the collar in *choker* consists of only one pigment cell type, while *parade*^{tj262} mutants have ectopic melanophores and iridophores. This suggests that, similarly to *choker,* the *parade*^{tj262} phenotype might be the results of a defect in maintenance of the VS.

The above examples show that *parade*^{tj262} mutants have a combination of phenotypes that has not been observed in any other mutants before. From our observations in *parade*^{tj262} mutants we propose the following speculative model for the appearance of the *parade*^{tj262} phenotype (Fig. 7.1). We propose that during migration on the medial pathway iridophore precursors and sympathetic neuron precursor cells respond to *parade* expression in the ventral half of the embryos e.g. the somites or the aorta. *parade* is responsible for regulating the proliferation of iridophores and sympathetic neurons (Fig. 7.1 A). Iridophores move then into the VS (Fig. 7.1 B). A second signal, an environmental factor, expressed above the VS holds the iridophores and melanophores in the VS (Fig. 7.1 C). We propose that this environmental cue is directly or indirectly regulated by *parade.* Like in wild-type embryos iridophore precursors and sympathetic precursors migrate along the medial pathway in *parade*^{tj262} mutants (Fig. 7.1 D). Loss of *parade* results in decreased proliferation of sympathetic neurons and over-proliferation of iridophores (Fig. 7.1 E). The supernumerary iridophores migrate into the VS like in wild-type embryos (Fig. 7.1 E). However, loss of the environmental signal because of the loss of *parade* leads to some chromatophores, melanophores and iridophores, leaving the VS and migrate in the ectopic position.

From our model we would predict an early increase in iridoblast/iridophore numbers as indeed was observed. We would also predict an early decrease of sympathetic neuron (precursor) numbers. We were not able to check this yet, as no early markers are available yet. A screen being performed at the moment (A. Boyd, T. Chipperfield and R. Kelsh) will hopefully discover the earlier markers to test this hypothesis.

If our model is correct transplantation of *parade*^{tj262} iridophore precursors into wild-type embryos should result in normal iridophore numbers and patterning. We tried to do cell transplantation experiments, labelling donor cells with rhodamine/biotin, to observe the behaviour of iridophores and to test for cell autonomy of *parade*. Unfortunately this

proved very difficult for a variety of reasons. Firstly iridophores possess auto-fluorescening properties making it difficult to detect which iridophores contain rhodamine. Secondly, as the numbers of ectopic cells in *parade*^{tj262} mutants is so variable it is hard to judge if transplanted wild-type cells adopt a position in the ventral stripe because of coincidence, because they possess different properties or because of non-existence of the proposed environmental cue.

Once the gene mutated in *parade*^{tj262} is identified homology studies might give us an indication as to its function. Also *in situ* hybridisation experiments will allow us to study its expression and this may be very revealing.

A variety of different experimental approaches will help us to understand the mechanisms underlying the *parade*^{tj262} phenotype further. So far we were unable to identify the reason for the increase in iridophore numbers and ectopic positioning of the chromatophores. We attempted to examine changes in regulation of cell numbers using *alk* as a marker for iridoblasts/iridophores. To see if there was an increase in proliferating or apoptosing iridoblasts/iridophores, we to tried to combine *alk in situ* hybridisation with PH3 antibody or TUNEL staining respectively. Unfortunately, both double protocols did not work even after initial modifications to the protocols. Further adjusting of the protocols should help us solve this question. Once the gene and the lesion in *parade*^{tj262} is identified we will also be able to genotype embryos following experiments such as *in situ* hybridisations. This will allow us to study, using *alk in situ* hybridisation, when the increase in iridophore numbers first occurs. In addition crossing *parade*^{tj262} into transgenic lines where expression of GFP is under the control of the *sox10* promoter might help towards identifying the mechanism responsible for the increase of VS iridophore numbers. Even though other pigment cells will also be GFP-positive, both excessive proliferation and death of GFP-positive cells should be visible in a timelapse study of *parade*^{tj262}; *sox10*::GFP embryos in comparison to *sox10*::GFP wild-type embryos. When checking for an increase in proliferation timelapse studies of a sufficient length should allow us to determine the fate of the cells that were proliferating excessively. Timelapse studies should also be able to help us confirm our observation that the ectopic cells in *parade*^{tj262} mutants are located in the VS before migrating into the ectopic position.

Identification of the mechanisms responsible for the phenotype of *parade*^{tj262} mutants should give us more information on regulation of iridophore and sympathetic neuron

numbers during zebrafish development. In addition it should give us further insight into maintenance of the VS.

Chapter VIII References

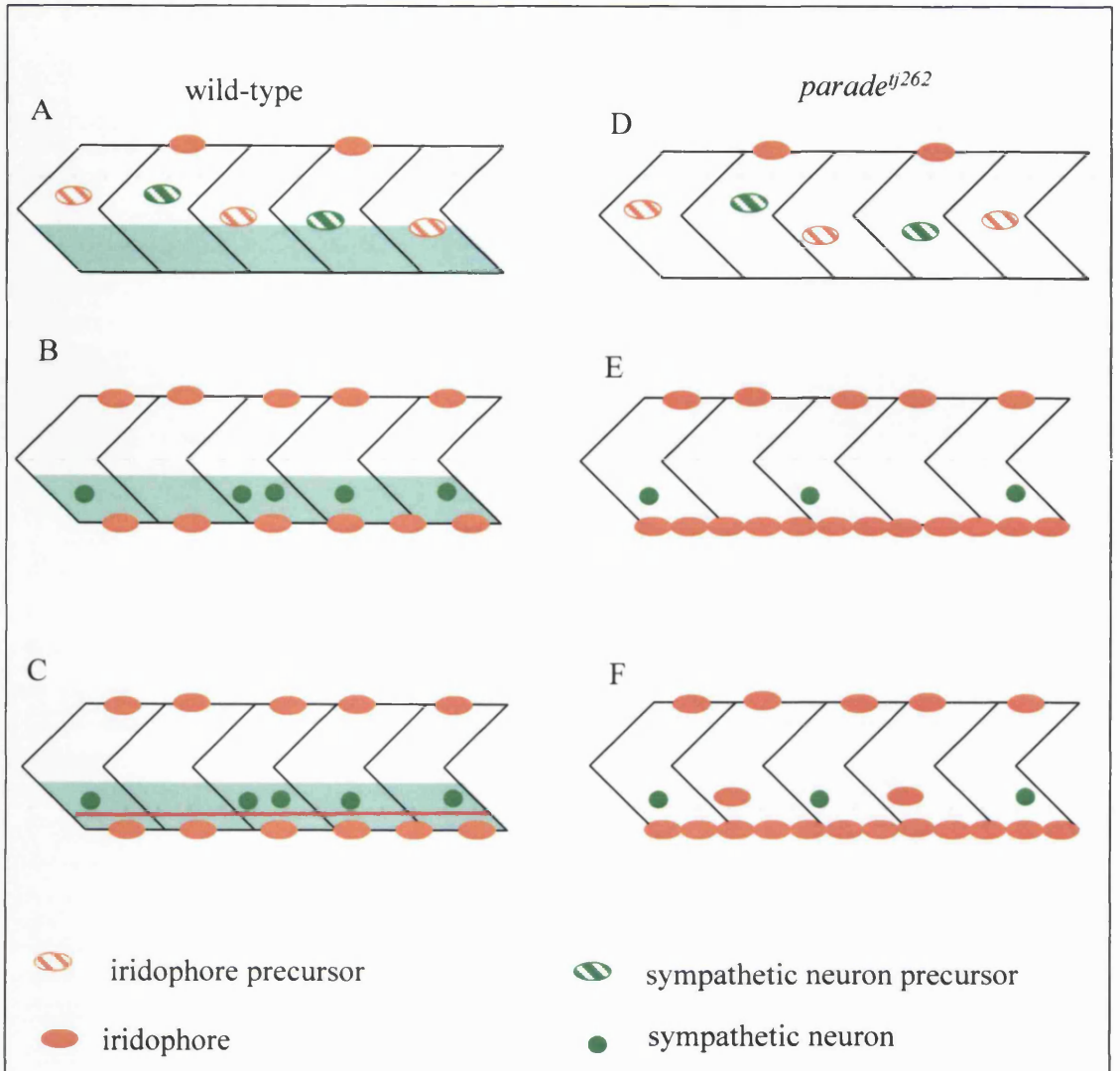

Fig. 7.1: Model for development of the *parade*^{tj262} phenotype
During development iridophore and sympathetic neuron precursors migrate along the medial pathway (A, D). *parade* expression (here shown in blue in the ventral half of the embryos) in wild-type embryos controls the proliferation rate of both (B). Loss of *parade* leads to an increase in proliferation of iridophores and a reduction of proliferation of sympathetic neuron precursors (E). Once iridophores have reached the VS, expression of *parade* is directly or indirectly necessary for expression of an environmental signal (shown as red line) above the VS to keep chromatophores in the VS (C). Loss of the signal because of loss of *parade* leads to some chromatophores leaving the VS (F). Melanophores are not shown, but like iridophores some leave the VS due to loss of the environmental signal.

Amores, A., Force, A., Yan, Y. L., Joly, L., Amemiya, C., Fritz, A., Ho, R. K., Langeland, J., Prince, V., Wang, Y. L. et al. (1998). Zebrafish hox clusters and vertebrate genome evolution. *Science* **282**, 1711-4.

Amsterdam, A., Nissen, R. M., Sun, Z., Swindell, E. C., Farrington, S. and Hopkins, N. (2004). Identification of 315 genes essential for early zebrafish development. *Proc Natl Acad Sci U S A* **101**, 12792-7.

Amundsen, T., Forsgren, E. (2001). Male mate choice selects for female coloration in a fish. *PNAS* **98**, 13155-13160.

An, M., Luo, R. and Henion, P. D. (2002). Differentiation and maturation of zebrafish dorsal root and sympathetic ganglion neurons. *J Comp Neurol* **446**, 267-75.

Aoki, Y., Saint-Germain, N., Gyda, M., Magner-Fink, E., Lee, Y. H., Credidio, C. and Saint-Jeannet, J. P. (2003). Sox10 regulates the development of neural crest-derived melanocytes in *Xenopus*. *Dev Biol* **259**, 19-33.

Asai, R., Taguchi, E., Kume, Y., Saito, M. and Kondo, S. (1999). Zebrafish leopard gene as a component of the putative reaction-diffusion system. *Mech Dev* **89**, 87-92.

Aybar, M. J. and Mayor, R. (2002). Early induction of neural crest cells: lessons learned from frog, fish and chick. *Current Opinion in Genetics & Development* **12**, 452-458.

Bagnara, J. T. (1978). On the Development of Pigment Patterns in Amphibians. *Amer. Zool.* **18**, 301-312.

Bagnara, J. T. (1991). An historical perspective on pigment cell biology from the editor. *Pigment Cell Res* **4**, 2-6.

Bagnara, J. T. (1998). Comparative Anatomy and Physiology of Pigment Cells in Nonmammalian Tissues. Oxford: Oxford University Press.

Bagnara, J. T. (1999). The Emergence of Pigment Cell Biology: A personal view. *Pigment Cell Res* **12**, 48-65.

Bagnara, J. T., Matsumoto, J., Ferris, W., Frost, S. K., Turner, W. A., Jr., Tchen, T. T. and Taylor, J. D. (1979). Common origin of pigment cells. *Science* **203**, 410-5.

Bagnara, J. T., Taylor, J. D. and Hadley, M. E. (1968). The dermal chromatophore unit. *J Cell Biol* **38**, 67-79.

Baroffio, A., Dupin, E. and Le Douarin, N. M. (1991). Common precursors for neural and mesectodermal derivatives in the cephalic neural crest. *Development* **112**, 301-5.

Baroffio, A., Dupin, E. and Ledouarin, N. M. (1988). Clone-Forming Ability and Differentiation Potential of Migratory Neural Crest Cells. *Proceedings of the National Academy of Sciences of the United States of America* **85**, 5325-5329.

Barrallo-Gimeno, A., , Holzschuh, J., , Driever, W., and Knapik, E. W. (2004). Neural crest survival and differentiation in zebrafish depends on mont blanc/tfap2a gene function. *Development* **131**, 1463-77.

Barsh, G. S. (2003). What controls variation in human skin color? *PLoS Biol* **1**, E27.

Baxter, L. L., Hou, L., Loftus, S. K. and Pavan, W. J. (2004). Spotlight on spotted mice: a review of white spotting mouse mutants and associated human pigmentation disorders. *Pigment Cell Res* **17**, 215-24.

Bazigou, E., Apitz, H., Johansson, J., Loren, C. E., Hirst, E. M., Chen, P. L., Palmer, R. H. and Salecker, I. (2007). Anterograde Jelly belly and Alk receptor tyrosine kinase signaling mediates retinal axon targeting in Drosophila. *Cell* **128**, 961-75.

Belmadani, A., Tran, P. B., Ren, D., Assimacopoulos, S., Grove, E. A. and Miller, R. J. (2005). The chemokine stromal cell-derived factor-1 regulates the migration of sensory neuron progenitors. . *J Neurosci* **25**, 3995-4003.

Berg, J. M., Tymoczko, J. L. and Stryer, L. (2002). Biochemistry. *New York: W. H. Freeman and Co.*

Bronner-Fraser, M. and Fraser, S. (1989). Developmental potential of avian trunk neural crest cells in situ. *Neuron* **3**, 755-66.

Bronner-Fraser, M. and Fraser, S. E. (1988). Cell lineage analysis reveals multipotency of some avian neural crest cells. *Nature* **335**, 161-4.

Budd, P. S., Antoniou, J., Mellor, A. L. and Jackson, I. J. (1997). Sooty foot, a novel mouse mutation that affects the pigmentation of exposed skin, but not hair, maps to chromosome 2. *Mamm Genome* **8**, 631-5.

Chong, S. W., Nguyen, T. T., Chu, L. T., Jiang, Y. J. and Korzh, V. (2005). Zebrafish id2 developmental expression pattern contains evolutionary conserved and species-specific characteristics. *Dev Dyn* **234**, 1055-63.

Collins, F. S. (1992). Positional cloning:Let's not call it reverse anymore. *Nature Genetics* **1**, 3-6.

Cooper, C. L., Brady, G., Bilia, F., Iscove, N. N. and Quesenberry, P. J. (1997). Expression of the Id family helix-loop-helix regulators during growth and development in the hematopoietic system. *Blood* **89**, 3155-65.

Dickmeis, T., Rastegar, S., Lam, C. S., Aanstad, P., Clark, M., Fischer, N., Rosa, F., Korzh, V. and Strahle, U. (2002). Expression of the helix-loop-helix gene id3 in the zebrafish embryo. *Mech Dev* **113**, 99-102.

Dorsky, R. I., Raible, D. W. and Moon, R. T. (2000). Direct regulation of nacre, a zebrafish MITF homolog required for pigment cell formation, by the Wnt pathway. *Genes & Development* **14**, 158-162.

Dupin, E., Glavieux, C., Vaigot, P. and Le Douarin, N. M. (2000). Endothelin 3 induces the reversion of melanocytes to glia through a neural crest-derived glial-melanocytic progenitor. *Proc Natl Acad Sci U S A* **97**, 7882-7.

Dupin, E., Real, C., Glavieux-Pardanaud, C., Vaigot, P. and Le Douarin, N. M. (2003). Reversal of developmental restrictions in neural crest lineages: transition from Schwann cells to glial-melanocytic precursors in vitro. *Proc Natl Acad Sci U S A* **100**, 5229-33.

Dutton, K. A., Pauliny, A., Lopes, S. S., Elworthy, S., Carney, T. J., Rauch, J., Geisler, R., Haffter, P. and Kelsh, R. N. (2001). Zebrafish *colourless* encodes *sox10* and specifies non- ectomesenchymal neural crest fates. *Development* **128**, 4113-4125.

Elworthy, S., Lister, J. A., Carney, T. J., Raible, D. W. and Kelsh, R. N. (2003). Transcriptional regulation of *mitfa* accounts for the *sox10* requirement in zebrafish melanophore development. *Development* **130**, 2809-2818.

Elworthy, S., Pinto, J. P., Pettifer, A., Cancela, M. L. and Kelsh, R. N. (2005). Phox2b function in the enteric nervous system is conserved in zebrafish and is sox10-dependent. *Mech Dev* **122**, 659-69.

Engeszer, R. E., Ryan, M.J., Parichy, D.M. (2004). Learned Social Preference in Zebrafish. *Curr Biol* **14**, 881-884.

Englund, C., Loren, C. E., Grabbe, C., Varshney, G. K., Deleuil, F., Hallberg, B. and Palmer, R. H. (2003). Jeb signals through the Alk receptor tyrosine kinase to drive visceral muscle fusion. *Nature* **425**, 512-6.

Epperlein, H. H., Lofberg, J. and Olsson, L. (1996). Neural crest cell migration and pigment pattern formation in urodele amphibians. *Int J Dev Biol* **40**, 229-38.

Erickson, C. A., Duong, T. D. and Tosney, K. W. (1992). Descriptive and experimental analysis of the dispersion of neural crest cells along the dorsolateral path and their entry into ectoderm in the chick embryo. *Dev Biol* **77**, 251-272.

Erickson, C. A., Goin, T.A. (1995). Avian neural crest cells can migrate in the dorsolateral path only if they are specified as melanocytes. *Development* **121**, 915-925.
Erickson, C. A. and Goins, T. L. (1995). Avian neural crest cells can migrate in the dorsolateral path only if they are
specified as melanocytes. *Development* **121**, 915-924.
Faraco, C. D., Vaz, S. A., Pastor, M. V. and Erickson, C. A. (2001). Hyperpigmentation in the Silkie fowl correlates with abnormal migration of fate-restricted melanoblasts and loss of environmental barrier molecules. *Dev Dyn* **220**, 212-25.
Fitch, K. R., McGowan, K. A., van Raamsdonk, C. D., Fuchs, H., Lee, D., Puech, A., Herault, Y., Threadgill, D. W., Hrabe de Angelis, M. and Barsh, G. S. (2003). Genetics of dark skin in mice. *Genes Dev* **17**, 214-28.
Fraser, S. E. and Bronner-Fraser, M. (1991). Migrating Neural Crest Cells in the Trunk of the Avian Embryo Are Multipotent. *Development* **112**, 913-920.
Fujii, R. (2000). The regulation of motile activity in fish chromatophores. *Pigment Cell Res* **13**, 300-19.
Geisler, R. (2002). Mapping and cloning. In *Zebrafish : a practical approach*, (ed. C. Nuesslein-Volhard and R. Dahm), pp. 175-212. Oxford: Oxford University Press.
Geisler, R., Rauch, G., Geiger-Rudolph, S., Albrecht, A., van Bebber, F., Berger, A., Busch-Nentwich, E., Dahm, R., Dekens, M., Dooley, C. et al. (2007). Large-scale mapping of mutations affecting zebrafish development. *BMC Genomics* **8**, 11.
Geisler, R., Rauch, G. J., Baier, H., van Bebber, F., Bross, L., Dekens, M. P., Finger, K., Fricke, C., Gates, M. A., Geiger, H. et al. (1999). A radiation hybrid map of the zebrafish genome. *Nat Genet* **23**, 86-9.
Geissler, E. N., Ryan, M. A. and Housman, D. E. (1988). The dominant-white spotting (W) locus of the mouse encodes the c-kit proto-oncogene. *Cell* **55**, 185-92.
Gilbert, S. F. (2000). Developmental Biology. Sunderland, Massachusetts: Sinauer Associates, INC.
Haffter, P., Granato, M., Brand, M., Mullins, M. C., Hammerschmidt, M., Kane, D. A., Odenthal, J., vanEeden, F. J. M., Jiang, Y. J., Heisenberg, C. P. et al. (1996a). The identification of genes with unique and essential functions in the development of the zebrafish, *Danio rerio*. *Development* **123**, 1-36.
Haffter, P., Odenthal, J., Mullins, M. C., Lin, S., Farrell, M. J., Vogelsang, E., Haas, F., Brand, M., vanEeden, F. J. M., FurutaniSeiki, M. et al. (1996b). Mutations affecting pigmentation and shape of the adult zebrafish. *Development Genes and Evolution* **206**, 260-276.
Halloran, M. C. and Berndt, J. D. (2003). Current Progress in Neural Crest cell Motility and Migration and Future Prospects for the Zebrafish Model System. *Dev Dyn* **228**.
Harris, M. L. and Erickson, C. A. (2007). Lineage Specification in Neural Crest Cell Pathfinding. *Dev Dyn* **236**, 1-19.
Henion, P. D. and Weston, J. A. (1997). Timing and pattern of cell fate restrictions in the neural crest lineage. *Development* **124**, 4351-4359.
Herbarth, B., Pingault, V., Bondurand, N., Kuhlbrodt, K., Hermans-Borgmeyer, I., Puliti, A., Lemort, N., Goossens, M. and Wegner, M. (1998). Mutation of the Sry-related *Sox10* gene in *Dominant megacolon*, a mouse model for human Hirschsprung disease. *Proceedings of the National Academy of Sciences of the United States of America* **95**, 5161-5165.
Hild, M., Dick, A., Rauch, G. J., Meier, A., Bouwmeester, T., Haffter, P. and Hammerschmidt, M. (1999). The smad5 mutation somitabun blocks Bmp2b signaling

during early dorsoventral patterning of the zebrafish embryo. *Development* **126**, 2149-2159.
Hirata, M., Nakamura, K., Kanemaru, T., Shibata, Y. and Kondo, S. (2003). Pigment cell organization in the hypodermis of zebrafish. *Dev Dyn* **227**, 497-503.
Hirata, M., Nakamura, K. and Kondo, S. (2005). Pigment cell distributions in different tissues of the zebrafish, with special reference to the striped pigment pattern. *Dev Dyn* **234**, 293-300.
Hodgkinson, C. A., Moore, K. T., Nakayama, A., Steingrimsson, E., Copeland, N. G., Jenkins, N. A. and Arnheiter, H. (1993). Mutations at the mouse microphthalmia locus are associated with defects in a gene encoding a novel basic-helix-loop-helix-zipper protein. *Cell* **74**, 395-404.
Hosoda, K., Hammer, R. E., Richardson, J. A., Baynash, A. G., Cheung, J. C., Giaid, A. and Yanagisawa, M. (1994). Targeted and natural (piebald-lethal) mutations of endothelin-B receptor gene produce megacolon associated with spotted coat color in mice. *Cell* **79**, 1267-76.
Hou, L., Arnheiter, H. and Pavan, W. J. (2006). Interspecies difference in the regulation of melanocyte development by SOX10 and MITF. *PNAS* **103**, 9081-9085.
Hrabe de Angelis, M. H., Flaswinkel, H., Fuchs, H., Rathkolb, B., Soewarto, D., Marschall, S., Heffner, S., Pargent, W., Wuensch, K., Jung, M. et al. (2000). Genome-wide, large-scale production of mutant mice by ENU mutagenesis. *Nat Genet* **25**, 444-7.
Hukriede, N., Fisher, D., Epstein, J., Joly, L., Tellis, P., Zhou, Y., Barbazuk, B., Cox, K., Fenton-Noriega, L., Hersey, C. et al. (2001). The LN54 radiation hybrid map of zebrafish expressed sequences. *Genome Res* **11**, 2127-32.
Hukriede, N. A., Joly, L., Tsang, M., Miles, J., Tellis, P., Epstein, J. A., Barbazuk, W. B., Li, F. N., Paw, B., Postlethwait, J. H. et al. (1999). Radiation hybrid mapping of the zebrafish genome. *Proc Natl Acad Sci U S A* **96**, 9745-50.
Hurley, S. P., Clary, D. O., Copie, V. and Lefcort, F. (2006). Anaplastic lymphoma kinase is dynamically expressed on subsets of motor neurons and in the peripheral nervous system. *J Comp Neurol* **495**, 202-12.
Ide, H. (1978). Transformation of Amphibian Xanthophores into Melanophores in Clonal Culture. *J Exp Zool* **203**, 287-294.
Ide, H. and Hama, T. (1976). Transformation of Amphibian Iridophores into Melanophores in Clonal Culture. *Dev Biol* **59**, 297-302.
Iwahara, T., Fujimoto, J., Wen, D., Cupples, R., Bucay, N., Arakawa, T., Mori, S., Ratzkin, B. and Yamamoto, T. (1997). Molecular characterization of ALK, a receptor tyrosine kinase expressed specifically in the nervous system. *Oncogene* **14**, 439-49.
Jackson, I. J. (2004). The G-netics of dark skin. *Nat Genet* **36**, 935-6.
Jager, R., Hahne, J., Jacob, A., Egert, A., Schenkel, J., Wernert, N., Schorle, H. and Wellmann, A. (2005). Mice transgenic for NPM-ALK develop non-Hodgkin lymphomas. *Anticancer Res* **25**, 3191-6.
Jen, Y., Manova, K. and Benezra, R. (1997). Each member of the Id gene family exhibits a unique expression pattern in mouse gastrulation and neurogenesis. *Dev Dyn* **208**, 92-106.
Jesuthasan, S. (1996). Contact inhibition collapse and pathfinding of neural crest cells in the zebrafish trunk. *Development* **122**, 381-389.
Jia, L., Cheng, L. and Raper, J. (2005). Slit/Robo signaling is necessary to confine early neural crest cells to the
ventral migratory pathway in the trunk. *Dev Biol* **282**, 411-421.

Johnson, S. L., Africa, D., Walker, C. and Weston, J. A. (1995). Genetic control of adult pigment stripe development in zebrafish. *Dev Biol* **167**, 27-33.
Kee, Y. and Bronner-Fraser, M. (2005). To proliferate or to die: role of Id3 in cell cycle progression and survival of neural crest progenitors. *Genes Dev* **19**, 744-55.
Kelly, P. D., Chu, F., Woods, I. G., Ngo-Hazelett, P., Cardozo, T., Huang, H., Kimm, F., Liao, L., Yan, Y. L., Zhou, Y. et al. (2000). Genetic linkage mapping of zebrafish genes and ESTs. *Genome Res* **10**, 558-67.
Kelsh, R. N. (2004). Genetics and evolution of pigment patterns in fish. *Pigment Cell Res* **17**, 326-36.
Kelsh, R. N. (2006). Sorting out Sox10 functions in neural crest development. *Bioessays* **28**, 788-98.
Kelsh, R. N., Brand, M., Jiang, Y. J., Heisenberg, C. P., Lin, S., Haffter, P., Odenthal, J., Mullins, M. C., van Eeden, F. J. M., Furutani-Seiki, M. et al. (1996). Zebrafish pigmentation mutations and the processes of neural crest development. *Development* **123**, 369-389.
Kelsh, R. N. and Eisen, J. S. (2000). The zebrafish *colourless* gene regulates development of non- ectomesenchymal neural crest derivatives. *Development* **127**, 515-525.
Kelsh, R. N., Inoue, C., Momoi, A., Kondoh, H., Furutani-Seiki, M., Ozato, K. and Wakamatsu, Y. (2004). The Tomita collection of medaka pigmentation mutants as a resource for understanding neural crest cell development. *Mech Dev* **121**, 841-59.
Kelsh, R. N. and Raible, D. W. (2002). Specification of zebrafish neural crest. *Results Probl Cell Differ* **40**, 216-36.
Kelsh, R. N., Schmid, B. and Eisen, J. S. (2000). Genetic analysis of melanophore development in zebrafish embryos. *Developmental Biology* **225**, 277-293.
Keynes, R. J. and Stern, C. (1988). Mechanisms of vertebrate segmentation. *Development* **103**, 413-429.
Kimmel, C. B., Ballard, W. W., Kimmel, S. R., Ullmann, B. and Schilling, T. F. (1995). Stages of embryonic development of the zebrafish. *Dev Dyn* **203**, 253-310.
Kitamura, K., Takiguchi-Hayashi, K., Sezaki, M., Yamamoto, H. and Takeuchi, T. (1992). Avian neural crest cells express a melanogenic trait during early migration from the neural tube:observations with the new monoclonal antibody, "MEBL-1.". *Development* **114**, 367-378.
Knapik, E. W., Goodman, A., Atkinson, O. S., Roberts, C. T., Shiozawa, M., Sim, C. U., Weksler-Zangen, S., Trolliet, M. R., Futrell, C., Innes, B. A. et al. (1996). A reference cross DNA panel for zebrafish (Danio rerio) anchored with simple sequence length polymorphisms. *Development* **123**, 451-60.
Knapik, E. W., Goodman, A., Ekker, M., Chevrette, M., Delgado, J., Neuhauss, S., Shimoda, N., Driever, W., Fishman, M. C. and Jacob, H. J. (1998). A microsatellite genetic linkage map for zebrafish (Danio rerio). *Nat Genet* **18**, 338-43.
Kondo, S. (2002). The reaction-diffusion system: a mechanism for autonomous pattern formation in the animal skin. *Genes Cells* **7**, 535-41.
Kondo, S. and Asai, R. (1995). A reaction-diffusion wave on the skin of marine angelfish *Pomacanthus*. *Nature* **376**, 765-768.
Krull, C. E. (2001). Segmental organization of neural crest migration. *Mechanisms of Development* **105**, 37-45.
Krull, C. E., Collazo, A., Fraser, S. E. and Bronner-Fraser, M. (1995). Segmental migration of trunk neural crest: time-lapse analysis reveals a role for PNA-binding molecules. *Development* **121**, 3733-43.

Krull, C. E., Lansford, R., Gale, N. W., Collazo, A., Marcelle, C., Yancopoulos, G. D., Fraser, S. E. and Bronner-Fraser, M. (1997). Interactions of Eph-related receptors and ligands confer rostrocaudal pattern to trunk neural crest migration. *Current Biology* **7**, 571-580.

Kwok, C., Korn, R. M., Davis, M. E., Burt, D. W., Critcher, R., McCarthy, L., Paw, B. H., Zon, L. I., Goodfellow, P. N. and Schmitt, K. (1998). Characterization of whole genome radiation hybrid mapping resources for non-mammalian vertebrates. *Nucleic Acids Res* **26**, 3562-6.

LaBonne, C. and Bronner-Fraser, M. (1999). Molecular mechanisms of neural crest formation. *Annual Review of Cell and Developmental Biology* **15**, 81-112.

Land, M. F. (1972). The physics and biology of animal refelctors. *Prog Biophys Mol Biol* **24**, 75-106.

Lane, P. W. and Liu, H. M. (1984). Association of Megacolon With a New Dominant Spotting Gene (Dom) in the Mouse. *Journal of Heredity* **75**, 435-439.

Le Douarin, N. (2004). The avian embryo as a model to study the development of the neural crest: a long and still ongoing story. *Mech Dev* **121**, 1089-1102.

Le Douarin, N. M. and Dupin, E. (1993). Cell Lineage Analysis in Neural Crest Ontogeny. *Journal of Neurobiology* **24**, 146-161.

Le Douarin, N. M. and Dupin, E. (2003). Multipotentiality of the neural crest. *Curr Opin Genet Dev* **13**, 529-36.

Le Douarin, N. M. and Kalcheim, C. (1999). The Neural Crest. New York: Cambridge University Press.

Lee, H. O., Levorse, J. M. and Shin, M. K. (2003). The endothelin receptor-B is required for the migration of neural crest-derived melanocyte and enteric neuron precursors. *Developmental Biology* **259**, 162-175.

Lele, Z., Folchert, A., Concha, M., Rauch, G. J., Geisler, R., Rosa, F., Wilson, S. W., Hammerschmidt, M. and Bally-Cuif, L. (2002). parachute/n-cadherin is required for morphogenesis and maintained integrity of the zebrafish neural tube. *Development* **129**, 3281-94.

Liao, E. H., Hung, W., Abrams, B. and Zhen, M. (2004). An SCF-like ubiquitin ligase complex that controls presynaptic differentiation. *Nature* **430**, 345-50.

Lister, J. A., Close, J. and Raible, D. W. (2001). Duplicate mitf genes in zebrafish: Complementary expression and conservation of melanogenic potential. *Developmental Biology* **237**, 333-344.

Lister, J. A., Robertson, C. P., Lepage, T., Johnson, S. L. and Raible, D. W. (1999). *nacre* encodes a zebrafish microphthalmia-related protein that regulates neural-crest-derived pigment cell fate. *Development* **126**, 3757-3767.

Lopes, S., Yang, X., Müller, J., Carney, T., McAdow, A. R., G.J., R., Schafer, M., Jacoby, A. S., Hurst, L. D., Haffter, P. et al. (in prep.).

Loren, C. E., Englund, C., Grabbe, C., Hallberg, B., Hunter, T. and Palmer, R. H. (2003). A crucial role for the Anaplastic lymphoma kinase receptor tyrosine kinase in gut development in Drosophila melanogaster. *EMBO Rep* **4**, 781-6.

Loring, J. F. and Erickson, C. A. (1987). Neural crest cell migratory pathways in the trunk of the chicken embryo. *Dev Biol* **121**, 220-236.

Lyden, D., Young, A. Z., Zagzag, D., Yan, W., Gerald, W., O'Reilly, R., Bader, B. L., Hynes, R. O., Zhuang, Y., Manova, K. et al. (1999). Id1 and Id3 are required for neurogenesis, angiogenesis and vascularization of tumour xenografts. *Nature* **401**, 670-7.

Maderspacher, F. and Nusslein-Volhard, C. (2003). Formation of the adult pigment pattern in zebrafish requires leopard and obelix dependent cell interactions. *Development* **130**, 3447-57.
Malicki, J., Schier, A. F., SolnicaKrezel, L., Stemple, D. L., Neuhauss, S. C. F., Stainier, D. Y. R., Abdelilah, S., Rangini, Z., Zwartkruis, F. and Driever, W. (1996). Mutations affecting development of the zebrafish ear. *Development* **123**, 275-283.
Martinsen, B. J. and Bronner-Fraser, M. (1998). Neural crest specification regulated by the helix-loop-helix repressor Id2. *Science* **281**, 988-91.
Martinsen, B. J., Frasier, A. J., Baker, C. V. and Lohr, J. L. (2004). Cardiac neural crest ablation alters Id2 gene expression in the developing heart. *Dev Biol* **272**, 176-90.
Marusich, M. F., Furneaux, H. M., Henion, P. D. and Weston, J. A. (1994). Hu Neuronal Proteins Are Expressed in Proliferating Neurogenic Cells. *Journal of Neurobiology* **25**, 143-155.
McCallion, A. S. and Chakravarti, A. (2001). EDNRB/EDN3 and Hirschsprung disease type II. *Pigment Cell Res* **14**, 161-9.
Melby, A. E., Kimelman, D. and Kimmel, C. B. (1997). Spatial regulation of floating head expression in the developing notochord. *Dev Dyn* **209**, 156-65.
Mellgren, E. M. and Johnson, S. L. (2004). A requirement for kit in embryonic zebrafish melanocyte differentiation is revealed by melanoblast delay. *Dev Genes Evol* **214**, 493-502.
Mellgren, E. M. and Johnson, S. L. (2005). kitb, a second zebrafish ortholog of mouse Kit. *Dev Genes Evol* **215**, 470-77.
Milos, N., Dingle, A. D. and Milos, J. P. (1983). Dynamics of pigment pattern formation in the zebrafish, Brachydanio rerio. III. Effect of anteroposterior location of three-day lateral line melanophores on colonization by the second wave of melanophores. *J Exp Zool* **227**, 81-92.
Mochii, M., Ono, T., Matsubara, Y. and Eguchi, G. (1998). Spontaneous transdifferentiation of quail pigmented epithelial cell is accompanied by a mutation in the Mitf gene. *Dev Biol* **196**, 145-59.
Montero-Balaguer, M., Lang, M., Sachdev, S., Knappmeyer, C., Stewart, R. A., De La Guardia, A., Hatzopoulos, A. K. and Knapik, E. (2006). The mother superior mutation ablates foxd3 activity in neural crest progenitor cells and depletes neural crest derivatives in zebrafish. *Dev Dyn* **235**, 3199-212.
Moreira, J. and Deutsch, A. (2005). Pigment pattern formation in zebrafish during late larval stages: a model based on local interactions. *Dev Dyn* **232**, 33-42.
Morin-Kensicki, E. M. and Eisen, J. S. (1997). Sclerotome development and peripheral nervous system segmentation in embryonic zebrafish. *Development* **124**, 159-167.
Morris, S. W., Kirstein, M. N., Valentine, M. B., Dittmer, K. G., Shapiro, D. N., Saltman, D. L. and Look, A. T. (1994). Fusion of a kinase gene, ALK, to a nucleolar protein gene, NPM, in non-Hodgkin's lymphoma. *Science* **263**, 1281-4.
Morrison-Graham, K. and Takahashi, Y. (1993). Steel factor and c-kit receptor: from mutants to a growth factor system. *Bioessays* **15**, 77-83.
Murray, J. D. (1981). On pattern formation mechanisms for lepidopteran wing patterns and mammalian coat markings. *Philos Trans R Soc Lond B Biol Sci* **295**, 473-96.
Nakamura, M., Tobin, D. J., Richards-Smith, B., Sundberg, J. P. and Paus, R. (2002). Mutant laboratory mice with abnormalities in pigmentation: annotated tables. *J Dermatol Sci* **28**, 1-33.

Neuman, T., Keen, A., Zuber, M. X., Kristjansson, G. I., Gruss, P. and Nornes, H. O. (1993). Neuronal expression of regulatory helix-loop-helix factor Id2 gene in mouse. *Dev Biol* **160**, 186-95.

Nishimura, E. K., Yoshida, H., Kunisada, T. and Nishikawa, S. I. (1999). Regulation of E- and P-cadherin expression correlated with melanocyte migration and diversification. *Dev Biol* **215**, 155-66.

Nolan, P. M., Peters, J., Strivens, M., Rogers, D., Hagan, J., Spurr, N., Gray, I. C., Vizor, L., Brooker, D., Whitehill, E. et al. (2000). A systematic, genome-wide, phenotype-driven mutagenesis programme for gene function studies in the mouse. *Nat Genet* **25**, 440-3.

Norton, J. D. (2000). ID helix-loop-helix proteins in cell growth, differentiation and tumorigenesis. *J Cell Sci* **113 (Pt 22)**, 3897-905.

Oakley, R. A., Lasky, C. J., Erickson, C. A. and Tosney, K. W. (1994). Glycoconjugates Mark a Transient Barrier to Neural Crest Migration in the Chicken-Embryo. *Development* **120**, 103-114.

Oakley, R. A. and Tosney, K. W. (1991). Peanut agglutinin and chondroitin-6-sulfate are molecular markers for tissues that act as barriers to axon advance in the avian embryo. *Dev Biol* **147**, 187-206.

Painter, K. J., Maini, P. K. and Othmer, H. G. (2000). Development and applications of a model for cellular response to multiple chemotactic cues. *J Math Biol* **41**, 285-314.

Parichy, D. M. (1996a). Salamander pigment patterns: how can they be used to study developmental mechanisms and their evolutionary transformation? *Int J Dev Biol* **40**, 871-84.

Parichy, D. M. (1996b). When neural crest and placodes collide: interactions between melanophores and the lateral lines that generate stripes in the salamander Ambystoma tigrinum tigrinum (Ambystomatidae). *Dev Biol* **175**, 283-300.

Parichy, D. M. (2006). Evolution of danio pigment pattern development. *Heredity* **97**, 200-10.

Parichy, D. M., Mellgren, E. M., Rawls, J. F., Lopes, S. S., Kelsh, R. N. and Johnson, S. L. (2000a). Mutational analysis of endothelin receptor b1 (rose) during neural crest and pigment pattern development in the zebrafish Danio rerio. *Developmental Biology* **227**, 294-306.

Parichy, D. M., Ransom, D. G., Paw, B., Zon, L. I. and Johnson, S. L. (2000b). An orthologue of the *kit*-related gene *fms* is required for development of neural crest-derived xanthophores and a subpopulation of adult melanocytes in the zebrafish, *Danio rerio*. *Development* **127**, 3031-3044.

Parichy, D. M., Rawls, J. F., Pratt, S. J., Whitfield, T. T. and Johnson, S. L. (1999). Zebrafish *sparse* corresponds to an orthologue of *c-kit* and is required for the morphogenesis of a subpopulation of melanocytes, but is not essential for hematopoiesis or primordial germ cell development. *Development* **126**, 3425-3436.

Parichy, D. M., Turner, J. M. and Parker, N. B. (2003). Essential role for puma in development of postembryonic neural crest-derived cell lineages in zebrafish. *Developmental Biology* **256**, 221-241.

Pavan, W. J. and Tilghman, S. M. (1994). Piebald lethal (sl) acts early to disrupt the development of neural crest-derived melanocytes. *Proc Natl Acad Sci U S A* **91**, 7159-63.

Pelletier, I., Bally-Cuif, L. and Ziegler, I. (2001). Cloning and developmental expression of zebrafish GTP cyclohydrolase I. *Mechanisms of Development* **109**, 99-103.

Pietzsch-Rohrschneider, I. (1977). The influence of phenylthiourea (PTU) on the pigment epithelium and the photoreceptor cells in the developing retina of Haplochromis burtoni (Cichlidae, Teleostei). *Cell and Tissue Research* **178**, 279-283.
Postlethwait, J. H., Woods, I. G., Ngo-Hazelett, P., Yan, Y. L., Kelly, P. D., Chu, F., Huang, H., Hill-Force, A. and Talbot, W. S. (2000). Zebrafish comparative genomics and the origins of vertebrate chromosomes. *Genome Res* **10**, 1890-902.
Pulford, K., Lamant, L., Morris, S. W., Butler, L. H., Wood, K. M., Stroud, D., Delsol, G. and Mason, D. Y. (1997). Detection of anaplastic lymphoma kinase (ALK) and nucleolar protein nucleophosmin (NPM)-ALK proteins in normal and neoplastic cells with the monoclonal antibody ALK1. *Blood* **89**, 1394-404.
Quigley, I. K. and Parichy, D. M. (2002). Pigment pattern formation in zebrafish: A model for developmental genetics and the evolution of form. *Microscopy Research and Technique* **58**, 442-455.
Raible, D. W. and Eisen, J. S. (1994a). Restriction of neural crest cell fate in the trunk of the embryonic zebrafish. *Development* **120**, 495-503.
Raible, D. W. and Eisen, J. S. (1994b). Specification and Commitment in Zebrafish Trunk Neural Crest Development. *Developmental Biology* **163**, 536-536.
Raible, D. W., Wood, A., Hodsdon, W., Henion, P. D., Weston, J. A. and Eisen, J. S. (1992). Segregation and early dispersal of neural crest cells in the embryonic zebrafish. *Dev Dyn* **195**, 29-42.
Ransom, D. G., Bahary, N., Niss, K., Traver, D., Burns, C., Trede, N. S., Paffett-Lugassy, N., Saganic, W. J., Lim, C. A., Hersey, C. et al. (2004). The zebrafish moonshine gene encodes transcriptional intermediary factor 1gamma, an essential regulator of hematopoiesis. *PLoS Biol* **2**, E237.
Rauch, G.-J., Granato, M. and Haffter, P. (1997). A polymorphic zebrafish line for genetic mapping using SSLPs on high-percentage agarose gels. *Tech. Tips Online T01208.*
Rawls, J. F., Mellgren, E. M. and Johnson, S. L. (2001). How the zebrafish gets its stripes. *Developmental Biology* **240**, 301-314.
Reedy, M. V., Faraco, C. D. and Erickson, C. A. (1998a). The Delayed Entry of Thoracic Neural Crest Cells into the Dorsolateral Path Is a Consequence of the Late Emigration of Melanogenic Neural Crest Cells from the Neural Tube. *Dev Biol* **200**, 234-246.
Reedy, M. V., Faraco, C. D. and Erickson, C. A. (1998b). Specification and migration of melanoblasts at the vagal level and in hyperpigmented Silkie chickens. *Dev Dyn* **213**, 476-85.
Santiago, A. and Erickson, C. A. (2002). Ephrin-B ligands play a dual role in the control of neural crest cell migration. *Development* **129**, 3621-3632.
Sawai, S. and Campos-Ortega, J. A. (1997). A zebrafish Id homologue and its pattern of expression during embryogenesis. *Mech Dev* **65**, 175-85.
Schilling, T. F. and Kimmel, C. B. (1994). Segment and Cell-Type Lineage Restrictions During Pharyngeal Arch Development in the Zebrafish Embryo. *Development* **120**, 483-494.
Schonthaler, H. B., Lampert, J. M., von Lintig, J., Schwarz, H., Geisler, R. and Neuhauss, S. C. (2005). A mutation in the silver gene leads to defects in melanosome biogenesis and alterations in the visual system in the zebrafish mutant fading vision. *Dev Biol* **284**, 421-36.
Shah, N. M., Groves, A. K. and Anderson, D. J. (1996). Alternative neural crest cell fates are instructively promoted by TGF beta superfamily members. *Cell* **85**, 331-343.

Sherman, L., Stocker, K. M., Morrison, R. and Ciment, G. (1993). Basic fibroblast growth factor (bFGF) acts intracellularly to cause the transdifferentiation of avian neural crest-derived Schwann cell precursors into melanocytes. *Development* **118**, 1313-26.
Shiroishi, T. (2001). [A large-scale mouse mutagenesis with a chemical mutagen ENU]. *Tanpakushitsu Kakusan Koso* **46**, 2613-8.
Sick, S., Reinker, S., Timmer, J. and Schlake, T. (2006). WNT and DKK determine hair follicle spacing through a reaction-diffusion mechanism. *Science* **314**, 1447-50.
Southard-Smith, E. M., Kos, L. and Pavan, W. J. (1998). *Sox10* mutation disrupts neural crest development in *Dom* Hirschsprung mouse model. *Nature Genetics* **18**, 60-64.
Stemple, D. L. and Anderson, D. J. (1992). Isolation of a Stem-Cell for Neurons and Glia from the Mammalian Neural Crest. *Cell* **71**, 973-985.
Stocker, K. M., Sherman, L., Rees, S. and Ciment, G. (1991). Basic FGF and TGF-/M influence commitment to melanogenesis in neural
crest-derived cells of avian embryos. *Development* **111**, 635-645.
Strmac, M. and Braunbeck, T. (1999). Effects of triphenyltin acetate on survival, hatching success, and liver ultrastructure of early life stages of zebrafish (Danio rerio). *Ecotoxicol Environ Saf* **44**, 25-39.
Svetic, V., Hollway, G., Elworthy, S., Chipperfield , T., Davison, C., Adams, R., Eisen, J., Ingham, P., Currie, P. and Kelsh, R. (2007). Sdf1a patterns zebrafish melanophores and links the somite and melanophore pattern defects in choker mutants. *Development* **134**, 1011-22.
Thisse, B., Pflumio, S., Fürthauer, M., Loppin, B.,, Heyer, V., Degrave, A., Woehl, R., Lux, A., Steffan, T., Charbonnier, X. Q. and Thisse, C. (2001). Expression of the zebrafish genome during embryogenesis (NIH R01 RR15402). *ZFIN Direct Data Submission.*
Tickle, C. (2000). Limb development: an international model for vertebrate pattern formation. *Int J Dev Biol* **44**, 101-8.
Tosh, D. and Slack, J. M. (2002). How cells change their phenotype. *Nat Rev Mol Cell Biol* **3**, 187-94.
Tosney, K. W. (2004). Lond-Distance Cue From Emerging Dermis Stimulates Neural Crest Melanoblast migration. *Dev Dyn* **229**, 99-108.
Turing, A. M. (1952). The chemical basis for morphogenesis. *Philos Trans R Soc Lond B* **237**, 32-72.
Van Raamsdonk, C. D., Fitch, K. R., Fuchs, H., de Angelis, M. H. and Barsh, G. S. (2004). Effects of G-protein mutations on skin color. *Nat Genet* **36**, 961-8.
Vernersson, E., Khoo, N. K., Henriksson, M. L., Roos, G., Palmer, R. H. and Hallberg, B. (2006). Characterization of the expression of the ALK receptor tyrosine kinase in mice. *Gene Expr Patterns* **6**, 448-61.
Wang, H. U. and Anderson, D. J. (1997). Eph family transmembrane ligands can mediate repulsive guidance of trunk neural crest migration and motor axon outgrowth. *Neuron* **18**, 383-396.
Watanabe, M., Iwashita, M., Ishii, M., Kurachi, Y., Kawakami, A., Kondo, S. and Okada, N. (2006). Spot pattern of leopard Danio is caused by mutation in the zebrafish connexin41.8 gene. *EMBO Rep* **7**, 893-7.
Westerfield, M. (1995). The Zebrafish Book. Eugene: University of Oregon Press.
Weston, J. A. and Butler, S. L. (1966). Temporal factors affecting localization of neural crest cells in the chicken embryo. *Dev Biol* **14**, 246-66.

Woods, I. G., Kelly, P. D., Chu, F., Ngo-Hazelett, P., Yan, Y. L., Huang, H., Postlethwait, J. H. and Talbot, W. S. (2000). A comparative map of the zebrafish genome. *Genome Res* **10**, 1903-14.
Woods, I. G., Lyons, D. A., Voas, M. G., Pogoda, H. and Talbot, W. S. (2006). nsf is essential for organization of myelinated axons in zebrafish. *Curr Biol* **16**, 636-48.
Yokota, Y. (2001). Id and development. *Oncogene* **20**, 8290-8.
Yokota, Y., Mansouri, A., Mori, S., Sugawara, S., Adachi, S., Nishikawa, S. and Gruss, P. (1999). Development of peripheral lymphoid organs and natural killer cells depends on the helix-loop-helix inhibitor Id2. *Nature* **397**, 702-6.
Yokota, Y., Mori, S., Narumi, O. and Kitajima, K. (2001). In vivo function of a differentiation inhibitor, Id2. *IUBMB Life* **51**, 207-14.
Yokota, Y., Mori, S., Nishikawa, S. I., Mansouri, A., Gruss, P., Kusunoki, T., Katakai, T. and Shimizu, A. (2000). The helix-loop-helix inhibitor Id2 and cell differentiation control. *Curr Top Microbiol Immunol* **251**, 35-41.
Yoshida, H., Kunisada, T., Kusakabe, M., Nishikawa, S. and Nishikawa, S. I. (1996). Distinct stages of melanocyte differentiation revealed by anlaysis of nonuniform pigmentation patterns. *Development* **122**, 1207-14.
Zarnescu, O. (2007). Ultrastructure of the skin melanophores and iridophores in paddlefish, Polodon spathula. *Micron* **38**, 81-84.
Zhang, J. J., Talbot, W. S. and Schier, A. F. (1998). Positional cloning identifies zebrafish *one-eyed pinhead* as a permissive EGF-related ligand required during gastrulation. *Cell* **92**, 241-251.
Ziegler, I. (2003). The pteridine pathway in zebrafish: regulation and specification during the determination of neural crest cell-fate. *Pigment Cell Res* **16**, 172-82.